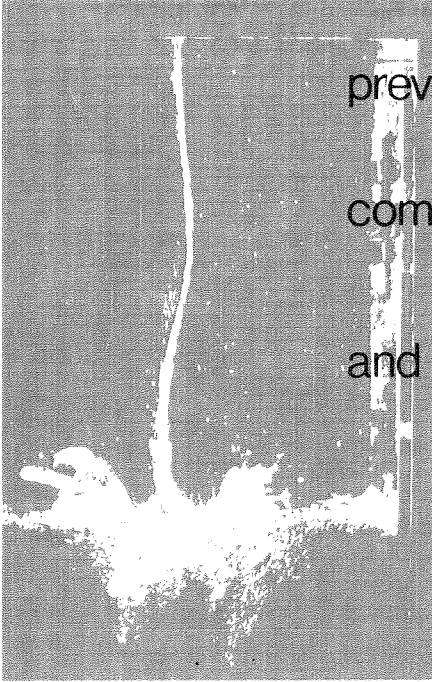


flow-induced gate vibrations

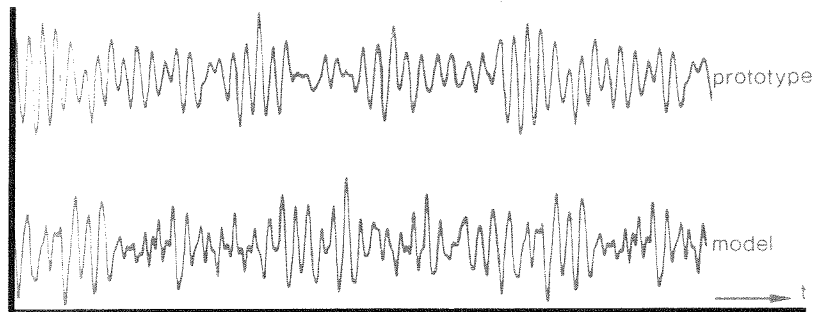


prevention of self-excitation

computation of dynamic gate

behaviour

and the use of models



p. a. kolkman

flow-induced gate vibrations

prevention of self-excitation

computation of dynamic gate

behaviour

and the use of models



p. a. kolkman

flow-induced gate vibrations

prevention of self-excitation
computation of dynamic gate
behaviour
and the use of models

proefschrift

ter verkrijging van de graad van doctor in de technische wetenschappen aan de **technische hogeschool delft**, op gezag van de rector magnificus prof. dr. ir. h. van bekkum, voor een commissie aangewezen door het college van dekanen te verdedigen op donderdag 17 juni 1976 te 16.00 uur door

paul albert kolkman

civiel ingenieur, geboren te amsterdam

Dit proefschrift is goedgekeurd door de promotoren
prof. ir. H. J. Schoemaker
prof. ir. A. A. van Douwen

Stellingen behorend bij het proefschrift „Flow-Induced Gate Vibrations” door P. A. Kolkman.

1. Instabiele hydroëlastische trillingen hangen meestal niet samen met het instabiel loslaten van stroming.
2. De „zuigkracht” bij rioolschuiven is vooral te reduceren door de bovenbelasting te verlagen, d.w.z. de spleten die de schuifschacht voeden zodanig te dimensioneren dat de waterstand in de schacht lager is dan overeenkomt met de druk bovenstrooms van de schuif.
3. Een van de moeilijkste aspecten bij het ontwerpen van trillingsmodellen van schuiven is de geometrische reproductie.
4. Resultaten van trillingsonderzoek van rioolschuiven moeten kritisch bekeken worden als deze verkregen zijn met een model met een niet korrekte rioollengte of als het model geplaatst is geweest in een gesloten circuit.
5. Als het model van een schuif met overstortend water niet trilt, geeft dit nog geen garantie dat de werkelijke schuif trillingsvrij is.
6. Vergelijking (IV. 17), welke aangeeft dat de dempende werking van vloeistof op een trillend voorwerp evenredig is met het aangestroomde oppervlak, met de dichtheid van de vloeistof en met de stroomsnelheid, wordt wat betreft de laatste term kwalitatief bevestigd door het toepassen van een steunzeil bij trawlers.
7. Onderzoek naar luchtstroming kan in de meeste gevallen gedaan worden in watermodellen. Hebben deze soms reeds voordelen boven luchtmodellen bij het onderzoek naar windhinder, de voordelen worden groot bij onderzoek van luchtstromingen waarbij dichtheidsverschillen een rol spelen, zoals tocht, of verspreiding van rook in een gelaagde atmosfeer.
8. Het vele onderzoek op het gebied van hydroëlastische verschijnselen dat gedaan wordt aan cilindres, heeft eerder vertroebelend dan verhelderend gewerkt op het inzicht in het dynamische gedrag van schuiven.
9. Het stellen van regels en beperkingen omdat de mensen niet aan vrijheid toe zouden zijn, werkt kinderlijk gedrag in de hand.
10. Ouders van kinderen jonger dan 18 jaar dienen, als zij een volledige baan hebben, niet te promoveren.
11. Op de T.H.D. dient, meer dan nu het geval is, gestimuleerd te worden dat pas afgestudeerden die hiervoor aanleg hebben, een promotieonderzoek verrichten.

12. Bij onderwijsprojecten in het kader van ontwikkelingshulp dient men rekening te houden met de mogelijkheid dat de opgeleiden na dit onder-richt geen handenarbeid meer wensen te verrichten.
13. De akties die worden ondernomen om de Oosterschelde open te houden gaan er impliciet van uit dat de kwaliteit van het Noordzeewater vol- doende blijft om het huidige ecologische systeem in stand te houden. Nagegaan moet worden of er voldoende gronden voor deze verwachting zijn.
14. Het welzijnsgevoel kan, bij gelijke kosten, versterkt worden door de starre elementen van inkomensverwerving te vervangen door aan de individuele omstandigheden aangepaste. Te denken is aan:
 - tijdsduur van werken
 - leeftijd van pensionering
 - hoogte van inkomen
 - verloop van de inkomenslijn met de tijd
 - hoogte van het pensioen

ERRATA:

p. 38 line 1

"This is a lower order of equation (I.19)" has to be read as:

"Introducing the general solution $y = Y_0 e^{st}$ results in a cubic equation in s (comparable with the quartic equation (I.22) which resulted from the coupled equations (I.19 and 20))"

p. 102 line 14

$Y_0 = \sin \omega t$ should be read as $y = Y_0 \sin \omega t$

p. 110 below (IV.13): 10^6 has to be read as 10^{-6}

p. 116 line 12 becomes: $F = \frac{1}{2} \rho L^2 C_D (V^2 - 2V\dot{y} + \dot{y}^2)$

Preface

This book has been written with three aims:

- to serve as a thesis;
- to make me conscious of the state of my knowledge after more than 15 years of experience in the field of gate dynamics; and
- to make available this knowledge for gate design and future research.

Those who are experienced in applied structural mechanics will find in Chapter I, the first part of Chapter II and in Chapters III and V much that fits in with their experience and knowledge. The designer can avoid a number of design errors when he applies the instability indicator introduced in Chapter III, which indicates when extra danger of unstable vibrations is to be expected.

Chapters II and IV are relatively long and go into many details, because in the course of years, by sheer necessity, a lot of research has been done on theory and on scale models in relation to unstable vibrations and the determination of the added mass of water and hydrodynamic damping.

Chapter VI, finally, could not be missed, where so much of the knowledge has been obtained by means of the technique of scale models, of which the Dutch Public Works Ministry gave me the opportunity to verify the results with laborious and costly prototype investigations.

An attempt has been made to find connections in certain fields with the great experience which has since many years been built up by the aeronautical laboratories. However, it also appeared that the vibration mechanisms of slender and streamlined bodies in flow differ on many points from those of gates, which partly block the stream.

I would like to mention two important books, which were published a few years ago and which stimulated me to undertake this work, namely the design handbook on gates "Stahlwasserbau"^x and the report on the

Preface

Symposium on "Flow-Induced Vibrations" organized in 1972 by the IUTAM/IAHR^{***}, which report presents the state of the art in this field lying so exactly between the fluid dynamics and the applied structural mechanics and involving so many different disciplines.

To many I owe a debt of gratitude for the help they gave me in achieving this work, both in the Delft Hydraulics Laboratory, where from the beginning the importance was recognized of developing this specialization and where colleagues of my own branch and also in the mathematics and instrumentation branches gave their essential support, and outside the Laboratory, where designers have endeavoured to realize gate designs in intensive co-operation with the Laboratory. Being grateful to the many who helped with typewriting, with drawings, with photography and reproduction, I feel that Mr. J.C. Hoogewerff has to be mentioned in particular, because when he improved my English, he inspired me at the same time to rethink many unclear reasonings and formulations.

I was in the happy circumstances that my family, the Delft Hydraulics Laboratory, the Delft Technical University and my violin teacher permitted me to organize things in such a way that too great a stress could be prevented, circumstances which seem to be rare and for which I am indebted to my wife and my two sons in particular.

* G. Wickert and G. Schmauszer "Stahlwasserbau", published in 1971 by Springer-Verlag, Berlin.

*** Eduard Naudascher (ed.) "Flow-Induced Structural Vibrations", Symposium held in 1972 in Karlsruhe and sponsored by the International Union of Theoretical and Applied Mechanics and the International Association of Hydraulic Research, published in 1974 by Springer-Verlag, Berlin.

Contents

PREFACE	V
LIST OF SYMBOLS	XI
GLOSSARY OF LESS COMMON EXPRESSIONS	XV
CHAPTER I INTRODUCTION	1
I.1. Summary	1
I.2. Description of different types of flow-induced vibration	2
I.3. Added mass, hydrodynamic damping, hydrodynamic rigidity and hydrodynamic excitation	6
I.4. Self-excitation or negative hydrodynamic damping	10
I.5. Structures in water and air	15
I.6. Gate and valve vibrations	17
I.7. Design requirements in relation to gate and valve vibrations	23
CHAPTER II SELF-EXCITING VIBRATIONS OF GATES AND VALVES	29
II.1. Summary	29
II.2. Introduction	29
II.3. General description of the computation method for self-exciting vibrations	36
II.4. Self-exciting vibrations of a water curtain or overflow nappe enclosing an air pocket	38
II.5. Self-exciting vibrations of a plug valve	39
II.6. The minimum "reduced" frequency required for stability of an undamped plug valve	46
II.7. Experimental data to check the plug valve theory	47
II.8. Estimate of maximum forces in the resilient gate suspension	48
	VII

Contents

II.9.	Self-exciting vibrations of a reversed Taintor valve	49
II.10.	Experimental data to check the Taintor valve theory	52
II.11.	Possibility of application of the theory to cylinder valves	53
II.12.	Self-exciting vertical vibrations of gates	54
II.13.	Vertical gate vibrations with damping due to wave radiation	61
II.14.	Discharge fluctuations and wave production	64
II.15.	Experimental data to check the theory for vertical gate vibrations	67
II.16.	Computation of the additional length coefficient c_L and the radiation coefficient c_r	69
II.17.	Determination of the force coefficient c_F	78
CHAPTER III PREVENTION OF SELF-EXCITATION IN GATE DESIGN; A SIMPLIFIED APPROACH USING AN INDICATOR		83
III.1.	Summary	83
III.2.	Introduction	83
III.3.	Discussion on the validity of the indicator for self-exciting vibrations	87
III.4.	Examples of design factors which can lead to self-exciting vibrations	88
CHAPTER IV HYDRODYNAMIC MASS AND DAMPING		101
IV.1.	Summary	101
IV.2.	Theoretical concepts	101
	2a. General aspects of hydrodynamic mass and damping	101
	2b. The added mass in stagnant water	106
	2c. The added mass in flowing water	112
	2d. Water damping in stagnant and flowing water	115
IV.3.	Computation methods and examples of computation	119
	3a. The added mass	119
	3b. The wave radiation	123
	3c. The damping by flow	125
IV.4.	Summary of determinative parameters	134
	4a. The added mass	134
	4b. The water damping	137

Contents

CHAPTER V THE RESPONSE OF GATES TO EXCITATION BY TURBULENCE PRESSURES	141
V.1. Summary	141
V.2. Introduction	141
V.3. Hydrodynamic excitation	142
V.4. Passive response of a single oscillator to random excitation	145
V.5. Parameters which determine the response of an oscillator in fluid flow	147
V.6. Measurement results in gate models of the single oscillator type	151
V.7. Discussion on the behaviour of continuously elastic gates	153
V.8. The relation between structure response and fatigue of materials	154
CHAPTER VI THE USE OF PHYSICAL MODELS IN VIBRATION RESEARCH	157
VI.1. Summary	157
VI.2. Introduction	157
VI.3. Types of physical models for vibration research	159
VI.4. Air models for gate research	163
VI.5. The reliability of models	164
APPENDIX A INSTABILITY OF A VERTICAL WATER-CURTAIN CLOSING AN AIR-CHAMBER	167
Summary	167
Introduction	167
A. Theoretical study	168
B. Experimental study	169
Conclusion	173
Appendix I, Calculation of the momentary curtain shape due to a harmonic pressure variation	174
Appendix II, Cushion rigidity and damping, related to harmonic oscillation	176
Figures	179

Contents

APPENDIX B ANALYSIS OF VIBRATION AND DAMPING MEASUREMENTS ON A REVERSED TAINTOR VALVE	183
Summary	183
Introduction	183
Choice of dimensionless parameters	185
Representative amplitude	187
Analysis of the water damping	187
The model	189
Results of measurements with a valve opening $d/D = 0.3$	192
Conclusions	198
APPENDIX C MODELS WITH ELASTIC SIMILARITY FOR THE INVESTIGATION OF HYDRAULIC STRUCTURES	201
Hydraulic reproduction laws	202
Elastic properties of models	205
Combination for flow without free liquid surface	206
Combination for flow with free liquid surface	207
Model research and verification measurements on the Hagestein visor gates	209
Further application of elastic similarity models	211
Figures	212
REFERENCES	217
ABSTRACT	225
SAMENVATTING (DUTCH ABSTRACT)	225

List of symbols

a	arm of lift force	m
a	wave amplitude	m
A_0, A_1, A_2	factors	
A_c	culvert cross-sectional area	m^2
A_g	effective gap area (Fig. II. 1 and II. 6)	m^2
A_{g0}	initial gap area	m^2
A'_g	variation of gap area due to vibration	m^2
b	width of valve lip or gate lip	m
B	valve lip or gate lip area	m^2
c	wave celerity (propagation velocity)	ms^{-1}
c	damping factor	$kg s^{-1}$
c_e	excitation coefficient	
c_F	force coefficient	
c'_F	dynamic force coefficient	
c_i	inertia coefficient	
c_k	rigidity coefficient $\{k A_{g0} / \rho A_c^2 g \Delta H_o (dA_g / dy)\}$	
c_L	length coefficient (effective culvert length = $L + c_L A_c / L_c$)	
c_{Ld}	length coefficient at downstream side	
c_{Lu}	length coefficient at upstream side	
c_m	mass coefficient = $m / \rho A_c L$	
c_p	pressure coefficient	
c'_p	dynamic pressure coefficient	
c_{rd}	radiation coefficient at downstream side	
c_{ru}	radiation coefficient at upstream side	
c_s	suction coefficient	
c_{se}	self-excitation coefficient	
c_w	damping factor due to water	$kg s^{-1}$
c_ϕ	lift coefficient per unit of angle	rad^{-1}

List of symbols

$C_{I_g}, C_{II_g}, C_{I_w}, C_{II_w}$	influence factors	
C_{air}	compressibility of air	$\text{kgm}^{-1} \text{s}^{-2}$
C_D	drag coefficient	
D	drag force	kgms^{-2}
E_1	power radiated by waves per unit width	kgms^{-3}
E_2	power transferred by the gate into the water per unit width	kgms^{-3}
f	frequency	s^{-1}
f_n	natural frequency (or eigen-frequency) (cycl. s^{-1})	s^{-1}
F	(external) hydrodynamic force	kgms^{-2}
F'	force variation due to vibration	kgms^{-2}
F_D	drag force	kgms^{-2}
F_s	static force	kgms^{-2}
F_{qs}	quasi-static force	kgms^{-2}
F_d	dynamic force	kgms^{-2}
F_{max}	maximum (internal) force	kgms^{-2}
F_w	hydrodynamic force	kgms^{-2}
Fr	Froude number (V/\sqrt{gL})	
g	acceleration of gravity	ms^{-2}
h	water depth	m
h_c	culvert height	m
h_d	water depth downstream of gate	m
h_u	water depth upstream of gate	m
H	pressure head (= $p/\rho g$)	m
I_p	polar moment of inertia	kgm^2
k	spring rigidity	kgms^{-2}
k_{hc}	hydrodynamic counter-rigidity (force variation/displacement)	kgms^{-2}
k_p	polar spring rigidity	$\text{kgm}^2 \text{s}^{-2}$
L	lift force	kgms^{-2}
L	culvert length	m
L	length representative of flow pattern	m
L'	imaginary additional culvert length	m
L_c	circumferential length	m
m	mass of structure	kg
m_w	added water mass	kg
M	rotative moment	$\text{kgm}^2 \text{s}^{-2}$

List of symbols

n	integer	
n	co-ordinate perpendicular to surface	m
n_L	scale factor of model related to length	} etc.
n_V	scale factor of model related to viscosity	
p	e^{pt} is a measure of self-amplification	s^{-1}
p	pressure	$kgm^{-1} s^{-2}$
p'	dynamic pressure	$kgm^{-1} s^{-2}$
p_n	pressure related to the n^{th} Fourier component	$kgm^{-1} s^{-2}$
q_n	discharge of the n^{th} source	$m^3 s^{-1}$
Q	discharge	$m^3 s^{-1}$
Q_0	initial discharge	$m^3 s^{-1}$
Q'	discharge variation due to vibration	$m^3 s^{-1}$
$\dot{Q}' = \ddot{Q}$	discharge variation per unit of time	$m^3 s^{-2}$
r	radius (at the seal) of cylinder valve	m
R	hydraulic radius	m
Re	Reynolds number (VL/v)	
s	complex number determining damped free vibration ($y = Ye^{st}$)	s^{-1}
S	reduced frequency ($f\delta/\sqrt{2g\Delta H}$ or fL/V)	
S_n	reduced natural frequency = $f_n L/V$	
Strouhal number: S related to dominant excitation frequency		
t	time	s
T	wave period	s
u	velocity component in x direction	ms^{-1}
u'	variation of u due to vibration	ms^{-1}
U_0	reference velocity	ms^{-1}
v	water velocity	ms^{-1}
v	velocity component in y direction	ms^{-1}
v'	variation of v due to vibration	ms^{-1}
$v'_{v'}$	water velocity variation relative to the vibrating gate	ms^{-1}
v_g	velocity of gate vibration	ms^{-1}
V	reference velocity	ms^{-1}
V_0	amplitude of velocity fluctuation	ms^{-1}
V_1, V_2 etc.	velocities related to Fourier components	ms^{-1}
w	culvert width	m
w	velocity component in z direction	ms^{-1}

List of symbols

w'	variation of w due to vibration	ms^{-1}
$W(f)$	power density spectrum as function of f (= frequency)	
$W(S)$	power density spectrum as function of S	
$W_P(f)$	power density of pressure fluctuation	$\left\{ \begin{array}{l} kg^2 m^{-2} s^{-3} \\ kg^2 m^{-2} s^{-4} \end{array} \right.$
$W_P(S)$		
$W_F(f)$	power density of force fluctuation	$\left\{ \begin{array}{l} kg^2 m^2 s^{-3} \\ kg^2 m^2 s^{-4} \end{array} \right.$
$W_F(S)$		
x	distance	m
x, y and z	co-ordinates	m
y	displacement due to vibration	m
$\dot{y} = dy/dt$		ms^{-1}
$\ddot{y} = d^2y/dt^2$		ms^{-2}
$\dddot{y} = d^3y/dt^3$		ms^{-3}
Y_o	vibration amplitude	m
z	vertical displacement due to vibration	m
$\alpha, \beta, \gamma, \epsilon$	coefficients	
γ	relative damping (damping/critical damping, or $c/2\sqrt{km}$)	
δ	opening under gate, or gap width	m
δ_o	initial value of δ	m
ΔH	head difference across valve or gate	m
ΔH_o	initial head difference	m
$\Delta H'$	additional head difference due to vibration	m
$\dot{\Delta H}' = d(\Delta H')/dt$		ms^{-1}
ΔH_m	additional head difference due to inertia of water	m
ΔH_d	head difference due to vibration, downstream effect	m
ΔH_u	head difference due to vibration, upstream effect	m
ϵ	ratio of band width of frequency and f_n	
θ	coefficient related to the force	
λ	wave length	m
λ_n	wave length of n^{th} Fourier component	m
μ	discharge coefficient	
μ	viscosity	$kgm^{-1} s^{-1}$

Glossary

ν	kinematic viscosity (μ/ρ)	$m^2 s^{-1}$
ρ	density of water	kgm^{-3}
ρ_{air}	density of air	kgm^{-3}
σ	surface tension	$kg s^{-2}$
τ	shear tension	$kgm^{-1} s^{-2}$
ϕ	phase angle	rad
ϕ	wing angle	rad
ϕ_0	amplitude of rotation	rad
ϕ	velocity potential	$m^2 s^{-1}$
Φ	dimensionless power spectral density of a unified spectrum	
Φ_F	dimensionless power spectral density of force	
Φ_P	dimensionless power spectral density of pressure	
ω	angular velocity of vibration	rad s^{-1}
ω_n	natural (or eigen-) angular velocity of vibration	rad s^{-1}
::	sign for proportionality	
*	sign for multiplication	
$\overline{y^2}$ etc;	—refers to the time-averaged value = $\lim_{T \rightarrow \infty} \frac{1}{T} \int_0^T () dt$	
(IV. 22)	equation 22 of Chapter IV	
[]	refers to reference list	

GLOSSARY OF LESS COMMON EXPRESSIONS

<i>Active Response</i>	- A movement with increasing amplitude, caused by an initial disturbance
<i>Added Mass</i>	- Expression indicating that a part of the fluid forces is proportional to the vibrational acceleration, with the result that natural frequencies drop and vibration modes change (other expressions: hydrodynamic mass, virtual mass)
<i>Cauchy Number</i>	- Dimensionless number for the spring rigidity k ; k is divided by the hydrodynamic reference force $\rho V^2 L^2$ per unit length L : $Ca = k/\rho V^2 L$
<i>Cavitation</i>	- Boiling of liquid at normal ambient temperature, caused by low pressure (often locally and momentarily only) resulting from flow conditions
<i>Divergence</i>	- Instability caused by permanent flow forces; an initial disturbance inducing an extra flow force greater than the restoring spring force

Glossary

- Drag Force* - Component of the flow force in the direction contrary to the main velocity
- Dynamic Force* - Part of the fluctuating forces with frequencies at and near to the resonance frequency of a structure
- Eigen-frequency* - Frequency belonging to an eigen-vibration (other expression: natural frequency)
- Eigen-load* - Load distribution which causes deflections equal to the ones belonging to an eigen-vibration
- Eigen-vibration* - Vibration of an undamped system with more than one degree of freedom in which a complete equilibrium exists between acceleration forces of the masses and the rigidity forces; to each eigen-vibration belongs one vibration mode (eigen-mode) and one frequency (eigen-frequency). Each system has a number of eigen-vibrations equal to the number of degrees of freedom
- Fluid Resonance* - A mechanism in the flow which causes the excitation forces to be purely harmonic
- Flutter* - Unstable flow-induced vibrations of wings, propellor blades, bridges etc.; generally, a coupling by the flow of two degrees of freedom is involved
- Forced Vibration* - Vibration at which the structure reacts passively to the flow forces, without inducing additional flow excitation
- Free Oscillation* - Vibratory movement without external excitation, caused by an initial disturbance
- Froude Number* - Dimensionless number representing the relation between fluid pressures due to flow (ρV^2) and to gravity (ρgh) : $Fr = V^2/gh$
- Galloping* - Self-excited vibrations of bodies in flow (see Chapter I, par. 4)
- Hydrodynamic Damping* - Expression indicating that a part of the fluid forces are related to the vibration velocities and operative in opposite direction
- Hydrodynamic Counter-rigidity* - Expression introduced to explain that at a sudden gate displacement (at which the flow initially remains constant) forces are operative in the direction of and proportional to this displacement
- Hydrodynamic Rigidity* - Expression indicating that a part of the fluid force counteracts the displacement of a vibratory movement
- Internal Force* - Force in the spring of a single oscillator

Glossary

- Lift Force* - Component of the flow force perpendicular to the direction of the main velocity
- Mechanical Damper* - Any damping element which is not related to the fluid flow; included are friction effects, structural damping, hydraulic shock absorbers, etc.
- Mechanical Damping* - The damping value of mech. dampers expressed in terms of linear damping
- Natural Frequency* - See: Eigen-frequency
- Natural Load* - See: Eigen-load
- Negative Damping* - Expression indicating that an unstable vibration can be described by equation (I. 3) when a negative value is introduced for the damping value c
- Power Density Spectrum* - See foot-note Chapter V, par. 3
- Quasi-Static Force* - Fluctuating force with frequencies far below the lowest eigen-frequency of a structure
- Random Excitation* - Forces which are irregular in time and place
- Reduced Frequency* - Dimensionless number for excitation frequencies (f); multiplying the frequency with the ratio of a representative length L and the flow velocity V ; $S = fL/V$. See also: Strouhal number
- Reduced Natural Frequency* - Dimensionless number for the natural frequency (f_n), resulting in $S_n = f_n L/V$
- Relative Damping* - Ratio damping/critical damping, in which the critical damping is the value at which an initial motion no longer becomes an oscillation
- Resonance Frequency* - The frequency at which the frequency response graph of a damped structure shows a maximum (without damping, the resonance frequency equals the natural frequency)
- Reversed Taintor Valve* - Valve having a sector gate with horizontal axis, placed in a rectangular culvert (fig. II. 3) and with the flow directed to the concave side
- Taintor Gate* - Sector gate with horizontal axis with the flow directed to the (smooth) convex side
- Reynolds Number* - Dimensionless number expressing the relation between the dynamic pressure (ρV^2) and the viscous shear stress in flows ($\mu \partial V / \partial n$ or $\mu V/L$). $Re = VL\rho/\mu$
- Self-Controlling Vibration* - Vibration with such amplitude and frequency that the excitation forces of turbulence and eddies synchronize over the length of the structure, resulting in an increase of excitation

Glossary

- Self-Exciting Vibrations* - Unstable vibrations which, after an initial disturbance, are self-amplifying due to flow forces
- Single Oscillator* - Single-mass spring system, (damped or undamped) with one degree of freedom
- Stable Vibrations* - Free vibrations which have, after an initial disturbance, a decreasing amplitude
- Stationary Vibration* - A harmonic oscillation, with constant amplitude and frequency
- Strouhal Number* - Dimensionless number for the dominant frequency of a force spectrum $S = fL/V$
- Sub-Critical Flow* - Expression used for cylinders in flow with unstable flow separation. At sub-critical Reynolds numbers, the turbulence in the boundary layer is small and the Reynolds number does not influence the Strouhal number and the drag force coefficient
- Super-Critical Flow* - Expression used for cylinders in flow with unstable flow separation. At super-critical Reynolds numbers the boundary layer at the cylinder surface is fully developed at the flow separation point and the Strouhal number and the drag force coefficient tend to become constant
- Thoma Number* - Dimensionless number expressing the relation between the average flow pressure available above the vapour pressure of the liquid ($p - p_v$) and the dynamic flow pressure ($\frac{1}{2}\rho V^2$) at the point where cavitation begins (incipient cavitation): $\sigma_i = (p - p_v) / \frac{1}{2}\rho V^2$
- Unified Power Density Spectrum* - Power density spectrum expressed as a function of non-dimensional parameters, with an area equal to unity
- Unstable Vibrations* - Free vibrations which have, after an initial disturbance, a growing amplitude
- Weber Number* - Dimensionless number expressing the relation between the dynamic flow pressure (ρV^2) and the fluid pressure related to surface tension ($\sigma/\text{curvature}$ or σ/L), or: $We = \rho V^2 L / \sigma$

Chapter I

Introduction

1. SUMMARY

A review is presented of different kinds of dynamic forces and the resulting vibrations, which may occur in bodies in fluid flow. In the hydrodynamic forces related to vibrations, the following elements can be distinguished:

- the hydrodynamic excitation;
- the added mass;
- the hydrodynamic rigidity;
- the hydrodynamic damping; and
- the self-excitation (or negative hydrodynamic damping).

Self-excitation phenomena are illustrated by the mechanisms of galloping, flutter, and the automatically pulsating hydraulic ram.

The vibrations which may occur in gates are classified into:

- forced vibrations, where the structure reacts passively to a dynamic external load;
- self-controlling vibrations, where the vibratory movement is strong enough to synchronize the external load mechanism, resulting in a certain increase of the effective excitation; and
- self-exciting vibrations, where an initial small disturbance produces a mechanism in which the mechanical and hydrodynamic systems are coupled in such a way that the hydrodynamic excitation increases with the vibration amplitude and which leads to an ever-increasing (unstable) vibration, limited finally by non-linear effects.

Design requirements for gates and valves are aimed at the prevention of self-exciting vibrations, the reduction of the rate of self-control, and sufficient structural strength and rigidity to withstand the hydrodynamic load, including the dynamic excitation by turbulence and the vorticity induced by the gate itself.

Chapter I. Introduction

2. DESCRIPTION OF DIFFERENT TYPES OF FLOW-INDUCED VIBRATION

When the dynamic behaviour of a gate or a valve is analyzed, the designer tends to consider the structure as a mechanical system. It is, for instance, considered as a suspended elastic structure with internal damping. If the load of the flowing water is known in the aspects of place, direction and time, there exist all sorts of methods to compute the response of such a mechanical system. (In the following, all factors, apart from the hydrodynamic ones, will be described in "mechanic" terms, also when hydraulic dampers, rubber elasticity and damping, or frictional forces are involved.)

Considering the mechanical system in its simplest appearance, the single, linearly damped oscillator with one degree of freedom, its behaviour follows from the classical equation of motion:

$$m\ddot{y} + c\dot{y} + ky = F(t) \tag{I. 1}$$

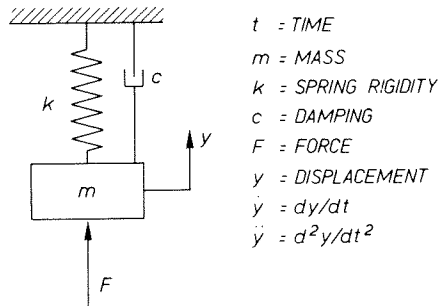


FIG. I. 1

For different load types, solutions for y are known. They are defined as *the passive response of the oscillator*.

a. In response to harmonic excitation ($F \cos \omega t$), the final vibration becomes:

$$y = Y \cos (\omega t - \phi) = \frac{(F/k) \cos (\omega t - \phi)}{\sqrt{(1 - \omega^2/\omega_n^2)^2 + (c^2/km)(\omega^2/\omega_n^2)}} \tag{I. 2}$$

$$\tan \phi = c\omega/(k - m\omega^2)$$

This solution is valid after initial disturbances are damped out.

I. 2 Different types of flow-induced vibration

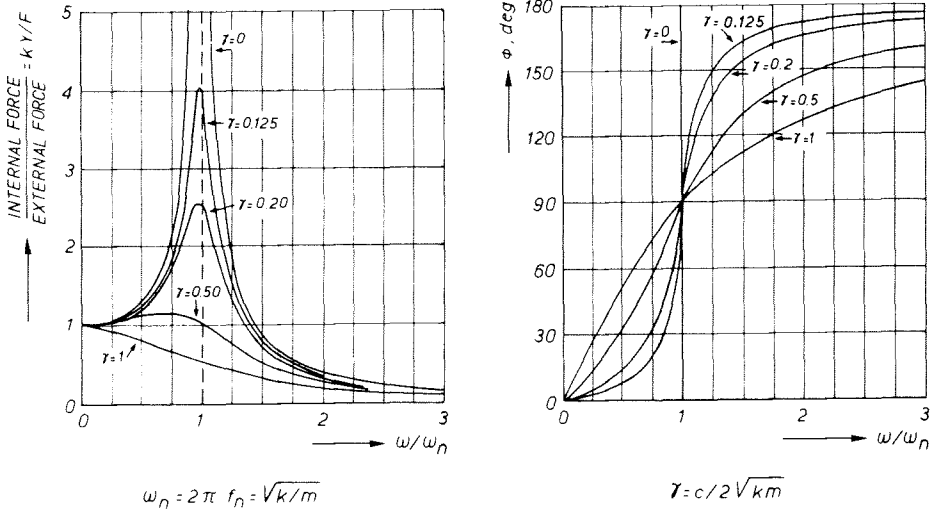


FIG. I. 2

Because each periodic load can be decomposed by Fourier analysis into a number of harmonic loads, the equation (I. 2) is always applicable, on the condition that the damper and spring are linear.

b. Free oscillations.

Free oscillation occurs after an initial disturbance; the basic equation is (I. 1), but now with the external force F equal to zero:

$$m\ddot{y} + c\dot{y} + ky = 0 \quad (\text{I. 3})$$

The solution for y is:

$$y = Y_0 e^{-\gamma \omega_n t} \cos(\sqrt{1 - \gamma^2} \omega_n t + \alpha) \quad (\text{I. 4})$$

wherein: $\omega_n = \sqrt{k/m}$ = natural (or eigen) angular frequency (I. 5)

$$\gamma = c/2\sqrt{km} = \text{relative damping} \quad (\text{I. 6})$$

($c = 2\sqrt{km}$ is the critical damping; if c is still greater, the free movement is no longer an oscillatory one)

$$-\gamma \omega_n = p = -c/2m$$

Chapter I. Introduction

Y_0 and α depend on the conditions present at the moment $t = 0$ when free oscillation starts.

The exponent $(-\gamma \omega_n t)$ determines whether the free oscillation is stable ($\gamma > 0$) or unstable ($\gamma < 0$). In the following, some examples will show that $\gamma < 0$ can occur in structures in flow; this is *the active response of the oscillator*.

c. The response to random excitation with a wide frequency band.

This is relevant to excitation by turbulent water pressures. The statistical properties of these fluctuating pressures in stationary flow are also stationary and can be described as a frequency-distributed power density spectrum^{*}, defined as:

$$W(f), \text{ with } \int_0^{\infty} Wdf = \lim_{T \rightarrow \infty} \frac{1}{T} \int_{t-T}^t (F-\bar{F})^2 d\tau = F'^2 \quad (\text{I. 7})$$

(f = frequency of excitation; F' = dynamic force, which is the standard deviation of the force fluctuation around the mean value \bar{F})

The response of the oscillator to random excitation has been analyzed by Thomson and Barton [97], assuming that the power spectrum is a smooth continuous function and that the oscillator is so lightly damped that the response at and near the natural frequency dominates the response at other frequencies. This results in a response only depending on $W(f_n)$, the power density at the natural frequency. The response is:

$$\overline{y^2} = \pi f_n W(f_n) / 4 k^2 \gamma \quad (\text{I. 8})$$

in which

$$\overline{y^2} = \lim_{T \rightarrow \infty} \frac{1}{T} \int_{t-T}^t y^2 d\tau$$

(y is defined as the dynamic component of the displacement)

^{*} The word power suggests the dimension of F^2 , being energy/time; but it is not. The following definition (Harris and Crede [36], 1961, Volume I, p. I-22) is used: "Power Spectral Density is the limiting mean square value (e.g. of acceleration, velocity, displacement, stress or other random variable) per unit band width, i.e., the limit of the mean square value in a given rectangular band width divided by the band width, as the band width approaches to zero".

I. 2 Different types of flow-induced vibration

When a structure in flow is considered, it appears that the flow force has components proportional to \ddot{y} , to \dot{y} and to y . It can also be said that the flowing fluid affects the mass m , the damping c , and sometimes the rigidity k of the structure; and this effect can be represented by values added to m , c and k . The added values in water, to be introduced as m_w , c_w and k_w will, in general, be dependent on the flow velocity and can moreover depend on the vibration frequency and amplitude of the structure. The excitation force exerted by the water is partly independent of the vibration of the structure, but also partly dependent on the vibration amplitude and frequency. In general equation, (I. 1) can be presented as:

$$(m + m_w) \ddot{y} + (c + c_w) \dot{y} + (k + k_w) y = F_w(t) \quad (\text{I. 9})$$

In this way it is logical to define F_w as the part of the force which is independent of the vibration itself.

Sometimes the motion-dependent force is still analyzed as if it were a right hand term. Petrikat [81], in his analysis of results obtained in gate models, estimated values of m_w and c_w ; the excitation force which remained appeared to be still motion-dependent.

The equation (I. 9) can give information on the stability of a system, if all hydrodynamic forces, which are motion-dependent, are considered to be left-hand terms.

If m_w , c_w and k_w are constants, the reaction to an initial disturbance will be similar to equation (I. 4), and it can be concluded whether the reaction on the disturbance will damp out, or strengthen. The relative damping is:

$$\gamma = \frac{c + c_w}{2 \sqrt{(k + k_w) (m + m_w)}} \quad (\text{I. 10})$$

If $\gamma > 0$ the structure is stable, if $\gamma < 0$ instability occurs.

This analysis will be more complicated if $(m + m_w)$, $(c + c_w)$, and $(k + k_w)$ are dependent on the frequency and amplitude of the vibration. This dependence is caused by the fact that in reality the linear presentation of terms is a simplification.

If the equation of motion shows non-linear terms, with \ddot{y} being replaced by a function $f(\ddot{y})$, \dot{y} by $f'(\dot{y})$ and y by $f''(y)$, solution methods are

Chapter I. Introduction

available which have been developed for the Van de Poll equations; a summary thereof is given by Bavink and Grasman [9]. At the symposium on Flow-Induced Structural Vibrations (1972), Parkinson presented a review of mathematical models [73] aimed to represent the different types of motion-dependent and motion-independent forces on cylindrical bodies. In Chapters II to V, detailed analyses will be given of motion-dependent and motion-independent hydrodynamic forces acting on gates. A short presentation follows in the next paragraphs.

3. ADDED MASS, HYDRODYNAMIC DAMPING, HYDRODYNAMIC RIGIDITY AND HYDRODYNAMIC EXCITATION

The "added mass" m_w :
 m_w has been analyzed by Lamb [54] on p. 76 of his handbook. He considered a two-dimensional strip, vibrating perpendicular to its greatest width and submerged in an infinite body of fluid. The (potential) flow caused by the vibration is fully in phase with the vibration. So, the total kinetic energy at the moment of maximum velocity is a measure of the added water mass, which can be described as an imaginary quantity of water coupled to the strip and following its movement. In reality, however, the flow pattern is infinite, with the vibration amplitude decreasing with increasing distance. The imaginary added water mass of a strip equals the volume of water in a circular cylinder with a diameter equal to the strip width. For vibrating circular or elliptical cylinders, the imaginary added water mass remains the same, i.e. the volume of a circular cylinder with a diameter equal to the transverse dimension of the vibrating cylinder perpendicular to the direction of vibration.

With a free water surface, the vibration of all water particles also remains in phase with the vibration of the structure as long as wave radiation is negligible; for gate vibration this assumption is valid (see Chapter IV). Under these circumstances, a potential flow occurs; the condition at the free water surface is that the potential remains zero during the vibration. In 1933 Westergaart [107] computed the added mass for a barrage, in order to be able to compute the water load at a sudden horizontal movement during an earthquake; he made a simplifying assumption of the flow pattern. Schoemaker [90] calculated the added mass for the horizontal vibration of a gate on a high sill; the computations were confirmed by the experiments of Allersma [7]. Other publications on

I. 3 Added mass, damping, rigidity; hydrodynamic excitation

added mass are from Zienkiewicz and Nath [109] (the use of an electric analogue to solve the potential flow equation), Birkhoff [15] (a resumé of basic assumptions), Gal [31] (the added mass of a sector gate) and Wendel [106] (the added mass of prisms and cylinders in submerged condition with free water surface). When wave radiation is of importance, at relatively low frequencies, m_w tends to decrease.

The water damping c_w :

The c_w factor has not often been discussed as such, but elements of it can be found in the literature. For instance, Biesel [13] analyzed the waves radiated by wave generators. Lamb [43] discussed the energy dissipation through the viscosity of the fluid when the fluid oscillates parallel to the boundary (par. 345 in his handbook). Moreover, the results of the analysis of flutter and galloping, which are two types of unstable or self-exciting vibration, are also applicable when the flow leads to positive damping and stable vibration.

Another element of energy dissipation is found in the drag force, which normally is proportional to the square of velocity. This, now, can be considered in relation to the difference in velocity between the water and the vibrating body. In relation to investigations with elastic models of the weir gates at Hagestein, this concept was proposed in 1959 [45]. The analysis resulted in a linear damping value c_w proportional to the water velocity; see Appendix B, page 188. The concept is used more often now, but at the symposium on flow-induced vibrations in Karlsruhe [43] in 1973, this led to a discussion by Hunt [39] of investigations by King and Prosser [43].

Non-linear elements can interfere with damping; for instance, in stagnant water the drag force leads to a damping proportional to the square of the vibration velocity: $F_{\text{drag}} = C_D * \text{area} * \frac{1}{2} \rho \dot{y} |\dot{y}|$. In such a case, linearization techniques are used, introducing an equivalent linear damping which gives, under steady state vibration conditions, equal energy dissipation over one period (Appendix B, page 188). In the next paragraph the occurrence of negative c_w values will be discussed.

The hydrodynamic rigidity, k_w :

A part of k_w follows from variation of buoyancy when vibration has a vertical component. For common gate designs, even when buoyancy boxes are used, k_w appears to be of minor importance. For most cases, such boxes are completely submerged to obtain a weight compensation indepen-

Chapter I. Introduction

dent of the water level and gate position; in this case k_w will be zero. If a gate is only supported by its buoyancy boxes, which have an immersion depth D , its resonance frequency will be $f_n = \frac{1}{2\pi} \sqrt{g/D}$. When $D = 1$ m, f_n will be 0,5 cycles/sec., which is low compared with any conceivable frequency of a gate; this shows that the hydrodynamic rigidity is small compared with the suspension rigidity.

A rigidity factor caused by flow is the vane effect, this is one of the elements which play a role in wing flutter calculations. In the example of Fig. I. 4, this rigidity becomes negative because F acts upstream of the axis of rotation.

k_w forces counteract the m_w forces. When determined by experiments, the two are sometimes expressed together in a resultant m_w , which then will depend on the vibration frequency.

The hydrodynamic excitation, F_w :

In the following, only motion-independent forces are considered. In a steady flow, the excitation forces F_w acting on a body show frequencies proportional to the velocity of the oncoming flow and inversely proportional to the reference diameter of the body. This important discovery was made by Strouhal in 1878 for telephone wires whistling in the wind and was used later to generalize that, for any body, the dominant frequency of excitation f is proportional to V (velocity) and L^{-1} (L = reference length).

$$\frac{fL}{V} = S \text{ (geometry)} \quad (\text{I. 11})$$

fL/V is the so-called Strouhal number

The geometry referred to is related both to body shape and to flow pattern. For the excitation of valves, (I. 11) is directly applicable; for gates this is not always the case, because velocity variations are related to changes of the free water surface level which can result in an essential change of the flow geometry.

Excitation force amplitudes can be expressed in terms of $c_e \rho V^2 \times$ area, in the same way as for stationary hydrodynamic forces. Viscosity effects of the fluid are expressed in the Reynolds number (the influence of which is weak under conditions encountered for gates):

I. 3 Added mass, damping, rigidity; hydrodynamic excitation

$$\frac{\text{Force}}{\rho L^2 V^2} = f \text{ (geometry, Reynolds number)} \quad (\text{I. 12})$$

(f means: function of)

Strouhal numbers for differently shaped cylinders and steel profiles are presented in [17], [88] and [107] as functions of the Reynolds number; while for slide valves, butterfly valves and sector valves, Abelev presented the dominant Strouhal numbers of the hydrodynamic excitation forces in [1], [2] and [3].

In reality, a non-vibrating body will, except for the case of circular or elliptical cylinders (and this only in a limited range of Reynolds numbers), seldom be excited at one single frequency; and then the excitation has to be described in terms of a power density spectrum as introduced on page 4.

Fung [30] made use of the property that the spectral density can be described as:

$$\int_0^{\infty} W df = \text{force}^2 \text{ (wherein force}^2 \text{ is a value averaged over time)}$$

Now introducing the force = $c_F (\frac{1}{2}\rho V^2 * \text{area})$ and presenting f in a non-dimensional way as $fL/V = S$, in a similar way as has been done in equation (I. 11), he derived the following expression for the response of a single oscillator:

$$\overline{y^2} = \frac{1}{T} \int_0^{\infty} y^2 dt = (c_F \frac{1}{2} \rho V^2 * \text{area})^2 \frac{L}{V} \frac{1}{8m^2 \omega_n^3 \gamma} \phi(S_n) \quad (\text{I. 13})$$

The symbols are those of Fig. I. 1 and I. 2.

$\phi(S)$ is the non-dimensional unified power density spectrum, which is a function of S and depends on the flow geometry and the Reynolds number only. S_n is the value of S at the resonance frequency f_n and is equal to $f_n L/V$. This topic will be further analysed in Chapter V.

For gates this approach was first applied to the analysis of measurements made in models of the Hagestein weir [46], but in Appendix B a simplified expression has been introduced to present the passive response to excitation by turbulence.

Chapter I. Introduction

Experimental evidence showed that the simplified expression is valid and did indeed depend only on the flow geometry (the Reynolds number having negligible effect).

4. SELF-EXCITATION OR NEGATIVE HYDRODYNAMIC DAMPING

As can be seen in equation (I. 10), an unstable vibration occurs when the total damping of a structure plus ambient water ($c + c_w$) becomes negative.

In Fig. I. 1 the damping force acting on the mass is negative in relation to the \dot{y} direction, and proportional to \dot{y} . If the total damping is $(c + c_w) < 0$, the force F will act in the direction of the vibration velocity and continuously transfer energy from the flow to the vibrating body. The solution of equation (I. 3) for free oscillation of linearly damped systems is given by equation (I. 4), which for $\gamma < 0$ gives a vibration of which the amplitude Y will grow continuously with:

$$\left. \begin{aligned} \text{in which} \quad Y &= e^{-\gamma \omega_n t} = e^{pt} \\ p &= -(c + c_w)/2(m + m_w) \end{aligned} \right\} \quad \text{(I. 14)}$$

Thus, the amplitude would grow infinitely. In practice, however, amplitudes are physically limited, mechanically or by c_w becoming a function of the vibration amplitude.

An example of self-exciting vibration of a body in fluid flow has been found by Den Hartog and described in his handbook [27] p. 302/303. It concerns non-circular wires, the fluid forces on which follow from the stationary equations of lift and drag. The phenomenon of self-excitation, which can occur in a body having one degree of freedom, is known as *galloping*.

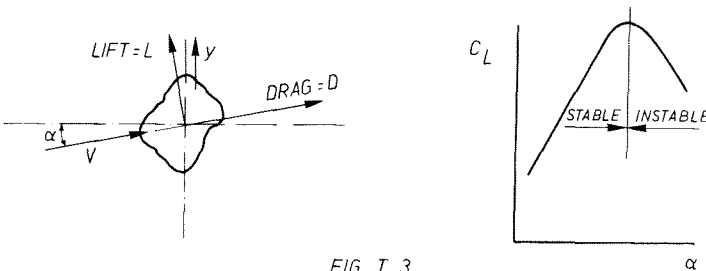


FIG. I. 3

I. 4 Self-excitation

A vibration with one degree of freedom, in y direction, is now considered. The force in y direction per unit length, due to the flow velocity V, equals:

$$F_y = L \cos \alpha + D \sin \alpha = \frac{1}{2} \rho V^2 D (C_L \cos \alpha + C_D \sin \alpha) \quad (\text{I. 15})$$

The vibration causes the flow velocity relative to the body to decrease by $\dot{y} \sin \alpha$, while the angle of incidence α decreases by $(\dot{y}/V) \cos \alpha$. All equations can be linearized, assuming $|\dot{y}| \ll V$.

The extra force related to the vibration becomes:

$$F_y' = - (\partial F_y / \partial \alpha) (\dot{y}/V) \cos \alpha - (\partial F_y / \partial V) \dot{y} \sin \alpha$$

This results in:

$$F_y' = \frac{1}{2} \rho V D \dot{y} \left\{ - C_D (1 + \sin^2 \alpha) - \sin \alpha \left(\frac{\partial C_D}{\partial \alpha} \cos \alpha + C_L \cos \alpha \right) - \frac{\partial C_L}{\partial \alpha} \cos^2 \alpha \right\} \quad (\text{I. 16})$$

The structure becomes unstable when the extra force F_y' is in phase with the vibration velocity, that is when:

$$\partial F_y' / \partial \dot{y} = F_y' / \dot{y} > 0 \quad (\text{I. 17})$$

In practice this happens when α is small; the criterion for stability then becomes:

$$\partial C_L / \partial \alpha + C_D < 0 \quad (\text{I. 18})$$

A first indication of the possibility of galloping is that $\partial C_L / \partial \alpha < 0$ (Fig. I. 3); this can occur in profiles where, when the angle of incidence α decreases, the flow gets attached over a greater area at the upper side.

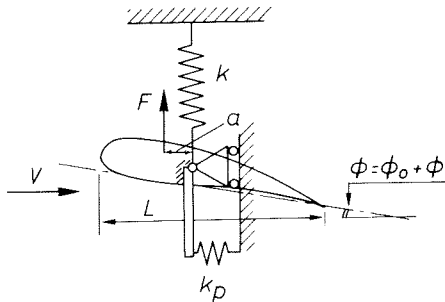
The values of C_L and C_D , which are functions of α , can be determined experimentally under constant flow conditions, but application of the results in the computation of non-stationary cases is only reliable for low-frequency vibrations.

Another type of self-exciting vibrations are the *flutter vibrations* of wings. Negative damping occurs in transsonic flow; but when two or more degrees of freedom are involved, damping can also become negative in

Chapter I. Introduction

subsonic flow due to the coupling of the different vibrations. A survey of literature on flutter is presented by Ashley [8].

The phenomenon will be demonstrated by the simplified case of a wing which is suspended at its centre of gravity. This point can move in vertical sense, while the wing also can rotate around this point.



- k = RIGIDITY (VERTICAL)
- k_p = POLAR RIGIDITY
- m = MASS
- I_p = POLAR MOMENT OF INERTIA
- F = LIFT FORCE
- V = WIND VELOCITY
- L = PROFILE LENGTH
- ϕ = WING ANGLE
- $M = \alpha F$ = MOMENT OF FORCE

FIG. I.4

The equations for the fluid forces are presented in a general form, including all possible coupling terms. When the vibration velocities are small compared with the flow velocity, only linear terms need to be considered. This is a correct assumption when only beginning vibrations are studied.

Displacement:

$$m\ddot{y} + ky = L_y y + L_{\dot{y}} \dot{y} + L_{\ddot{y}} \ddot{y} + L_{\phi} \phi + L_{\dot{\phi}} \dot{\phi} + L_{\ddot{\phi}} \ddot{\phi} \quad (I. 19)$$

Rotation:

$$I_p \ddot{\phi} + k_p \phi = M_{\phi} \phi + M_{\dot{\phi}} \dot{\phi} + M_{\ddot{\phi}} \ddot{\phi} + M_y y + M_{\dot{y}} \dot{y} + M_{\ddot{y}} \ddot{y} \quad (I. 20)$$

All terms with L and M depend on the flow velocity and follow from theory or experiment.

Equations (I. 19 and 20) can be solved by introducing the following expressions for the freely oscillating coupled wing motion:

$$\left. \begin{aligned} y &= Y_0 e^{st} \\ \phi &= \phi_0 e^{st} \end{aligned} \right\} \quad (I. 21)$$

I. 4 Self-excitation

(Y_0 is real, ϕ_c and $s = p + iq$ are complex)

After elimination of Y_0 and ϕ_0 , the solution of s for each velocity \bar{v} can be found.

s is a complex number ($p + iq$), and any solution wherein $p > 0$ indicates that the vibration is incremental or unstable.

s has to be found from an equation of the following type:

$$s^4 + A_3s^3 + A_2s^2 + A_1s + A_0 = 0 \quad (\text{I. 22})$$

The stability or instability of vibrations obeying such equations have been analyzed by Routh and Hurwitz, a short summary of which can be found in Den Hartog's handbook on Mechanical Vibrations [27] p. 311 for the third degree equation. Solutions for higher degree equations can be found in the paper of Sherman et al. [94].

A special kind of instability can occur when $\omega = 0$. This is the static instability or *divergence*, which occurs when a change of the wing angle ϕ causes the flow to induce an extra rotative moment which is greater than the restoring moment due to the polar rigidity. This is the case when

$$\frac{\partial(aF)}{\partial\phi} > k_p \quad (\text{I. 23})$$

Analysis of the flutter equations has become possible after Theodorsen [96] derived, in 1935, the lift and moment factors L and M for a thin airfoil, using potential flow calculations.

The solution method described above has two major disadvantages:

- the L and M factors depend in reality on the vibration frequency, the value of which follows from the solution of the equations; this implies an iterative procedure. Experimentally found values of the coefficients L and M are published by Bergh [11].
- the L and M factors are only known for harmonic vibrations and can be different for incremental or decremental vibrations.

To overcome these disadvantages, another procedure has been developed, assuming that steady state vibrations are obtained by application of (imaginary) mechanical dampers, for translation as well as for rotation.

Chapter I. Introduction

The values of the damping factors, c and c_p , needed to obtain a steady state vibration, are then computed.

The basic equations (I. 19) and (I. 20) are thus transformed into:

$$\text{Displacement:} \quad m\ddot{y} + c\dot{y} + ky = L_y y + \dots \text{ etc.} \quad (\text{I. 24})$$

$$\text{Rotation} \quad : \quad I_p \ddot{\phi} + c_p \dot{\phi} + k_p \phi = M_\phi \phi + \dots \text{ etc.} \quad (\text{I. 25})$$

The solutions for harmonic vibration are now:

$$y = Y_o e^{i\omega t} \quad \text{and} \quad \phi = \phi_o e^{i\omega t} \quad (\text{I. 26})$$

(Y_o and ω real, ϕ_o complex).

Now ω is introduced as a known quantity, by which all L and M factors become fully determined.

After elimination of Y_o and ϕ_o one complex equation remains, of which the real and the imaginary part give two conditions from which c and c_p can be solved. This calculation has to be done for a whole series of ω values. In the ω range where c and c_p both are positive and greater than the real available mechanical damping factors, the deficit (or non-available) damping will in reality cause an incremental or unstable vibration. At which ω value the unstable vibration will really occur, follows from the condition that the coupled torsion and translation vibrations need to have the same increment.

Also for flutter vibrations, initial disturbances will continuously increase in amplitude until the coefficients will change or the structure will collapse. For a safe design, instabilities should not occur, not even at smaller amplitudes.

Since the accident with the Tacoma bridge, flutter analysis has been introduced in the civil engineering world [101], [87]. The wind load coefficients are determined in wind tunnel tests.

The last type of unstable vibration to be mentioned is the instability due to *buffeting*. This instability is related to an instability of the separation point between attached flow and flow separation. The important variation of the flow forces is partly independent of and partly dependent on the vibration itself. The phenomenon is mainly related to particular airplane manoeuvres, during which the incident flow

I. 5 Structures in water and air

angle (or wing tilt) becomes very great.

5. STRUCTURES IN WATER AND AIR

Because self-excited vibrations have been much more studied for structures in air than for structures in water, an attempt is made to judge in how far similar or different phenomena are to be expected for structures in air and in water.

Differences are due to difference in the type of structure, difference in circumstances (velocity range of the flow) and difference in the relation between the mass of the structure and the added mass of the fluid. Some points must be mentioned:

- a. A first difference is that resonance frequencies become considerably lower in water, due to the added water mass.
- b. Valves and gates are different from wings and other bodies in air flow, because they are meant to regulate the flow in a pipe or a canal. This means that some of the gate and valve vibrations directly cause flow obstruction variations, which result in head difference variations across the structure.
- c. Similar wing structures in water and in air (or similar valves in water and in air) will have different reduced natural frequencies ($S_n = f_n L/V$), due to the fact that in water the velocity V has to be reduced by $\sqrt{\rho_w/\rho_{air}}$ to obtain the same load (which is proportional to $\frac{1}{2}\rho V^2 L^2$). Although the resonance frequency f_n in water will also be lower due to the added water mass, this reduction is smaller than the reduction of V . The structure in water will have a greater value of S_n .
- d. In addition to the increase of S_n for structures in water, the ratio of the forces due to damping or self-excitation to forces due to permanent flow will increase for equal vibration amplitudes. Damping forces and self-excitation forces appear to be mainly proportional to $\rho V \dot{y} L^2$ (see Chapter II and IV), as has also been found for galloping in equation (I. 16). Their relation to the permanent-flow forces, proportional to $\rho V^2 L^2$ remains unchanged when \dot{y} and V are proportionally reduced. As S_n is greater in water, the ratio of the vibrational velocity with amplitude $2\pi f_n Y_0$ to the flow velocity V will, for equal Y_0 values, be greater in water than in air.
- e. It is still a matter of discussion whether wings in air and in water are

equally well described by the computations of the type Theodorsen has made.

Abrahamson [6] stated that the results of flutter experiments on hydrofoils compare unfavourably with theory, whereas in air some safety still exists for the whole range of S_n values. Theoretically, there is no reason for this discrepancy.

- f. Free surface conditions of water are different from any boundary condition in air flow.

An example of the importance of point b in vibration problems of gates, is given by the mechanism of the hydraulic ram. This is a high-head pump which transfers the energy of a great low-head flow to a small high-head discharge. A complete description of the workings of the ram is presented in [86].

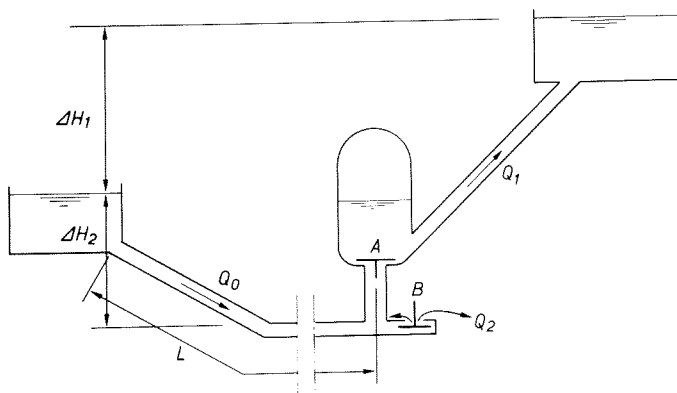


FIG. I.5

During constant flow conditions, one-way valve A would be closed, because of the head difference ΔH . One-way valve B is closed by the dynamic head, whose force is greater than the weight of the valve member (which even can be partly compensated by a spring). In this system constant flow cannot occur, and an intermittent one will occur when valve B has been opened a first time.

When valve B is opened at a discharge of zero, the head difference across B will disappear and the whole head ΔH_2 in the feed pipe is used for the acceleration of water therein. The increasing discharge exercises an increasing force in closing direction on valve B and before an equilibrium discharge is reached, valve B closes.

I. 6 Gate and valve vibrations

This leads to a high pressure at the valves A and B (water hammer) and, due to the pipe flow inertia, the flow Q will (as far as the compressibility of water can be neglected) not change abruptly. Consequently, relief valve A will open to let the flow escape through the lift pipe the moment valve B closes. The water flows into the accumulator and to the upper reservoir. During a certain time, the discharge head ΔH_1 plus the weight of valve A will cause a deceleration of the pipe flow and, when $Q_0 = 0$, valve A will close. This closing causes a piston effect by which Q_0 becomes negative during a short moment. Because A is closed, this negative Q_0 cannot change abruptly and water has to be taken in through valve B, which opens. The cycle recommences. The function of the accumulator is to prevent extremely high pressures, which could occur at the sudden inflow at valve A.

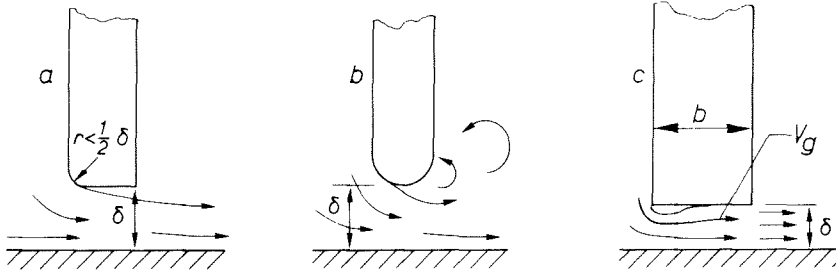
In computations of unstable vibrations of gates and valves, the inertia of the water plays a dominant role. Mechanisms similar to that of the hydraulic ram can explain most of these vibrations. Such vibrations are analyzed in Chapter II.

6. GATE AND VALVE VIBRATIONS

Research on gates and valves, relating to unstable vibrations and excitation by flow, is mainly applied model research, aimed to develop shapes which are least sensitive to vibration and to determine dominant flow-induced excitation frequencies.

Regarding to shape, the main conclusion is that separation of flow at the gate edges must be stable. Rounded edges are only acceptable at the upstream side, and then only when the radius of curvature is not too small, so that no separation can occur at the curvature. When rectangular seals are used, at small gate openings reattachment of flow can also give rise to instabilities. These instability phenomena are comparable with the phenomenon of buffeting.

The first research on the shape of seals was published by Müller in 1933 [60]; later a great number of publications followed, of which especially those of Petrikat [78 and 81] and Krummet [53] have to be mentioned. They come to the conclusion that the flow must remain fully attached until the end of the edge is reached.



INSTABILITIES AT GATE EDGES
 a AND b: SEPARATION AT A CURVATURE
 c: UNSTABLE REATTACHMENT

FIG. I.6

Whenever possible, sharp edges should be applied in order to reduce the area upon which pressure pulsations, related to instabilities of flow separation and/or reattachment, can act. On this point a compromise is necessary because of strength requirements and often because watertightness in closed position of the gate is wanted; this leads to the application of rubber seals. Vibration behaviour of rubber seals in relation to their deformability has been presented by Lyssenko and Chepajkin [57]. Solutions for rubber seals in relatively sharp edges are proposed by Petrikat [81] and Schmidgall [89], but both come to the conclusion that a thin rubber strip does not automatically lead to a safe design for all circumstances.

Sometimes gates are used without any special seal: a retaining plate, with stiffening girders at the downstream side, protrudes under the last girder and the plate edge is sharpened. This solution is presented by Schmidgall [89], Murphy [62] and Petrikat [81]. To reduce the leakage in closed position, rubber or lead can be embedded in the culvert bottom [81].

An effective means of reducing the danger of vibration is to keep the girders in air; this is applicable to Taintor and sector gates on spillway crests and at outlet culverts of high-head dams. The smooth retaining plate is at the upstream side. The supercritical jet flow under the gate has to flow away down a slope or in free air, so that no hydraulic jump can occur near the gate or the valve. The lower edge should be as sharp as possible; however, the seal shape should be well designed, as it was with such an edge that Schmidgall [89] found heavy vibrations in

1. 6 Gate and valve vibrations

his original design. A review of design criteria in relation to gate vibrations is included in literature survey presented in the handbook of Wickert and Schmauszer [108].

Research on dominant excitation frequencies led to the determination of the necessary resonance frequencies to prevent resonance phenomena ($\omega/\omega_n \sim 1$ in Fig. I. 2). This leads to certain rigidity demands. In the same way as for bodies in flow (equation (I. 11)) for gate excitation at the seals also a dominant excitation frequency is determined by means of the value of the Strouhal number $S = f b/V$ or $S = f \delta/V$ (f = excitation frequency, δ = gap height, b = seal width as shown in Fig. I. 6c, V = average velocity in the gap).

There is a single relation between S and the configuration relation b/δ Naudascher [64 and 69] presented the results of several investigations on rectangular seals and other configurations. For the seals, it was found that $S = f \delta/V$ varies between 0.2 (for $\delta/b = 0.25$) and 0.32 (for $\delta/b = 0.55$). In [67] he showed the general trend, for various structures, of the vibration amplitude being a function of f/f_n (f = excitation frequency, f_n = natural frequency).

The tendency of designing gates and valves with sharper edges results (because the critical S value does not change) in higher excitation frequencies. If it is not possible to raise the resonance frequency too, the demand becomes that the latter lies well below the dominant excitation frequency. However, this solution is unsafe: already the fact that the head difference is, in general, variable makes that the excitation frequency can shift downwards, and also there remains the risk that higher resonance modes may interfere. Experiences of Petrikat and Minor [82], and Schmidgall [89] showed how gates at high heads become critical at vibration frequencies well under the dominant excitation frequencies. In model tests of the Volkerak dam, the author observed S values of about 0.03 [25]. Recently, Naudascher and Locher [70] published experimental results showing S values of 0.01 - 0.03 for a configuration similar to that of a nearly entirely raised valve gate with rectangular seal (in a position where flow reattachment can occur). There was found a tendency of increased force amplitudes at greater vibration amplitudes. The experiments of Petrikat and Minor [82] and of Schmidgall [89] also showed that at much lower values of S heavy vibrations do occur; these lower values are related to high-head gates with relatively sharp edges. In Chapter II there will be presented a theory that can explain these

Chapter I. Introduction

low S values in relation to self-excited vibrations.

The work of Abelev [1, 2 and 3] on Strouhal numbers related to the total pulsating force on gates has already been mentioned.

Naudascher [66] presented a study on flow phenomena which are sensitive to feedback phenomena within the flow itself (fluid resonance). This study has recently been further developed in co-operation with Martin and Padmanabhan [58]. By comparison with instability studies, done by others, of shear flow instability, the existence is concluded of critical velocity patterns at gate edges where reattachment occurs. Moreover, it has been supposed, parallel to what has been found by Schwarz for overflow nappes [92] and to other vibration phenomena, that self-excitation is related to the distance between the points of flow separation and flow reattachment (for flow patterns similar to those of Fig. I. 6c), so that an $(n + \frac{1}{4})$ number of wave lengths is equal to this distance (wave length defined as vibration period multiplied by the velocity of the gap flow). This leads to a series of Strouhal numbers of 0.2, 0.6, 0.8 etc. No experimental evidence has been found yet for higher values of S than 0.4.

The excitation force amplitude has first been studied by Petrikat [78] in 1953, followed by later studies partly in co-operation with others [81, 82 and 83]. The evaluation of experiments was done in such a way that the excitation force was a right hand term in equation (I. 9). However, in the two papers last named, he found that the force amplitude increases with the vibration amplitude, which shows a certain tendency of self-excitation.

A systematic experimental study of the force amplitudes acting on a rectangular gate seal during gate vibration was presented in 1974 by Hardwick [35]. This study was concentrated on a range of the reduced frequency, $S = f b / V_{\text{gap}}$, between 0.3 and 0.45 and was done for $\delta = 0.66 b$. In one of the figures he presented the excitation coefficient in the way proposed by Petrikat:

$$C_A = F / \rho g b (d_1 - d_2) \times \text{span}$$

This coefficient is based on the same principle as equation (I. 12), taking into consideration that $\rho g (d_1 - d_2)$ is proportional to ρV^2 and that $b \times \text{span}$ represents the area L^2 on which the pressures act in vertical sense. (d_1 and d_2 are the water depths at opposite sides of the

I. 6 Gate and valve vibrations

gate)

By presenting C_A as function of the vibration amplitude Y_0 (made dimensionless as Y_0/b), it was shown that for small vibration amplitudes the force has a constant amplitude component ($C_A \sim 0.5$) plus a component proportional to the vibration amplitude. The C_A coefficient increases by a factor 2 to 4 (depending on S) and reaches its maximum at the relative small vibration amplitude values between 0.015 and 0.03. This indicates that the vibration is not a purely self-exciting one, because then a larger range of amplitudes would be involved wherein the force is proportional to Y_0 , as has been found for galloping and flutter.

A demand in relation to the prevention of self-exciting vibrations is that the total load from weight and hydrodynamic forces is such that all wheels, articulation points, etc. are loaded in one definite direction. Otherwise, chattering can occur, which is always critical for the onset of vibrations. Murphy [62 and 5] introduced this criterium to judge the maximum allowable hydrodynamic (static + dynamic) force on valves. It has also been found in a model study of the inlet sluice of the Volkerak dam at the Delft Hydraulics Laboratory [25] that a wheel gate becomes critical when it is raised so far that the upper wheels just get loose from their rails. The author observed damage to lock culvert valves, which was probably due to vibration when the gate was retracted for a major part into its recess, which position caused unloading of the upper wheels. By a correct recess shape, continuous wheel loading can be obtained for nearly the whole range of gate positions. Slide valves are not sensitive to this problem, if the slide bearing supports the gate over its entire range.

Gates with simultaneous under- and overflow behave in the same way as a body in infinite flow. A dominant Strouhal number can be defined, but now depending on the ratio between gate height and water depths. A low frequency vortex street will occur. Such a gate has been studied by Naudascher [63]. Partensky [74 and 75] studied a resonance phenomenon in mitre gates, provoked by a periodic wave, released upstream by simultaneous underflow and overflow of a weir gate.

Studies on self-excitation (active response) of gates and valves are only few. In the handbook of Den Hartog [27], some qualitative analyses of different valves are presented. The valve behaviour in a pipe flow system has been presented by several authors, for instance by Harding [34] and Urata [103]. The computation method is similar to the

one used in electrical systems, computing the impedance of the pipe flow and using the relation between local water pressures and the elastic valve behaviour. Abelev [4] presented the principles of a computation method for vibration of a slide valve placed in a short culvert, a method which he improved a few times after earlier publications. His method is based on a system wherein the vibrations cause discharge fluctuations. Due to inertia effects in the flow (especially of importance in the narrow slits between gate and culvert shaft), pressure fluctuations result in an energy transfer from the flow to the vibrating structure.

A type of vibration which leads to an active response after an initial disturbance, but which is again completely different from galloping or flutter, is the *self-excitation of gates with overflowing water*.

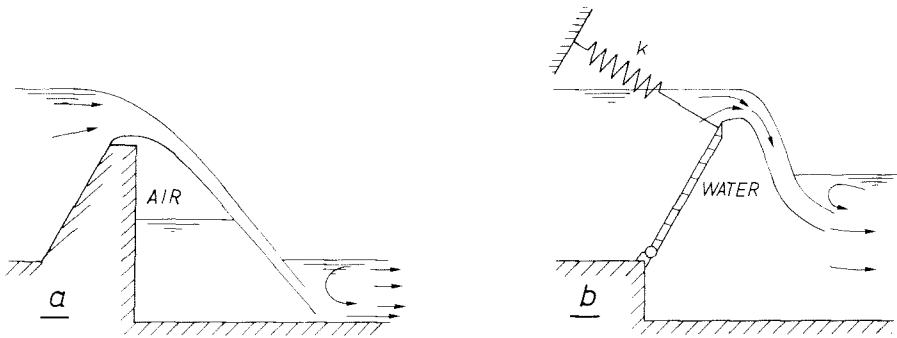


FIG I.7

Type a is sensitive to self-excitement when the overflow nappe has a limited thickness. The maximum nappe thickness was investigated by Partensky for a rigid gate [76].

For case b, where vibrations occur particularly at greater discharges, it seems that the effect of the weakness of the air cushion is replaced by the weakness of the gate suspension. However, the gate vibration now does not only affect place and shape of the falling nappe, but also causes a fluctuation of the discharge. In case a, the elastic air cushion leads to a phenomenon wherein the air pressure fluctuations cause the nappe to vibrate, which results in a volume variation of the air cushion, which again provokes nappe vibration. In an elastic gate this instability is greatly reinforced. The remedy of making a connection between the air cushion and the outside air has been studied,

1. 7 Design requirements

among others, by Fischer [29]. Simplified theoretical approaches were made by Petrikat [78] and Pariset [72]. A more complete one was presented by Schwarz [92]. He proved by numerical calculation of nappe vibration caused by an assumed pressure fluctuation of the air cushion, that at certain frequencies energy transfer can result from the nappe to the air cushion. This calculation was repeated in an analytical way by Treiber [99]. Results of calculations of those frequencies at which maximum energy transfer occurs are in accordance with measured vibration frequencies, but disagreement is found when the calculation is complemented with the introduction of air rigidity; see also Appendix A.

Vibration of valves in high-head structures (say > 10 m) can be caused by cavitation, occurring when local low pressures cause low-temperature boiling. Because cavitation is a special, extended field of investigation, this topic is not treated in this book. For gate and valve design, the conclusion is that cavitation must be prevented by designing the structure in such a way that pressures near valves and gates are always high enough. A compilation of observations in this field is given by Knapp, Daily and Hammit [44]; illustrative pictures of cavitation damage near valves are presented by Douma [28]. When aeration is applied at culvert valves to relieve the low pressure zones, insufficient aeration results in unstable flow, which can cause vibrations and extremely high pulsating pressures. Design requirements are presented in the handbook of Wickert and Schmauszer, par. 10. 3 [109]

7. DESIGN REQUIREMENTS IN RELATION TO GATE AND VALVE VIBRATIONS

To distinguish different types of vibrations, the classification introduced in 1963 by Naudascher [64] is used.

Self-exciting vibrations; these are the unstable vibrations which are, after an initial disturbance, self-amplifying. Among these are galloping, flutter and buffeting.

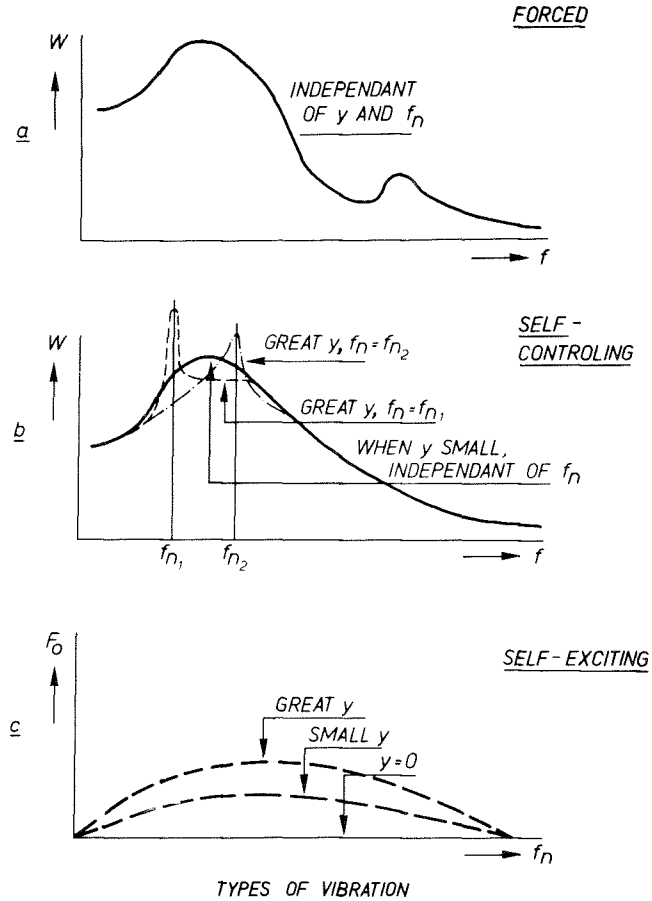
Forced vibrations; these are the vibrations of structures reacting passively to a hydrodynamic excitation force, which force in turn is not influenced by the vibration.

Self-controlling vibrations; the structure reacts passively to the hydrodynamic excitation force, but, starting from a certain vibration amplitude, this force is influenced by the vibration. This will be the case when an initially irregular, turbulent, three-dimensional flow pattern

Chapter I. Introduction

is synchronized by the vibration; the force fluctuations at different places of the structure will then also be synchronized. This results in an increased, but limited, effective force amplitude.

Sometimes the turbulence will change so that the dominant excitation frequency comes nearer to the resonance frequency of the structure.



TYPES OF VIBRATION

FIG. I. 8

The three types of vibration are illustrated in Fig. I. 8. Fig. a shows that with forced vibrations, which result generally from random excitation, the force function W is not influenced by the natural frequency f_n of the structure; nor is it influenced by the vibration amplitude Y . Fig. b shows that with self-controlling vibrations the force is affected by the vibration at greater amplitudes: the band width narrows, but the total force amplitude ($\sqrt{\int_0^{\infty} Wdf}$) does not increase substantially and, from a

1. 7 Design requirements

certain amplitude value, a maximum excitation is reached. An increase of the force amplitude is effected by synchronization of the eddy field of the vibrating structure; the importance of this phenomenon depends on the length/width ratio of the body. With self-exciting vibrations, Fig. 8c, the force amplitude F_0 will increase with the amplitude of the vibration, initially even proportionally thereto. The force is purely periodic; the period depends on the resonance frequency and can be influenced by the self-excitation mechanism. The magnitude of self-excitation depends on the natural frequency. At very great amplitudes, the force is usually limited physically by non-linearities, sometimes in the mechanical and sometimes in the flow system.

A good gate design in relation to vibration is a gate with a low level of vibration. The expression often used in public tenders is that a "vibration-free design" is required. But, using the classification mentioned above, the best one can claim for a design is that it is free of self-excited vibrations and has a low degree of self-control; still there remains a structure placed in a highly turbulent flow field (turbulence is greatly related to the energy loss of the flow when the gate or valve is in a partially closed position). Due to the dynamic pressures, a dynamic response of the structure will always occur.

For a good design the following rules should be applied:

- a. The shape has to be such that self-exciting vibrations are prevented whenever possible; if, under some hydraulic conditions, self-excitation can still be expected, measures of prevention have to be taken in the form of sufficient rigidity and/or sufficient mechanical damping. In judging the shape, especially of small leakage gaps, it has to be taken into account that the shape is influenced by wear of the seals and that the gate position can be altered by wear of the pivots. Structural members should offer no risk of galloping. When natural friction is introduced as a safety factor, an analysis has to be made of the character of this (non-linear) damping, and one must be sure that this damping will always occur.
- b. Resonance frequencies of the whole gate or of members in submerged condition have to be well above the dominant turbulence or eddy frequencies in order to prevent resonance phenomena and also to prevent that great amplitudes can cause extra excitation forces (self-controlling vibrations).

Chapter I. Introduction

- c. Sufficient strength and stiffness has to be available to withstand forced vibrations (so that no unacceptable tensions or unacceptable vibration amplitudes will be caused by the static and dynamic hydrodynamic loads).
- d. Reversal of the direction of forces has to be prevented in order to avoid the influence of play in pivots or hammering of wheels. Pretensioning can be applied as an additional means to fulfill this requirement.
- e. The occurrence of unstable free water surfaces near gates and valves has to be prevented. These can result from incomplete aeration or cavitation and can lead to pulse loads. Also a variation of the compressibility of the fluid due to the presence of air can give rise to instabilities.

To fulfill all these requirements, different hydraulic aspects must be studied, available literature must be classified, more systematic research programmes must be undertaken. In the end, it can be expected that this will lead to design criteria for the different types of gates and valves by which their dynamic behaviour can be completely described.

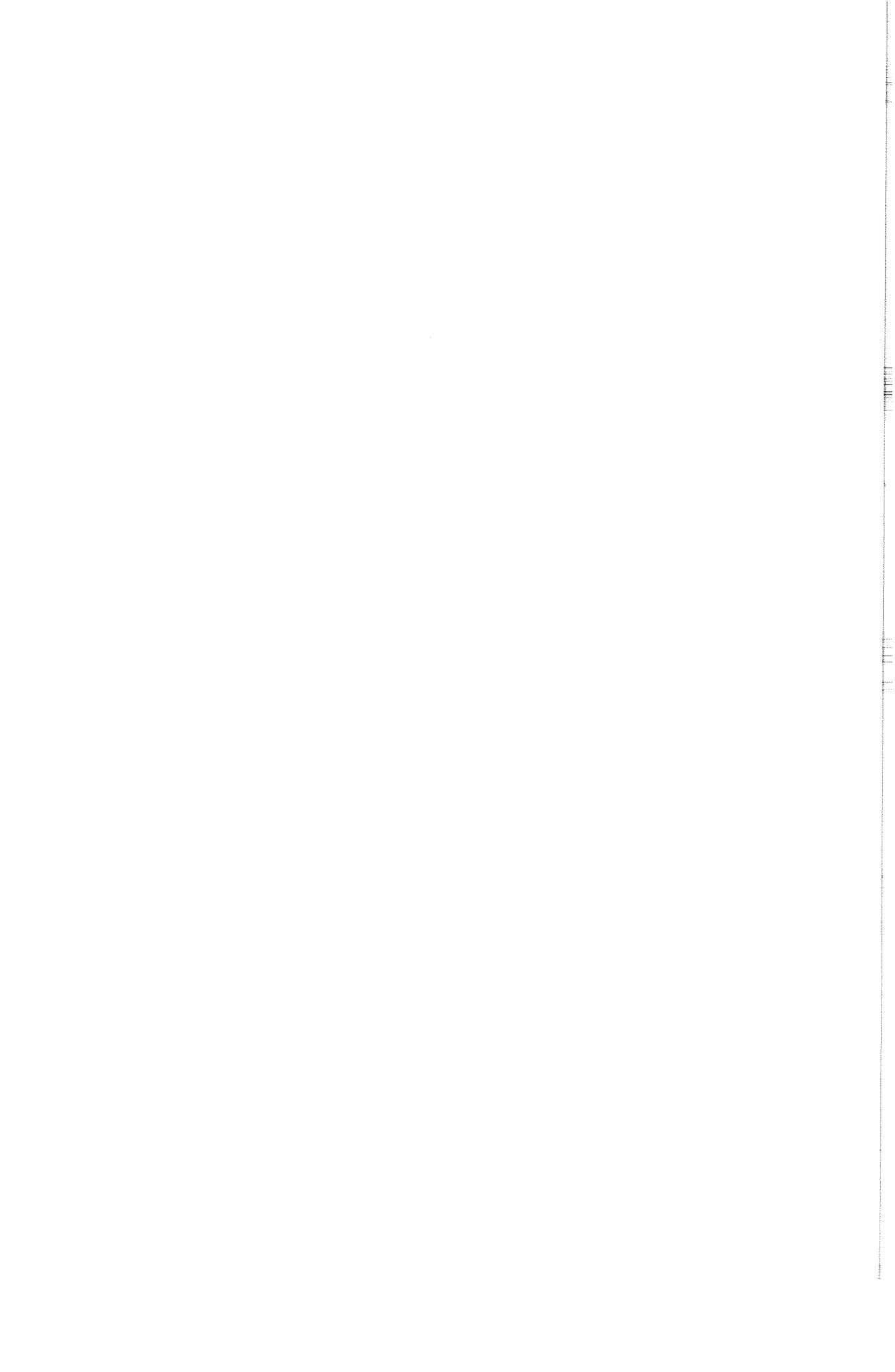
These are of the following character:

- All parameters are to be presented in a non-dimensional form to permit their application regardless of the size of the structure and of hydrodynamic conditions.
- The valve or gate design must be free of self-exciting vibrations, with a possible exception for a well defined narrow range of critical conditions (for instance gate positions).
- Water mass and damping are to be presented for all circumstances (gate or valve openings, water levels or pressure differences).
- The dominant excitation frequencies have to be quantified to find designs wherein the resonance frequencies are well above the excitation frequencies.
- Vibrations can, except under certain critical conditions, be described as forced vibrations, to which the dynamic response of the structure can be calculated from the power density spectrum of the excitation force. Limits of acceptable vibration amplitudes within which no self-controlled vibrations occur are to be indicated.
- Possible self-exciting vibrations in the critical ranges must be

I. 7 Design requirements

analyzed theoretically so that the amount of damping required to prevent or to reduce these vibrations can be calculated.

The following chapters deal with various design criteria: In Chapter II, a computation method is presented for self-exciting vibrations and results are given for several types of valves and gates; a similar approach is presented in Appendix A for unstable vibrations of a vertical water curtain and some of the conclusions are of importance for gates with overflow. In Chapter III, indications are presented with which the risk of self-exciting vibrations can be detected. In Chapter IV, the added mass and damping are analyzed and for a few cases computation methods are given. In this chapter also an adequate non-dimensional presentation is suggested, illustrated by the measurements to be found in Appendix B. In Chapter V, parameters are developed to present in a non-dimensional way the passive response to random turbulence excitation (forced vibrations), illustrated again by the measurements on a valve in Appendix B. Finally, in Chapter VI and in Appendix C, the possibilities of model research are summarized; the reliability of elastic models is discussed with the aid of model/prototype test results.



Chapter II

Self-exciting vibrations of gates and valves

1. SUMMARY

Three mechanisms of self-exciting vibrations, occurring in many different gates and valves, are analyzed:

- Vibrations caused by the water-air cushion system at overflow gates
- Vibrations of a plug valve in nearly closed condition (similar vibration mechanisms occur in a cylinder valve and in a reversed Taintor valve)
- Vibrations of nearly closed slide and wheel valves and gates.

The method of analysis consists in the calculation of discharge fluctuations and pressure fluctuations near the structure, due to an assumed harmonic vibration. To balance the extra forces caused by the pressure fluctuations, a rigidity and damping factor in the gate support is introduced into the calculation; the gate mass is taken into account. The values of rigidity and damping depend on the frequency of vibration. If the real mechanical rigidity is known, the frequency of the vibration is fully determined by it. By comparing, at this frequency, the real mechanical damping with the calculated one, it can be concluded whether self-exciting vibrations will or will not occur.

2. INTRODUCTION

As mentioned in Chapter I, to prevent self-exciting vibrations is a primary design requirement for gates and valves. The following aspects are of importance (each being related to the hydrodynamic conditions):

- a. the shape of the gate or valve, of the recess and of the slots, and the location of bulkheads, etc , which have to be seen in relation to

Chapter II. Self-exciting vibrations

- the flow direction and waterlevels;
- b. the rigidity of the structure;
- c. damping by the structure itself and by additional dampers; and
- d. play in pivots, wheels, etc.

Sub a

As mentioned in Chapter I, par. 6, the modern tendency in gate design is that unstable flow separation or flow reattachment has to be prevented. This leads to sharp edges to establish well-defined flow separation points, while downstream of these separation points, girders are placed well away from the separated flow to make sure that no reattachment can occur. Another design requirement is the reduction of areas on which pressure pulsations related to instabilities of flow separation and/or reattachment can act; this is another argument for the application of sharp edges. However, strength considerations and the use of seals limit the possibilities. Solutions for rubber seals which follow this demand as far as possible do not always lead automatically to a design which is safe under all circumstances. Sometimes gates are designed without any special seal: the retaining plate, with stiffening girders at its downstream side, projects below the lowermost girder and has a sharpened edge. Such a design results in some leakage in closed position. A rubber or lead strip embedded in the bottom prevents this.

An effective method of reducing the danger of vibration is to keep girders in air. This is applicable to Taintor and sector gates on spillway crests and to outlet culverts of high-head dams. The smooth retaining plate of the gate is then at the upstream side and does not cause any flow instability; its lower edge is shaped as sharp as possible. Downstream, the jet flow has to be fully aerated so that no hydraulic jump can occur.

In this Chapter, a theoretical analysis is presented of self-exciting vibrations, of which one case (par. 12) is related to flow near valve and gate edges. The analysis of vertical vibrations of gates and valves results in the conclusion that no blunt edges should be applied where suction forces can occur. This conclusion is important for the design of edges.

Another type of vibration, which is more or less independent of the cross-section of the seal, is the horizontal vibration of valves when their seals (bottom, top and/or side seals) are just loose from the seats. The analysis in par. 5 of a plug valve enables computation of this type of

II. 2 Introduction

vibration. It can be concluded that no tapered gates which have narrow slits over a certain range of gate positions should be applied. Also, when a relieve system is used to free the valve from its seat before raising, a sufficient gap width should be provided, the magnitude of which can be calculated. Similar considerations can be applied to the reversed Taintor valve with a protruding upper seal, as well as to a cylinder valve.

A special case of instabilities are the self-exciting vibrations which can occur at the overflow of weirs and gates. Self-exciting vibrations occur when the pressure fluctuations in the air enclosed between the gate and the falling nappe, caused by nappe oscillations, are transferred to the upper part of the nappe, so that new nappe oscillations are excited. This mechanism is presented in par. 4 of this chapter and in Appendix A. Also, in this case the self-exciting mechanism is not necessarily due to instability of flow at a separation point; such an instability of separation could, however, strengthen the vibration. Prevention of this type of vibration is achieved by the provision of openings through which the air pocket is in communication with the constant atmospheric pressure. The best solution to obtain this communication is the provision on the gate crest of elements which protrude through the overflowing nappe (see further handbook of Wickert and Schmauszer [108])

In Chapter III, a more general method will be presented which enables optimal shaping in the design of gates and prediction of possible critical points in the design; a number of critical configurations are shown.

Sub b and c

One of the requirements of a good design is that its resonance frequency must be widely different from the dominant excitation frequency and, when the mass of the gate and the value of the added water mass are known, this results in the requisite rigidity.

Owing to this point of view, an important part of the vibration research is concentrated on the dominant excitation frequency f (see Chapter I, par. 6). This is usually represented by the Strouhal number $S=fL/V$; L = gate edge thickness b or gate raise δ , V = gap velocity. The tendency of designing gates and valves with sharper edges results (because the critical S value remains the same) in higher excitation frequencies. It is advisable to raise the resonance frequency well above it; the demand that

Chapter II. Self-exciting vibrations

the latter lies well below the dominant excitation frequency is not safe enough. The fact that the head difference is variable makes that the excitation frequency can shift downwards and also there remains a risk that higher resonance modes interfere.

The analysis presented in this chapter deals with purely *self-exciting vibrations*. For different types of valves and gates, the prevention of self-excitation leads to a relation between the critical valve or gate opening and the rigidity and damping of the hoist system. It is also shown that for vertical vibrations the critical value of S_n ($= f_n \delta_o / v$ in which f_n = resonance frequency in submerged condition, δ_o = gap width, and $v = \sqrt{2g \Delta H}$, wherein ΔH = head difference across the gap, and g = acceleration of gravity) is not limited to a certain range: the valve is critical when a suction force occurs at the seal. It appears that if the thickness of the seal (in flow direction) is reduced, the excitation force amplitude can increase in some cases (in a certain range of the S_n value). Maximum excitation is to be expected at S_n values in the range of 0.02 to 0.1. This analysis of self-exciting vibrations is complementary to that of forced vibrations, and their results lead to complementary conclusions concerning gate design.

In general, the experience of the author shows that a high rigidity of a gate and its suspension form an extra guard against self-exciting vibrations, and this is in accordance with the theoretical solutions. One exception has been found: at a gate with overflow, where a thick nappe occurred and the air pocket under the nappe had been sucked empty, stiffening of the suspension had an adverse effect. For this case, a solution against the vibration was found in the aeration of the nappe.

Sub d

A demand in relation to the prevention of self-exciting vibrations is that the resulting load from weight and hydrodynamic forces is such that all wheels, articulations, etc. are loaded in one definite direction. Otherwise, play can interfere, which is always critical for the onset of vibrations (see again Chapter I, par. 6). In some cases preloading of the wheels can be introduced by means of counter-pressure wheels. Pre-tensioning of the hoist sometimes can be achieved with a spring. Extra weight of the gate can have an adverse effect, due to an increase of dynamic forces at lower resonance frequencies. To calculate the resulting force, a careful

II. 2 Introduction

analysis has to be made of the stationary and the non-stationary hydrodynamic forces. The stationary forces on culvert gates depend greatly on the size of leakage gaps, because these determine the waterlevel in the gate shaft, which in its turn determines to a large extent the resulting downpull. The stationary hydrodynamic forces are not further analyzed in this book.

RELATION BETWEEN THE PRESENT METHOD OF ANALYSIS AND OTHER PUBLISHED METHODS

Only few authors have tried to present mathematically the vibration phenomena of valves and gates. An exception form the *instabilities of a nappe overflowing a gate* and enclosing an air pocket, for which various authors considered the possibility of energy transfer from the oscillating nappe to the air cushion (energy transfer per period = \int_0^T rate of

decrease of air volume \times pressure surplus of air $\times dt$). The result of this analysis is that instabilities can arise at a series of definite frequencies, the values of which correspond to experimental ones.

First to be mentioned are the publications dealing with design questions: Petrikat [79], who also introduced the combination of nappe oscillation and gate vibration, Pariset [72] and Minor [59]. More theoretically of interest is the analysis of Schwarz [92], who arrived at an accurate determination of the energy transfer after first determining the shape of the oscillating nappe. The pressure fluctuation acts perpendicular to the nappe, and so the path of each water particle can be calculated by a step by step method. This work was followed up by Treiber [99], Cremer [16], Randsford [85] and Binnie [14]. Last named author especially considered the influences of turbulence in the boundary layer of air, and of the surface tension. Pertensky and Sar Khloeng [76] determined the limit value of the nappe thickness at which nappe oscillations occur.

The mechanism of *vibration of plug valves* is indicated in the handbook on Mechanical Vibrations by Den Hartog [60], p. 318, but without mathematical presentation. Harding [34] and Urata [103] published an analysis of valves in pipes, wherein the different elements, pipe, valve and spring, were considered in terms of input - output systems, of which the impedance was determined. The way of computation is very similar to

Chapter II. Self-exciting vibrations

that used for electrical circuits and servo systems. Abelev [4] treated the horizontal vibration of a slide valve (the type of vibration of fig. III. 17). In all the computations, the inertia of the water due to pipe flow plays a role similar to what has been presented in Chapter I for the hydraulic ram. The work of Abelev is of special interest, because he schematized the non-linear hydraulic losses of the leakage gap into a first and a second term of the Taylor series, with which he could not only arrive at the magnitude of self-excitation, but could also compute the limit amplitude. This amplitude gives zero energy transfer per time period from the water to the oscillating gate.

In the computation of paragraph 5 of this chapter, a few simplifications are introduced, leading to practical results which are still widely applicable, also to other valves than the reversed Taintor valve and the cylinder valve.

The mechanism of vertical vibrations has not yet been clearly presented by other authors. Petrikat, [79] and [82], concentrates on finding excitation coefficients; he supposes that the excitation is caused at the low pressure regions, where the flow is sensitive to separation. Naudascher's search for instabilities concentrates on instabilities in the flow itself, and he concludes that certain velocity patterns near the gate are more likely to cause instabilities than others. He also concludes, from considerations similar to those discussed for nappe oscillation, that a series of frequencies are susceptible to instability phenomena [56, 63, 65, 70]. In fact his results are not related to self-exciting vibrations, because the tendency of instability is not generated by gate vibrations.

The computations regarding self-exciting vibrations presented in this chapter, (par. 13) should, at this moment, only be seen as a concept, because quantitative experimental data are scarce. Qualitative agreement has been found in so far, that it appears that only seals with low-pressure zones (due to rounded edges or to flow reattachment) are susceptible to self-exciting vibrations (critical shapes are presented by Petrikat [79], Müller [60] and Krummet [53]). Another qualitative agreement can be found in the character of the waves produced in the water when gates vibrate. Purely vertical vibrations cause waves radiating parallel to the gate; horizontal vibrations produce a cross pattern of waves.

II. 2 Introduction

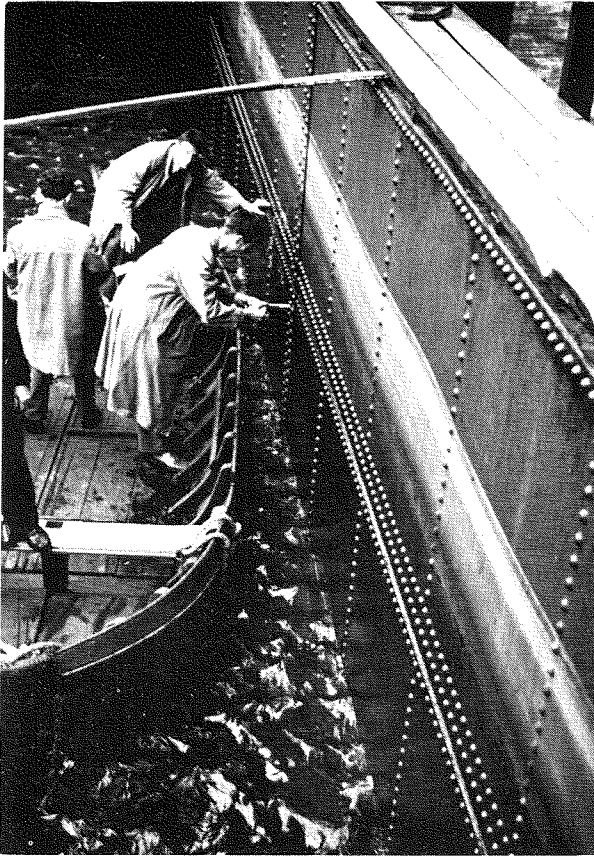


Plate II. 1 Wave pattern caused by horizontal vibration with an amplitude of 5 mm.

The latter can be explained by assuming that they are caused by the discharge fluctuations in the leakage gap at the ends of the gate. The computations of par. 15 show that the mechanism of self-exciting vibrations is related to relatively important discharge fluctuations.

Since the analysis of self-excitation presented hereafter shows clearly the different parameters involved, this can be the starting point for a systematic research to obtain the separate coefficients. Though the coefficients introduced are supposed to be constant and, in principle, can be determined with a non-vibrating gate under permanent flow conditions, experience with airfoil flutter shows that coefficients can vary

Chapter II. Self-exciting vibrations

with frequency and amplitude. So, accurate results can only be obtained by force measurements during harmonic oscillation. Such a study was presented by Bergh [11], who determined the coefficients for wing flutter computation.

3. GENERAL DESCRIPTION OF THE COMPUTATION METHOD FOR SELF-EXCITING VIBRATIONS

The analysis presented in this chapter assumes infinitely small vibration amplitudes, which leads to linear equations. After the linearized differential equations have been derived, a stationary vibration is introduced. The rigidity (k) of the resilient gate or valve suspension (in the case of nappe oscillation, this is the air cushion rigidity) and the mechanical damper (c), which are needed to sustain this vibration, are then calculated. These calculated values of k and c are compared with the actual values. Because k and c are functions of the frequency of vibration, the actual value of k now determines the frequency of the real vibration. The value of c at this frequency is compared with the value of the real damper; if the actual value is smaller than the calculated one, the vibration can be supposed to be unstable. If the real system has no mechanical damping, a sufficient condition for self-excitation is that the computed damping is positive. This method was first chosen for the analysis of the oscillation of an overflow nappe or a falling water curtain (Appendix A). The methods by means of which the solution of the basic equations could result in an incremental or decremental solution of the type $y = y_0 e^{st}$ (s is a complex number) appeared to be very complex and elaborate. Graphical methods could not be considered because a set of equations had to be solved simultaneously. Step by step methods are possible but are only of interest when other methods fail, because only specific solutions are obtainable. The method of introducing a stationary vibration is an extension of the method of determining the energy transfer per period of time that has been developed by Schwarz [92] for the overflow nappe.

The mechanism of the oscillation of a nappe enclosing an air pocket is as follows:

If the air cushion is (as the result of incidental nappe oscillation) subjected to a pressure fluctuation, the water particles in the nappe are accelerated perpendicular to their flow path. Consequently, the particle

II. 3 Computation method

path will fluctuate around the original one. The oscillating nappe shape can be analyzed and waves can be recognized (Appendix A, fig. 3). Now, the volume variation of the air enclosed by the nappe has to cause the pressure fluctuations with which the calculation started (with correct phase and amplitude). This leads to certain conditions of rigidity and damping of the air cushion (as functions of the assumed frequency). Because these values are only calculated ones, negative values can also occur. Comparison with the real rigidity leads to the determination of the real frequencies that will occur, and of these only the ones which have a positive calculated damping of the air can physically exist.

The analysis of the mechanism of valve and gate vibration goes as follows:

A harmonic gate vibration is assumed. This vibration causes a variation of the discharge capacity of the valve and leakage gaps. The flow has to accelerate or to decelerate to arrive at a new equilibrium, but this is connected to a variation of the head difference across the valve. For instance, when the discharge capacity of the gap is decreased, a deceleration of the flow in the pipe is caused by the valve, resulting in an increased head difference across the valve and consequently in extra hydrodynamic forces on the valve: horizontal forces and sometimes also extra suction at the seal. These forces transfer energy to the oscillating valve if they are in phase with and in the direction of the vibration velocity. This is the case when the extra horizontal or suction forces are in the direction of the valve displacement giving rise to the decrease of discharge capacity. In the calculations, these extra hydrodynamic forces have to be balanced by the rigidity and damping of the suspension system, or of the wheels or other supports. Again, these calculated rigidity and damping values, which are a function of the frequency of vibration, are compared with the real ones. The rigidity of the suspension or support determines the real frequency of vibration, and the real damping compared with the calculated value determines whether the vibration is stable or unstable. With this type of calculation, the harmonic vibration is introduced into a differential equation of the following type:

$$\frac{d^3 y}{dt^3} + A_2 \frac{d^2 y}{dt^2} + A_1 \frac{dy}{dt} + A_0 y = 0 \quad (\text{II. 1})$$

See equation (II. 10).

Chapter II. Self-exciting vibrations

This is a lower order of equation (I. 19), and Den Hartog proposes in p. 286 of his handbook [27] the application of the Routh and Hurwitz stability criterion to see whether the (undamped or damped) structure is stable or unstable. However, with the method of introducing an arbitrary damper, so that the vibration becomes a purely harmonic one, the arbitrary damper is a direct measure of the damper to be applied to suppress the instability. Moreover, this method has a wider applicability, because the coefficients A_0 , A_1 and A_2 are only assumed to be constant; if experimental verification would show that these coefficients vary with frequency (this was found in the flutter phenomena of airfoils), experiments can be done with harmonic oscillations and the values of A_0 , A_1 and A_2 can then be introduced into the computations.

Introducing the harmonic oscillation $y = Y_0 e^{i\omega t}$ in equation (II. 1) results in:

$$(-i\omega^3 - A_2\omega^2 + iA_1\omega + A_0) Y_0 e^{i\omega t} = 0,$$

giving two equations:

$$\omega^2 = A_1 = A_0/A_2 \tag{II. 2}$$

From these equations the support rigidity and mechanical damping can be found for each frequency. Then again, the actual rigidity will determine the vibration frequency and the actual damping will determine whether the vibration is stable or unstable.

Remark: If the computed damping is a negative one, the vibration is stable; i.e. a negative damper (which produces energy) would be needed to sustain a harmonic oscillation. The value of negative damping now in fact is a measure of the hydrodynamic energy absorption; this is the hydrodynamic damping. This means that the calculations of self-exciting vibrations for certain frequencies also give information on the hydrodynamic damping.

4. SELF-EXCITING VIBRATIONS OF A WATER CURTAIN OR OVERFLOW NAPPE ENCLOSING AN AIR POCKET

The analysis of this problem, given in Appendix A, has been presented in 1972 at the IUTAM/IAHR symposium [68] and has to be considered as a continuation of the work of Schwarz [92]. A new element in this computation is that the water-air system is considered as a whole.

II. 4 Water curtain or overflow nappe

Instabilities of the air water system only occur when the overflow nappe or water-curtain is thin (data on limit values have been investigated by Partensky and Sar Khloeung [76]). When the gate is elastic, vibrations occur also at greater nappe thicknesses and also under conditions wherein the air cushion has disappeared; these cases, however, are not further analyzed. The computations of Appendix A show definitely under which conditions of rigidity and damping of the air cushion the system becomes unstable. Experiments show that a higher cushion rigidity than the computed one also can lead to unstable vibrations. But then, however, the system often needs a strong initial disturbance before vibration starts. This indicates that non-linear effects are not negligible; these have not been taken into account in the theoretical analysis.

It has been found experimentally that a low air cushion rigidity leads more easily to oscillations of the overflow nappe. This leads to the important conclusion that model research on self-exciting nappe oscillations is rather unsafe for the prediction of oscillations, which conclusion is of particular importance when minimum dimensions of aeration systems have to be designed for the reduction of air pressure fluctuations in the cushion. The analysis in Appendix A includes the computation of the behaviour of the falling water curtain in response to a pressure pulsation in the air cushion, leading to a periodic volume variation of the air cushion. An extension of this calculation to other nappe shapes, including the parabolic overflow nappe of a weir, is given by Treiber [99]. His results could be combined with the ones of Appendix A. Further study of the influence of the non-linear effects which cause the divergence between computations and experiment is desirable.

5. SELF-EXCITING VIBRATIONS OF A PLUG VALVE

The computation of self-exciting vibrations follows after the introduction of a number of simplifying assumptions:

1. The water is supposed to be incompressible; this implies that the first resonance frequency related to a sound wave is high compared with the frequencies of valve vibration (For an open-ended tube such resonance occurs when $4L = \text{compression wave velocity} \times T$, wherein T is the time period of one vibration cycle).
2. Aeration or cavitation phenomena do not occur.
3. The water viscosity has no effect.

Chapter II. Self-exciting vibrations

4. All hydraulic losses, except those at the valve gap, are neglected.
As the computation will show that vibrations occur at small gap widths, this assumption is for most cases a reasonable one. Related to this assumption is the phenomenon that there is a negligible regain of pressure, after the discharge through the gap has redistributed itself over the culvert cross-section.
5. The value of the length of L is at least a few times the culvert height h_c , so that it can be assumed that L is representative of the inertia of the water. In the computation this inertia is introduced as if over the whole length the discharge is evenly distributed over the culvert cross-section. The flow inertia in the leakage gap is neglected.
6. The discharge coefficient μ is supposed to remain constant during the vibration.

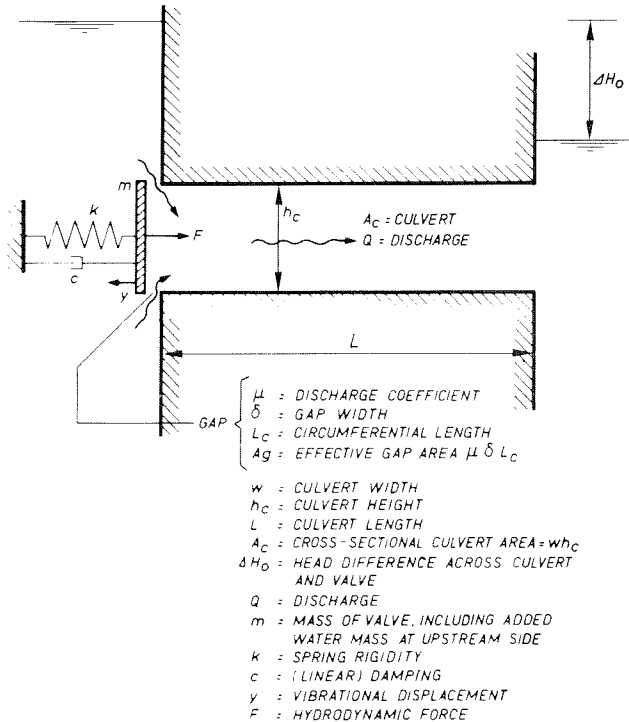


FIG. II. 1

II. 5 Plug valve

In the computation, it is assumed that there is an imaginary damping c of such magnitude that the vibration is a purely harmonic one; the water-damping is neglected. This *imaginary* damping value, which follows from the computation, is supposed to be at the transition of the *real* damping values related to unstable and to the stable vibrations. The stability of the vibrations is ensured when the real damping value is greater than the imaginary one. When the real mechanical damping is zero, the condition for stability is that the calculation gives a negative value for the assumed damping.

Although all computations are done for a closed culvert, for a gate in an open channel a hypothetical length of the water column can also be estimated with the aid of the data of par.17, and so the same type of self-exciting vibrations can occur at gates in open channels when the seals get loose at the edges.

It is assumed that the variable parameters Q , A_g and ΔH vary within a small amplitude around an average value equaling the value of a permanent flow condition.

$$Q = Q_o + Q', \quad A_g = A_{go} + A'_g \quad \text{and} \quad \Delta H = \Delta H_o + \Delta H'$$

$$\dot{Q} = \dot{Q}', \quad \dot{A}_g = \dot{A}'_g \quad \text{and} \quad \dot{\Delta H} = \dot{\Delta H}'$$

Three basic equations can be derived:

- Force equation (dynamic part) which follows from an equilibrium of forces acting on the mass:

$$F' = \rho g A_c \Delta H' = -m \ddot{y} - c \dot{y} - k y \quad (\text{II. 3})$$

(y = displacement due to the vibration, $\dot{y} = dy/dt$, $\ddot{y} = d^2y/dt^2$;
 $\Delta H'$ = head difference increase across the valve due to the vibration).

- Discharge equation, which follows from the classical equation for discharge capacity plus the piston effect of the gate:

$$Q = A_g \sqrt{2g \Delta H} - A_c \dot{y} \quad (\text{II. 4})$$

(ΔH is the local head difference across the valve; $\Delta H = \Delta H_o + \Delta H'$)

- Acceleration equation of the water column; the head difference increase across the valve is related to a head decrease downstream of the valve, and this leads to a pressure differential across the culvert of $-\rho g \Delta H'$ which will accelerate the water column therein:

Chapter II. Self-exciting vibrations

$$-\rho g \Delta H' = \rho L (dv/dt), \text{ or}$$

$$\Delta H' = -\frac{L}{g A_c} \dot{Q} \quad (\text{II. 5})$$

The first derivative of equation (II. 4) becomes:

$$\dot{Q} = \dot{Q}' = \sqrt{2g \Delta H_o} (dA_g/dy) \dot{y} + \frac{1}{2} A_{go} \sqrt{\frac{2g}{\Delta H_o}} \Delta \dot{H}' - A_c \ddot{y} \quad (\text{II. 6})$$

and equation (II. 5 and 6) result in:

$$\Delta H' = -\frac{L \sqrt{2g \Delta H_o}}{g A_c} (dA_g/dy) \dot{y} - \frac{1}{2} \frac{L A_{go}}{g A_c} \sqrt{\frac{2g}{\Delta H_o}} \Delta \dot{H}' + \frac{L}{g} \ddot{y} \quad (\text{II. 7})$$

In this derivation it is presupposed that for permanent flow conditions $\Delta H = \Delta H_o$. The value dA_g/dy is the gap variation per unit of vibrational displacement; in the case of Fig. II. 1 this value becomes μL_c . In other cases, for instance when the seat is inclined, the vibrational displacement y causes a smaller gap variation.

The other information on $\Delta H'$ is available from equation (II. 3):

$$\Delta H' = \frac{-m \ddot{y} - c \dot{y} - k y}{\rho g A_c} \quad (\text{II. 8})$$

and

$$\Delta \dot{H}' = \frac{-m \ddot{\dot{y}} - c \ddot{y} - k \dot{y}}{\rho g A_c} \quad (\text{II. 9})$$

Remark: When the equations (II. 7) and (II. 8) are considered, they appear to be linear equations of the second order with coupled parameters ΔH and y , and at first sight they are comparable with the wing flutter equations (I. 19) and (I. 20). Although physically the head difference ΔH can not be compared with the airfoil angle ϕ , mathematically a similar approach is possible.

Combining (II. 8 and 9) with (II. 7) results in:

$$\frac{m \ddot{y} + c \dot{y} + k y}{\rho g A_c} - \frac{L \sqrt{2g \Delta H_o} (dA_g/dy)}{g A_c} \dot{y} + \frac{L A_{go}}{A_c \sqrt{2g \Delta H_o}} \frac{m \ddot{y} + c \ddot{y} + k \dot{y}}{\rho g A_c} + \frac{L}{g} \ddot{y} = 0$$

or:

II. 5 Plug valve

$$\begin{aligned} & \frac{L A_{g0} m}{A_c^2 \rho g \sqrt{2g \Delta H_0}} \ddot{y} + \left(\frac{L A_{g0} c}{A_c^2 \rho g \sqrt{2g \Delta H_0}} + \frac{m}{\rho g A_c} + \frac{L}{g} \right) \ddot{y} + \\ & + \left(\frac{L A_{g0} k}{A_c^2 \rho g \sqrt{2g \Delta H_0}} + \frac{c}{\rho g A_c} - \frac{L \sqrt{2g \Delta H_0} (dA_g/dy)}{g A_c} \right) \dot{y} + \\ & + \frac{k}{\rho g A_c} y = 0 \end{aligned} \quad (\text{II. 10})$$

In this equation the harmonic motion $y = Y_0 e^{-i\omega t}$ is introduced, in which Y_0 and ω are real. Equation (II. 10) then results into two conditions:

Real part:

$$- \left(\frac{L A_{g0} c}{A_c^2 \rho g \sqrt{2g \Delta H_0}} + \frac{m}{\rho g A_c} + \frac{L}{g} \right) \omega^2 + \frac{k}{\rho g A_c} = 0$$

or:

$$\omega^2 = \frac{k}{m \left(1 + \frac{\rho A_c L}{m} + \frac{L A_{g0} c}{m A_c \sqrt{2g \Delta H_0}} \right)} \quad (\text{II. 11a})$$

Imaginary part:

$$\begin{aligned} - \frac{L A_{g0} m}{A_c^2 \rho g \sqrt{2g \Delta H_0}} \omega^3 + \left(\frac{L A_{g0} k}{A_c^2 \rho g \sqrt{2g \Delta H_0}} + \frac{c}{\rho g A_c} - \right. \\ \left. - \frac{L \sqrt{2g \Delta H_0} (dA_g/dy)}{g A_c} \right) \omega = 0 \end{aligned}$$

or:

$$\omega^2 = \frac{k}{m} \left\{ 1 + \frac{A_c \sqrt{2g \Delta H_0} c}{L A_{g0} k} - \frac{\rho A_c (2g \Delta H_0) (dA_g/dy)}{k A_{g0}} \right\} \quad (\text{II. 11b})$$

Two new coefficients are now introduced:

- the mass coefficient $c_m = m/\rho A_c L$; this is the relation between the valve mass (incl. the added mass of water upstream) and the water mass

Chapter II. Self-exciting vibrations

in the culvert downstream; and
 - the rigidity coefficient $c_k = \frac{k A_{go}}{\rho A_c (2g \Delta H_o) (dA_g/dy)}$

The physical meaning of c_k is the following:

When the valve moves with an abrupt displacement y , the inertia of the water in the culvert causes the discharge to remain constant, the local head difference ΔH across the valve changes and so does the hydrodynamic force $F = \Delta H \rho g A_c$. This change of the force F is proportional to y , and we can speak of a hydrodynamic counter-rigidity $k_{hc} = -dF/dy$. The hydrodynamic force due to k_{hc} is in a direction opposite to the restoring force of the spring. In the case of fig. II. 1, k_{hc} is positive. Now c_k is the ratio between the spring rigidity and the hydrodynamic counter-rigidity; i.e. $c_k = k/k_{hc}$.

Definition: c_k is positive when the hydrodynamic counter-rigidity counteracts the spring rigidity.

Equation (II. 11a and 11b) can now be written as follows:

$$\omega^2 = \frac{k}{m \left(1 + \frac{1}{c_m} + \frac{L A_{go} c}{m A_c \sqrt{2g \Delta H_o}} \right)} \quad (\text{II. 11c})$$

$$\omega^2 = \frac{k}{m} \left(1 - \frac{1}{c_k} + \frac{A_c \sqrt{2g \Delta H_o} c}{L A_{go} k} \right) \quad (\text{II. 11d})$$

These equations also hold good when the valve is placed at the downstream end of the culvert, but then c_k is negative. Condition for the design of a stable, undamped valve is that the equations above have a solution wherein the imaginary damping $c < 0$.

Equations (II. 11c and 11d) can be abbreviated to:

$$\omega^2 = \frac{k}{m} \frac{1}{\left(1 + \frac{1}{c_m} + \alpha \frac{c}{m} \right)} = \frac{k}{m} \left(1 - \frac{1}{c_k} + \beta \frac{c}{k} \right) \quad (\text{II. 11e})$$

wherein α and β are positive coefficients in which only geometric and hydrodynamic parameters are involved. The value of c can be calculated from (II. 11e):

$$\frac{\alpha \beta}{m k} c^2 + \left\{ \frac{\alpha (c_k - 1)}{c_k m} + \frac{\beta (c_m + 1)}{c_m k} \right\} c + \frac{1}{c_m} - \frac{1}{c_k} - \frac{1}{c_k c_m} = 0$$

II. 5 Plug valve

A valve without a mechanical damper is stable when both roots of the imaginary damping value c are negative. This is reached when:

$$\frac{1}{c_m} - \frac{1}{c_k} - \frac{1}{c_k c_m} > 0 \left\{ \begin{array}{l} \underline{a} \ c_k > 0 \text{ and } c_k > c_m + 1 \\ \underline{b} \ c_k < 0 \text{ and } c_k < c_m + 1 \end{array} \right.$$

The determinative condition for stability is that either

$$c_k > c_m + 1 \quad (\text{II. 12a})$$

or

$$c_k < 0 \quad (\text{II. 12b})$$

This means that a valve with its seat at the upstream side is not subject to self-excited vibrations. A discussion of the physical aspects of this result can be found in the introduction of chapter III.

If there is mechanical or hydrodynamic damping, equations (II. 11a and 11b) can be combined:

$$\begin{aligned} \omega^2 &= \frac{k}{m} \left\{ \frac{1}{1 + \frac{1}{c_m} \left(1 + c \frac{A_{go}}{\rho A_c^2 \sqrt{2g \Delta H_o}} \right)} \right\} = \\ &= \frac{k}{m} \left\{ 1 - \frac{1}{c_k} \left(1 - c \frac{1}{\rho L \sqrt{2g \Delta H_o} (dA_g/dy)} \right) \right\} \end{aligned}$$

and finally in:

$$c_k = \left(1 + c_m + \frac{c A_{go}}{\rho A_c^2 \sqrt{2g \Delta H_o}} \right) \frac{1 - \frac{c}{\rho L \sqrt{2g \Delta H_o} (dA_g/dy)}}{1 + \frac{c A_{go}}{\rho A_c^2 \sqrt{2g \Delta H_o}}} \quad (\text{II. 13})$$

From this last equation, a relation between c_k and c can be found for every hydrodynamic condition, which relation leads to the necessary minimum damping value in the range $0 < c_k < c_m + 1$.

Note:

If the culvert is short, in calculations with equation (II. 13) a correction has to be introduced in the culvert length L , because of the additional inertia of the pulsating discharge in the transition zone before the discharge is evenly distributed over the culvert cross-section.

Chapter II. Self-exciting vibrations

This effect interferes only in the term $c/\rho L \sqrt{2g \Delta H_0} (dA_g/dy)$ of equation (II. 13). The corrected length can be described as $L = \text{culvert length} + c_L \times \text{hydraulic radius}$, wherein c_L depends on the ratio $\delta_0/\text{hydr. radius}$ and can be read from the graph of fig. II. 14 (Fig. II. 14 mentions h/δ as parameter, but in this case it has to be read as $\text{hydr. rad.}/\delta$. The hydraulic radius is A_c/L_c).

6. THE MINIMUM "REDUCED" FREQUENCY REQUIRED FOR STABILITY OF AN UNDAMPED PLUG VALVE

Equation (II. 12), the stability condition for a valve without mechanical damping, can also be expressed in terms of a demand for a *minimum reduced frequency*. This is a dimensionless number with the character $f_n L/V$. ($f_n = \text{natural frequency}$; $L = \text{a representative length}$, for which the gate opening δ_0 is taken; and $V = \text{a representative velocity}$, $\sqrt{2g \Delta H_0}$). The natural frequency f_n is computed from

$$f_n = \frac{\text{support rigidity}}{2\pi (\text{gate mass} + \text{water mass in the culvert})}$$

When the definitions $c_k = \frac{k A_{go}}{\rho A_c (2g \Delta H_0) (dA_g/dy)}$ and $c_m = \frac{m}{\rho A_c L}$

and the condition $c = 0$ are introduced in the equation (II. 11a) the result is:

$$\omega^2 = \frac{k}{m \left(1 + \frac{\rho A_c L}{m} \right)}$$

$$\text{or } \omega^2 = \frac{k}{\rho A_c L (1 + c_m)} = \frac{c_k \rho A_c 2g \Delta H_0 (dA_g/dy)}{\rho A_c L (1 + c_m) A_{go}}$$

Introducing the condition for stability, $c_k > 1 + c_m$, we get:

$$\omega^2 \geq \frac{2g \Delta H_0}{L A_{go} / (dA_g/dy)}$$

In the case of the plug valve, $A_{go} = \mu \delta_0 L_c$ and $dA_g/dy = \mu L_c$. Because μ is supposed to be constant:

$$\frac{\omega \delta_0}{\sqrt{2g \Delta H_0}} \geq \sqrt{\frac{\delta_0}{L}}$$

II. 7 Experimental data, plug valve

This can be seen as a demand for a reduced natural frequency:

If the natural frequency f_n is calculated from spring rigidity and mass, including the water mass in the pipe, and if the velocity is defined as the local maximum velocity $\sqrt{2g \Delta H_0}$, a safe design for a plug valve requires the following relation between the reduced natural frequency and the gap width:

$$S_n = \frac{f_n \delta_0}{V} \geq \frac{1}{2\pi} \sqrt{\frac{\delta_0}{L}} \quad (\text{II. 14})$$

7. EXPERIMENTAL DATA TO CHECK THE PLUG VALVE THEORY

Equation (II. 13) has been checked for the culvert valves of the Kreekrak navigation lock. The roller gates were designed, because of severe demands for watertightness in closed position, with a continuous rubber seal at their downstream face (fig. II. 2).

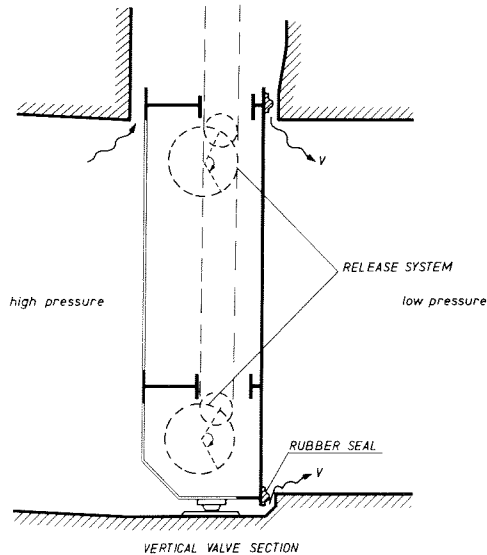


FIG. II. 2

Before raising, the gate was moved from the seat in upstream direction; a gap was created similar to that of fig. II. 1. In the hydraulic model, the bending rigidity of the gate was reproduced by a stiff gate supported by a single spring. This gate came into a self-excited vibration. A cursory analysis of the report [24] leads to the conclusion that c_m must have been of the order of 0.3. The theoretical c_k value

Chapter II. Self-exciting vibrations

for a safe design consequently had to be at least 1.3. In the test, c_k was somewhat smaller than unity.

In the modified model, which did not come into vibration, the gap width was increased and measures were taken to reduce (dA_g/dy) , because it was supposed that bending of the gate in reality leads only to variation of the gap area (due to vibration) at the middle of the gate. The c_k value estimated for the final model was about 2. This agrees with the theoretical value required for c_k .

The uncertainties in the estimates are due to the fact that in the mass of the gate is included the upstream added water mass, which in a case like fig. II. 2 is difficult to estimate.

8. ESTIMATE OF MAXIMUM FORCES IN THE RESILIENT GATE SUSPENSION

Experience at the Kreekrak gate model [24] shows that in some cases an increase of amplitude causes the gate to hit its seat. If the resilient suspension has to be designed so that the undamped valve can withstand all possible forces, the maximum force can be computed with equation (II. 12a). For the case of fig. II. 1:

$$dA_g/dy = \mu L_c \quad (\text{see the remark made after equation (II. 7)}).$$

The widest critical gap at which vibrations can occur is characterized by:

$$c_k = 1 + c_m \quad (\text{see equation (II. 12a)}).$$

Furthermore:

$$c_k = \frac{k \mu \delta_o L_c}{\rho A_c 2g \Delta H_o \mu L_c} = \frac{k \delta_o}{2\rho g A_c \Delta H_o}$$

The maximum spring force occurs when at this valve opening (δ_o) the valve touches its seat as the result of a vibration amplitude equal to δ_o . This force equals $k \delta_o$.

$$F_{\max} = k \delta_o = c_k 2\rho g A_c \Delta H_o = 2 c_k * (\text{static load})$$

Because $c_k = 1 + c_m$, the total force due to the vibration is:

$$F_{\max} = (2 + 2 c_m) * (\text{static load})$$

II. 9 Reversed Taintor valve

The total force, including the static load, becomes:

$$F_{\text{tot}} = (3 + 2 c_m) * (\text{static load})$$

This means that when there is no damper (and for safety reasons the unknown water damping has been neglected), this force is independent of the chosen suspension rigidity. However, when the critical gap width occurs during opening or closing of the gate, the critical gap width range will decrease proportionally to the rigidity value, and consequently the critical range will be passed in a shorter time. To obtain a reduction of F_{tot} , only a damper is effective.

9. SELF-EXCITING VIBRATIONS OF A REVERSED TAINTOR VALVE

The reversed Taintor valve has been used as a non-aerated valve in lock culverts (see [62] and [23]). The low-pressure region downstream of the valve is not connected to the atmosphere, because the shaft has a high water-level. Sometimes the valve is slightly aerated downstream by means of aeration tubes and fine lateral distribution grids to prevent wall erosion by cavitation by means of small air bubbles [84]. This has to be considered as an emergency measure; the efficiency of a lock system is reduced by aeration: air pockets endanger the water distribution in culverts with branches, possible detergents in the water will foam, and ships sink deeper because of the reduced water density.

The sector shaped gate is a guarantee for a rigid structure; and when sideward movements are prevented by sliding seals, which are leakage-free over the whole gate way, its dynamic behaviour can be considered as a single oscillator wherein only rotational vibrations around the pivot axis can occur. The type investigated at the Delft Hydraulics Laboratory (see [23] and Appendix B) had a sharp and rigid bottom edge formed by the retaining plate itself, and sealing was effected with a rubber slab embedded in the culvert bottom. In the original design, sealing at the culvert ceiling was effected with a rubber seal attached to a lip B of the gate (see fig. II. 3). At small valve openings, heavy vibrations occurred, which are dealt with in the following computation scheme.

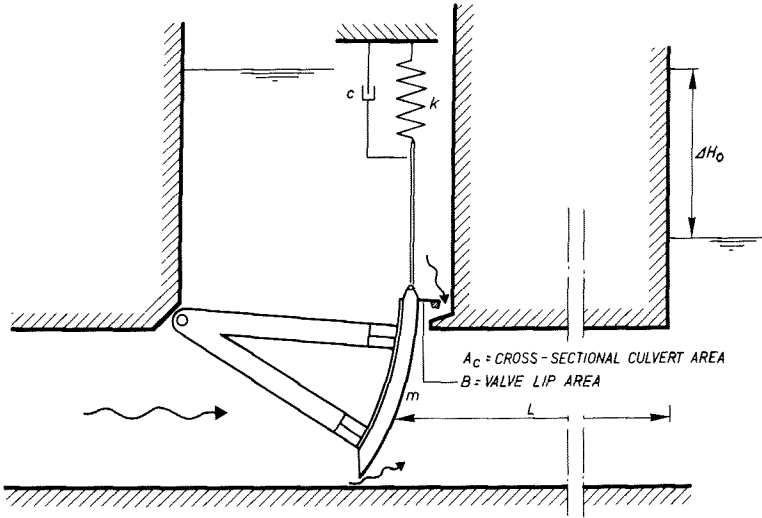


FIG II.3

The leakage gap at small openings is both at the top and at the bottom of the gate. The total effective gap area is again called A_g . The variation of the gap area caused by vibration is defined as (dA_g/dy) , as in the preceding paragraph. Also the same assumptions are made; and the following basic equations can be derived for vibration in vertical direction:

- Force equation, similar to (II. 3)

$$F = \rho g B \Delta H' = - m \ddot{y} - c \dot{y} - ky \tag{II. 15}$$

For m , the virtual mass of the water around all girders upstream of the retaining plate has to be estimated. The polar moment of inertia around the pivot axis has to be reduced to an equivalent mass hanging on the suspension spring.

- Discharge equation, similar to (II. 4)

$$Q = A_g \sqrt{2g \Delta H} - B \dot{y} \tag{II. 16}$$

- Acceleration of the water column in the culvert, similar to (II. 5)

$$\Delta H' = \frac{-L}{g A_c} \ddot{Q} \tag{II. 17}$$

Again, when the culvert is short, a correction on the length L has to be estimated. The analysis results in a similar expression for the suspension rigidity as has been found in the preceding paragraph.

II. 9 Reversed Taintor valve

If

$$c_m = \frac{m A_c}{\rho L B^2}$$

and

$$c_k = \frac{k A_{g0}}{\rho B 2g \Delta H_o (dA_g/dy)}$$

the following equation is obtained:

$$c_k = \left(1 + c_m + \frac{c A_{g0}}{\rho B^2 \sqrt{2g \Delta H_o}} \right) \frac{1 - \frac{c A_c}{\rho L B \sqrt{2g \Delta H_o}} (dA_g/dy)}{1 + \frac{c A_{g0}}{\rho B^2 \sqrt{2g \Delta H_o}}} \tag{II. 18}$$

The differences between the equations (II. 13) and (II. 18) follow from the fact that L is representative of the extra head difference across the valve due to the inertia of the water in the culvert. Whereas in the case of the plug valve the piston effects cause a displacement of the gate resulting in an acceleration of the culvert flow velocity v of $dv/dt = \ddot{y}$, reversed Taintor valve vibration only causes displacement of the water by the gate lip B. When this water displacement is distributed over the whole culvert cross-sectional area A_c , the acceleration in the culvert becomes $dv/dt = \ddot{y} B/A_c$. This means that the culvert length L is reduced to an effective length $L B/A_c$. The extra head difference, due to the inertia of the water, only acts on the gate lip B instead of on the whole gate area A_c , as was the case in the preceding paragraph. This means that the factor $A_c L$ is now reduced to $L B^2/A_c$, while in the other terms the area A_c is reduced to B.

Again, to be on the safe side when designing the valve, it is enough to compute c_k in case there is no mechanical damping.

$$c_k \geq 1 + c_m$$

Because c_k varies with the valve position, there can always be found a critical gate opening A_{g0} . When the gate has a smaller opening, self-exciting vibrations will occur.

Note:

When calculating c_m , the length L has to be increased by $c_L \times$ culvert height, wherein c_L follows from the graph of fig. II. 14. For h/δ must be read A_c/B which is equal to the relation culvert height/gate lip width.

Chapter II. Self-exciting vibrations

When using equation (II. 18), in the term in which both c and L occur, the length L is the culvert length increased by $\frac{1}{2} c_L h_c$.

A remedy against self-exciting vibrations lies in the suppression of the gate lip B .

Another solution is proposed, among others, by Krummet [53]. Fig. II. 4 is the application in the Kainji Dam project^{*}. In Krummet's solution, a stiff rubber seal is used in combination with a metal lip at the seat, which lip reduces the pressure differential across the seal. A further reduction of the maximum vibration can be obtained by the application of a damper.

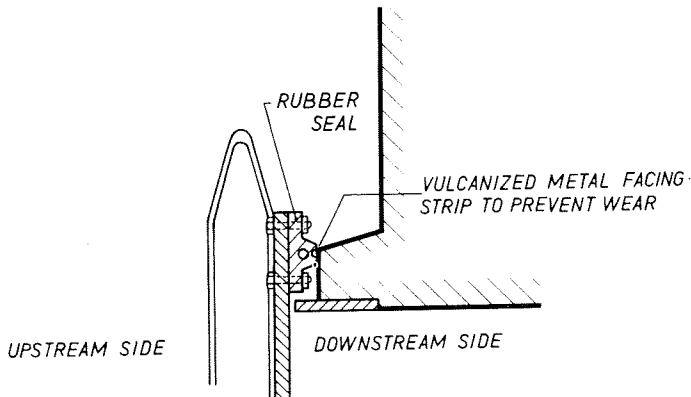


FIG. II. 4

10. EXPERIMENTAL DATA TO CHECK THE TAINTOR VALVE THEORY

In a model investigation of a reversed Taintor valve for a 25 m head navigation lock, it was tested at which gate opening the gate condition was at the transition between the vibrating and the non-vibrating stage. The vibrations found during the model tests occurred at a small valve opening. From the results^{*} it could be concluded that the critical situation appeared at $c_m = 26.5$ and $c_k = 29$. This agrees quite well with the relation $c_k = c_m + 1$. However, from an analysis wherein the still-water damping, measured in the model, was also taken into account, a c_k value of about 10 had to be expected.

^{*} Results can be made available from the Delft Hydraulics Laboratory.

II. 11 Cylinder valve

11. POSSIBILITY OF APPLICATION OF THE THEORY TO CYLINDER VALVES

The problems with a cylinder valve can be similar to those of the Taintor valve. When, the gate seal radius r is distance b greater than the central core radius (see fig. II. 5), the area $2\pi r b = B$ is equivalent to the gate lip of the reversed Taintor valve.

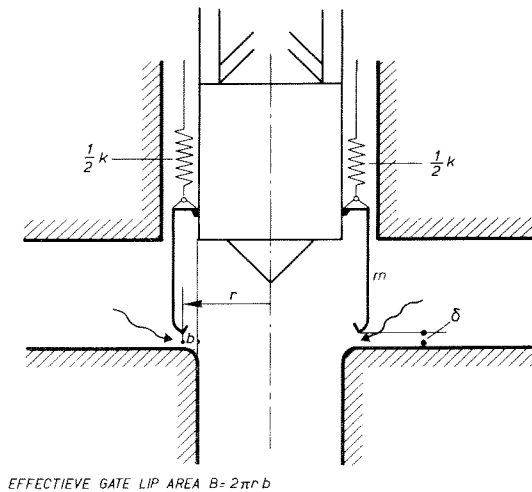


FIG. II.5

The leakage gap A_g consists partly of the gap underneath the gate and partly of the leakage near the upper seal. The variation of the gap width with the vertical vibrational displacement (dA_g/dy) will only occur below. If the culvert is short, a fictive length has to be added to represent the extra inertia in the transition zone where the locally induced velocity fluctuations are distributed over the cross-sectional culvert area. This fictive added length is difficult to determine exactly in this case. It seems reasonable, however, to compute the value c_m with a culvert length including the valve height, to use the ratio $b/\text{hydraulic radius}$ instead of δ/h to find the value c_L in fig. II. 14 and to take $c_L \approx \text{hydr. rad.}$ as the virtual length to be added.

In this analysis it has been presupposed that there is a rigid support of the central core. If this is not the case, and if the valve is connected to the core, a self-exciting vertical vibration can occur like that of a plug valve.

With the cylinder valve, no special experience has been gained as yet to check the theoretical minimum value of c_k for a vibration-free design. A remedy against self-exciting vibrations can be found in reducing the radius differential b to zero, or, if the upper water-level is not too high and aeration is permitted, in omitting the upper seal and using a gate cylinder of such height that its upper part projects above the upstream water. This solution has been proposed for the cylinder valve in the weir in the Lower Rhine at Amerongen, which had to be replaced because of damage due to dynamic loads.

12. SELF-EXCITING VERTICAL VIBRATIONS OF GATES

In this paragraph, a computation scheme is presented that explains the occurrence of self-exciting vertical vibrations in valves and gates at nearly closed position.

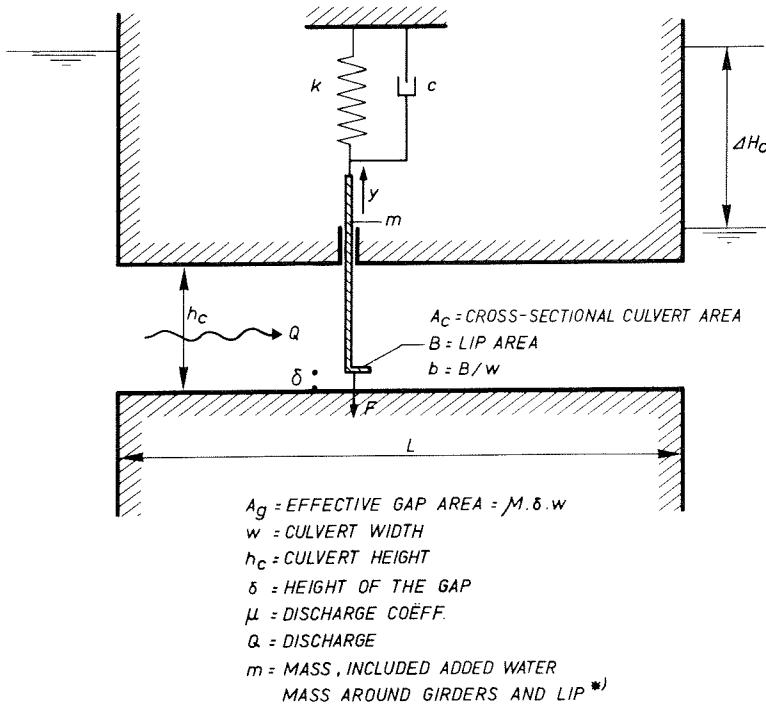


FIG. II. 6

* See fig. IV. 6.

II. 12 Vertical vibrations

The assumptions for the computation are the same as in par. 5. Though in the computation scheme of fig. II . 6 the inertia of the water is again due to the length L of the closed culvert, it will be shown that for free-surface flow an equivalent length can be introduced. The wave radiation at free-surface flow is neglected in the first analysis; firstly because the radiated energy is small at higher frequencies and secondly because the simpler results enable one to see which factors are the dominant causes of instability. The basic equations in this computation are the same ones as in par. 5.

- Force equation

$$F' = c_F \rho g B \Delta H' = - m \ddot{y} - c \dot{y} - ky \quad (\text{II. 19})$$

The value of c_F is further discussed in par. 7B of this chapter.

- Discharge equation

$$Q = A_g \sqrt{2g \Delta H} \quad (\text{II. 20})$$

ΔH is the local head difference across the gap. The value of the discharge coefficient, which is included in A_g , will be discussed for a rectangular valve edge in par. 17.

- Acceleration of the water column

$$\Delta H' = \frac{-L}{g A_c} \dot{Q} \quad (\text{II. 21})$$

With a short culvert length it is important to know that the length L has to be increased by a term $(2 c_L + b/\delta) h_c$, see equation (II. 49), in which c_L can be read from the graph of fig. II. 14. The factor 2 is due to the fact that pressure pulsation, related to discharge fluctuations, arises both upstream and downstream of the valve.

For the *free-surface flow* the equation is:

$$\Delta H' = - (c_{Lu} + c_{Ld} + b/\delta) \frac{\dot{Q}}{g w} = - c_L \frac{\dot{Q}}{g w} \quad (\text{II. 21a})$$

This equation is derived in par. 16; see equation (II. 54). The length coefficients c_{Lu} and c_{Ld} can be read from the graph of fig. II. 17, wherein the value of c_L depends on the relation δ/h so that the upstream water depth results in the value c_{Lu} , and c_{Ld} follows from the downstream conditions. In fact, the inertia effect of the water has now not been related to the acceleration of the culvert flow velocity (\dot{Q}/A_c) , but to the acceleration of the gap flow velocity $(\dot{Q}/w \delta)$; and

Chapter II. Self-exciting vibrations

the equivalent length to be introduced in equation (II. 21) is $c_L \delta$, instead of the culvert length L . The value $(L/gA_c) \dot{Q}$ in equation (II. 21) now changes into:

$$(c_L \delta / g w \delta) \dot{Q} = (2 c_L / gw) \dot{Q}, \text{ so}$$

$$\Delta H' = - 2 c_L \frac{\dot{Q}}{gw}$$

Note:

The displacement of water due to the vibration movement has not been treated separately. When, during the vibration movement the gate moves downwards, water has to be pressed away and at the same time an equal amount of water will be sucked in above the lip. For this reason, the effect is only a local additional flow, resulting in an added mass effect, which in normal cases will be small compared with the gate mass (see chapter IV, fig. 6b).

When the equations (II. 19, 20 and 21) are worked out in the same way as in par. 5, this results in:

$$c_k^{-1} = 2 c_F \rho g B \Delta H_o (dA_g / dy) / k A_{go}$$

and:

$$c_k^{-1} = \frac{c}{k} \frac{A_c \sqrt{2g \Delta H_o}}{A_{go} L} + \frac{c A_{go} L}{c A_{go} L + m A_c \sqrt{2g \Delta H_o}} \quad (\text{II. 22})$$

c_k has kept the same meaning as in par. 5: the relation between the spring rigidity of the suspension and the hydrodynamic counter-rigidity, calculated under the assumption that the discharge remains constant. The head, and consequently the suction force, varies with the gate opening which can result in a hydrodynamic counter-rigidity. Equation (II. 22) can be simplified because c_k^{-1} will be small; in fact it is the relation between the suction force and the force necessary to suck the gate onto the bottom seat. Assuming that $A_{go} = \mu w \delta$ and $\partial A_g / \partial y = \mu w (\partial \delta / \partial y) \equiv \mu w$, equation (II. 22) becomes:

$$c_k^{-1} = \frac{2 c_F \rho g B \Delta H_o}{k \delta_o} = \frac{c}{k} \frac{h_c \sqrt{2g \Delta H_o}}{\mu \delta_o L} + \frac{c}{m} \frac{\mu \delta_o L}{h_c \sqrt{2g \Delta H_o}} \quad (\text{II. 23})$$

When we introduce the symbols S_n (reduced natural frequency):

II. 12 Vertical vibrations

$$S_n = \frac{f_n \delta_o}{V} = \frac{\omega_n \delta_o}{2\pi \sqrt{2g \Delta H_o}} \quad \text{and} \quad \omega_m^2 = \frac{k}{m},$$

equation (II. 23) can be changed into:

$$c = c_F \rho B \sqrt{2g \Delta H_o} \frac{\mu(L/h_c)}{1 + 4\pi^2 \mu^2 (L/h_c)^2 S_n^2} \quad (\text{II. 24})$$

When the correction for the culvert length is taken into account, the c_L value of fig. II. 14 can be introduced into this equation:

$$c = c_F \rho B \sqrt{2g \Delta H_o} \frac{\mu(L/h_c + 2c_L)}{1 + 4\pi^2 \mu^2 (L/h_c + 2c_L)^2 S_n^2} \quad (\text{II. 24a})$$

c is a measure for the energy transfer from the flow to the mechanical system, which is also a measure for the self-excitation magnitude.

For $c_F > 0$, a continuous self-amplifying vibration will occur. If the excitation is small, the envelope curve of the vibration graph will show the function:

$$y = Y_o e^{\gamma \omega_n t}$$

$$\gamma = \frac{c}{2m \omega_n} = \frac{1}{2} \mu c_F \frac{\rho B \delta/m}{2\pi S_n h_c/L + 8\pi^3 S_n^3 \mu^2 L/h_c}$$

For free-surface flow equation (II. 24) results in:

$$c = c_F \rho B \sqrt{2g \Delta H_o} \frac{\mu(c_{Lu} + c_{Ld} + \frac{b}{\delta})}{1 + 4\pi^2 \mu^2 (c_{Lu} + c_{Ld} + \frac{b}{\delta})^2 S_n^2} \quad (\text{II. 24b})$$

If information exists on damping of the girders in the water or on linear damping of the mechanical system, the equations (II. 23 and 24) can be used to calculate the minimum necessary rigidity, the maximum allowable head difference etc. Self-excited vertical vibrations will be mainly effected when the lower gate edge is so shaped that the pressure distribution therebelow causes a suction force. Additional effects will be discussed in par. 7b. The predominance of suction is in agreement with the experience that with a rectangular edge profile instability

Chapter II. Self-exciting vibrations

occurs mainly at openings smaller than the seal width; the low-pressure zones occur because of flow reattachment. The same holds true for semi- or quarter-circular edges; it is most probable that circular edges are not instable because of the instability of flow separation, but because low-pressure zones occur near the separation point. Until now, there exists no more than qualitative experimental evidence for the equations (II. 22, 23 and 24), namely that in all cases where in self-exciting vibrations have occurred the gate edge profile is such that suction forces can be expected.

The results of the equations (II. 24a and 24b) can be presented in a single graph, if c_i (the inertia coefficient) is introduced:

$$c_i \begin{cases} = L/h_c + 2c_L & \text{for a closed culvert} \\ = c_{Lu} + c_{Ld} + b/\delta & \text{for free-surface flow} \end{cases}$$

A measure for self-excitation is c , which has been introduced into the computation as the value of a (hypothetical) mechanical damper which makes the vibration a stationary one. The value of c is presented in fig. II. 7 in a dimensionless way; the dimensionless self-excitation coefficient c_{se} is introduced:

$$c_{se} = c/c_F \rho B \sqrt{2g \Delta H_o}$$

When conclusions are drawn from fig. II. 7, the following points must be taken into consideration:

- c_F follows from equation (II. 60) and depends on the geometry and on the waterlevels. The highest value is reached when suction occurs, that is, for a rectangular seal profile, when δ is smaller than or equal to $0.65 b$.
- μ can vary with the gap height; it can vary between 0.6 and 1 , depending on edge profile and gap height. For the rectangular seal of equation (II. 64), there is found $\mu = 0.895$ when reattachment of flow occurs, and $\mu = 0.6 - 0.65$ when reattachment does not occur.
- The resulting self-excitation is the summation of c and other damping factors. The water-damping by flow mainly depends on the water velocity and is roughly proportional thereto (see Chapter IV).
- At low frequencies, wave radiation can cause additional damping.

II. 12 Vertical vibrations

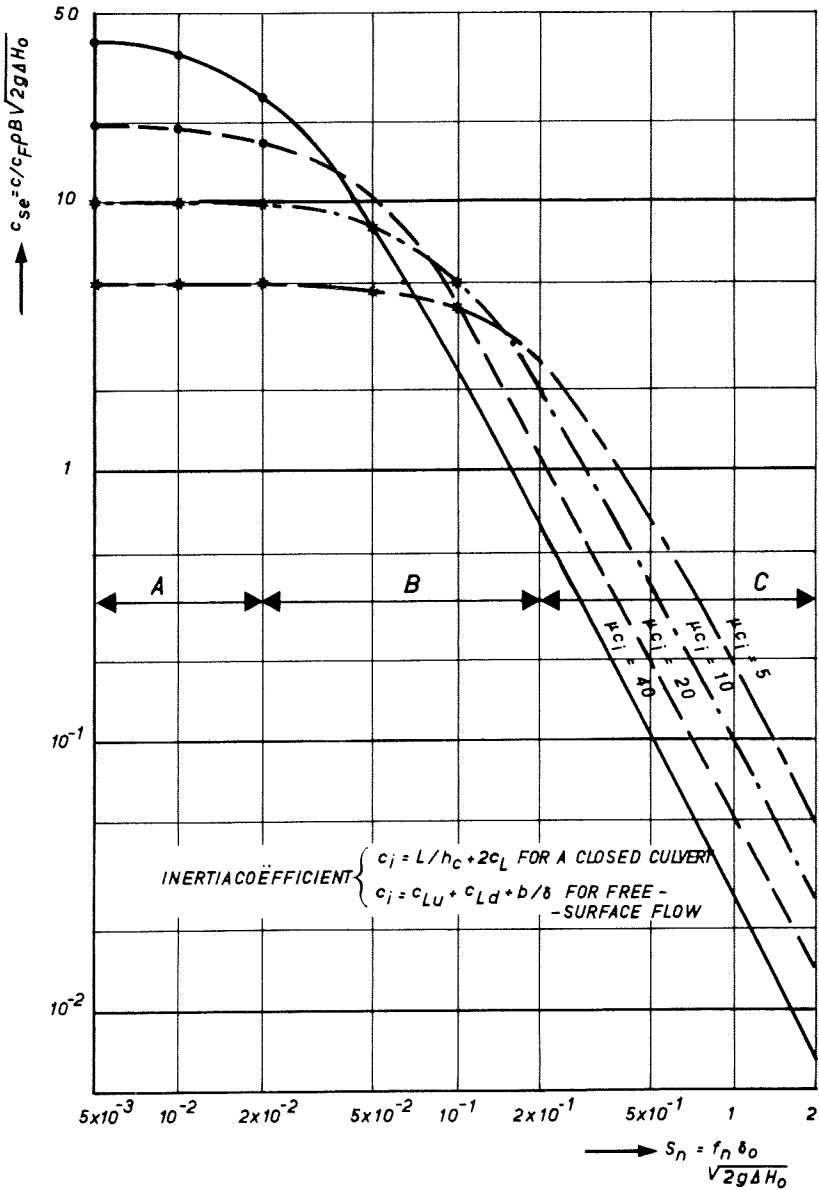


FIG. II. 7

When considering fig. II. 7, three zones can be discerned: A where c_{se} is roughly constant; C where $c_{se} \propto S_n^{-2}$; and the intermediate zone B. It will now be tried to define for a rectangular sectioned lower edge of a gate, which are the most critical conditions.

Chapter II. Self-exciting vibrations

- When certain hydrodynamic conditions are given, more safety is obtained by an increased rigidity, because S_n is then increased and c_{se} decreases.
 - When the edge thickness is reduced, a comparable critical condition occurs when $\delta/b = 0.65$. For this gate opening (keeping the head difference and the resonance frequency of the structure the same), S_n and B will decrease proportionally to b . The resultant excitation c will tend to increase in zone C, because c_{se} increases proportionally to b^{-2} . The increase of c will not be fully proportional to b^{-1} , because c_i tends to increase; but this effect will not be great. In zone A, the self-excitation decreases, because the lip area B has been reduced, while c_{se} remains constant. The greatest self-excitation can be expected in zone B.
 - When the gate is lowered beyond the critical gate opening $\delta/b = 0.65$, c_F will decrease (see equations (II. 60 and 65)). S_n will decrease ($\propto \delta$) and so c_{se} will in zone C increase ($\propto \delta^{-2}$). In zone A, the self-excitation will decrease, because c_{se} remains constant and c_F decreases. This effect is somewhat, but not totally, compensated by the increase of the coefficient c_i . In this case also, the greatest self-excitation can be expected in zone B.
 - A greater head difference tends to increase the self-excitation, especially in zone C (S_n decreases because $\sqrt{2g \Delta H_0}$ increases); but in zone A, both the self-excitation and the hydrodynamic damping will increase proportionally to $\sqrt{2g \Delta H_0}$, so the effect of ΔH will not be large.
- A discussion on the physical aspects of this solution can be found in the introduction of Chapter III.

In the preceding analysis it was found that with a seal causing a resultant suction force, instability can occur at all head differences and for each suspension spring rigidity and/or reduced natural frequency. In practice, however, this is not the case. This is probably due to the effect of hydrodynamic damping. Still little information is available on this damping, and for safety its effect has to be underestimated. However, there is one term of the hydrodynamic damping of which an estimate is available: the effect of wave radiation. For completeness the result of this analysis will be presented in the following paragraph, although no great influence of this damping is found.

II. 13 Vertical vibrations with damping

13. VERTICAL GATE VIBRATIONS WITH DAMPING DUE TO WAVE RADIATION

The fluctuating flow is, by equation (II. 21), related to a pressure head difference proportional to the flow variation \dot{Q}' . This is the mechanism by which energy transfer can occur, which then will radiate. The additional head due to the radiation at the upstream side of the gate can be represented by the function:

$$\Delta H'_u = f(Q', \omega, h_u, \delta, w, g)$$

(h_u = water depth upstream of the gate; $\Delta H'_u$ = the pressure head variation just upstream of the gap).

From dimensional considerations, by considering the flow to be two-dimensional and from knowing from wave theory that $\Delta H'_u \propto Q'$ when Q' is small, the following formula can be set up:

$$c_{ru} = \frac{\Delta H'_u g w}{Q' \omega} = f\left(\frac{\delta_o}{h_u}, \frac{\omega^2 h_u}{g}\right) \quad (\text{II. 25a})$$

(c_{ru} = radiation coefficient at the upstream side)

Parallel reasoning for the downstream side leads to the equation:

$$c_{rd} = \frac{\Delta H'_d g w}{Q' \omega} = f\left(\frac{\delta_o}{h_d}, \frac{\omega^2 h_d}{g}\right) \quad (\text{II. 25b})$$

wherein the index d refers to the downstream side.

This is a simplified expression, because the influence of the flow velocity near the free water surface on the wave velocity is neglected. So, the effect of wave radiation can be written as:

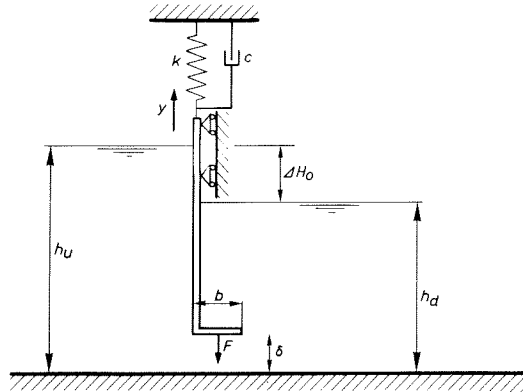
$$\Delta H'_r = \Delta H'_u + \Delta H'_d = -\frac{Q' \omega}{g w} (c_{ru} + c_{rd}) \quad (\text{II. 26})$$

In the same way as in equation (II. 21a), the inertia effect of the water can be expressed by the equation (see equation (II. 54):

$$\Delta H'_m = - (c_{Lu} + c_{Ld} + b/\delta) \frac{\dot{Q}'}{g w} \quad (\text{II. 27})$$

But now c_{Lu} is a function of both δ_o/h_u and $\omega^2 h_u/g$, whereas in equation (II. 21a) the latter had no effect. The term b/δ results from the inertia of the water under the gate; b is the length of the gate seal in flow direction.

Chapter II. Self-exciting vibrations



w = CANAL WIDTH
 A_g = EFFECTIVE GAP AREA
 B = GATE LIP AREA = $b w$
 F = FORCE
 h = WATER DEPTH
 u = UPSTREAM d = DOWNSTREAM

FIG. II. 8

The basic equations for computation now become:

- Force equation

$$F' = c_F \rho g B \Delta H' = -m\ddot{y} - c\dot{y} - ky \quad (\text{II. 28})$$

- Discharge equation

$$Q = A_g \sqrt{2g \Delta H} \quad (\text{II. 29})$$

ΔH = local head difference across the gap.

- Acceleration of the water column with damping by radiation

$$\Delta H_0 = \Delta H + (c_{ru} + c_{rd}) \frac{Q'}{g w} + (c_{Lu} + c_{Ld} + b/\delta) \frac{\dot{Q}}{g w} \quad (\text{II. 30})$$

From these equations, the same procedures have been followed as before and the resulting equations become:

$$\omega^2 = \frac{k}{m} \left[1 - \frac{c_F 2g \Delta H_0 \rho B (dA_g/dy)}{k A_{go}} + \frac{c}{k} \left\{ \frac{w \sqrt{2g \Delta H_0}}{(c_{Lu} + c_{Ld}) A_{go}} + \frac{\omega(c_{ru} + c_{rd})}{c_{Lu} + c_{Ld}} \right\} \right] \quad (\text{II. 31a})$$

and

II. 13 Vertical vibrations with damping

and

$$\omega^2 = \frac{k \left\{ 1 - \frac{(c_{ru} + c_{rd}) \omega c_F \rho B (dA_g/dy) \sqrt{2g \Delta H_o}}{k w} + \frac{(c_{ru} + c_{rd}) \omega A_{go}}{w \sqrt{2g \Delta H_o}} \right\}}{m \left\{ 1 + \frac{(c_{ru} + c_{rd}) \omega A_{go}}{w \sqrt{2g \Delta H_o}} + \frac{(c_{Lu} + c_{Ld} + b/\delta) A_{go}}{w \sqrt{2g \Delta H_o}} \frac{c}{m} \right\}} \quad (\text{II. 31b})$$

These equations have not been analyzed in detail, but they can serve as a base for further experimental work. A check has been made, whether the condition $c_F < 0$ is still sufficient for safe design. This is always the case when $\rho B \delta / m < \mu^2 c_F (c_{Lu} + c_{Ld})^{-2}$. This condition is always fulfilled in practice.

It is of interest which maximum head difference a gate can withstand without need of mechanical damping, supposing that all the energy loss is due to wave radiation; $c = 0$. With the reasonable assumption that all terms between the brackets are much smaller than unity, the following expression can be derived after having denominated the small terms ϵ_1 , ϵ_2 , etc. Equation (II. 31) can now be written (the terms with c being equal to zero) as:

$$\omega^2 = \frac{k}{m} (1 - \epsilon_1) = \frac{k (1 - \epsilon_2 + \epsilon_3)}{m (1 + \epsilon_4)}$$

This results in:

$$1 - \epsilon_1 + \epsilon_4 \sim 1 - \epsilon_2 + \epsilon_3$$

or:

$$\begin{aligned} 1 - \frac{c_F 2g \Delta H_o \rho B (dA_g/dy)}{k A_{go}} + \frac{\omega (c_{ru} + c_{rd}) A_{go}}{w \sqrt{2g \Delta H_o}} &= \\ = 1 - \frac{(c_{ru} + c_{rd}) \omega c_F \rho B (dA_g/dy) \sqrt{2g \Delta H_o}}{k w} + \\ + \frac{\omega (c_{ru} + c_{rd}) A_{go}}{w \sqrt{2g \Delta H_o}} \end{aligned}$$

or:

$$\frac{c_F 2g \Delta H_o \rho B (dA_g/dy)}{k A_{go}} = \frac{(c_{ru} + c_{rd}) \omega c_F \rho B (dA_g/dy) \sqrt{2g \Delta H_o}}{k w}$$

Chapter II. Self-exciting vibrations

or:

$$\frac{\omega \sqrt{2g \Delta H_o}}{\omega A_{go} (c_{ru} + c_{rd})} = 1$$

Introducing the reduced natural frequency, defined in the same way as in equation (II. 24), and with $A_{go} = \mu \delta_o$ we find:

$$S_n = \frac{1}{2\pi} \frac{\omega \delta_o}{\sqrt{2g \Delta H_o}} = \frac{1}{2\pi (c_{ru} + c_{rd})} \quad (\text{II. 32})$$

The c_r values are calculated for some schematized cases and the results are presented in fig. II. 18. This under the assumption that the flow through the gap is so small that the velocities of the water in the upstream and downstream basins are small enough not to effect a wave velocity of (g/ω) , and that the flow related to the permanent discharge does not disturb the potential flow caused by the flow fluctuations. Use has been made of a new developed computation programme of the Delft Hydraulics Laboratory [12].

Validity of the computations leading to equation (II. 32) can only be expected for small δ/h values; otherwise the uneven flow distribution in the gap will interfere. The graphs of fig. II. 18 have been extended also for greater δ/h values; this can be used for other calculations of radiated energy, for instance when a flow which is evenly distributed over the culvert area debouches into a free-surface basin. It can be seen that equation (II. 32) leads to such extremely high S_n values that for most cases other damping factors will be of more importance than wave radiation. As has been stated before, not much information exists on other hydrodynamic damping factors, such as damping coefficients of struts and girders in the flow.

14. DISCHARGE FLUCTUATIONS AND WAVE PRODUCTION

Surface waves caused by vibration are mainly produced at the upstream side of gates. Downstream, the relative high surface velocity in the eddy, directed toward the gate, suppresses wave radiation. If $V > g/4\omega$, it can be proved that no radiation can even occur. (see fig. IV. 5 with the text belonging to it). In models, this velocity limit is greater than $g/4\omega$, because of the influence of surface tension.

With horizontal vibrations, the radiated waves are deep-water waves; this is due to the relatively high frequency of the vibrations

II. 14 Discharge fluctuations and waves

(Deep-water waves are produced when the waterdepth $h \gg \pi g/\omega^2$). The maximum wave amplitude can become $a = 2Y_0$ (a = wave amplitude, Y_0 = vibration amplitude), but only when the approach velocity of the upstream water is small (see equation (IV.30)). With the vertical vibrations, waves are radiated with their crests parallel to the gate (plate II. 2), which is partly due to the discharge fluctuations under the gate. Horizontal vibrations mostly produce a cross pattern of waves, the amplitude of which can be spectacular (pp. 35 and 65 (pl. 3); a spectacular picture has been presented by Petrikat and Minor [82]). This cross pattern is a combination of waves generated by the gate itself and generated at the corners by discharge fluctuations. The horizontal vibrations are excited by a mechanism similar to that which has been shown for the plug valve, and these vibrations are also connected with discharge fluctuations in the leakage gap between the side seal of the gate and their seats.

The discharge fluctuations caused by vertical vibrations can be calculated with the equations (II. 20 and 21a). Equation (II. 20) presents the discharge $Q = A_g \sqrt{2g \Delta H}$, in which the gap area is $\mu \delta w$. The velocity fluctuations in the gap follow from the differentiation of the equation:

$$\dot{v} = \frac{\dot{Q}}{w \delta_0} = \frac{\mu}{\delta_0} \sqrt{2g \Delta H_0} \dot{y} + \frac{\mu}{2} \sqrt{\frac{2g}{\Delta H_0}} \Delta H \dot{H} \quad (\text{II. 33})$$

From equation (II. 21a), which describes the extra head across the gate due to inertia, $\Delta H' = - (c_{Lu} + c_{Ld} + b/\delta_0) \dot{Q}/gw = - c_i \dot{Q}/gw$ follows:

$$\Delta H' = - c_i \delta_0 \dot{v}/g \quad (\text{II. 34})$$

Now the equations (II. 33 and 34), thus obtained, can be solved if a stationary vibration is introduced:

$y = Y_0 e^{i\omega t}$, $v = V e^{i\omega t}$, $\Delta H' = \Delta H' e^{i\omega t}$; Y_0 and ω are real, while V and $\Delta H'$ are complex. Working out the equations (II. 33 and 34) and dividing all terms by $e^{i\omega t}$ results in:

$$i\omega V = \frac{\mu}{\delta_0} \sqrt{2g \Delta H_0} Y_0 i\omega + \frac{\mu}{2} \sqrt{\frac{2g}{\Delta H_0}} \Delta H' i\omega \quad (\text{II. 35})$$

$$\Delta H' = - c_i \delta_0 i\omega V/g \quad (\text{II. 36})$$

Combining these two equations gives:

$$i\omega V = \frac{\mu}{\delta_0} \sqrt{2g \Delta H_0} Y_0 i\omega + \frac{\mu}{2} \sqrt{\frac{2g}{\Delta H_0}} \frac{c_i \delta_0 \omega^2}{g} V \quad (\text{II. 37})$$

Chapter II. Self-exciting vibrations

or:

$$V = \frac{\frac{\mu}{\delta_o} \sqrt{2g \Delta H_o} i}{i\omega - \frac{\mu}{2} \sqrt{\frac{2g}{\Delta H_o}} \frac{c_i \delta_o \omega^2}{g}} \omega Y_o \quad (\text{II. 38})$$

This last equation is simplified by introducing the reduced natural frequency S_n and dividing the numerator and denominator by i .

$$S_n = \frac{\omega \delta_o}{2\pi \sqrt{2g \Delta H_o}}$$

$$V = \frac{\mu/2\pi S_n}{1 + i\mu c_i / 2\pi S_n} \omega Y_o \quad (\text{II. 39})$$

From this equation, the relation between the amplitudes of V and ωY_o is found:

$$\bar{V} = \frac{\mu}{2\pi S_n \sqrt{1 + \mu^2 c_i^2 / 4\pi^2 S_n^2}} \omega \bar{Y}_o \quad (\text{II. 40})$$

If S_n is of the order of 0.01, μ of the order of 1 and c_i of the order of 10, $\bar{V}/\omega \bar{Y}_o \sim 13.5$. If S_n is smaller, the relation becomes approximately:

$$\bar{V}/\omega \bar{Y}_o \sim \mu/2\pi S_n \quad (\text{II. 41})$$

If wave radiation is negligible, the waterlevel fluctuations near the gate can be presented as the vertical water velocity, which belongs to the potential flow created by the discharge fluctuations. If the gap under the gate is small, the discharge $V\delta_o$ can be considered as a single source at the bottom. At a distance R this causes a radial velocity of $2V\delta_o/\pi R$. At the water surface, at a distance h from the source, the potential is zero; the water surface acts as a negative mirror (for this concept, see par. 16). Near the gate, the water surface is at distance h from the source; this gives a vertical velocity of $2v\delta_o/\pi h$ for the positive source, but the virtual negative source, created by mirroring, doubles this velocity. So, the water velocity becomes at first approximation $\frac{4}{\pi} \frac{\delta_o}{h} v$.

II. 15 Experimental data of vertical vibrations

In this computation, however, there should have been introduced a positive mirroring at the bottom. This leads to a reduction of the fluctuation by about 20% ($\cong 1 - 3^{-1} + 5^{-1} - 7^{-1}$ etc.); so, roughly, the water velocity v in the gap is reduced at the water surface by a factor δ_o/h . Equation (II. 41) means that for the range wherein a maximum of self-excitation occurs (zone B of fig. II. 7, i.e. $2 \cdot 10^{-2} < S_n < 10^{-1}$), the velocity fluctuations near the gap caused by discharge fluctuations are greater than the vertical vibration velocities of the gate. Near the surface, this is probably not true, because δ_o/h becomes so small that the influence of discharge fluctuations is less than the horizontal vibration component of the gate. The waves produced by discharge fluctuations at the side seals can be of much greater importance, because the discharge fluctuations partly take place near the water surface.

15. EXPERIMENTAL DATA TO CHECK THE THEORY FOR VERTICAL GATE VIBRATIONS

Experimental work to verify the relations of equation (II. 24) is still poor or even non-existent. There is a general experience that great rigidity is a way to prevent self-exciting vibrations in gates.

It has been found by the author in different experiments (see Plates II. 2 and 3, but also in others) that the type of vibration occurring at nearly closed gates is a self-exciting one; when the vibration is stopped it restarts exponentially. The S_n values roughly correspond to those in zone B. An indication that discharge fluctuations (and the related inertia of the flow) indeed play an important role, are the waves near the gate. This is illustrated by Plate II. 2, which shows the wave pattern generated by a model gate in purely vertical vibration. In Plate II. 3, the waves show an interference pattern, of which a part seems to come from the corners. This can be explained by the discharge fluctuations in the gap between the side seals and their seats. Plate II. 1 shows a similar phenomenon at a lock gate in predominantly horizontal vibration. The analysis of the discharge fluctuations is given in par. 14.

In 1975 research has been started to investigate the self-exciting vibrations at low S_n values. Although as yet no definite conclusions can be drawn, the strongest vibrations did indeed occur in zone B of fig. II. 7 as was discussed at the end of par. 13. The excitation forces seem to be lower than the calculated forces. This was qualitatively expected, because no hydraulic damping was introduced into the computation.

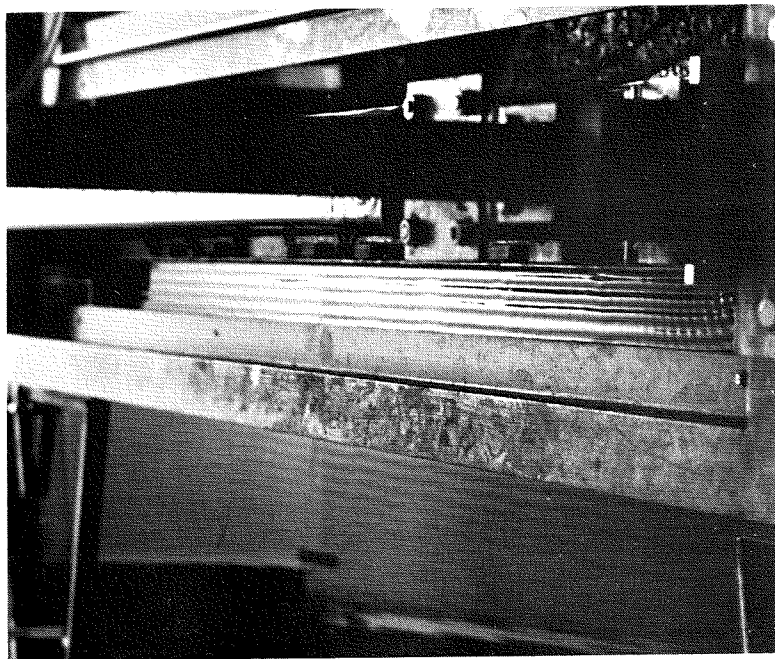


Plate II. 2

Wave radiation due to vertical vibration.

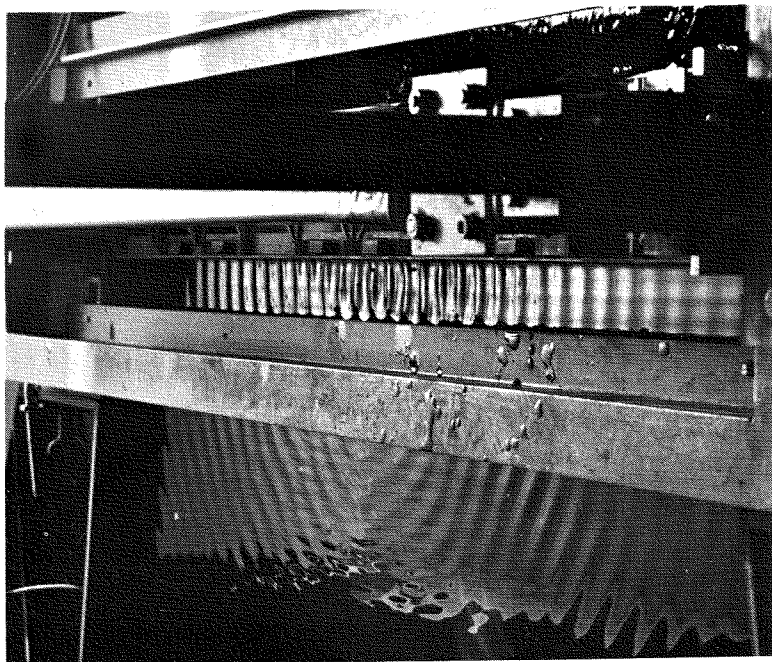


Plate II. 3

Radiation due to predominantly horizontal vibration.

Model investigation of a 30 m span gate; ΔH between 0,5 and 4 m (ref. [25]).

II. 16 Length coeff. c_L and radiation coeff. c_r

16. COMPUTATION OF THE ADDITIONAL LENGTH COEFFICIENT c_L AND THE RADIATION COEFFICIENT c_r

In par. 5 the culvert length L is used to express the inertia effect of the water. This is done under the assumption that the flow through the gap is spread immediately over the entire cross-sectional culvert area and that the transition does not produce an additional inertia effect. In effect, a more complete calculation can be done under the assumption that the flow pattern caused only by the discharge fluctuation is a potential flow, which can be considered to be superposed on the permanent flow. For still-water conditions, it will be shown in Chapter IV that a high-frequency oscillating flow indeed is a potential flow. In the following computations wave radiation is neglected. Two cases will be treated:

a. Closed culvert.

The pulsating gap flow under the vertically vibrating gate is supposed to be evenly distributed over the gap area. At the bottom and at the top of the culvert positive mirroring of the system can be assumed, because no flow through top and bottom wall can take place. The mirroring is repeated infinitely; this means that the gate and the gap flow behave like an infinitely long wall with regularly spaced pulsating portions in the following way:

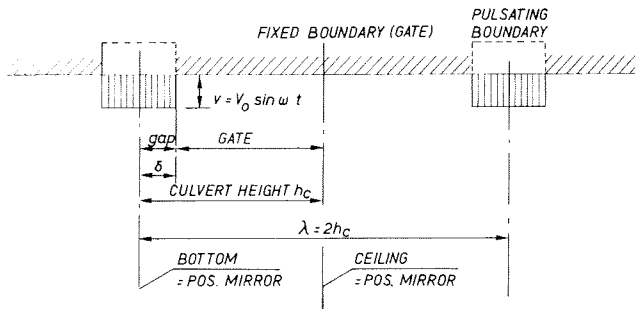


FIG. II. 9

This problem can be solved by finding the Fourier components, the lowest component of which has a wave length λ . As each component can be treated as a standing wave, the pressure distribution on the lateral wall can be found with the wave theory.

Chapter II. Self-exciting vibrations

b. Open channel.

Positive mirroring occurs at the bottom. However, at the free water surface, the mirroring is negative; this is in accordance with the constant pressure condition at the free surface when wave radiation (caused by gravity) is neglected; the potential remains zero, while in the water a fluctuating potential occurs. The result is an infinite boundary of the water fluctuating in the following way:

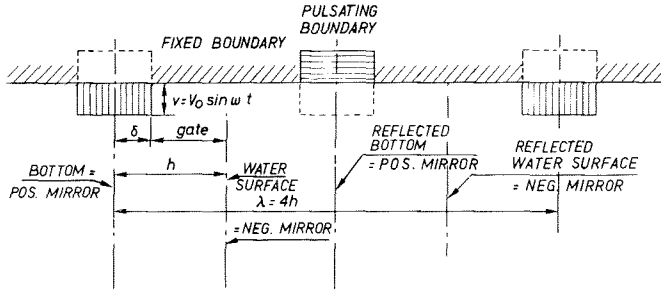


FIG II. 10

The method, based on a concept of Becker [10], has been developed by Schoemaker [90] for the computation of the added water mass at vibrating gates. Another effort has been made by Lange [55], but his final result with negative mirroring at the free water surface has not been published.

Computation of the closed culvert

For this computation, the flow velocity amplitude of fig. II. 10 can be considered as the superposition of the fluctuating mean culvert velocity V_1

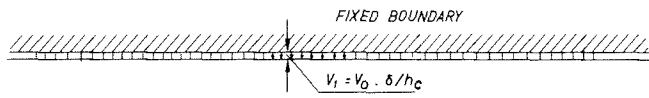


FIG II. 11

and a velocity fluctuation V_2 , whose resultant culvert flow is equal to zero.

II. 16 Length coeff. c_L and radiation coeff. c_r

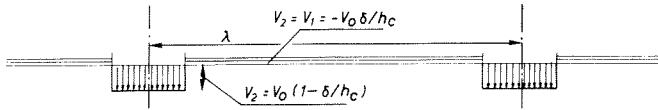


FIG. II.12

The effect of velocity V_1 has already been taken into account by introducing the culvert length L . The resulting pressure fluctuation

$\Delta p = \rho \frac{L}{wh_c} \dot{Q}$ has been used in equation (II. 5, II. 17 and II. 21) by introducing $\Delta H' = \Delta p / \rho g$. In the following only the *additional (imaginary) culvert length* due to V_2 is calculated. The Fourier components of V_2 are:

$$V_2 = V_1 \cos 2\pi x / \lambda \dots\dots\dots + V_n \cos n 2\pi x / \lambda \text{ (the sine components are zero)}$$

with:

$$V_n = \frac{4}{2\pi n} V_0 \sin n 2\pi \delta / \lambda \tag{II. 42}$$

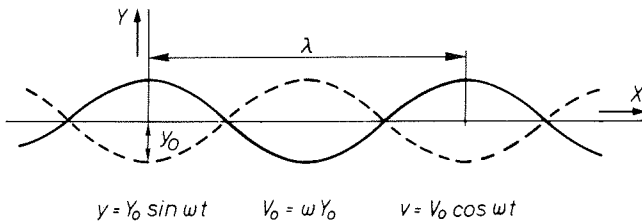


FIG. II.13

All pressures caused by a fluctuating boundary are proportional to the accelerations of this boundary. The relation between the pressures at the boundary and the sinus-shaped acceleration can be found with the theory of standing waves. The pressures of the standing wave just below the original free water surface line (fig. II. 13) are:

$$p = - \rho g y \sin \omega t$$

The corresponding vertical acceleration of the water surface is

$$\frac{dv}{dt} = - \omega^2 y \sin \omega t \text{ (with } \omega^2 = 2\pi g / \lambda_n \text{)}$$

Chapter II. Self-exciting vibrations

This means that

$$p = + \frac{\rho g}{2} \frac{dv}{dt} = \frac{\rho \lambda}{2\pi} \frac{dv}{dt} \quad (\text{II. 43})$$

The pressures related to the n^{th} Fourier component (with $\lambda_n = \lambda/n$) of the velocity fluctuation of equation (II. 42) are:

$$p_n = \rho \frac{dv_o}{dt} \frac{4}{2\pi n} \frac{\lambda}{n} \sin n 2\pi \delta/\lambda \cos n 2\pi x/\lambda \quad (\text{II. 44})$$

The average pressure at the gap becomes:

$$\bar{p}_n = \frac{1}{\delta} \int_0^\delta p_n dx \quad (\text{II. 45})$$

or from (II. 44):

$$\bar{p}_n = \rho \delta \frac{dv_o}{dt} \left(\frac{\lambda}{\delta}\right)^2 \frac{4}{(2\pi n)^3} \sin^2 n 2\pi \delta/\lambda \quad (\text{II. 46})$$

The total pressure at the gap becomes:

$$\bar{p} = \rho \delta \frac{dv_o}{dt} \left(\frac{\lambda}{\delta}\right)^2 \frac{4}{(2\pi)^3} \sum_{n=1}^{\infty} \frac{1}{n^3} \sin^2 n 2\pi \delta/\lambda \quad (\text{II. 47})$$

which can be written as:

$$p = c_L \rho \delta dv/dt$$

c_L has been calculated for different δ/h_c values (with $\lambda = 2h_c$).

δ/h_c	0.01	0.025	0.05	0.1	0.2
c_L	2.72	2.14	1.69	1.25	0.82

The c_L has been plotted in fig. II. 14. The additional culvert length to be introduced follows from the consideration that the inertia has to be expressed in terms of v_{culvert} instead of v_{gap} ($v_{\text{culvert}} = v_{\text{gap}} \delta/h_c$).

$$p = c_L \rho \delta (h_c/\delta) (dv_{\text{culvert}}/dt) = c_L \rho h_c (dQ/dt) / A_c$$

Q = momentary pulsating discharge, A_c = cross-sectional culvert area.

The extra head ($\Delta H' = p/\rho g$) becomes
$$\Delta H' = \frac{c_L h_c}{g A_c} \dot{Q} \quad (\text{II. 48})$$

II. 16 Length coeff. c_L and radiation coeff. c_r

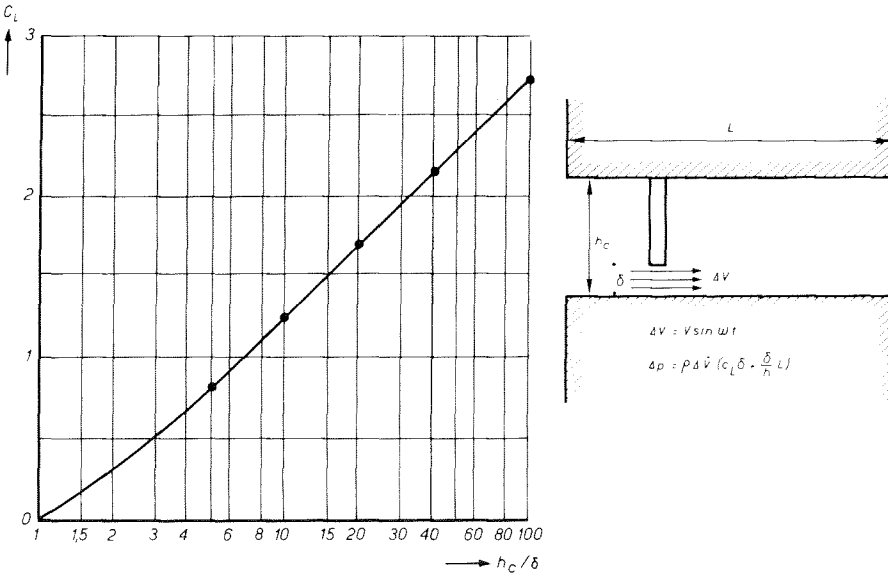


FIG. II.14

The original expression for the inertia of the water was for instance in equation (II. 5):

$$\Delta H' = - \frac{L}{g A_c} \dot{Q}$$

This means that if the gate is at the up- or downstream end of the culvert, an additional length of $(c_L h_c)$ has to be introduced. If the gate is midway in the culvert, this additional length is to be added both up- and downstream of the gate. If a vertically vibrating gate is considered whose gap length b in the flow direction is too great to be omitted, the additional length becomes:

$$L' = (2c_L + \frac{b}{\delta}) h_c \tag{II. 49}$$

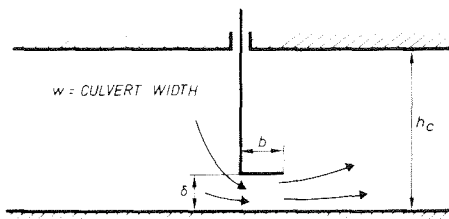
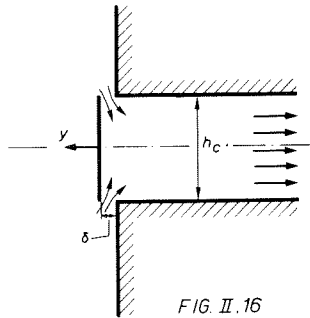


FIG II.15

Chapter II. Self-exciting vibrations

In some cases the gap flow is perpendicular to the culvert; for instance in fig. II. 16.



For this case no computations have been made. However, for practical purposes it can be assumed that c_L has roughly the same value, but in the two-dimensional case of fig. II. 16, $L' = c_L h_c$ becomes:

$$L' = c_L \left(\frac{1}{2} h_c \right)$$

In the case of a circular or rectangular valve with a circumferential gap, the hydraulic radius $R = L_c / A_c$ should be used ($L_c =$ the circumferential length):

$$L' = c_L R$$

If a plug valve vibrates, the mass of water in the culvert which is directly accelerated by the valve is determined by the culvert length L without an imaginary additional length, because this acceleration has immediate effect on the entire cross-sectional culvert area.

Computation of the inertia in free surface flow

The inertia of the water is calculated under the assumption that the acceleration of gravity can be neglected. This assumption is correct for high frequencies (more precisely: high $\omega^2 h/g$ values). The Mathematics Branch of the Delft Hydraulics Laboratory [12] made computations of the c_L values for several $\omega^2 h/g$ values. The computations presented below are to be seen as the limit value for $\omega^2 h/g \rightarrow \infty$. The result of both computations are shown in fig. II. 17. The analysis goes parallel to that of the closed culvert and is based on the pulsating boundary movement of

II. 16 Length coeff. c_L and radiation coeff. c_r

fig. II. 10. The Fourier components are:

$$V = V_1 \cos 2\pi x/\lambda + V_3 \cos 6\pi x/\lambda + \dots + V_n \cos n 2\pi x/\lambda$$

wherein n is an odd integer.

$$V_n = V_0 \frac{8}{2\pi n} \sin n 2\pi \delta/\lambda \quad (II. 50)$$

$$p_n = \rho \frac{dv_0}{dt} \frac{8\lambda}{(n 2\pi)^2} (\sin n 2\pi \delta/\lambda) (\cos n 2\pi \delta/\lambda) \quad (II. 51)$$

Introducing again $\bar{p}_n = \frac{1}{\delta} \int_0^\delta p_n dx$:

$$\bar{p} = \rho \delta \frac{dv_0}{dt} \frac{1}{\pi^3} \left(\frac{\lambda}{\delta}\right)^2 \sum_{\substack{n=1 \\ n=\text{odd}}}^{\infty} \frac{1}{n^3} \sin^2 n 2\pi \delta/\lambda \quad (II. 52)$$

which can be written as:

$$p = c_L \rho \delta \frac{dv}{dt} = c_L \rho (\dot{Q}/w) \quad (II. 53)$$

Q = discharge, w = gate width,

c_L has been calculated for different δ/h values (with $\lambda = 4h$):

δ/h	0.02	0.1	0.2	0.32	1
c_L	3.16	2.12	1.68	1.39	0.54

These values, combined with the results of [12] has been plotted in fig. II. 17. c_L is different at the upstream and downstream sides because of the different depths of water. For a complete gate, there have to be considered the values at the upstream side (c_{Lu}) and at the downstream side (c_{Ld}) and also the inertia of the water under the gate. This results in:

$$p = (c_{Lu} + c_{Ld} + b/\delta) \rho (\dot{Q}/w)$$

(b = width of gate lip, δ = gate elevation). Expressed in $\Delta H'$ (extra head difference across the gate due to the effect of inertia) this becomes:

$$\Delta H' = - \frac{p}{\rho g} = - (c_{Lu} + c_{Ld} + b/\delta) \dot{Q}/gw \quad (II. 54)$$

Chapter II. Self-exciting vibrations

The meaning of b/δ can be seen in fig. II. 15, where the effective horizontal water column subjected to inertia is $(c_L \delta)$; this has to be increased with the lip width b .

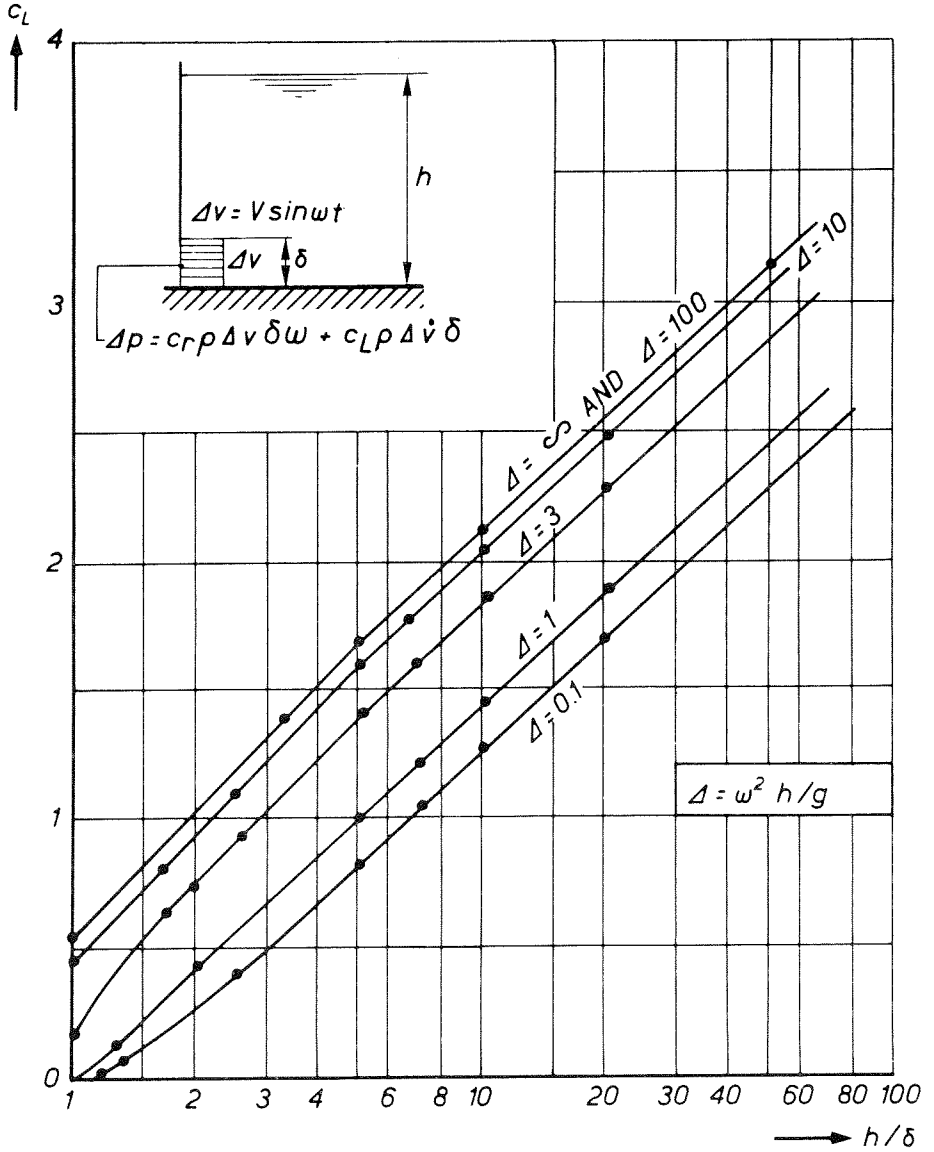


FIG II.17

II. 16 Length coeff. c_L and radiation coeff. c_r

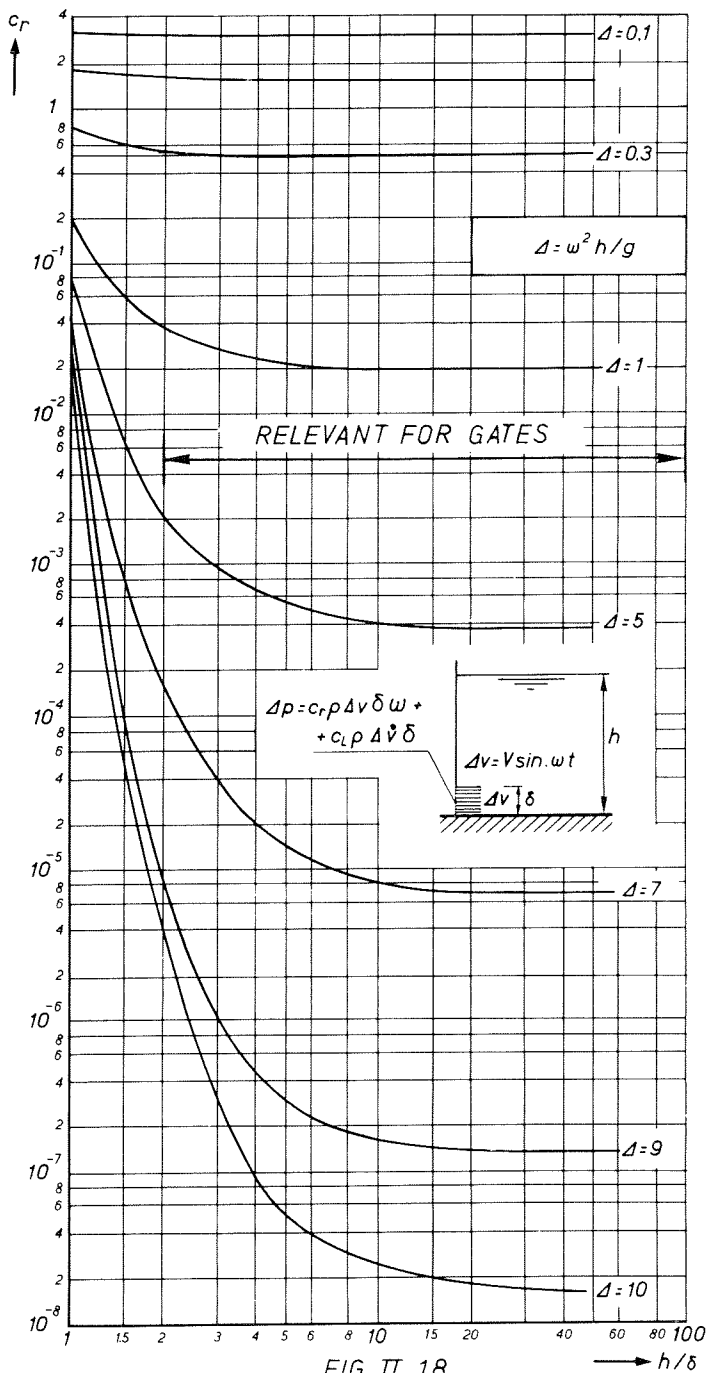


FIG. II. 18

$\rightarrow h/\delta$

Chapter II. Self-exciting vibrations

In fig. II. 17 it can be seen that with decreasing values of $\Delta = \omega^2 h/g$ the inertia effect on the water decreases. The radiation of energy will increase; and from the fluctuating discharge, energy must be transferred to the water to compensate this wave radiation. This results in the complete expression for p , wherein also the "out of phase" pressure is expressed by means of the radiation coefficient c_r , the value of which is presented in fig. II. 18 [12].

The computations have been checked for simple cases:

- a. For low $\omega^2 h/g$ values, the wave is a shallow water wave with a velocity of \sqrt{gh} , and the pressure distribution over the depth is a hydrostatic one so that the discharge at the bottom produces a wave with a height of $h' = q/\sqrt{gh} = v\delta/\sqrt{gh}$; this h' is now also representative of the pressure at the gap.
- b. For high h/δ values, an other check has been made, assuming that the radiation wave has a height "a" and a velocity g/ω (deep water wave), of which wave the radiation of energy is known. Moreover, the pressure at the bottom can be calculated and, together with the discharge pulsation, this determines the energy transfer from the pulsating discharge into the water. The energy balance requires that these two energies are equal, which is in accordance with the result of fig.

II. 18.

Because the simplified computations (without the effect of wave radiation) lead to potential flow patterns (see Chapter IV), all computation and analogue techniques existing for potential flow can also be applied to find c_L coefficients. These techniques are discussed in Chapter IV, par. 3^a, in relation to the determination of the added mass.

17. DETERMINATION OF THE FORCE COEFFICIENT c_F

The force coefficient c_F , introduced in equation (II. 19) and returning in equation (II. 24) and in the ordinate of fig. II. 7, is related to the suction force at the edges of gates and valves. The effect of such suction is supposed to be that, when acceleration or deceleration of the discharge causes an extra head difference across a valve or gate edge, the result is an extra suction force. This suction results from all the pressure differentials at the gate edges. When, for instance, the example of fig. II. 19a is considered under permanent flow condition, the pressure under the edge is a combined result of the pressure

II. 17 Force coefficient c_F

in the downstream zone 2, and the suction caused by the fact that the flow contraction in the intermediate gap section II is followed by an expansion towards the terminal gap section III. The upward hydrodynamic force can be expressed as:

$$F = \rho g H_2 B - c_s \rho g \Delta H_{12} B \quad (\text{II. 55})$$

in which the suction coefficient c_s has been introduced.

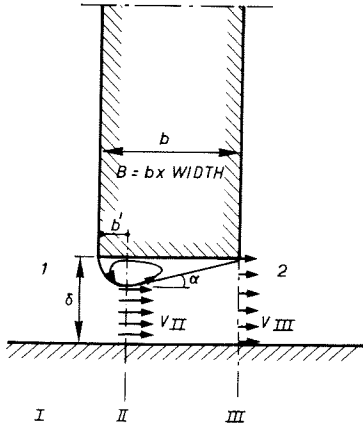


FIG. II.19^a

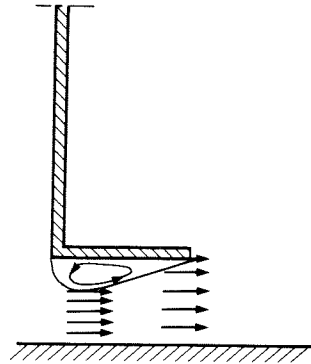


FIG. II.19^b

If only the dynamic component is considered, there follows from equation (II. 21a) that:

$$\Delta H'_{12} = - (c_{Lu} + c_{Ld} + b/\delta) \dot{Q}/gw \quad (\text{II. 56})$$

But the downstream head H_2 also is affected by discharge fluctuations and can be derived from equation (II. 53):

$$H'_2 = \frac{P_2}{\rho g} = c_{Ld} \dot{Q}/gw \quad (\text{II. 57})$$

The fluctuating force (positive in the direction of suction) becomes:

$$F' = - \rho g H'_2 B + c_s \rho g \Delta H'_{12} B = - \rho c_{Ld} (\dot{Q}/w) B - \rho c_s (c_{Lu} + c_{Ld} + b/\delta) (\dot{Q}/w) B \quad (\text{II. 58})$$

In equation (II. 19), the force coefficient has been introduced as if

Chapter II. Self-exciting vibrations

the average pressure on the gate edge is proportional to $\Delta H'_{12}$, which is in conformity with the last term of equation (II. 55) if $c_F = c_s$. However, the total force coefficient becomes:

$$c_F = c_s + c_{Ld} / (c_{Lu} + c_{Ld} + b/\delta) \quad (\text{II. 59})$$

In the example of fig. II. 19b, the part of the dynamic pressure due to discharge fluctuations, expressed by H'_{2} , will also act to some extent on the top surface of the lip, so the formula will become:

$$c_F = c_s + \theta c_{Ld} / (c_{Lu} + c_{Ld} + b/\delta) \quad (\text{II. 60})$$

It can be expected that for deep water and relative narrow lips θ tends to be small; whereas when the downstream jet from under the gate edge is a free jet, θ tends to be equal to 1. Exact determination of θ can be achieved by electrical analogue techniques or potential flow computation (Chapter IV). Generally applicable results are not yet available.

The suction coefficient c_s has to be determined in a hydraulic model under permanent flow conditions. For the rectangular section edges of fig. II. 19 a guess can be made:

If the contraction coefficient is 0.65, $\tan \alpha = 0.25$ and $b' = 0.4 \delta$, the flow reattaches at distance 1.8δ . Between the sections I and II, the contracting flow is accompanied by a constant low pressure: the one calculated for section II. Between section II and the point of reattachment, the flow expands again, while the pressure is assumed to increase linearly so that the low pressure can be considered to work on one half of this length. Thus, the low pressure works effectively on a length of 1.1δ . The energy head loss between the sections II and III is:

$$\Delta H = (v_{II} - v_{III})^2 / 2g$$

The pressure in section II follows from:

$$H_{II} + v_{II}^2 / 2g = H_{III} + v_{III}^2 / 2g + \Delta H$$

And from these equations can be derived:

$$H_{II} = H_{III} - 2 (v_{III}^2 / 2g) (v_{II} / v_{III} - 1) \quad (\text{II. 61})$$

The total head loss across the gap is:

II. 17 Force coefficient c_F

$$\begin{aligned}\Delta H_{12} &= (v_{II} - v_{III})^2/2g + v_{III}^2/2g = \\ &= v_{III}^2/2g \{ (v_{II}/v_{III} - 1)^2 + 1 \}\end{aligned}\quad (\text{II. 62})$$

In equation (II. 20) there was introduced $Q = A_g \sqrt{2g \Delta H}$, which, according to the symbols of fig. II.6, can be written as:

$$Q = \mu \delta w \sqrt{2g \Delta H} = \mu \delta w \sqrt{2g \Delta H_{12}} \quad (\text{II. 63})$$

By using equation (II. 62) and introducing $v_{III} = Q/w\delta$, the discharge coefficient μ now becomes:

$$\mu = \{ (v_{II}/v_{III} - 1)^2 + 1 \}^{-\frac{1}{2}} \quad (\text{II. 64})$$

If $v_{II} = 1.5 v_{III}$, $\mu = 0.895$.

This value of μ is valid for small gate openings ($b/\delta > 1.6$), in which reattachment of flow occurs. For greater gate openings, μ will be 0.6 or 0.65, i.e. approximately equal to the contraction coefficient.

When the flow reattaches and $v_{II} = 1.5 v_{III}$, there follows from equation (II. 62):

$$v_{III}^2/2g = \Delta H/1.25$$

From equation (II. 61) follows, assuming $v_{II}/v_{III} = 1.5$:

$$H_{II} = H_{III} - (2 \Delta H/1.25) (1.5 - 1) = H_{III} - \Delta H/12.5$$

Because the magnitude of the local low pressure relative to H_2 now is $\Delta H/1.25$ and because this acts on a flow length of 1.1δ , the suction force on the gate is:

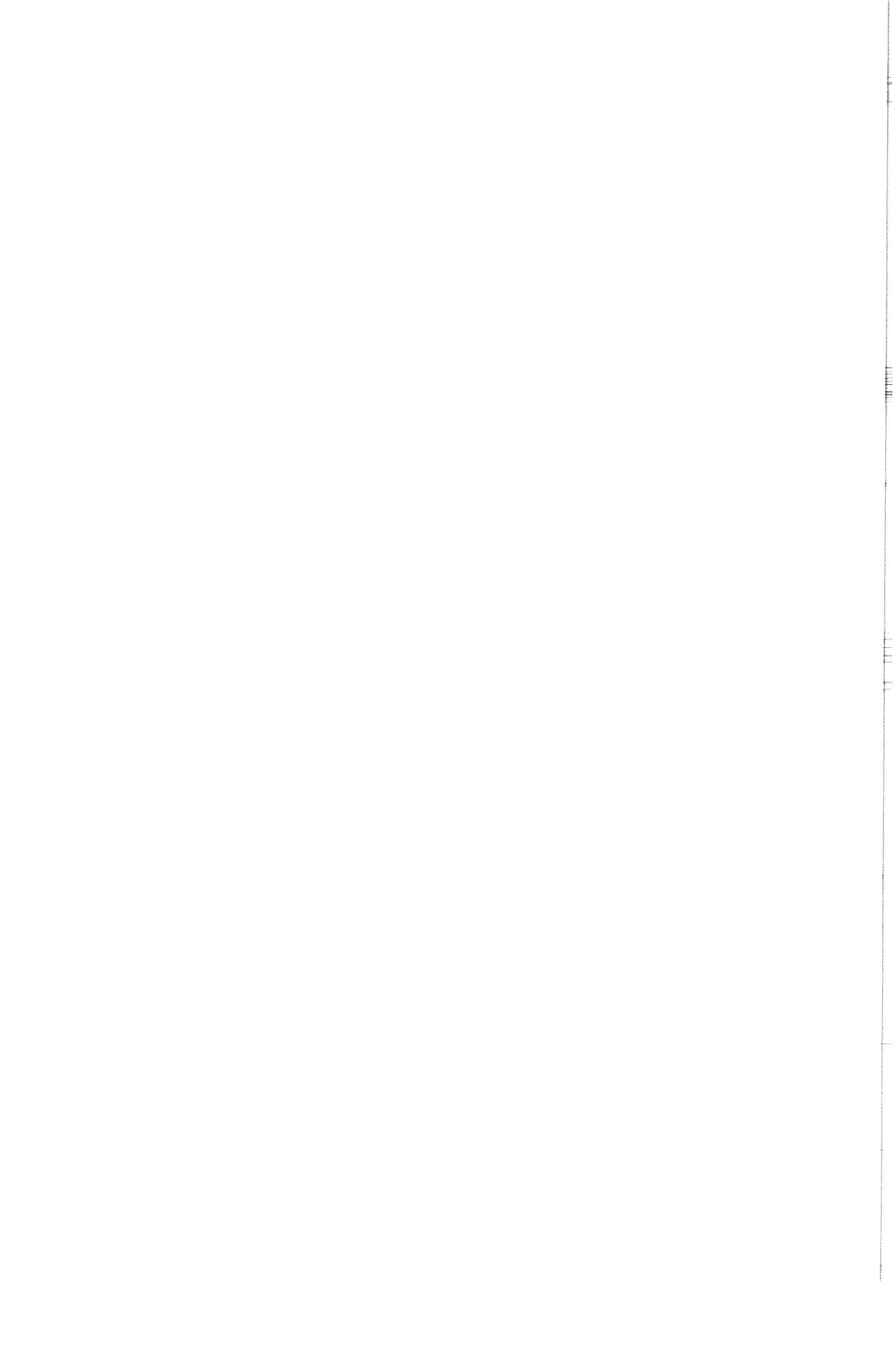
$$\Delta H c_s b = (\Delta H/1.25) 1.1 \delta$$

or

$$c_s = 0.88 \delta/b \quad (\text{II. 65})$$

The maximum value of δ at which the flow reattaches is $\delta = 0.6 b$.

$$c_{s \max} = 0.88 \cdot 0.6 = 0.53$$



Chapter III

Prevention of self-excitation in gate design; a simplified approach using an indicator

1. SUMMARY

An indicator is proposed for recognizing the points in the design of gates and valves that are critical for the occurrence of self-exciting vibrations. This indicator corresponds with the occurrence of the hydrodynamic counter-rigidity, introduced in Chapter II. Its applicability is illustrated in a number of examples. Other examples are presented where, by means of this indicator, self-exciting vibrations may be expected. The indicator can be used to improve designs in the preliminary stage, and to indicate on which points in further research extra attention must be paid.

2. INTRODUCTION

In Chapter II, two cases of self-exciting vibrations have been analyzed: one being a plug valve vibrating in the direction of the pipe flow, the other being a valve or gate vibrating perpendicular to the flow direction. These two examples will be used to illustrate the mechanism of self-exciting vibrations and to demonstrate the validity of the indicator to predict them.

In any mechanism wherein energy is transferred from a flowing medium to a vibrating structure, there is a force component in phase with the vibration velocity. This can be explained as follows, assuming that there is a vibration with an amplitude Y_0 :

the displacement is $y = Y_0 \sin \omega t$ and the force acting on the gate is

$$F = F_1 \sin \omega t + F_2 \cos \omega t.$$

Chapter III. Prevention of self-excitation using an indicator

The transfer of energy E to the structure by the force F during the period T is:

$$E = \int_0^T F ds = \int_0^T F \dot{y} dt = \int_0^T \left[F_1 \sin \omega t (\omega Y_0 \cos \omega t) + F_2 \cos \omega t (\omega Y_0 \cos \omega t) \right] dt$$

Because $\int_0^T \sin \omega t \cos \omega t dt = 0$ and $\int_0^T \cos^2 \omega t dt = \frac{1}{2}T$, this becomes

$$E = \frac{1}{2}T \omega Y_0 F_2 = \pi Y_0 F_2$$

So, only F_2 , which is in phase with \dot{y} , transfers energy.

The mechanism of self-excitation found in Chapter II can be described as follows:

When, for instance, the structure moves in the direction in which the width of the leakage gap decreases, the flow decreases and the water tends to be decelerated. This deceleration is due to the force exerted by the structure on the water, and this force is related to an increased head difference across the structure. Said force, which is equal to the force the water exerts on the structure, arises from the flow inertia. Momentarily, flow through the reduced leakage gap is greater than the equilibrium flow belonging to the reduced gap, and the resulting extra flow causes an increased head difference across the valve or the gate.

If the additional head difference across the structure results in a force on the structure in the direction of the initial movement thereof, the force tends to amplify this movement. In the case of vibration in the flow direction of a plug valve, this happens when the seat is on the downstream side of the valve; in the case of vertical vibration (i.e. perpendicular to the flow direction), this happens when the additional head difference causes vertical suction on the valve.

It is important to analyze which elements cause a force in phase with the vibrational displacement (like the forces caused by the mass or rigidity of a mechanical system), or in phase with the velocity of vibrational movement (like the forces of positive or negative damping in a mechanical system), of which only the latter force can transfer energy

III. 2 Introduction

to the vibrating structure. When a vibration of extremely low frequency is considered, the flow inertia will be of minor importance and the flow tends to follow the vibration in such a way that at each momentary gate or valve position there will be an equilibrium flow condition equal to the constant flow condition belonging to this valve position. As the flow velocity follows the gap width, the flow acceleration is proportional to the velocity of vibrational movement. Because the acceleration of flow is the element which causes the additional head difference across the structure, the force caused by it is proportional to the velocity of vibrational movements; it operates in the direction of this velocity and transfers energy from the flow to the structure.

If the vibration has a high frequency, the flow velocity will not follow the vibration and tends to remain constant. In this case, the constant flow will cause a positive additional head difference across the structure when the leakage gap is narrow, and a negative additional head difference when the gap is wide. This results in a force which is in phase with the displacement; i.e. the force does not transfer energy to the structure.

Still another phenomenon occurs in plug valves, wherein valve displacement induces pipe flow due to the pistoning effect. If plug valve vibration has a high frequency, the pipe flow tends to be constant; so, the pistoning effect has to be compensated by decreases and increases of the flow through the gap, causing head variations across the valve proportional to the vibrational valve velocity and acting as a damper.

When the equation (I. 8) is considered:

$$(m + m_w) \ddot{y} + (c + c_w) \dot{y} + (k + k_w) y = 0$$

then the foregoing leads to the conclusion that c_w is negative at low frequencies, tends to become zero at higher frequencies, and will become positive at high frequencies if pistoning effects occur. If a fictive mechanical damper c is applied in such a way that $(c + c_w) = 0$, the vibration becomes stationary. This means that c is at a maximum at low frequencies, tends to decrease to zero at higher frequencies and will be negative at high frequencies if pistoning effects occur. This agrees with the results of the analysis made in Chapter II.

The phenomena which cause self-exciting vibrations have one element in common: When the gap width decreases, the head difference across the valve or gate increases, because the flow inertia prevents an immediate

Chapter III. Prevention of self-excitation using an indicator

decrease of the flow velocity. If the additional head difference across the valve causes forces in the direction of initial valve movement, self-excitation can occur. When the frequency is very high, the same phenomena occur, but the forces are nearly in phase with the vibrational displacement. This leads to the following formulation of the *instability indicator*:

If a sudden initial movement of the gate causes additional hydrodynamic forces in the direction of this movement, assuming that the flow remains constant for a moment before changing in reaction thereon, a risk of self-exciting vibrations exists.

In logic: If a cause A (a sudden initial movement) results in an effect B (forces in the direction of the movement), a phenomenon C (the risk of self-exciting vibrations) is present.

In the examples treated hereafter, it is only investigated whether cause A results in effect B.

The forces generated by the flow, which remains constant for a moment, are related to the occurrence of the hydrodynamic counter-rigidity k_{hc} , the definition of which has been introduced in Chapter II, in the passage preceding the derivation of equation (II. 11). Additional forces are generated by the pressure gradient, which is related to acceleration or deceleration of the flow. For free-surface flow, this is expressed in the term $\theta c_{Ld} / (c_{Lu} + c_{Ld} + b/\delta)$ of equation (II. 60). For pipe flow, for example of fig. III. 17, the length L of the gap can give rise to low pressure near the gap when the flow decelerates.

Additional remarks about elements of instability:

Remark 1: A greater rigidity of the structure is favourable. Apart from the hydrodynamic counter-rigidity appearing at a sudden movement, it is possible that also at a slow movement the hydrodynamic forces counteract the rigidity; for instance, when a gate with a rectangular seal is used at a critical gate opening, it can happen that an extra lowering causes a rather sudden reattachment of flow (see fig. II. 19), resulting in an extra suction force. So, the lowering of the gate causes a hydraulic downpull, while the restoring force of the suspension spring (hoist) is in upward direction. This means that the effective spring rigidity is reduced. If the negative "rigidity" of the

III. 3 Validity of the indicator

fluid is greater than the spring rigidity, the structure is statically unstable. This is called divergence.

Remark 2: The water displacement by the vibrating structure (pistoning) has to be taken into consideration as a possible damping factor. This can be done by assuming a greater flow inertia, so that the pistoning effect has to be compensated by a flow variation through the gate opening or leakage gap. When this causes an additional head difference and a force in a sense opposite to the vibration velocity, there exists hydrodynamic damping.

3. DISCUSSION ON THE VALIDITY OF THE INDICATOR FOR SELF-EXCITING VIBRATIONS

The indicator for self-exciting vibrations has been developed in a purely empirical way from the examples of fig. III. 1 to 3 in the next paragraph. At first, the occurrence of the hydrodynamic counter-rigidity was considered to be sufficiently indicative. Vibrations predicted by the author and confirmed by experiments are discussed at fig. III. 13 and 20. The examples of fig. III. 3,4,6,9,10 and 17 can be found in several publications. Abelev [4] analyzed the case of fig. III. 17 after vibrations were found in the prototype. The indicator was first mentioned in an internal Delft University/Delft Hydraulics Laboratory paper [50] and was introduced in the discussions at the IAHR Symposium 1970 [49].

An attempt to establish such an indicator in relation to panel flutter has been published by Kornecki [52]. Kornecki concluded that the condition that the negative hydrodynamic rigidity has to be smaller than the spring rigidity is not only necessary to prevent divergence, but that it is also a sufficient condition for the prevention of vibration. This, however, appears not to be true in the cases treated in this and the preceding chapter.

For the cases analyzed in Chapter II, the indicator can be checked:

- The plug valve, with equations (II. 12a and 12b), was found to be stable when $c_k > c_m + 1$ or when $c_k < 0$.

The indicator states instability when: $k_{hc} \left(= \frac{1}{c_k} \times k \right) > 0$, i.e. $c_k > 0$

(k_{hc} = hydrodynamic counter-rigidity, k = spring rigidity). This means that the pistoning effect is neglected by the indicator. So, the use

Chapter III. Prevention of self-excitation using an indicator

of the indicator appears to be safe.

- For the vertical vibrations of equations (II. 22 and 24), the valve was found to be unstable ($c > 0$) for all cases wherein $c_k^{-1} > 0$.

This is in agreement with the indicator.

4. EXAMPLES OF DESIGN FACTORS WHICH CAN LEAD TO SELF-EXCITING VIBRATIONS

Examples 1 and 2 are not related to gates, but have triggered the development of the indicator.

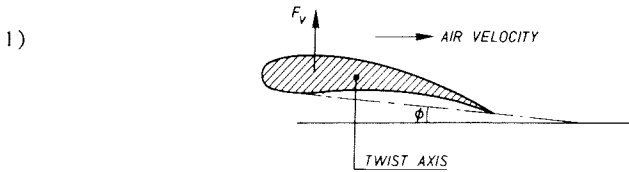


FIG III.1

Wing flutter: When the inclination ϕ increases, the total lift force F_v will increase also. Because F_v operates at about $\frac{1}{4}$ of the chord length and the twist axis lies farther to the rear, a rotative moment is formed which tends to increase the inclination ϕ . Because F_v also causes the wing to move upwards, the air flow at the leading edge of the wing will be decelerated; this results in an increased pressure and an increase of F_v . Much has been published on this subject, e.g. in Den Hartog's handbook [27], in the paper of Theodorsen [96] (explaining the dynamic fluid forces theoretically), and in the handbooks on aeroelasticity. For a literature review see [8]

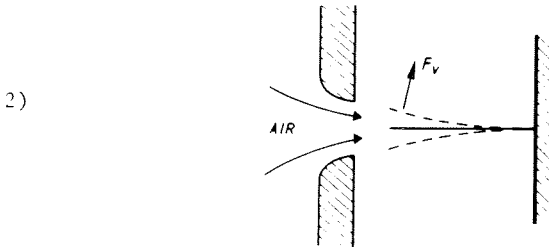


FIG III.2

This is the principle of the mouth-organ: When the resilient leaf moves from its rest position, the air flow exerts a force F_v in the same direction. Due to the flow inertia, the air flow at the front edge of the leaf

III. 4 Examples

is decelerated, resulting in a momentary increase of F_v .

3)

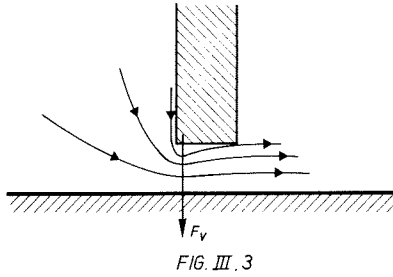


FIG. III.3

At small gate openings, the force F_v will be in downward direction. When the gate moves downwards, the flow will remain constant during the first moment, causing a momentary increase of the head difference across the gate. As F_v is roughly proportional to the head difference, the increase thereof reinforces F_v , which increases the downward movement of the gate. The flow inertia causes an increase of F_v , because the flow in the downstream zone has to be decelerated. The reverse happens when the gate moves upwards (a complete analysis has been given in Chapter II).

4)

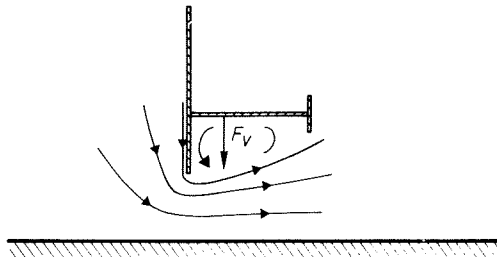
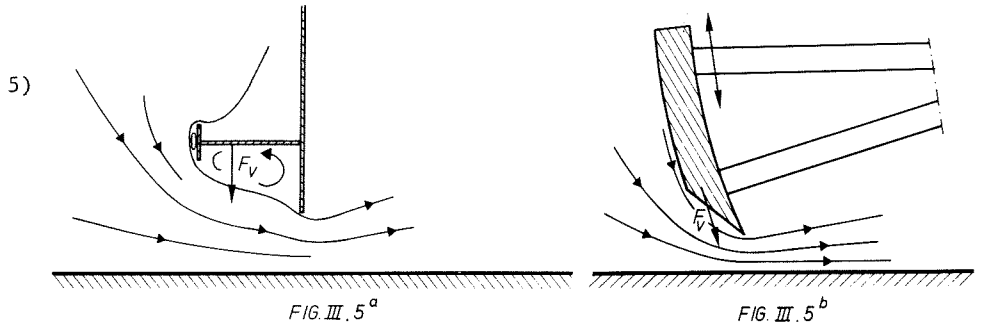
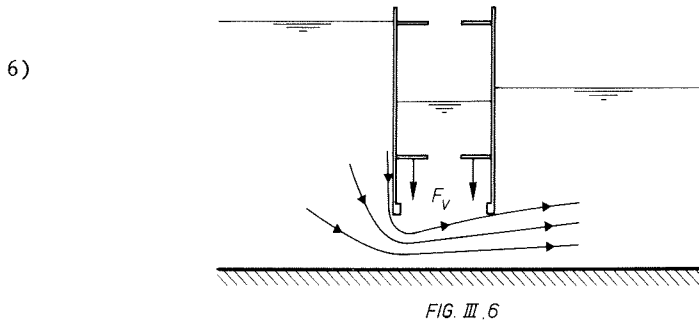


FIG III 4

If the reinforcement girder of the gate is situated relatively low, suction in downward direction will be exerted thereon, giving a result similar to 3).



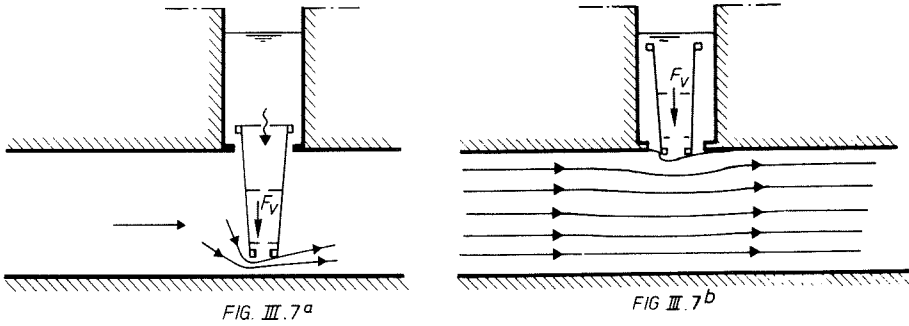
These cases are similar to 3) and 4). Fig. 5b is related to the land-side gates of the Haringvliet sluice, where self-exciting vibrations were found (Delft Hydraulics Laboratory study M 754, in progress).



At a double-plate gate, the flow reattaches at the downstream gate edge, when the gate raise is small, and this gives rise to the same phenomena as in 3), 4) and 5). If the horizontal beam is perforated, the momentary pressure fluctuations under the gate will be followed by the water between the plates, but with a delay. Thus, the gate itself acts as a sort of surge tank, which smoothes a pulsating pressure. At some frequencies, resonance of the water within the gate can occur (standing wave, or surge tank oscillation). Experience with this type of gate is unfavourable [25], unless the downstream plate ends much higher than the upstream one.

III. 4 Examples

7)



The case of a double-plate gate in a culvert is nearly the same as 6), but experience is more favourable [22], probably because the pressure in the valve shaft (when the gate is submerged) is higher than underneath the gate. This causes water flow through the interior of the gate, which compensates the low pressure underneath the gate and works like a damper: the losses of this flow at the gate girders produce damping forces proportional to the water velocity (Chapter IV). When the gate is almost entirely raised, another point of instability can occur at the position at which the flow is uncertain whether or not to reattach at the downstream gate edge (fig. 7b). When, for instance, the gate moves downwards, the flow separates from the downstream gate edge, the flow resistance increases, and the flow is decelerated. This causes an additional head difference across the gate, while F_v increases too.

8)

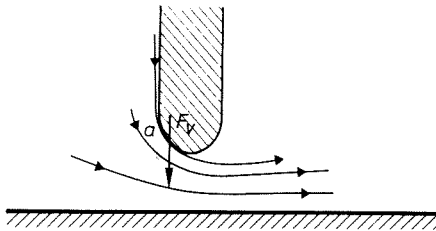


FIG. III. 8

At semi circular edges, the separation point is always situated in such a location that in a certain region (a) a low-pressure zone will occur, resulting in a downward force F_v . When e.g. the gate moves downwards, the discharge rate will remain constant during the first moment, causing

Chapter III. Prevention of self-excitation using an indicator

a momentarily increased head difference across the gate, resulting in an increase of F_v .

9)

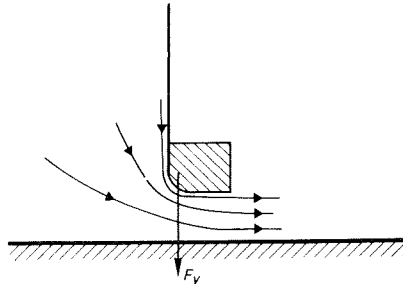


FIG. III. 9

This sealing beam works well at very small openings, but just before flow separation, there occurs a low pressure at the rounding and a similar situation arises as in 8).

10)

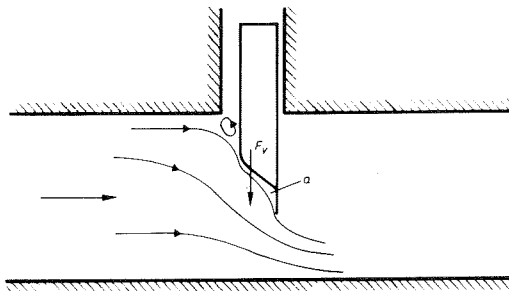


FIG. III. 10

This gate can give rise to a low-pressure region at (a), and is then similar to 8). If the gate is not too thin, low pressure does not necessarily occur.

11)

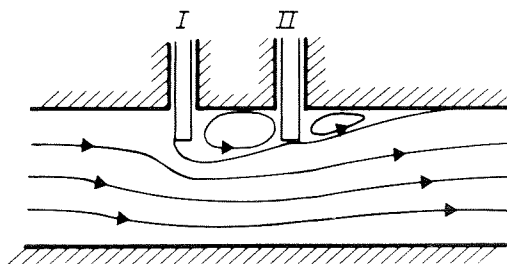


FIG. III. 11

III. 4 Examples

Where two valves are situated close behind each other, a lowering of gate I will make the flow separate from gate II. Consequently, the flow resistance will increase and, with constant flow, the head difference across valve I will increase also. When this additional head difference causes a suction force, the valve will become potentially unstable. When gate II is then lowered and the flow is still unattached, the flow will reattach at a certain moment and suction on gate II will occur. The suction force counteracts the restoring force of the spring (hoist) and this can cause divergence, which will increase the risk of vibration. The flow pattern of fig. III. 11 is unfavourable also, because there is an extremely low pressure between gates I and II, which can cause aeration or cavitation. Aeration of a culvert during valve closing can be dangerous: because of inertia, the flow downstream of the air pocket continues, decompressing the air, and after closure of the gate the water column returns and causes water-hammer.

12)

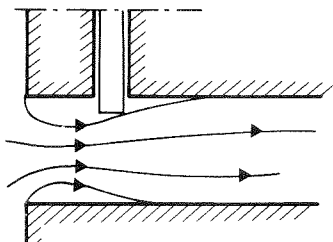


FIG. III. 12^a

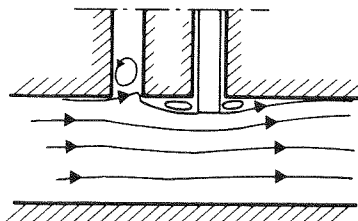


FIG. III. 12^b

Problems connected with reattachment of flow similar to example 11) can also result from bad shaping of the entrance to the culvert, or from open shafts and slots too close to the valve.

13)

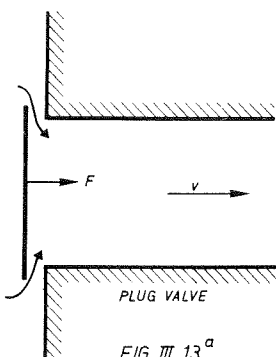
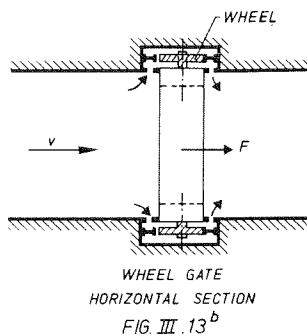


FIG. III. 13^a



WHEEL GATE
HORIZONTAL SECTION
FIG. III. 13^b

Chapter III. Prevention of self-excitation using an indicator

In both cases, when the gate moves to the right, the gap decreases. At a constant flow, the resulting additional head difference across the valve causes a force in the direction of the valve movement (a complete analysis is presented in Chapter II).

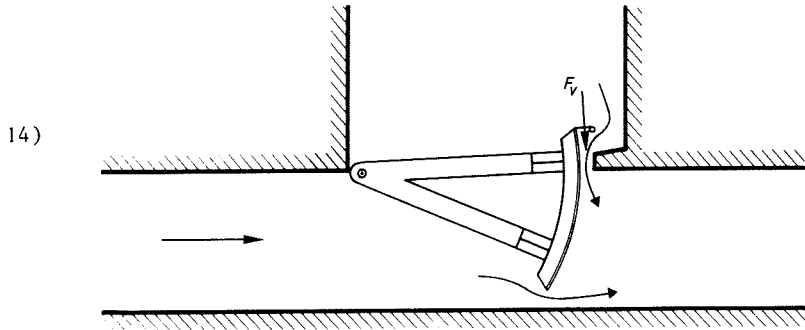


FIG. III.14

A reversed Taintor valve is relatively rigid, except in vertical direction. When its gate moves downwards, the flow at that moment causes an additional head difference across the valve, resulting in an additional vertical force in the direction of the gate movement (for complete analysis: see Chapter II).

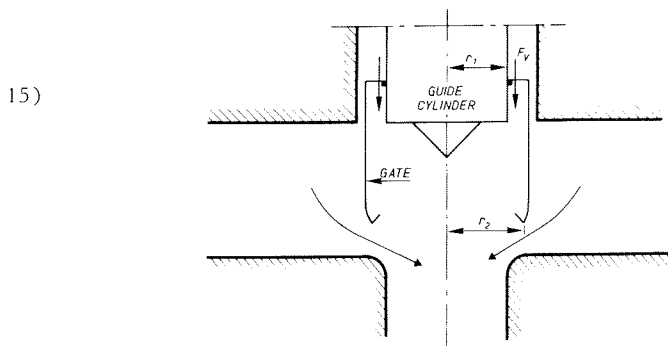
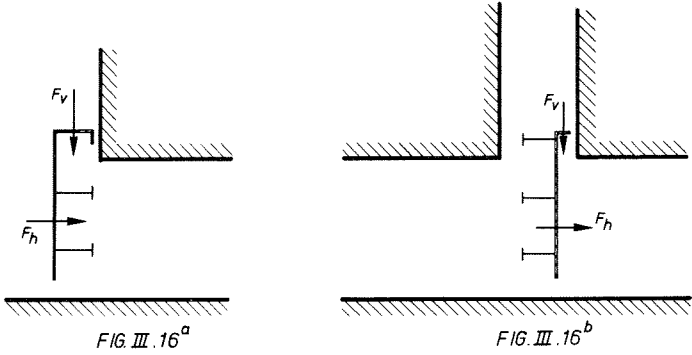


FIG. III.15

In a cylinder valve, if r_2 is substantially greater than r_1 , a downward gate movement causes an additional head difference resulting in a force F_v which tends to increase the downward displacement in the same way as in 14).

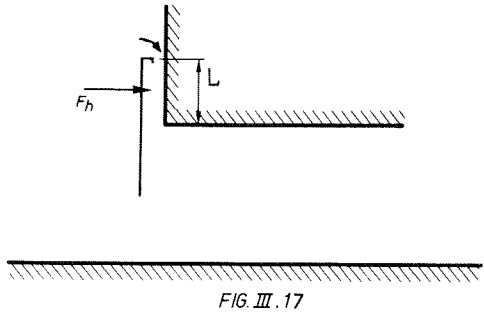
III. 4 Examples

16)



In these types of valve, an additional head difference occurs both when the gate moves in vertical direction and when it moves in horizontal direction. Each movement gives rise to both vertical and horizontal forces in a sense to increase the initial movement, thus exciting vibration. Also, coupling occurs between the two directions of vibration.

17)



When the gate is in a higher position than shown in 16), only the displacement in horizontal sense causes additional suction on the upper part of the gate. Especially in the narrow space with height L between the gate and the wall, the effect of flow inertia can be relatively important. This case has been analyzed in detail by Abelev [4].

18)

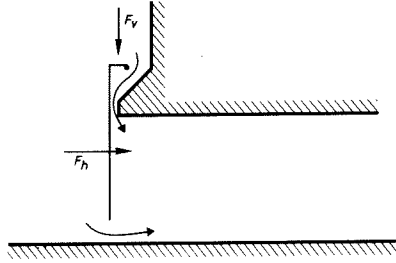


FIG. III. 18

In this case, vertical vibration of the upper lip of the gate also causes gap width variation. In other aspects this case is similar to 14-17).

19)

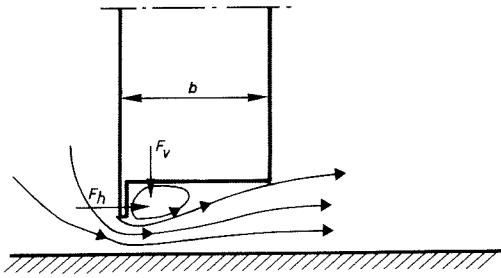


FIG. III. 19

In this example, the great dimension (b) of the gate in the direction of flow has the same effect as the height L in 17). When the gate moves downwards and the flow remains constant, the vertical force F_v tends to increase. Then deceleration of flow does not only lower the pressure at the downstream side of the gate, but the inertia of the water column (length b) causes a still lower pressure near the lip. This produces, at the same time, a vertical force and a horizontal force on the lip and so, coupling between different modes of vibration can be obtained. This type of vibration can also occur where labyrinth seals are used.

III. 4 Examples

20)

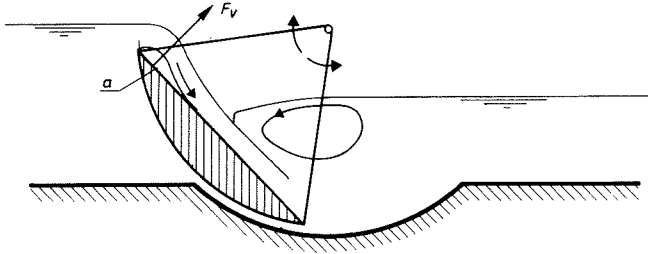


FIG. III. 20

The low pressure zone (a) beyond the top of the weir gate causes a rotating moment around the pivot axis. When the gate moves upwards, the overflow decreases, while downstream the nappe remains flowing at the same rate. This causes a further pressure reduction at (a).

21)

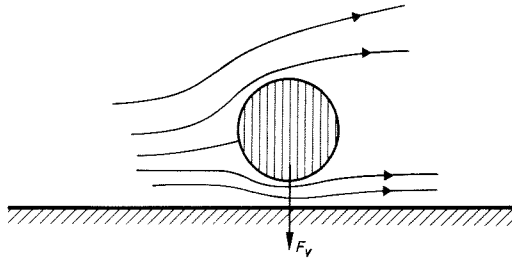


FIG. III. 21^a

Round (and many other) stop logs are unstable because of the suction force F_v at their lower part, described in 8). For round stop logs, the instability is reinforced by the fact that, when the log touches the bottom and the flow inertia effect has been damped out, an upward pressure occurs.

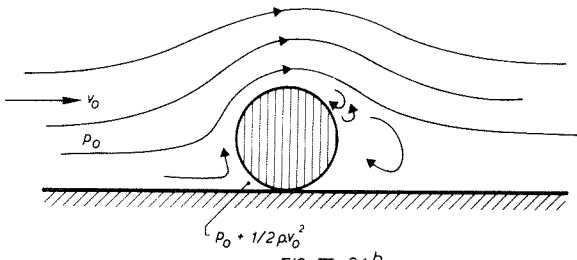


FIG. III. 21^b

Chapter III. Prevention of self-excitation using an indicator

The result is that there is not only a self-exciting regular vibration, but also an irregular movement of great amplitude.

22)

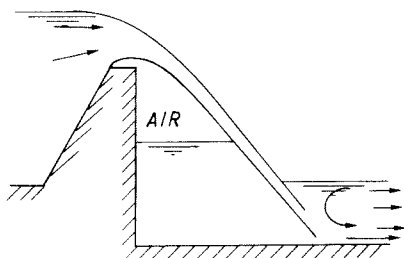


FIG. III 22

The instability of a nappe of water falling over a rigid weir and enclosing a body of air (see fig. I. 7a) is not well explainable with the indicator for self-exciting vibrations. One could, however, reason that if the nappe made an incidental forward movement, the pressure of the enclosed body of air would decrease, thereby causing a subsequent return of the nappe beyond its equilibrium position and a compression of the air. In this way, oscillation of the falling nappe could be initiated.

23)

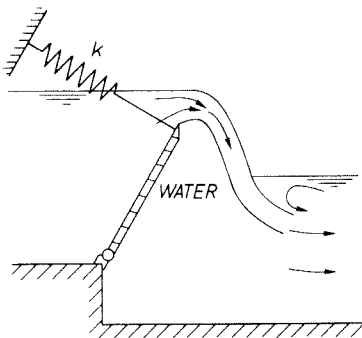
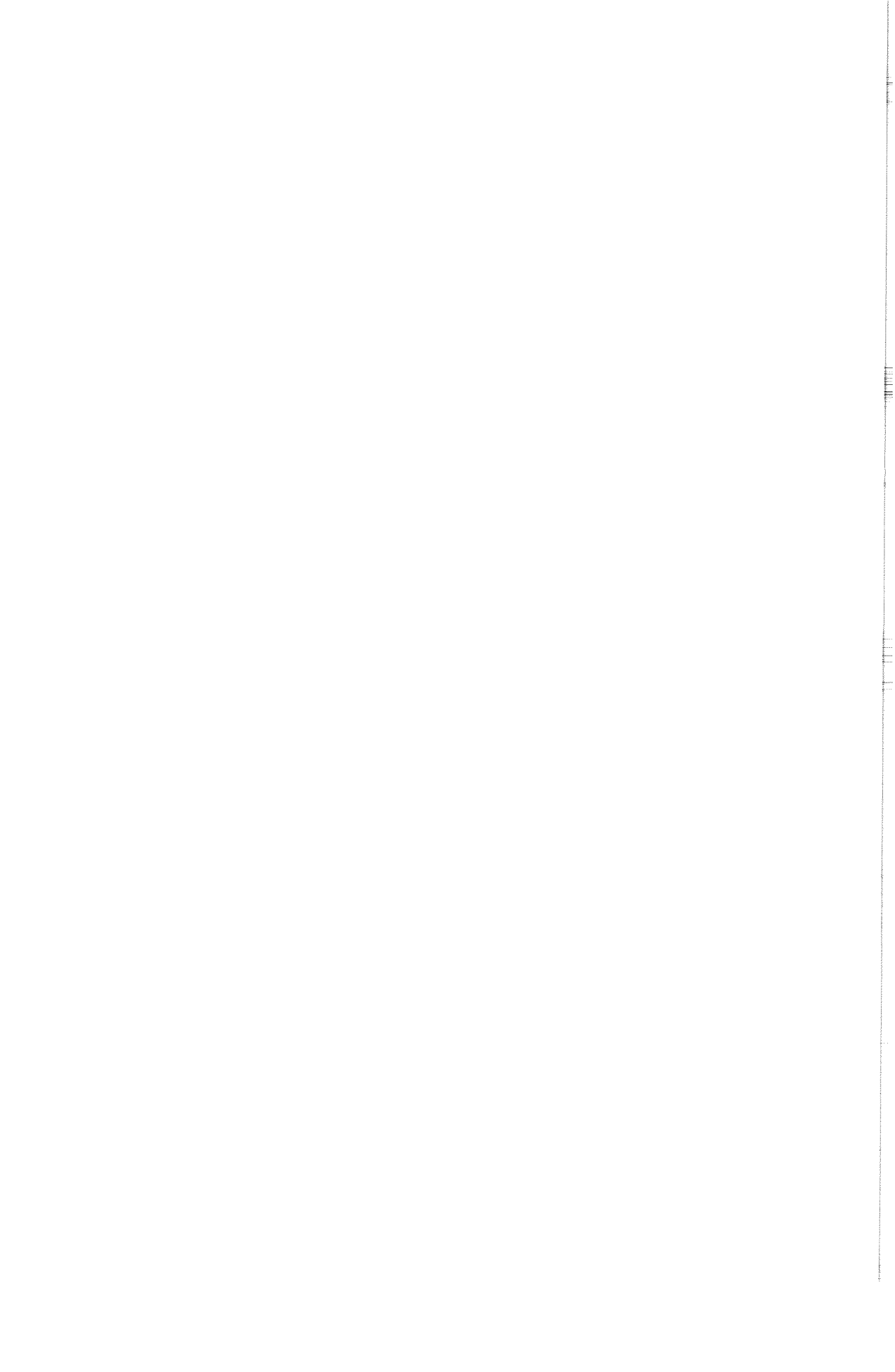


FIG. III.23

The overflow nappe without air underneath (similar to fig. I. 7b) behaves in approximately the same way as in 20). When a tiltable gate moves quickly forwards, the overflow decreases, because at its upstream side the gate makes place for water. The decreased overflow causes an additional pressure drop downstream of the gate. The decreased overflow is related

III. 4 Examples

only to a quick movement. In effect, this type of vibration can not be suppressed by the application of a more rigid hoist, but only by aeration.



Chapter IV

Hydrodynamic mass and damping

1. SUMMARY

Knowledge of the hydrodynamic mass (added mass) and damping is necessary for the computation of natural modes and natural frequencies of a structure, and also for the computation of self-exciting vibrations and the passive response of gates to hydrodynamic loads. Theoretical concepts are presented, together with computation methods applicable to a number of cases of vibrations of gates in flow. Some experimental data are discussed in relation to theory, among which the experiments on damping of a reversed Taintor valve which are presented in Appendix B.

2. THEORETICAL CONCEPTS

General literature on hydrodynamic mass (also called "added mass") and damping is referred to in Chapter I. In the following a qualitative estimate of the influence of certain pertinent parameters is derived from an analysis of the Navier-Stokes equation. Moreover, computation methods are presented, together with results of experiments leading to quantification for a number of cases.

Knowledge of the added mass is important, because gate and valve vibration analysis depends a great deal on it, not only for the determination of natural frequencies and the vibration modes belonging thereto, but, as shown in Chapter II, also for the analysis of self-exciting vibrations.

2a. GENERAL ASPECTS OF HYDRODYNAMIC MASS AND DAMPING

The behaviour of an oscillating structure can be described by

Chapter IV. Hydrodynamic mass and damping

combining the behaviour of a number of eigen-vibrations (= natural vibrations), each of which has a great similarity with the behaviour of a single oscillator.

As presented in Chapter I, equation (I. 1), a single oscillator is described by the equation:

$$\text{Force} = m\ddot{y} + c\dot{y} + ky \quad (\text{IV. 1})$$

The *general solution* of $m\ddot{y} + c\dot{y} + ky = 0$ is $y = Y_0 e^{st}$, which leads to:

$$s = \frac{-c}{2m} \pm \sqrt{\frac{c^2}{4m^2} - \frac{k}{m}}$$

For most cases of gate vibration $\frac{k}{m} > \frac{c^2}{4m^2}$, and from this condition the following general solution is derived:

$$y = e^{-\frac{c}{2m}t} (Y_1 \sin \sqrt{\frac{k}{m} - \frac{c^2}{4m^2}}t + Y_2 \cos \sqrt{\frac{k}{m} - \frac{c^2}{4m^2}}t) \quad (\text{IV. 2a})$$

The *particular solution* for periodic excitation is a periodic oscillation:

$$Y_0 = \sin \omega t$$

Introduced into equation (IV. 1) this gives:

$$F = -Y_0 m\omega^2 \sin \omega t + Y_0 c\omega \cos \omega t + Y_0 k \sin \omega t \quad (\text{IV. 2b})$$

At low frequencies of excitation, ω is small and $F \approx Y_0 k \sin \omega t$, so that the deflection is quasi-static with:

$$y = \text{force/rigidity} = F/k$$

Close to the resonance frequency, the spring force is approximately balanced by the mass acceleration. The eigen-frequency is by definition the value of ω at which there is complete balance:

$$Y_0 k = Y_0 m\omega_n^2$$

At higher frequencies, $m\omega^2 Y_0$ becomes dominant over the other forces and the response amplitude decreases rapidly:

$$Y_0 \approx F/m\omega^2$$

When a structure oscillates in submerged condition, the fluid, as will be shown later on, not only excites the structure by current and wave forces, but also gives rise to forces related to \ddot{y} and to \dot{y} . First named

IV. 2a General aspects

forces are *in phase* with the vibrational displacement $Y_0 \sin \omega t$ (*hydrodynamic mass* or in special cases *hydrodynamic rigidity*). The forces *out of phase* with the displacement (but in phase with the vibrational velocity) cause energy absorption (*hydrodynamic damping*) or energy production (*negative hydrodynamic damping* or *self-excitation*).

The hydrodynamic mass has no effect on the low-frequency response ($Y_0 = F/k$), nor has the real mass of the structure. But a shift will occur in the eigen-frequency of the structure because $Y_0 \omega_n^2 (m + m_{\text{water}})$ has to be balanced by the spring force $Y_0 k$.

For most of the vibration phenomena, important vibration amplitudes occur near or at the eigen-frequency. Because, at this frequency, spring and mass forces are in balance, a small excitation (which always turns out to act out of phase) is sufficient to cause a great amplitude. The increase of amplitude will continue till the damping force $c \omega Y_0$ balances the external force. For this reason, great interest has to be paid to hydrodynamic damping forces, even if these forces are an order of magnitude smaller than the forces due to the hydrodynamic mass.

Another aspect of the hydrodynamic mass and damping forces is their *coupling effect* when the vibrating structures have more than one degree of freedom. For the body of Fig. IV. 1, the added mass will be different for the different directions of vibration x and z , because the two flanges are of different size. The added mass concept can then be represented in the way of Fig. IV. 1b. But when the water pressures resulting from one degree of freedom also act on the degree of freedom in the other direction, the concept will change to that of Fig. IV. 1c. For more complicated cross-sections and more degrees of freedom, rotations and rotative moments also will play a role in the coupling.

An example of a coupling phenomenon has been found in a model investigation by the author [45] and is shown in Fig. IV. 2. The schematic representation of the forces at the gate section A-A shows that an upward acceleration causes a resultant force directed to the left ($F_2 > F_3$) and that F_2 and F_3 also cause a rotative moment. The vibration mode in submerged condition (found with vertical periodic excitation) shows a reversal of direction of the horizontal vibrations. This is clearly due to the coupling force ($F_2 - F_3$); the fact that the added mass is much greater for horizontal than for vertical movement only should have caused a decrease of horizontal amplitude.

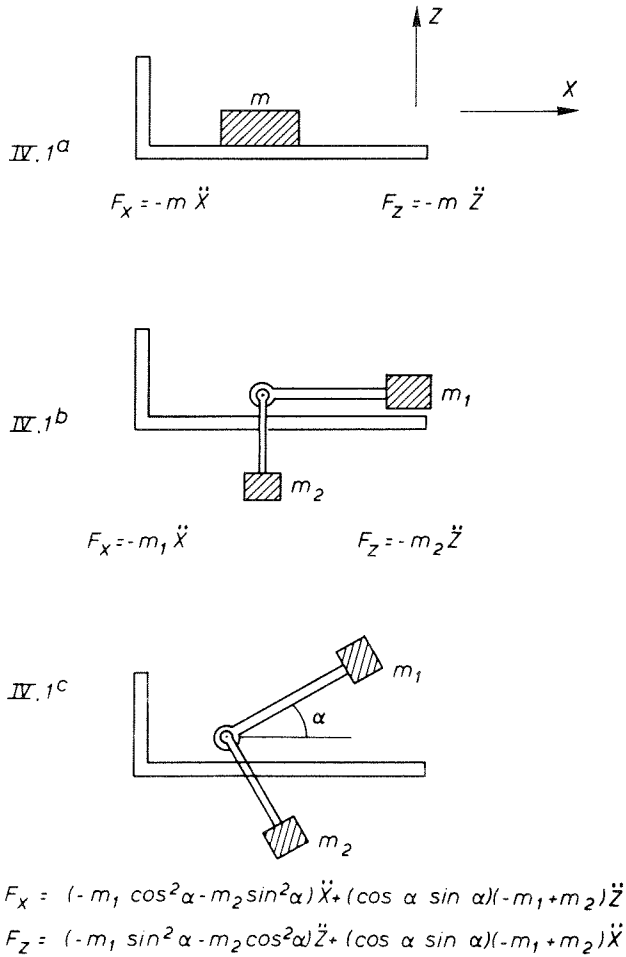
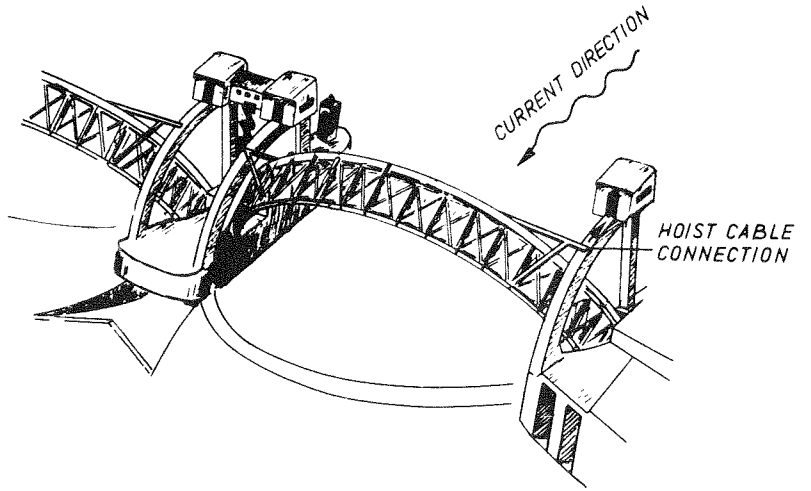


FIG. IV. 1

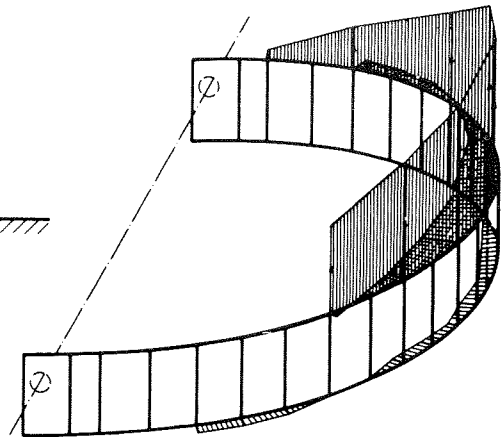
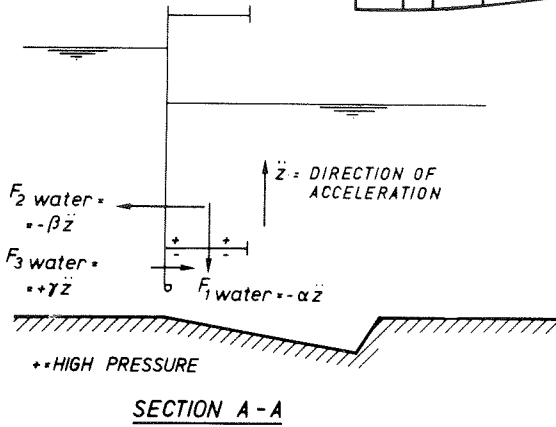
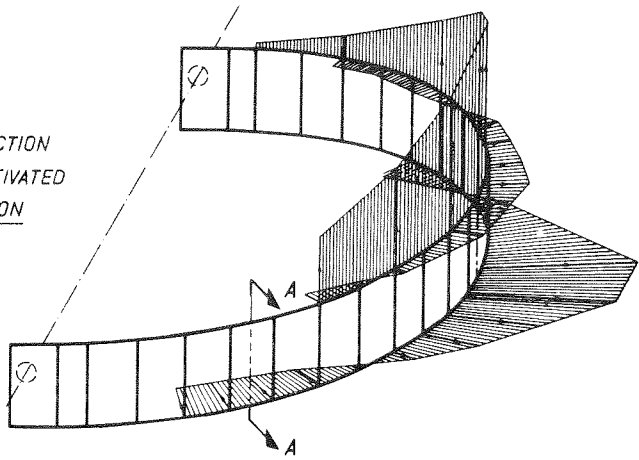
Also, the hydrodynamic damping forces act as a coupling between the different vibration modes, but because the damping forces are generally an order of magnitude smaller than the hydrodynamic mass forces, they will not change the pattern of the different vibration modes.

In the foregoing discussion, the hydrodynamic mass has been considered as the resultant force of all pressures resulting from the acceleration of the structure. Under certain conditions, which will be discussed in the next paragraph, it is possible that this mass will not be constant, but appears to be dependent on the frequency or amplitude of the vibration.

IV. 2a General aspects



STEREOMETRIC PROJECTION
OF THE VERTICALLY ACTIVATED
MODE, IN DRY CONDITION



SUBMERGED CONDITION

FIG. IV. 2

Chapter IV. Hydrodynamic mass and damping

In some cases there can also be a hydrodynamic rigidity. In general, this will only appear when the vibration causes a periodic change in the submergence depth of the structure (e.g., the heave frequency of the ship is determined by the equilibrium of the inertia force $(m + m_w) \omega^2 Y_0$ and the force due to submergence $k_{\text{water}} Y_0$). Occasionally the flow can cause hydrodynamic rigidity by the "windvane" effect. If, at periodic measurements, the in-phase forces are determined, separation of m_{water} and k_{water} is not always possible. It is then common to incorporate the hydrodynamic rigidity in the hydrodynamic mass and to introduce the force:

$$F = k Y_0 - m\omega^2 Y_0 = m'\omega^2 Y_0$$

In this case, m' clearly depends on ω .

2b. THE ADDED MASS IN STAGNANT WATER

The analysis of gate vibrations in stagnant water, induced by external excitation, does not seem of direct interest for the problem of flow-induced vibrations. It is, however, of interest because it can be seen as the limit condition of flow-induced vibration. Moreover, tests on natural vibration modes and natural frequencies, often done in stagnant water, are easier.

The analysis in this paragraph has been presented earlier in internal publications of the Delft Technical University by Schoemaker [91] and Kolkman [51].

It will be shown that, when a number of simplifying assumptions are made, the hydrodynamic mass becomes a constant factor, independent of ω and Y_0 . The flow caused by the vibration is, under the following assumptions, a potential flow. The assumptions are:

1. The vibration amplitude is small, so that the vibrating body can be described as a fixed body, on the surface of which pulsating sources and sinks are located, the discharge of each of which is equivalent to the water quantity displaced by the vibration in the area concerned.
2. The compressibility of water can be neglected.
3. The influence of viscosity on the water motion can be neglected.
4. Flow along all the boundaries can occur without hindrance.
5. Wave radiation at the free water surface can be neglected.
6. Mass and friction effects of the air can be neglected.
7. The water has a constant density.
8. Related to the fact that with the former simplifications only linear

IV. 2b Added mass in stagnant water

equations remain, the pressure pulsations in the liquid all have the same frequency as the body.

The equations for an incompressible fluid are:

$$\text{for continuity: } \frac{\partial u}{\partial x} + \frac{\partial v}{\partial y} + \frac{\partial w}{\partial z} = \nabla \cdot \bar{v} = 0 \quad (\text{IV. 3})$$

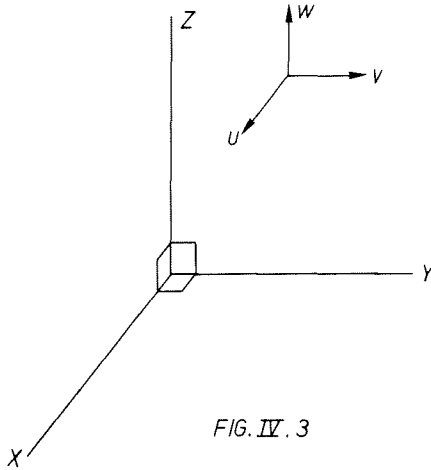
(u, v and w are the velocity components in x, y and z directions)

$$\text{for motion: } \rho \frac{\partial \bar{v}}{\partial t} + \rho (\bar{v} \cdot \nabla) \bar{v} = - \text{grad } p + \mu \Delta \bar{v} - \rho \times \text{grad } (g z) \quad (\text{IV. 4})$$

$$\text{or: } \rho \frac{\partial u}{\partial t} + \rho u \frac{\partial u}{\partial x} + \rho v \frac{\partial u}{\partial y} + \rho w \frac{\partial u}{\partial z} = - \frac{\partial p}{\partial x} + \mu \left(\frac{\partial^2 u}{\partial x^2} + \frac{\partial^2 u}{\partial y^2} + \frac{\partial^2 u}{\partial z^2} \right) - g(x)$$

The equations in y and z direction are similar.

$$g(x) = g(y) = 0 \text{ and } g(z) = g \text{ (acceleration of gravity)}$$



Because only small vibration amplitudes are dealt with, all non-linear terms disappear, and because according to the third assumption $\mu = 0$, equation (IV. 4) becomes now:

$$\rho \frac{\partial \bar{v}}{\partial t} = - \text{grad } (p + \rho g z) \quad (\text{IV. 5})$$

At the initial condition of $\bar{v} = 0$, the flow will remain rotation-free, due to the absence of shear forces, and the velocity pattern can be described with a pulsating velocity potential: $\phi_0(x, y, z) \sin \omega t$.

By introducing $\bar{v} = \text{grad } \phi$, equation (IV. 5) becomes $p_0 + p + \rho g z = - \rho \frac{\partial \phi}{\partial t}$

Chapter IV. Hydrodynamic mass and damping

and the pressure fluctuation at each point becomes:

$$p' = -\rho \frac{\partial \phi}{\partial t} \quad (\text{IV. 6})$$

For those surface areas of the body where the vibration of the body has a component normal to its surface, the condition for ϕ is:

$$v_n = \frac{\partial \phi}{\partial n} \quad (\text{IV. 7a})$$

At the other boundaries the equation becomes:

$$v_n = \frac{\partial \phi}{\partial n} = 0 \quad (\text{IV. 7b})$$

At the free water surface the approximate condition is:

$$\phi = 0 \quad (\text{IV. 7c})$$

(this is the case when the free-surface wave radiation is negligible).

Equations (IV. 7) determine the conditions at the water boundaries, which conditions in their turn determine the potential field.

As $v \propto \dot{\phi}$ and the pressures $p \propto \partial \phi / \partial t$, it is clear that the pressures are proportional to the acceleration of the structure only, independently of the frequency and amplitude of the vibration.

For the resultant force on the body the following ratios are obtained:

$$F \propto L^2 \rho \frac{\partial \phi}{\partial t} \propto \rho L^3 \frac{\partial v}{\partial t} \propto \rho L^3 \ddot{y}$$

(v is the momentary vibrational velocity, y the momentary displacement).

When this is compared with the force $F = m_w \ddot{y}$ caused by a constant added water mass m_w , the relation becomes:

$$m_w \propto \rho L^3 \quad (\text{IV. 8})$$

This means that when the simplifying assumptions are valid, m_w is constant and independent of vibrational frequency and amplitude.

Each mode of vibration, however, has its own quantity and distribution of the added water mass.

The physical meaning of the simplifications:

Sub 1

The amplitude Y_0 of the vibration $y = Y_0 \sin \omega t$ must be such that

$$Y_0 \ll L \quad (\text{IV. 9})$$

IV. 2b Added mass in stagnant water

L being a representative length of the body and fluid geometry.

If Y_0 is too great, the concept of pulsating, stationary sources and sinks ($y = 0$) is not valid.

The assumption (IV. 9) will nearly always be valid for gates; the breaking strength of the material restricts the allowable amplitude anyhow.

Sub 2

The compressibility gives rise to the radiation of waves. If the local velocity fluctuation is $u = U_0 \sin(\omega t \pm \frac{x}{c})$, in which c is the propagation velocity of the compression wave in water, the wave length λ of the compression wave becomes:

$$\lambda = 2 \pi c / \omega$$

The compressibility is to be neglected when $\lambda \gg L$ and so:

$$\frac{2 \pi c}{\omega} \gg L$$

or:

$$\omega \ll \frac{2 \pi c}{L} \quad (\text{IV. 10})$$

This assumption will always be true for gates, because L is some metres, $c > 1000$ m/s and ω is in the range of 0-50 rad/s in all practical cases. For valves in closed conduits, the theory is only valid for limited lengths of the pipe upstream and downstream of the valve.

Sub 3 and 4

The influence of the viscosity can be neglected in equation (IV. 4) when $\rho \frac{\partial \bar{v}}{\partial t} \gg \mu \Delta \bar{v}$. Because dv/dt is of the order of $\omega^2 Y_0$ and $\Delta \bar{v}$ of the order of $\omega Y_0 / L^2$, the condition is:

$$\rho \omega^2 Y_0 \gg \mu \omega Y_0 / L^2$$

or:

$$\frac{\rho \omega L^2}{\mu} = \frac{\omega L^2}{\nu} \gg 1 \quad (\text{IV. 11})$$

(ν = kinematic viscosity).

This will always be the case for gates, because ρ/μ is of the order of 10^6 sec/m^2 . The only point where $\Delta \bar{v}$ can be great is near sharp edges of the structure; there the viscosity will give rise to rotation and flow separation.

Near the boundaries slip flow occurs. The friction due to viscosity is

Chapter IV. Hydrodynamic mass and damping

treated by Lamb, Par. 345 [54].

When the boundary moves parallel to the flow with a velocity $u = U_0 \cos \omega t$, the flow at a distance n from the boundary moves parallel thereto with an amplitude:

$$u = U_0 e^{-\sqrt{\frac{\omega}{2\nu}} n} \cos \left(\omega t - \sqrt{\frac{\omega}{2\nu}} n \right)$$

(this is the solution of the equation $\rho \frac{\partial u}{\partial t} = \mu \frac{\partial^2 u}{\partial n^2}$)

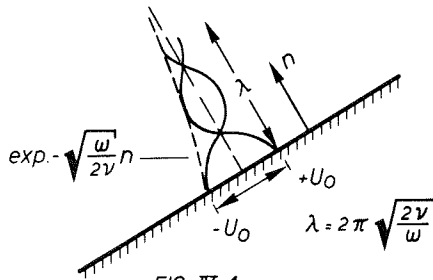


FIG. IV.4

The friction force becomes:

$$\frac{\tau}{\rho\nu} = -U_0 \sqrt{\frac{\omega}{2\nu}} \cos \omega t + U_0 \sqrt{\frac{\omega}{2\nu}} \sin \omega t \quad (\text{IV. 12})$$

The second term is the influence on the added water mass, the first is a damping factor.

A water sheet with a virtual mass and with a thickness δ should give a force

$$\tau_m = -\rho \delta \frac{\partial u}{\partial t} = \rho \delta \omega U_0 \sin \omega t$$

so the equivalent δ to the second term is:

$$\delta = \frac{\rho \nu U_0 \sqrt{\frac{\omega}{2\nu}}}{\rho \omega U_0} = \sqrt{\frac{\nu}{2\omega}} \quad (\text{IV. 13})$$

With ν of the order of 10^6 , a vibration of 1 c/sec. will give a sheet

thickness of $\delta = \frac{10^{-6}}{4\pi} \sim 0.3$ mm. This is negligible in gates, but can lead to a correction factor in hydraulic gate models.

IV. 2b Added mass in stagnant water

Sub 5

At the free surface the water-level fluctuations give rise to pressure fluctuations near the surface at variance with the assumption $p = 0$.

$$p' = \rho g z^* \quad \times$$

(p' = dynamic pressure component, z = momentary water-level above the still water surface).

$$\frac{dp'}{dt} = \rho g \frac{\partial z}{\partial t} = \rho g w \quad (w = \text{vertical water velocity at the free surface}).$$

Equation (IV. 5) remains valid and can be written as:

$$\rho \frac{\partial w}{\partial t} = - \frac{\partial}{\partial z} (p + \rho g z) = - \frac{\partial p}{\partial z} - \rho g$$

These two equations can be combined after calculating $\frac{\partial^2 p}{\partial t \partial z}$ from them:

$$\rho g \frac{\partial w}{\partial z} = - \rho \frac{\partial^2 w}{\partial t^2}$$

This leads to the condition that wave radiation can be neglected when

$$g \frac{\partial w}{\partial z} \ll \frac{\partial^2 w}{\partial t^2} \quad \text{or, considering that } \frac{\partial w}{\partial z} \text{ is of the order of } \omega Y/L \text{ and}$$

$$\frac{\partial^2 w}{\partial t^2} \text{ of the order of } \omega^3 Y \quad (Y = \text{amplitude of the local water oscillation}),$$

$$\frac{\omega^2 L}{g} \gg 1$$

(IV. 14)

Condition (IV. 14) can also be seen as the depth to which a surface wave still has influence on pressures. When the deep water wave length $\lambda = 2 \pi g/\omega^2$, the pressure decreases with depth; the 50% value occurs at a distance of $0.11 \lambda = 0.6 g/\omega^2$ below the free surface, and this distance should be small compared with the vertical gate dimensions.

In a submerged culvert valve, the determining dimension is the submergence depth related to 0.11λ .

\times In hydraulic models, the influence of the surface tension σ is not negligible and can cause a virtual increase of g . When the wave length is λ , the curvature of the water surface is $-z (2\pi/\lambda^2)$ and one gets $p' = \rho z (g + 4\pi^2 \sigma/\rho \lambda^2)$. σ being 0.074 N/m, p' doubles when $\lambda = 0.017$ m.

Chapter IV. Hydrodynamic mass and damping

The effect of $\omega^2 L/g$ is illustrated by the calculated water inertia shown in Chapter II, Fig. II. 17, where pressures in phase with the acceleration approach their limit value for $\omega^2 h/g > 10$.

Sub 6

The air friction is an order of magnitude smaller than the water friction. In equation (IV. 13) v of air is ten times greater, but the fact that δ becomes $\sqrt{10}$ times greater has no effect, because ρ is 10^3 times smaller.

Sub 7

The conditions at the interface between layers of different water density are comparable with the free surface condition, only the effect of gravity is greatly reduced (by a factor $\Delta\rho/\rho$). This means that when equation (IV. 14) is valid, it is certain that $\omega^2 L/(g\Delta\rho/\rho) \gg 1$.

2c. THE ADDED MASS IN FLOWING WATER

The vibrating body will superimpose upon the permanent flow condition at any point pressure and velocity fluctuations, which are mainly of the same frequency as the vibration.

In equation (IV. 4), all local velocities consist of a constant part v_0 and a fluctuating part v' , the latter being only an infinitesimal disturbance.

It is again the term $\rho \frac{\partial \bar{v}}{\partial t}$ ($= \rho \frac{\partial \bar{v}'}{\partial t}$) which will cause the added water mass effect.

However, the flow pattern of v' can be different from the one found in stagnant water. If, in equation (IV. 4), the additional velocities due to vibration are considered, the left hand part becomes in x direction:

$$\rho \frac{\partial u'}{\partial t} + \rho \left\{ (u + u') \frac{\partial (u + u')}{\partial x} + (v + v') \frac{\partial (u + u')}{\partial y} + (w + w') \frac{\partial (u + u')}{\partial z} \right\} \quad (\text{IV. 15})$$

Similar equations are found in y and z directions. In these equations, the terms u'^2 , v'^2 , etc. are negligible, (because $u' \ll u$, etc.) when only infinitesimal disturbances are considered. The same holds true for the products $u'v'$, etc. There only remain the terms:

$$\rho \frac{\partial u'}{\partial t} + \rho \left\{ u \frac{\partial u}{\partial x} + v \frac{\partial u}{\partial y} + w \frac{\partial u}{\partial z} \right\} + \rho \left\{ u' \frac{\partial u}{\partial x} + u \frac{\partial u'}{\partial x} + \text{etc.} \right\}$$

IV. 2c Added mass in flowing water

When the amplitude of u' remains constant but the frequency of vibration increases, the term $\rho \partial u' / \partial t$ tends to dominate, and again the extra velocity field tends to approach the one found in stagnant water. This occurs when:

$$\frac{\partial u'}{\partial t} \gg u' \frac{\partial u}{\partial x}$$

$\frac{\partial u'}{\partial t}$ is of the order of $\omega u'$, and $u' \partial u / \partial x$ of the order of $u'V/L$, so the additional flow becomes a potential one when:

$$\frac{\omega L}{V} \gg 1 \tag{IV. 16}$$

(All local velocities u , v and w are related to the reference velocity V).

In this case, the added water mass becomes the same as found in stagnant water.

Beside the condition of equation (IV. 16), the other *simplifying assumptions* of the preceding paragraph give rise to modified conditions for the validity of the potential flow solution for the computation of the added water mass.

Sub 1

The demand that the vibration amplitude is small remains unchanged.

Sub 2

The compression waves travel at a speed $V \pm c$, which results in the demand that:

$$\omega \ll \frac{2 \pi (c - V)}{L} \tag{IV. 10a)*}$$

For gates this demand is still no limitation; for all practical cases $V \ll c$ so that the equations (IV. 10 and 10a) pose approximately equal conditions.

Sub 3 and 4

The influence of viscosity in the laminar sublayer is proportional to the permanent and fluctuating velocity gradients; so the superposition does not give rise to new conditions.

* The equations numbered with "a" are equations modified due to the influence of flow.

Chapter IV. Hydrodynamic mass and damping

At increasing velocities, the sublayer gets thinner and the effect of viscosity decreases; so equation (IV. 11) is on the safe side.

There remains the classical condition that the flow pattern itself is no longer dependent on the viscosity when the Reynolds number is high enough:

$$Re = \frac{V L}{\nu} \gg 1 \tag{IV. 11a}$$

Sub 5

The radiation of free-surface waves can be neglected when the λ is small. Again, λ is a measure of the depth under the water surface, to which the wave pressures are still of importance. Because the orbital motion is greatest near the surface, the propagation velocity of waves is mainly determined by the local velocity near the water surface and equals:

$$c = v_{\text{surface}} + c_{\text{still water}}$$

λ can be calculated, taking into account that at both sides of a gate the surface velocity is directed towards the gate (Fig. IV. 5).

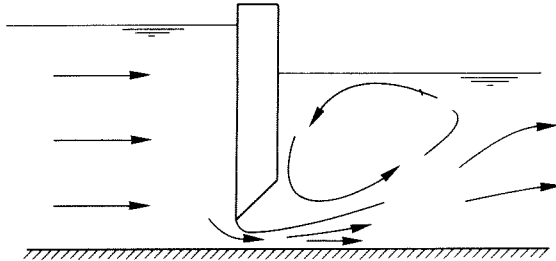


FIG. IV. 5

$$\lambda = (c - v) T = \left(\sqrt{\frac{g\lambda}{2\pi}} - v \right) \frac{2\pi}{\omega} \tag{T = 2\pi/\omega}$$

This results in a λ value to be calculated from:

$$\lambda^2 + \lambda \left(\frac{4\pi v}{\omega} - \frac{2\pi g}{\omega^2} \right) + \frac{4\pi^2 v^2}{\omega^2} = 0$$

It appears that λ becomes smaller when the water velocity increases, and when $v > \frac{g}{4\omega}$ no wave radiation occurs at all.

In practice, little wave radiation occurs; only upstream of a gate.

This occurs at horizontal gate vibration and also at vertical vibration

IV. 2d Water damping

caused by a discharge which varies periodically.

For flow, the conditions (IV. 14) for stagnant water is much on the safe side.

Sub 6 and 7

The conclusions drawn for stagnant water remain unchanged in flowing water: friction and mass of air are negligible just as density differences in water.

2d. WATER DAMPING IN STAGNANT AND FLOWING WATER

In stagnant water, the damping forces are due to the drag forces, to viscosity (resulting in friction along the skin plate and girders of a gate) and to wave radiation. In flowing water, the drag forces, but now related to the difference in velocity between the flow and the vibrating structure, become dominant.

The damping forces in flowing water

In the preceding paragraph, there has been found for a gate in a flow field that, when $\omega L/V \gg 1$ (equation (IV. 16)), the term $\partial u'/\partial t$ dominates the term $(u' \partial u/\partial x + u \partial u'/\partial x)$, etc. in equation (IV. 4) and that by this reason the added water mass remains unchanged relative to the stagnant water condition. This, however, does not mean that last named term has no effect: it generates damping forces, which are in phase with u' and out of phase with $\partial u'/\partial t$.

The fact that these damping forces are small compared with the acceleration forces does not detract from their importance; in a mechanical vibration system the damping forces are also relatively small compared with the rigidity forces and the inertial forces.

From equation (IV. 15) follows that, as u' , v' and w' are much smaller than u , v and w , only terms of the following character remain (apart from the "mass" terms $\rho \partial u'/\partial t$ etc. and neglecting the viscosity μ):

$$-\frac{\partial p}{\partial x} = \rho \left(u' \frac{\partial u}{\partial x} + u \frac{\partial u'}{\partial x} \text{ etc.} \right)$$

These terms represent out-of-phase forces, i.e. damping forces. This means that all the "damping" pressures caused by vibration are proportional to the permanent flow velocities and also proportional to the fluctuating velocities. The same holds true for the resulting force on the structure.

Chapter IV. Hydrodynamic mass and damping

In the equation of the single oscillator (IV. 1), the damping force $c_w \dot{y}$ will now be proportional to the working area (L^2), to $\rho \times (u, v$ and $w)$ and to \dot{y} ; so:

$$c_w :: \rho L^2 V \quad (\text{IV. 17})$$

Because, in a given flow field, u, v and w have at each point a constant relation to each other, they can be represented in terms of a reference velocity V . Equation (IV. 17) can be derived in a different way, as has been shown in Appendix B. When the flow and the vibration have the same direction, when the flow velocity dominates the vibration velocity, and when the drag coefficient is not influenced by the vibration amplitude, the force becomes:

$$F = \frac{1}{2} \rho L^2 C_D (V^2 - V \dot{y} + \dot{y}^2)$$

The first term is independent of the vibration, the last results in a force with a double frequency relative to the vibration frequency; only the second term is relevant and appears to be a damping force. This results in an expression for the water damping:

$$c_w = \rho L^2 C_D V \quad (\text{IV. 17}')$$

When no information is available on hydrodynamic damping, equation (IV. 17') can give a rough evaluation. However, when flow and vibration are not in the same direction, this equation can not be applied, but c_w will than also become proportional to $\rho L^2 C_D V$.

Equations (IV. 17 and 17') are demonstrated in Appendix B, Fig. 5, where the damping value of a fully submerged Taintor valve is presented. The damping value c (represented as R in Fig. 5) is made dimensionless by dividing it by $\rho V L^2$ and it is shown that the value $R/\rho V D W$ (D and W are the culvert height and width and DW can be considered as L^2) tends to become constant when the vibration amplitude is small. From experiments there is a clear tendency that at great ND/V values (this is the value $\frac{1}{2\pi} \omega L/V$ of equation (IV. 16)), and great Y_0/D values, the dimensionless damping value increases. This is due to the fact that for these cases the water velocity does no longer dominate the vibration velocity. For the example presented in Appendix B, the critical Y_0/D value, at which damping becomes dependent upon it, is remote from the amplitudes caused by flow. This will probably always be the case when a structure is designed in such a way that no self-excited vibrations occur.

IV. 2d Water damping

The skin friction and the drag force in stagnant water

The subject of skin friction has already been treated in the preceding paragraph. The effect of the skin friction due to vibration can be considered complementary to the skin friction due to the permanent flow. Because the shear stress in a sublayer is already proportional to the velocity gradient, the two can be combined as long as the laminar sublayer is not too thin. This means that the effect of skin friction in flowing water is equal to or smaller than that in stagnant water, provided that the additional flow pattern due to vibration is the same (condition of equation (IV. 16)). Skin friction can be derived from equation (IV. 12), in which the term in phase with the vibration velocity $u' = u_0 \cos \omega t$ is:

$$\tau = -\rho \nu U_0 \sqrt{\frac{\omega}{2\nu}} = -\rho \sqrt{\frac{\omega\nu}{2}} \times \dot{y} \quad (\text{IV. 18})$$

This shear stress works along all the plates and girder surfaces which are parallel to the direction of vibration. This area will be denominated by αL^2 , wherein L^2 shows the order of magnitude and α indicates that L^2 is related to the skin plate parallel to the vibration direction.*

The damping force becomes (in terms of c , as in equation (IV. 1)):

$$c_w \dot{y} = \rho \sqrt{\frac{\omega\nu}{2}} \alpha L^2 \dot{y},$$

so

$$c_w = \alpha L^2 \rho \sqrt{\frac{\omega\nu}{2}} \quad (\text{IV. 19})$$

Another damping element is formed by the viscosity effect near the sharp edges. Here, the potential concept leads to infinitely high velocities, which in practice always lead to flow separation and turbulence.

* To a small extent, the plates which are not parallel to the direction of vibration have also to be taken into account, because the flow induced by the vibration always has a component in the plate direction also, even when the plate is perpendicular to the vibration direction (for instance at the gate lip in Fig. IV. 6a). Although the shear stresses perpendicular to the vibration do not directly transmit energy, they produce turbulence and heat and so cause energy loss, which finally has to be compensated by energy input of the vibrating structure.

Chapter IV. Hydrodynamic mass and damping

At $\omega = 0$ and infinitely great vibration amplitudes the damping force $c_w \dot{y}$ in stagnant water tends to depend only on the drag force and so on the drag coefficient C_D :

$$\text{damping force} = - C_D \beta L^2 |\dot{y}| \dot{y} \tag{IV. 20}$$

L^2 now indicates the order of magnitude of the effective area and β indicates that this is related to the gate area perpendicular to the direction of vibration.

In Appendix B, (equation (12)) has been calculated, which is the equivalent c_w value, so that $c_w \dot{y}$ absorbs per period of a stationary vibration the same amount of energy as the force of equation (IV. 20). This results in the linearized damping factor:

$$c_w = \beta L^2 \frac{4}{3\pi} C_D \rho \omega Y_o \tag{IV. 21}$$

wherein

$$C_D = f (Y_o/L) \tag{IV. 21a}$$

The value C_D is not independent of the amplitude of vibration and is not equal to the C_D of stationary flow. The vortex street will be shorter under stagnant conditions.

The resultant value of c_w in stagnant water is now obtained by the summation of the values found in equations (IV. 19 and 21), assuming that the two factors do not interfere.

This seems reasonable, because they act chiefly on different parts of the structure.

$$c_w = \alpha L^2 \rho \sqrt{\frac{\omega v}{2}} + \beta L^2 \frac{4}{3\pi} C_D \rho \omega Y_o \tag{IV. 22}$$

In Fig. 4 of Appendix B, there is presented the measured water damping of a model of a reversed Taintor valve, made dimensionless by dividing it by $\rho DW \omega Y_o$ (in Fig. 4, R is the same as c_w and the culvert cross-section DW can be considered as L^2). From the combination with equation (IV. 22) follows:

$$\frac{R}{\rho D W \omega Y_o} = \frac{c_w}{\rho L^2 \omega Y_o} = \alpha \sqrt{\frac{v}{2 L^2 \omega}} \frac{L}{Y_o} + \frac{4}{3\pi} \beta C_D \tag{IV. 23}$$

When a rough guess is made of the effective valve area on which the viscous skin friction can act (about 5 times culvert cross-section), it appears that about 20 - 30% of the damping value presented in Fig. 4

IV. 3a Computation methods: added mass

of Appendix B can be related to this skin friction.

The systematic influence of the viscosity could, however, not be derived from the systematic influence of the value of ω , except to some extent for the very small Y_0/D value of 3.10^{-4} (i.e. a great L/Y_0 value in equation (IV. 23)).

It has been shown in Appendix B that under flow conditions, the influence of Y_0/L on C_D disappears, as does the significance of skin friction.

The radiation of waves

The influence of wave radiation on the forces acting on the structure is mainly of importance when the vibrating gate members or the retaining plate are near the free surface of the water. Due to the relatively high vibration frequencies of gates, the wave lengths of the radiated waves are short and consequently the resulting pressures are not sensible at the deeper parts of the gates. In the next paragraph it will be shown that, even at horizontal vibration of gates, the damping by wave radiation is unimportant compared to the damping due to the permanent flow. Only in the stagnant water conditions wave radiation can play a role.

An indication of the decreasing energy transfer at greater water depths is found in Fig. II. 18. When, over a constant height δ , there is a velocity fluctuation due to vibration, then at greater depths the value of h/δ increases and so does the value of $\omega^2 h/g$. In this Fig. it can be seen that that part of the pressure fluctuations, which is proportional to and in phase with the velocity and which leads to energy radiation, decreases greatly.

3. COMPUTATION METHODS AND EXAMPLES OF COMPUTATION

3a. THE ADDED MASS

As has been shown in the preceding paragraph, the conditions in stagnant water lead to the conclusion that the flow due to vibration is nearly a potential flow; the same holds true in the case of flowing water, when the dimensionless parameter $\omega L/V \gg 1$.

There are different methods of computing the potential flow:

- A. Conformal mapping, see Lamb [54]. Lamb found an analytical solution for an infinitely long, vibrating strip or cylinder: the added water mass appears to be $m = \frac{1}{4} \pi D^2$, in which D is the diameter of the

Chapter IV. Hydrodynamic mass and damping

cylinder or the width of the strip.

B. Computation methods, in which we imagine that a finite number (say n) of sources and sinks represents the boundaries. The flow of each source is computed in such a way that the velocity perpendicular to the surface is $\partial\phi/\partial n = 0$ for the non-vibrating part and $\partial\phi/\partial n = dy/dt$ for the vibrating part thereof. In a two-dimensional case in an infinite body of water $\phi = \frac{q_n}{2\pi} \ln r$ (r = radial distance from the source). These conditions lead to n equations for n unknown source discharges. This method is also suited to take into account free-surface conditions including wave radiation. When the bottom is horizontal and there is no reflection of radiated waves, it is possible to simplify the method so that, for each pulsating source at the gate surface, the potential flow pattern, including wave radiation, can be given in a general form. This general form was first presented by Becker [10]. This facilitates computation, because now only structure movements have to be programmed, while the bottom and water surface conditions are automatically fulfilled. A mathematical model is available and operational at the Delft Hydraulics Laboratory, developed for the purpose of computing the forces exerted by oncoming free-surface waves on solid structures. An investigation is in progress, to make this model applicable to the determination of added mass and wave radiation.

C. The electric analogon technique is described in its principles by Lamb in his handbook, par. 60^a, [54] and has been extended to three-dimensional problems by Zienkiewicz and Nath [109]. It solves the Laplace equation (eq. of continuity) under the supplementary condition that the flow is rotation-free. The free-surface condition is introduced as $\phi = 0$ (equation (IV. 7c)); this does not take into account wave radiation. The currents at the boundaries follow again from the condition $\partial\phi/\partial n = 0$ or $\partial\phi/\partial n = dy/dt$. The pressures follow from:

$$p = -\rho \frac{\partial\phi}{\partial t} \quad (\text{fluctuations with amplitude } \rho \omega \phi)$$

(ϕ is the voltage at the boundary, divided by the conductivity of the semi-conductor).

D. The Laplace equation for a horizontally vibrating vertical wall can be solved (including the effect of wave radiation) by finding the general solution, using the known linear solutions for waves.

IV. 3a Computation methods: added mass

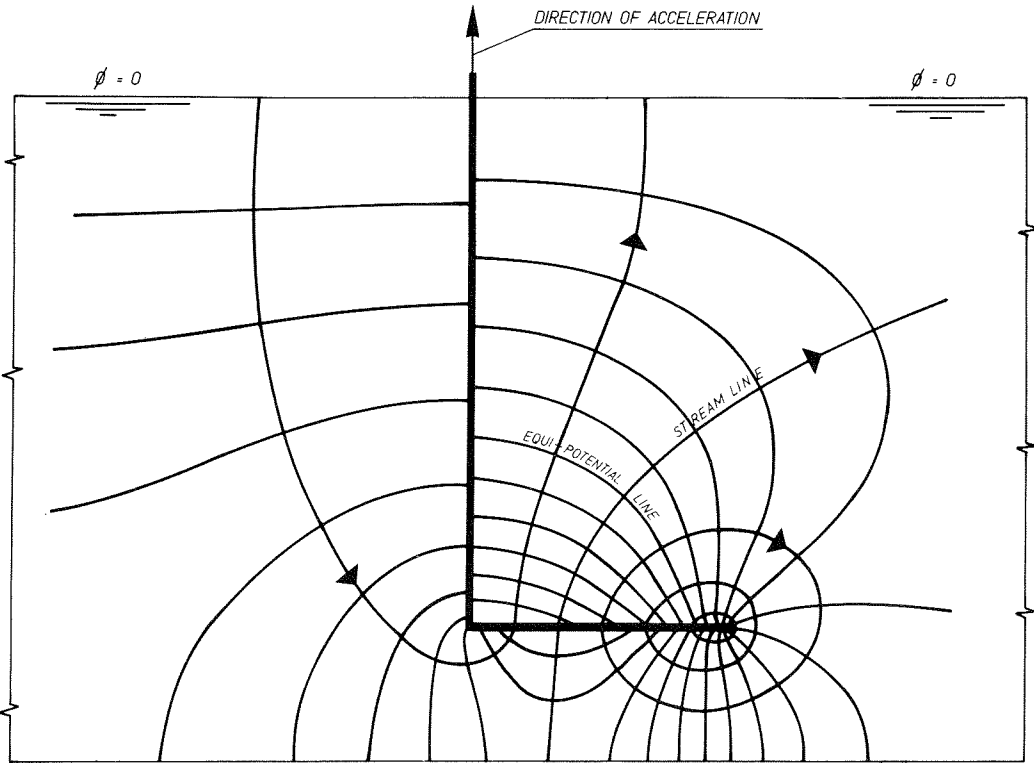


FIG IV. 6a EQUIPOTENTIAL AND STREAM LINES (L GATE)

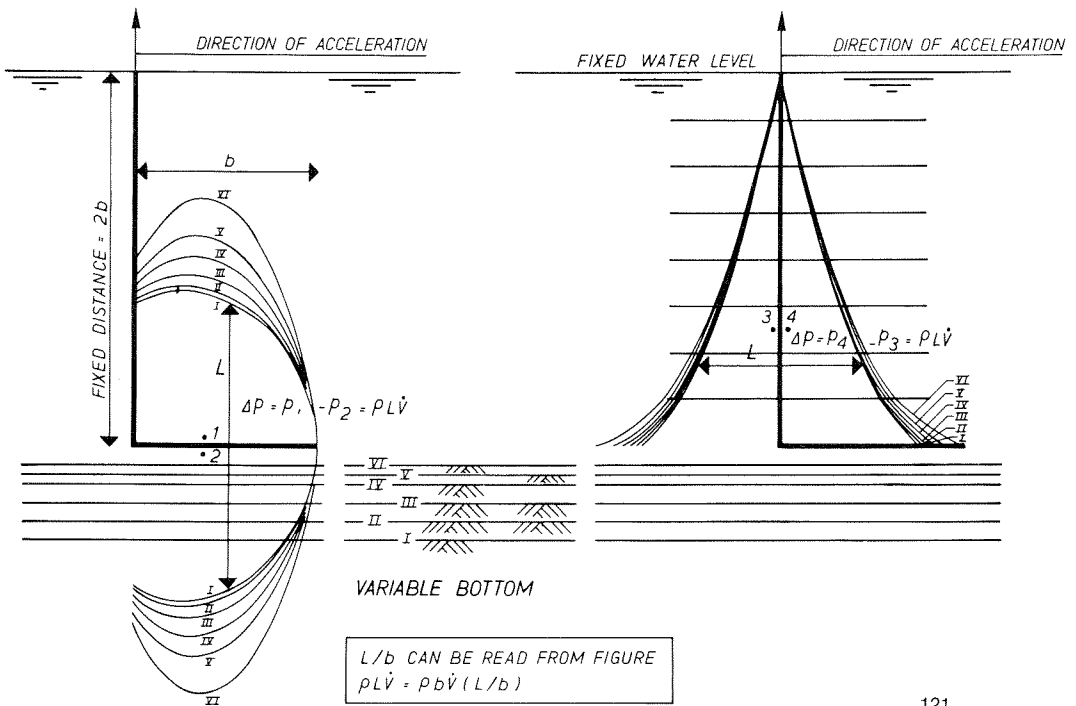


FIG. IV. 6^b FIXED WATER LEVEL, BOTTOM VARIABLE (L GATE)

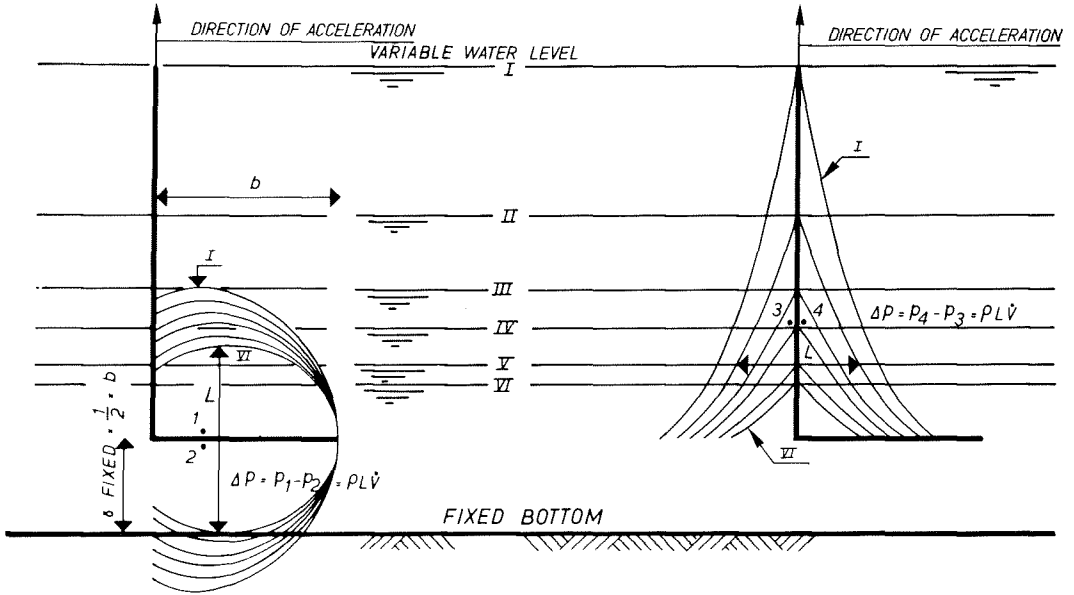


FIG. IV 6^c, FIXED BOTTOM, VARIABLE WATER LEVEL (L GATE)

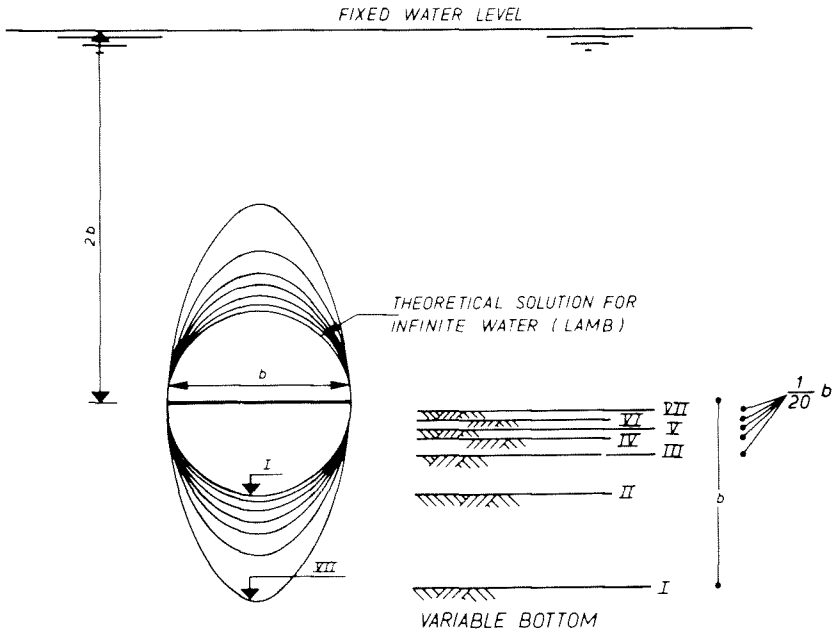


FIG. IV 6^d FIXED WATER LEVEL, VARIABLE BOTTOM (HORIZONTAL STRIP)

IV. 3b Computation methods: wave radiation

The boundary conditions at the wall have to be separated into series of which each term belongs to one wave. This method, developed in the Delft Hydraulics Laboratory by Berkhoff [12], is related to computation methods mentioned under B developed for the computation of forces on bodies subjected to wave action.

A similar method of solution, on the assumption that wave radiation can be neglected, is presented in Chapter II, par. 16; the results agree with those for high-frequency vibrations in the method indicated above.

E. Another computation method for added mass and wave radiation is the finite element method. At a recent symposium in Swansea (1974) [71], the possibilities of this technique were presented, but until now no experience seems available on its application to gates. For three-dimensional problems, its programming becomes elaborate.

The investigation method with an electric analogon has been used for the composition of Fig. IV. 6. These figures present the added mass of water and also the coupling forces in horizontal direction for a gate and for a strip under stagnant water conditions. The tests have been executed for stagnant water conditions, but the two water-levels can, in an electric analogon, also be at different heights. The test results were obtained in a Delft Hydraulics Laboratory investigation still in progress.

3b. THE WAVE RADIATION

Wave radiation represents generally only a small part of the total damping of a vibrating structure.

For horizontal vibration, wave radiation has been computed for stagnant deep water conditions, i.e. for the limit value (under flow conditions, the on-gate flow reduces wave length, the wave propagation velocity and therefore energy radiation; shallow water also reduces wave propagation velocity and energy radiation).

For horizontal vibration of a wall, the following computation of energy can be made (results are in accordance with the results of Fig. II. 8, determined with method C).

In the practical range of gates, all waves generated are deep water waves. The theory of deep water waves provides the equation:

$$\lambda = 2 \pi g / \omega^2 \quad (\text{IV. 24})$$

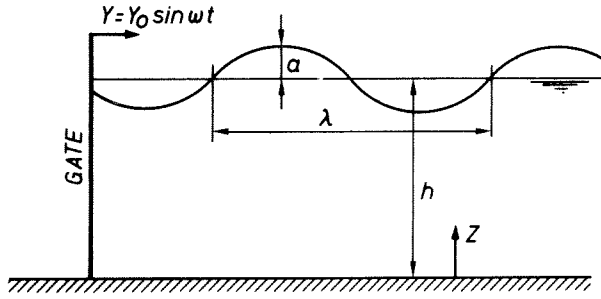


FIG. IV. 7

For $\lambda < 2 h$, the assumption of deep water waves is valid.

At an arbitrary height z above the bottom, pressure p and horizontal water velocity v due to the waves are:

$$p = \rho g a e^{-2 \pi (h-z)/\lambda} \sin \omega t \quad (\text{IV. 25})$$

$$v = \omega a e^{-2 \pi (h-z)/\lambda} \sin \omega t \quad (\text{IV. 26})$$

The energy transfer per unit of time and per unit of width over this section is:

$$E_1 = \frac{1}{T} \int_0^T \int_0^h v p dt dz = \frac{1}{8\pi} \rho g \omega a^2 \lambda (1 - e^{-4 \pi h/\lambda})$$

which for $h > \frac{1}{2}\lambda$ is approximately:

$$E_1 \sim \frac{1}{8\pi} \rho g \omega a^2 \lambda$$

and combined with (IV. 24):

$$E_1 = \frac{1}{4} \rho g^2 a^2 / \omega \quad (\text{IV. 27})$$

The energy transfer from the vibrating wall is:

IV. 3c Computation methods: damping by flow

$$\begin{aligned}
 E_2 &= \frac{1}{T} \int_0^T \int_0^h v p \, dt \, dz \\
 &= \frac{1}{T} \int_0^T \int_0^h (\omega Y_0 \sin \omega t) (\rho g a e^{-2 \pi(h-z)/\lambda} \sin \omega t) \, dt \, dz \\
 &= \frac{\lambda}{4\pi} \omega Y_0 \rho g a (1 - e^{-2 \pi h/\lambda}) \sim \frac{\lambda}{4\pi} \omega Y_0 \rho g a \quad (\text{IV. 28})
 \end{aligned}$$

Eliminating λ by means of (IV. 24) results in:

$$E_2 = \frac{1}{2} \rho g^2 a Y_0 / \omega \quad (\text{IV. 29})$$

From the energy balance between the wall and the section at the depth considered, there follows $E_1 = E_2$, which results in:

$$a = 2 Y_0 \quad (\text{IV. 30})$$

The energy absorption by a damper c of the mechanical system (IV. 1) is:

$$E_3 = \frac{1}{T} \int_0^T c \dot{y} y \, dt = \frac{1}{T} \int_0^T c \omega^2 Y_0^2 \sin^2 \omega t \, dt = \frac{1}{2} c \omega^2 Y_0^2$$

The equivalent value of c causing an energy absorption equal to the wave radiation follows from $E_3 = E_2$ and using (IV. 30):

$$c_{\text{wave}} = 2 \rho g^2 / \omega^3 \quad (\text{IV. 31})$$

c_{wave} = damping factor due to the wave, per unit of width of the gate.

3c. THE DAMPING BY FLOW

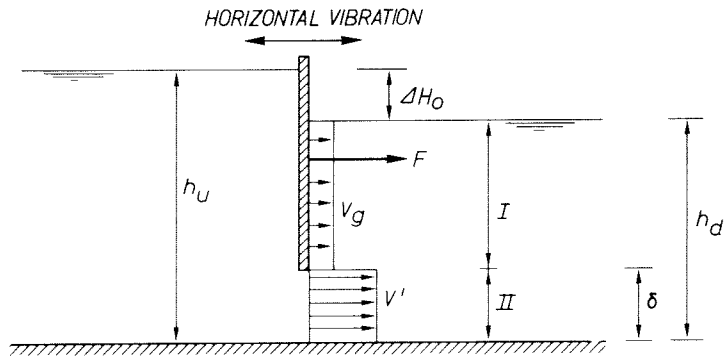
A. Horizontal vibrations

A computation method for water damping has been developed, assuming that the head loss of the flow under the gate is the determining factor for the energy dissipation and that wave radiation can be neglected. Both the hydrodynamic mass and damping are found by this method, but the results are mainly of interest for the damping.

Chapter IV. Hydrodynamic mass and damping

For the sake of simplicity, it is assumed that the discharge and discharge fluctuation across the gap of the gate are well distributed over the length of the gap. The momentary discharge is assumed to be related to the local momentary head difference across the gap.

It is also assumed that the frequency of vibration is so high, in accordance with equation (IV. 16), that the pressure pulsations in the water are related only to the periodic acceleration of the boundary; both the gate acceleration and the first derivative of the discharge fluctuation under the gate are considered.



$$v_{water} = v_0 + v'$$

F = FORCE ACTING ON THE GATE

FIG. IV. 8

The dynamic pressure in depth zone I is due partly to the acceleration of the gate \dot{v}_g and partly to the water velocity fluctuation \dot{v}' ; the force can be described as:

$$F_{\text{downstream}} = F_d = - C_{I_g} \rho \dot{v}_g \delta^2 - C_{I_w} \rho \dot{v}' \delta^2$$

The value δ has been chosen as length parameter, because this reference length is the same for the upstream and downstream conditions. The coefficients C_{I_g} , etc. will be determined later on. The total force (per unit of width) working on the gate (i.e. the combined effect of the added water mass and the damping force) is:

$$\begin{aligned}
 F_I &= - \rho \delta^2 \left\{ (C_{I_{g_{up}}} + C_{I_{g_{down}}}) \dot{v}_g + (C_{I_{w_{up}}} + C_{I_{w_{down}}}) \dot{v}' \right\} \\
 &= - \rho \delta^2 (\alpha \dot{v}_g + \beta \dot{v}')
 \end{aligned}
 \tag{IV. 32}$$

IV. 3c Computation methods: damping by flow

In the same way it can be formulated that the force over depth zone II, which is responsible for the velocity fluctuation, equals:

$$\begin{aligned}
 F_{II} &= -\rho \delta^2 \left\{ (C_{IIg_{up}} + C_{IIg_{down}}) \dot{v}_g + (C_{IIw_{up}} + C_{IIw_{down}}) \dot{v}' \right\} \\
 &= -\rho \delta^2 (\gamma v'_g + \epsilon \dot{v}')
 \end{aligned}
 \tag{IV. 33}$$

The relation between discharge and force under constant conditions is:

$$v_w = \mu \sqrt{2g\Delta H} = \mu \sqrt{\frac{2\Delta p}{\rho}} = \mu \sqrt{\frac{2 \text{ Force II}}{\rho \delta}}$$

A small fluctuation of the velocity will be linearly related to the force fluctuation over depth zone II:

$$v'_w = \frac{1}{2} \mu \sqrt{\frac{2}{\rho \delta}} \frac{\Delta \text{ Force}}{v_w}$$

It seems reasonable to calculate the head loss from the difference in velocity between the water and the gate, so:

$$v'_w = v' - v_g$$

Introducing also $\Delta \text{ Force}' = F_{II}$ we get:

$$v' - v_g = \frac{\mu}{\sqrt{2\rho \delta}} \frac{F_{II}}{v_w}
 \tag{IV. 34}$$

Equations (IV. 32 - 34) are sufficient to eliminate v' and F_{II} and to find the relation between v_g and F_I . The following expressions are introduced for the periodic fluctuations:

$$\left. \begin{aligned}
 v_g &= v_g e^{i\omega t} \\
 v' &= v' e^{i\omega t} \\
 F_I &= F_I e^{i\omega t} \\
 F_{II} &= F_{II} e^{i\omega t}
 \end{aligned} \right\} (v_g \text{ and } \omega \text{ real; } v', F_I \text{ and } F_{II} \text{ complex})$$

Now the three equations are rewritten with all terms divided by $e^{i\omega t}$:

$$F_I = -\rho \delta^2 \omega (i \alpha v_g + i \beta v')
 \tag{IV. 35}$$

$$F_{II} = -\rho \delta^2 \omega (i \gamma v_g + i \epsilon v')
 \tag{IV. 36}$$

$$v' - v_g = \frac{\mu F_{II}}{\sqrt{2\rho \delta * \rho g \delta \Delta H_0}}
 \tag{IV. 37}$$

Chapter IV. Hydrodynamic mass and damping

Combining (IV. 36 and 37) results in:

$$v' = v_g - \frac{\mu \rho \delta^2 \omega}{\rho \delta \sqrt{2g\Delta H_0}} (i \gamma v_g + i \epsilon v')$$

or:

$$v' = v_g \left(1 - i \frac{\gamma \mu \delta \omega}{\sqrt{2g\Delta H_0}} \right) : \left(1 + i \frac{\epsilon \mu \delta \omega}{\sqrt{2g\Delta H_0}} \right) \quad (\text{IV. 38})$$

Now F_I can be computed with (IV. 35 and 38), but first we introduce the reduced frequency:

$$S = \frac{f \delta}{\sqrt{2g\Delta H}}$$

or:

$$\frac{\omega \delta}{\sqrt{2g\Delta H}} = 2 \pi S \quad (\text{IV. 39})$$

Equation (IV. 38) now becomes:

$$v' = v_g \frac{1 - i \gamma \mu 2\pi S}{1 + i \epsilon \mu 2\pi S}$$

or:

$$v' = v_g \frac{1 - i (\epsilon + \gamma) \mu 2\pi S - \epsilon \gamma \mu^2 4\pi^2 S^2}{1 + \epsilon^2 \mu^2 4\pi^2 S^2} \quad (\text{IV. 40})$$

Introducing this in (IV. 32) gives:

$$\begin{aligned} F_I &= -\rho \delta^2 \omega v_g \left\{ i \alpha + i \beta \frac{1 - i (\epsilon + \gamma) \mu 2\pi S - \epsilon \gamma \mu^2 4\pi^2 S^2}{1 + \epsilon^2 \mu^2 4\pi^2 S^2} \right\} \\ &= -\rho \delta^2 \omega v_g \left\{ \frac{(\epsilon + \gamma) \mu 2\pi S}{1 + \epsilon^2 \mu^2 4\pi^2 S^2} \beta + i \left(\alpha + \frac{1 - \epsilon \gamma \mu^2 4\pi^2 S^2}{1 + \epsilon^2 \mu^2 4\pi^2 S^2} \beta \right) \right\} \quad (\text{IV. 41}) \end{aligned}$$

If this force on the gate is compared with the equivalent force due to the added water mass m_w and the virtual water damping c_w , it can be described as:

$$F_I = -m_w \dot{v}_g - c_w v_g$$

IV. 3c Computation methods: damping by flow

After introducing again the fluctuation $F_I e^{i\omega t}$, this becomes:

$$F_I = -i m_w \omega v_g - c_w v_g \quad (\text{IV. 42})$$

So there follows from (IV. 41 and 42):

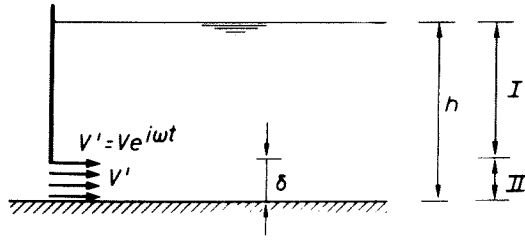
$$m_w = \rho \delta^2 \left(\alpha + \frac{1 - \epsilon \gamma (\mu 2\pi S)^2}{1 + \epsilon^2 (\mu 2\pi S)^2} \beta \right) \quad (\text{IV. 43})$$

$$c_w = \rho \delta^2 \omega \frac{(\epsilon + \gamma) \mu 2\pi S}{1 + \epsilon (\mu 2\pi S)} \beta \quad (\text{IV. 44})$$

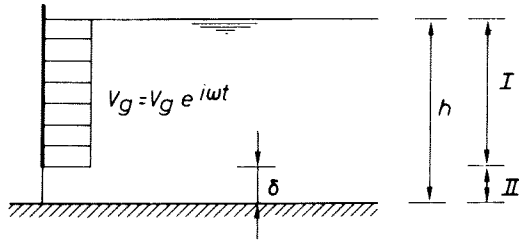
As it can be seen from the equations (IV. 32 and 33), the coefficients α , β , γ and ϵ have to be calculated from the coefficients C_I and C_{II} for the gate and for the gap. This is done in the same way as in Chapter II, par. 16.

In Fig. IV. 10 the results are shown of the computation of the forces in the gap due to discharge fluctuations in the gap. In fact, the coefficient C_{IIw} of Fig. IV. 10 is the same as the coefficient c_L of equation (II. 53), which is presented in Fig. II. 17. Only $c_L \rho \delta \dot{v}'$ in Fig. II. 17 is the pressure, and Fig. IV. 10 shows the force $p \delta = (C_{IIw}^{up} + C_{IIw}^{down}) \rho \delta^2 v'$.

The coefficient α has earlier been calculated for the Delft Hydraulics Laboratory investigation of the Haringvliet gates to derive the added water mass when the gate stands on a sill (published by Allersma [7], Fig. 3a). These results have been used to check the calculations made of the coefficients α , β , and ϵ . The calculation itself will not be presented in the following. All the computations have been made under the assumption that no wave radiation occurs, firstly because for all practical purposes the $\omega^2 h/g$ values are so great that they do not longer influence the pressures (see Fig. II. 17), and secondly because in flowing water the effect of wave radiation decreases with increasing flow velocity.



$$F_I = -(C_{IW \text{ up}} + C_{IW \text{ down}}) \rho \delta^2 \dot{v}' = -\beta \rho \delta^2 \dot{v}'$$



$$F_{II} = -(C_{IIg \text{ up}} + C_{IIg \text{ down}}) \rho \delta^2 \dot{v}_g = -\gamma \rho \delta^2 \dot{v}_g$$

$$F_I = -(C_{Ig \text{ up}} + C_{Ig \text{ down}}) \rho \delta^2 \dot{v}_g = -\alpha \rho \delta^2 \dot{v}_g$$

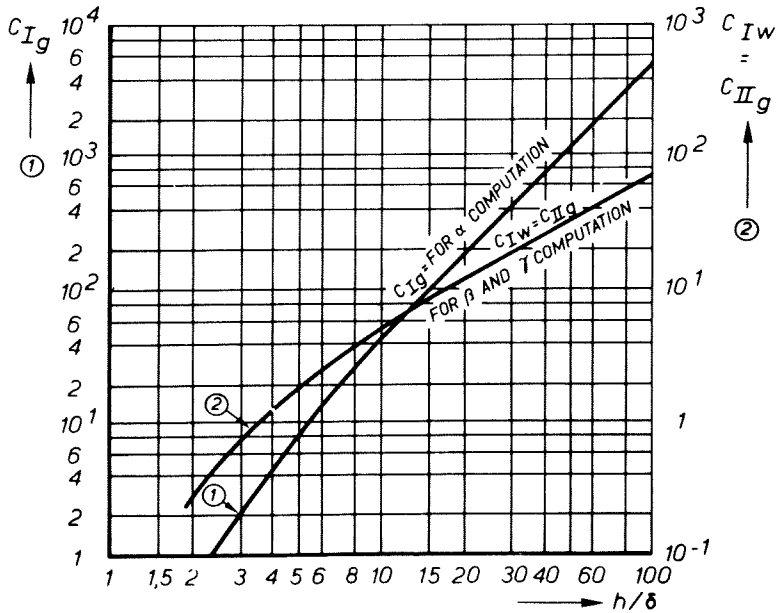


FIG. IV. 9

IV. 3c Computation methods: damping by flow

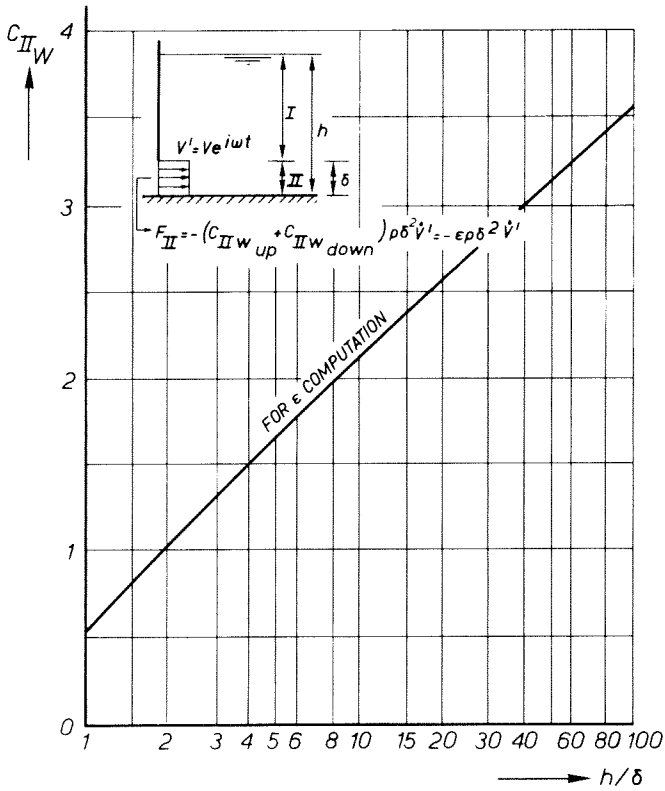


FIG. IV. 10

The computation of m_w and c_w has been made for different values of S , (h_{down}/δ) and $(\Delta H/\delta)$, and the results can be found in Table IV. 1. The computed results could be roughly checked with experimental results, as presented in Table IV. 2. It can be seen that their order of magnitude tallies, and also that the influence of wave radiation is of no importance.

When the gate is submerged, or when a culvert valve is considered, the computations go in the same way, but these cases are not further analyzed. A special case is the plug valve treated in Chapter II, par. 5 and Fig. II. 1, where the values of c_k and c_m are discussed for which $c > 0$ (indicating feedback vibration) and for which $c < 0$ (indicating hydrodynamic damping). This computation, however, is of no practical importance, because the design is already safe enough when the gate is free of self-exciting vibrations.

Chapter IV. Hydrodynamic mass and damping

TABEL IV. 1 The added water mass and water damping for horizontal gate vibration.
The values are per unit of width.

$$\mu = q/\delta \sqrt{2g\Delta H}$$

$$S = \frac{\omega\delta}{2\pi \sqrt{2g\Delta H}}$$

h_1/δ	$\Delta H/\delta$	$m_{\text{water}}/\rho\delta^2$				$c_{\text{water}}/\rho\delta^2$			
		0.003	$\mu S =$		0.3	0.003	$\mu S =$		0.3
			0.015	0.08			0.015	0.08	
2	1	3.70	3.62	2.75	2.17	0.073	0.34	0.79	0.34
	3	10.8	10.6	8.18	6.88	0.211	0.98	1.97	0.78
	10	77.1	75.5	62.6	57.5	1.22	5.57	9.05	3.26
	30	471	456	371	348	9.28	40.7	51.0	16.8
5	1	25.1	24.1	16.95	14.4	0.71	3.19	4.79	1.68
	3	42.8	41.2	31.1	27.9	1.05	4.67	6.39	2.17
	10	118.5	113.8	87.1	80.0	3.00	13.1	15.6	5.10
	30	622	598	488	464	13.9	58.4	58.9	18.5
20	1	414	387	282	264	14.6	59.6	51.7	15.7
	3	459	431	325	307	15.1	61.5	52.0	15.8
	10	625	582	436	412	23.4	85.5	73.5	21.8
	30	1480	1395	1129	1088	42.5	166	124.4	36.9
30	1	5272	4845	3842	3722	198	717	432	124.6
	3	5472	5044	4047	3928	198	716	428	123.5
	10	6074	5585	4459	4327	225	813	482	139
	30	7979	7363	5985	5826	282	1008	587	139

IV. 3c Computation methods: damping by flow

TABLE IV. 2 Comparison of the added water mass and water damping computed for horizontal gate vibration, with the results of gate model experiments (section model of Hagestein weir gate, D.H.L. report M 561^B [19], of which the values for different seal shapes [18] have been averaged. The values are per unit of width.

Gate opening m	h _{down} m	ΔH m	Frequency c/s	m _{water} (kg)		c _{water} (Ns/m)	
				computed	measured	computed	measured
0.48	4.45	0.41	1.03	13.300	14.500	16.000	25.000
			1.98	12.800	14.500	17.500	26.000
	4.85	1.60	0.9	23.400	21.700	31.200	43.000
			1.77	21.300	21.700	44.000	58.000
	4.52	3.00	0.87	31.000	24.600	31.000	47.500
			1.7	28.000	24.600	47.500	75.000

Remark 1

The test results only give an order of magnitude, because in the model, representing a prototype gate section of 3.7 m, the spacing between the flume walls was 10% wider than the gate section. The gap was sealed with a slack rubber membrane.

Also, some leakage could occur through the porous bottom; an indication thereof was the high value of about 1 measured for μ .

Remark 2

Due to wave radiation at the upstream side, $c_{\text{wave}} = 2 \rho g^2 / \omega^3$ according to equation (IV. 31) when the water velocity is low. For $N = 0.87$ c/s, $c_w = 1.200$ Ns/m per metre of gate length, and so its effect can be neglected.

Remark 3

All values are prototype values taken from the D.H.L. report, but measured in a 1 : 6 model.

The m_w was on scale 6^3 , the damping on scale $6^{5/2}$.

Chapter IV. Hydrodynamic mass and damping

B. Vertical vibrations

For the case of vertical gate vibrations no useful computation methods are available yet. If vertical damping of a gate is mainly due to the resistance (drag) of a number of girders in the flow, it can be expected that c_{water} will be proportional to the water velocity, as has been found in Appendix B, Fig. 5. Also, the results of model damping tests for the vertical vibration of the Hagestein weir gate, as presented in Delft Hydraulics Laboratory Report M 561^A [18], Fig. 32a, show that the damping is roughly proportional to V (or $\sqrt{2g\Delta H}$ in Fig. 32a). Some results of the damping tests on the Hagestein model can be found in [47]. The damping measured has as yet no general applicability because of the limitations of the model.

A special case wherein computation of vertical damping is possible, is the computation of the feedback vibration presented in Chapter II, par. 12 and Fig. II. 6. The c value in equation (II. 24) becomes negative when c_F is negative. This is the case when the lower edge of the gate is so designed that an uplift force occurs. The energy production of the (hypothetical) negative mechanical damper equals the energy absorption by the flow, and the factor c in equation (II. 24) is directly representative of the hydrodynamic damping c_w .

This computation may have some practical utility when a crenellated lower edge is applied for the prevention of vibration (so that only a part of the edge can be at a critical height and the other part will act as a damper). But until now, no real application has been found for such computation because too many factors are still unknown.

Appendix B (presented as a paper at the IAHR Symposium, 1970 [11]) is an illustration of how systematic research on gates and valves could be done, making use of the theory of the fundamental concepts of mass and damping dealt with in this chapter.

4. SUMMARY OF DETERMINATIVE PARAMETERS

4a. THE ADDED MASS

In par. 2 it has been found that $m_w :: \rho L^3$. (IV. 8)
The parameters ω (angular frequency), Y_0 (vibration amplitude), ν (kinematic viscosity), g (gravitational acceleration), c (propagation velocity of compression waves) and V (water velocity) have no perceptible effect if the following conditions are satisfied:

IV. 4a Determinative parameters: added mass

$$Y_o \ll L \quad (IV. 9)$$

$$\omega \ll \frac{2\pi (c - V)}{L} \quad (IV. 10a)$$

$$\frac{\omega L^2}{v} \gg 1 \text{ (in stagnant water conditions)} \quad (IV. 11)$$

$$\frac{VL}{v} \gg 1 \text{ (in flow condition)} \quad (IV. 11a)$$

$$\frac{\omega^2 L}{g} \gg 1 \quad (IV. 14)$$

$$\frac{\omega L}{V} \gg 1 \quad (IV. 16)$$

If the conditions (IV. 10 or 10a) are not completely satisfied, an additional m_w must be taken into account:

$$m_w' = \delta * (\text{Area} // Y_o) = \frac{v}{2\omega} * (\text{Area} // Y_o) \quad (IV. 12)$$

The complete expression of the added mass of water m_w with a determined geometry can be written as follows:

$$\frac{m_w}{\rho L^3} = f \left(\frac{\omega L}{v}, \frac{Y_o}{L}, \frac{VL}{v}, \frac{\omega^2 L}{g}, \frac{v}{c} \right) \quad (IV. 45)$$

As will be seen later on, the same dimensionless parameters from the right hand side of equation (IV. 45) also play a role in damping.

The force exerted on the gate by m_w is an order of magnitude greater than that exerted by water damping c_w , and experience shows that c_w is influenced much stronger by said parameters.

This is illustrated in Figs. II. 17 and 18, where, for similar cases, the pressures in phase with $\Delta \dot{v}$ (added mass) and in phase with Δv (water damping) are shown in relation to the parameter $\omega^2 h/g$, which is responsible for wave radiation. The damping parameter c_r (Fig. II. 18) depends completely on $\omega^2 h/g$, whereas the mass parameter c_L (Fig. II. 17) only gets a correction value for small $\omega^2 h/g$ values.

To check whether the parameters indeed have influence in a given situation, it is sufficient to compare the situation with similar cases, where data of m_w are directly available; or, if effect on c_w is known to be negligible, it can be inferred that the effect on m_w can also be neglected. In considering the influence of the various parameters, it has to be taken into account that variations of m_w are not very influential in the

Chapter IV. Hydrodynamic mass and damping

analysis of vibration; its effect is supplemental to the mass of the gate itself, and the result of an error in the estimation of the total mass is a shift of the resonance frequency with:

$$\omega :: \sqrt{\text{rigidity/mass}}$$

Its influence on the mechanism of self-exciting vibration is not so sensitive either (see influence of c_i on c_{se} in Fig. II. 7).

Of the different parameters of equation (IV. 45) the influence will be demonstrated with some examples.

- a. $\frac{\omega L}{V}$: This value is proportional to the reduced frequency S as used in Table IV. 1 (see p. 132); in which can be seen that m_w varies only by a factor 1.7 at a variation of S between 0.003 and 0.3.
- b. $\frac{Y_0}{L}$: This parameter has an important effect on water damping in stagnant water conditions (Appendix B, Fig. 4), but in flowing water conditions its effect tends to disappear (Appendix B, Fig. 5); the effect of Y_0/L on the added water mass will even be much smaller.
- c. $\frac{VL}{v}$ (Reynolds number): Its effect will be mainly apparent in models of gates. In Appendix B it can be seen that even at zero water velocity its effect is negligible in a culvert model with a cross-section of 0.25 m square. In Fig. 4 of Appendix B is shown that only for the extremely small amplitude of 3.10^{-4} for Y_0/D (D = culvert height) a slight effect becomes apparent in the damping by the water. Though the effect of the Reynolds number can be of more importance when the gate is so shaped that unstable separation of flow can occur (cylindrical, etc.), its effect on the added water mass will still remain unimportant.
- d. $\frac{\omega^2 L}{g}$: In Fig. II. 17, only for h/δ values near 1 and for $\omega^2 h/g$ values under 10 some effect is seen. As the computations were made for stagnant water conditions, the real energy radiation will be still smaller than the value calculated, because the surface currents at both sides of the gate are directed towards the gate (see remark following equation (IV. 31)).
- e. $\frac{V}{c}$: This parameter only has some importance for valves in long culverts. Experience with water hammer computation shows that only when $\omega L/(c - V) \gtrsim 0.5$ (L = culvert length, c = propagation velocity of

IV. 4b Determinative parameters: water damping

compression waves), its effect has to be taken into account.

4b. WATER DAMPING

In par. 2d it has been found that in flow:

$$c_{w_1} :: \rho L^2 v \quad (IV. 17)$$

and in stagnant water:

$$c_{w_2} :: L^2 C_D \rho \omega Y_o \quad (IV. 21)$$

wherein

$$C_D = f (Y_o/L) \quad (IV. 21a)$$

The skin friction results in:

$$c_{w_3} :: \rho L^2 \sqrt{\omega v} \quad (IV. 19)$$

The wave radiation results in:

$$c_{w_4} :: \rho g^2 L / \omega^3 \quad (IV. 31)$$

Equation (IV. 31) was $c :: \rho g^2 / \omega^2$, but c was expressed per unit of width)

Knowing that in flowing water $c_w / \rho L^2 v$ is the dominant parameter, the total water damping can be expressed as:

$$\frac{c_w}{\rho L^2 v} = f \left(\frac{c_{w_2}}{c_{w_1}}, \frac{c_{w_3}}{c_{w_1}}, \frac{c_{w_4}}{c_{w_1}} \right) = f \left(\frac{\omega Y_o}{v}, \frac{Y_o}{L}, \frac{\omega v}{v^2}, \frac{g^2}{\omega^3 L v} \right) \quad (IV. 46)$$

But this can be rewritten with the following modifications:

$$\begin{aligned} \frac{\omega Y_o}{v} &= \left(\frac{\omega L}{v} \right) \left(\frac{Y_o}{L} \right) \\ \frac{\omega v}{v^2} &= \left(\frac{v L}{v} \right) \left(\frac{v}{\omega L} \right)^{-1} \\ \frac{g^2}{\omega^3 L v} &= \left(\frac{\omega^2 L}{g} \right)^{-2} \left(\frac{\omega L}{v} \right) \end{aligned}$$

Now equation (IV. 46) can be written as:

Chapter IV. Hydrodynamic mass and damping

$$\frac{c_w}{\rho L^2 V} = f' \left(\frac{\omega L}{V}, \frac{Y_o}{L}, \frac{VL}{v}, \frac{\omega^2 L}{g} \right)$$

The dimensionless parameters at the right hand side are the same as in equation (IV. 45), except that V/c is missing. This is due to the fact that the approach to the damping equations has been different from the more systematic approach to the added water mass; the damping equations are all derived assuming that the wave propagation velocity of the compression waves is relatively great. If this is not the case, V/c influences the flow field, and the equation becomes:

$$\frac{c_w}{\rho L^2 V} = f' \left(\frac{\omega L}{V}, \frac{Y_o}{L}, \frac{VL}{v}, \frac{\omega^2 L}{g}, \frac{V}{c} \right) \quad (\text{IV. 47})$$

(a) (b) (c) (d) (e)

Discussions of parameters:

ad (a) and (b):

The effect of the parameters $\omega L/V$ and Y_o/L can be illustrated by the test results of the reversed Taintor valve, presented in Appendix B. The hydrodynamic damping of this valve is mainly effected by flow action on the upstream girders.

In par. 2d (equation (IV. 17') and further on) it has been found that in flow the water damping factor c_w is related to the drag coefficient C_D :

$$C_D :: c_w / \rho V L^2$$

In stagnant water, it follows from equation (IV. 21) that:

$$C_D :: c_w / \rho L^2 \omega Y_o$$

From Figs. 4 and 5 of Appendix B follows that Y_o/L only influences C_D in stagnant water or in flow at extremely high Y_o/L values, values much higher than those which are induced by flow. This means that for reversed Taintor valves $\omega L/V$ and Y_o/D have no effect on $c_w / \rho L^2 V$.

Another instance of hydrodynamic damping occurs when the water damping results from forces at the lower gate edge. For vertical vibrations, the coefficient (-c) of equation (II. 24), which represents the flow damping when the gate lip is exposed to an uplift force ($c_F < 0$), is dependent on $\omega L/V$ (proportional to S_n in the equation). This can also be seen in Fig. II. 7.

IV. 4b Determinative parameters: water damping

For horizontal vibrations, $\omega L/V$ is also of importance; this is illustrated by the computation results of Table IV. 1 and the experimental results of Table IV. 2 (in Table IV. 1, S is again proportional to $\omega L/V$).

It should be of interest to have more information on the effect of different girder and gate shapes on the damping values. Because in a structure the separate girders will often be exposed to flow velocities in directions different from the vibration direction, the effect of this angle has to be studied too.

ad (c)

$\frac{VL}{v}$: In the small scale model described in Appendix B, it appeared that under all circumstances relevant to vibration analysis, the Reynolds number has no influence on c_{water} . As has been discussed before, attention must be paid to cases, wherein shapes are involved in which unstable flow separation can occur (cylinders, etc.).

As has already been shown, skin plate friction can be calculated with equation (IV. 19).

ad (d)

$\frac{\omega^2 L}{g}$: For some simplified cases (stagnant water), wave radiation has been calculated (see Fig. II. 18 and equation (IV. 31)), but this damping factor should not be used as the limiting factor in vibration calculations, as the flow velocities near the surface are directed towards the gate. These velocities reduce the radiation of energy. Experience shows that other damping factors dominate the damping caused by wave radiation.

ad (e)

V/c : The radiation of energy by compressing waves at purely harmonic vibrations is theoretically not existant when this energy is reflected by one of the boundaries (standing wave). In reality, however, the waves are partially damped by friction before they are reflected. No quantitative information is available on the parameter V/c , but in most cases it is to be expected that its effect is small as long as $\omega L \ll 2\pi (c - V)$; (see equation (IV. 10a)). In culverts, where the length L may be great, compression waves may influence dynamic valve behaviour.

Concluding remark:

As has been said, only relatively little information is available

Chapter IV. Hydrodynamic mass and damping

yet on water damping, especially for vertical vibrations of gates. For those vibrations for which water damping can not be quantified, response computations have to be kept on the safe side, assuming that only damping by material properties of the gate and the hoist system is available. This can lead to uneconomical designs for the improvement of which the technique of model research is available. (see Chapter VI and Appendix C.)

Chapter V

The response of gates to excitation by turbulence pressures

1. SUMMARY

From the known solution of the response of a single oscillator to random excitation, non-dimensional parameters are derived which characterize the gate response to hydrodynamic excitation. The parameters are checked by measurements on a model of a culvert valve, presented in Appendix B. The agreement can be considered as proof that the valve behaves passively only and that it is free of self-excitation.

2. INTRODUCTION

The following theory of the response of an oscillator to random excitation is based on computations by Thomson and Barton [97]. The response of a suspended object (cylinder) to random flow excitation has been presented by Fung [30], on the basis of which the author has published an analysis of vibration measurements on gates [46]. This analysis was later simplified in the way presented in Appendix B. No other literature was found wherein this type of analysis has been applied to gates and valves.

In the following paragraphs the analysis is presented in detail, because it lies at the base of judgement whether gate vibration is due to passive response or to feedback between vibrations and flow-excitation. Moreover, the compilation of parameters determining dynamic gate behaviour is based on this analysis. In an ideal gate design, possible sources of self-exciting vibrations are eliminated. Still, when the gate is partially raised, there remains a structure placed in a highly turbulent flow, the turbulence of which is mainly related to the loss of energy due to the gate itself.

Chapter V. Response to turbulence excitation

The excitation of a gate by turbulence generally leads to forces in the structure which are small compared to the permanent hydrodynamic load. This has been found in several model tests of low-head gates at the Delft Hydraulics Laboratory (weir gates of the Hagestein, Haringvliet and Volkerak Barrages). However, in high-head valves, often designed in such a way that the vertical load is very small, the turbulence load can be of predominant importance and of the same order as the weight of the valve, or more. Because a net uplift force is dangerous, inciting heavy vibration (especially if there is play in pivots, etc.), the analysis is of special importance for this type of valve. The research presented in Appendix B is related to a high-head valve.

The analysis of vibration data involves the calculation of hydrodynamic forces from vibration. Hydrodynamic damping will be introduced as if it were an external damping. This is based on the hypothesis that hydrodynamic damping is related only to the local average water velocity near the individual gate members (equation IV. 17') and that this average velocity is not influenced by turbulence or by periodic disturbances of the vibration itself.

3. HYDRODYNAMIC EXCITATION

- If flow around a structure has a determinate geometry, this flow can be characterized by a reference velocity V and a reference length dimension L .
- Apart from small viscosity effects in the shear layer, the resultant force on a body is determined by the pressures acting perpendicular to the boundary.
- All local pressures are proportional to $\frac{1}{2}\rho V^2$ in relation to a reference pressure within the flow.

$$p = c_p \frac{1}{2}\rho V^2 \quad (\text{V.1a})$$

$$p' = c'_p \frac{1}{2}\rho V^2 \quad (\text{V.1b})$$

(p = static pressure; p' = dynamic pressure; c_p and c'_p are the static and the dynamic pressure coefficient, respectively).

All the frequencies of the dynamic pressure are related to the local and momentary velocity (i.e. to V) and to the local size of the eddy current (i.e. to L), in such a way that the characteristic frequencies (f) are proportional to V/L , i.e.:

V. 3 Hydrodynamic excitation

$$f \propto VL^{-1} \quad (V.2)$$

This leads to the introduction of a new parameter $S = fL/V$ which is called the Reduced Frequency.

- If the flow is constant, the dynamic pressures are statistically stationary and their standard deviation becomes:

$$\sqrt{p'^2} = c_p' \frac{1}{2} \rho V^2 \quad (V.3)$$

The frequency distribution can be described with a power density spectrum $W_p(f)$, expressed by the formula:

$$\int_0^{\infty} W_p(f) df = \overline{p'^2} = c_p'^2 \left(\frac{1}{2} \rho V^2\right)^2$$

(The index p of W_p indicates that W is meant in relation to pressure).

Because of equation (V.2), this spectrum can be transformed into

$W_p\left(\frac{fL}{V}\right) = W_p(S)$ so that:

$$\int_0^{\infty} W_p(S) dS = \overline{p'^2} = c_p'^2 \left(\frac{1}{2} \rho V^2\right)^2 \quad (V.4)$$

The dimension of $W_p(S)$ is $(\rho V^2)^2$.

However, it is more common to use the normalized spectrum $\phi = f(S)$, characterized by $\int_0^{\infty} \phi dS = 1$, the introduction of which in (V.4) results in:

$$W_p(S) = c_p'^2 \left(\frac{1}{2} \rho V^2\right)^2 \phi_p \quad (V.5)$$

If c_p' and $\phi = f(S)$ are given, together with a known velocity V and a flow geometry with a representative length L , the power density spectrum $W_p(f)$ (taking into account that $S = fL/V$ and $dS = (df) \times L/V$) follows from:

$$c_p'^2 \left(\frac{1}{2} \rho V^2\right)^2 = \int_0^{\infty} W_p(f) df = \int_0^{\infty} W_p(S) dS = \int_0^{\infty} LV^{-1} \times W_p(S) df$$

- * The word power suggests the dimension of p'^2 , being energy/time, but this is not the case. The following definition (Harris and Crede 1961 [36], volume I, p. I-22) is used: "Power Spectral Density is the limiting mean square value (e.g. of acceleration, velocity, displacement, stress or other random variable) per unit band width, i.e. the limit of the mean-square value in a given rectangular band width divided by the band width, as the band width approaches to zero".

Chapter V. Response to turbulence excitation

Combined with (V.5) there follows:

$$W_p(f) = W_p(S) \times L/V = c_p'^2 (\frac{1}{2}\rho V^2)^2 LV^{-1} \phi_p \quad (V.6)$$

From (V.1) and (V.2) follows that the local pressure can be described by:

$$c_p = p/\frac{1}{2}\rho V^2 = f(\text{geometry of flow})$$

$$c_p' = \sqrt{p'^2}/\frac{1}{2}\rho V^2 = f(\text{geometry of flow})$$

$$\phi_p(S) = f(\text{geometry of flow})$$

The resultant force on the body, consisting of the effect of all the local pressures, can now also be expressed as a power density spectrum W_F with:

$$\int_0^\infty W_F(f) df = \overline{F'^2} = c_F'^2 (\frac{1}{2}\rho V^2 L^2)^2 \quad (V.7)$$

wherein F' is the dynamic component of the total force: $F = F_s + F'$.

In the same way as has been shown for the pressures, there can be introduced a normalized force spectrum $\phi_F = f(S)$.

The forces can now be expressed as follows:

The static force F_s by use of the coefficient c_F . This force coefficient c_F is a simplified presentation, because the three factors in x, y and z direction have to be considered.

$$c_F = F_s/\frac{1}{2}\rho V^2 L^2 = f(\text{geometry of flow}) \quad (V.8)$$

The dynamic force by the use of the coefficient c_F'

$$c_F' = \sqrt{F'^2}/\frac{1}{2}\rho V^2 L^2 = f(\text{geometry of flow}) \quad (V.9)$$

$$\phi_F(S) = f(\text{geometry of flow}) \quad (V.10)$$

The power density spectrum is to be used for the response calculation of an elastic structure:

$$W_F(f) = c_F'^2 (\frac{1}{2}\rho V^2 L^2)^2 LV^{-1} \phi_F \quad (V.11)$$

The equations (V.8, 9 and 10), if given in the three co-ordinates, form a complete representation of the excitation by flow.

Instead of the whole spectrum, sometimes only the value of S for W_{\max} is mentioned, called the Strouhall number. This information is sufficient only for checking if the resonance frequency of the structure is far enough from the main excitation frequency. Response calculations of

V. 4 Passive response to random excitation

structures using c'_F and the dominant S values are often presented as if all excitation takes place at only one single frequency. When the resonance frequency of the structure is close to the dominant excitation frequency, this calculation is valid only if the band width of excitation is small compared to the width of the peak of the response curve of the structure. With gates, a wide band excitation can always be expected. An exception is a gate with over- and underflow, wherein vortex shedding can be very regular (Naudascher [63], as is the case with cylinders in sub-critical flow. Another exception can occur when the effects of turbulence are filtered by a resonance system (for example standing waves in a shaft).

4. PASSIVE RESPONSE OF A SINGLE OSCILLATOR TO RANDOM EXCITATION

The following response calculation is based on the paper of Thomson and Barton [97].

Suppose the excitation force is described by:

$$W_F = \frac{\Delta F'^2}{\Delta f} = f(f) \quad (V.12)$$

This means that, at a frequency f , a band width is considered of:

$$f - \frac{1}{2}\Delta f < f < f + \frac{1}{2}\Delta f$$

In this band width, a part of $\overline{F'^2}$ is available, i.e. $\Delta(\overline{F'^2})$, which can be considered as the equivalent of a periodic excitation at a frequency f (provided that Δf is small). Consequently:

$$F = F_f \cos 2 \pi f t \quad (V.13)$$

and

$$\overline{\Delta F'^2} = \lim_{t \rightarrow \infty} \frac{F_f^2}{T} \int_0^t \cos^2(2 \pi f t) dt = \frac{1}{2} F_f^2 \quad (V.14)$$

The response of single oscillator follows from the single oscillator equation:

$$m\ddot{y} + c\dot{y} + ky = F_f \cos 2 \pi f t \quad (V.15)$$

In the presence of stationary excitation, all initial phenomena are damped out. Only the particular solution of equation (V. 15) remains (eq. I. 2), wherein:

$$y = y_f \cos(2 \pi f t - \phi)$$

and

$$Y_f = \frac{F_f/k}{\sqrt{(1 - f^2/f_n^2)^2 + c^2 * 4\pi^2 f^2/k^2}} \quad (V.16)$$

Chapter V. Response to turbulence excitation

When relative damping is introduced:

$$\gamma = \frac{c}{\text{critical}} = \frac{c}{2\sqrt{km}}$$

Equation (V.16) becomes:

$$Y_f = \frac{F_f/k}{\sqrt{(1 - f^2/f_n^2)^2 + 4\gamma^2 (f/f_n)^2}} \quad (\text{V.17})$$

When equation (V.17) is applied to all frequencies separated by an interval Δf , a power density spectrum is obtained of the response W_y :

$$\begin{aligned} W_y/W_F &= Y_f^2 / F_f^2 = \\ &= \frac{1}{k^2 \{(1 - f^2/f_n^2)^2 + 4\gamma^2 (f/f_n)^2\}} \end{aligned} \quad (\text{V.18})$$

Assuming that $\gamma \ll 1$, the response is mainly determined by the power density spectrum of the force W_F at the natural frequency f_n ; ($f_n = \frac{1}{2}\pi \sqrt{\frac{k}{m}}$). Only a small band width is of interest. (How large this is, will be discussed later.)

Upon the introduction of $(\frac{f}{f_n}) = 1 + \epsilon$, in which ϵ varies from $-\epsilon_0$ to $+\epsilon_0$, with $\epsilon_0 \ll 1$, equation (V.18) becomes:

$$\begin{aligned} W_y/W_F &= \frac{1}{k^2 \{[1 - (1 + \epsilon)^2]^2 + 4\gamma^2 (1 + \epsilon)^2\}} \approx \\ &\approx \frac{1}{k^2 (4\epsilon^2 + 4\gamma^2)} \end{aligned} \quad (\text{V.19})$$

The total response $\overline{y^2}$ is now considered, supposing that W_F is constant over the whole frequency range:

$$\begin{aligned} \overline{y^2} &= \int_0^\infty W_y df = \int_0^\infty W_F \frac{1}{k^2 (4\epsilon^2 + 4\gamma^2)} df \approx \\ &\approx \int_{-\epsilon_0}^{+\epsilon_0} \frac{W_F f_n}{4k^2 (\epsilon^2 + \gamma^2)} d\epsilon = \frac{W_F f_n}{4k^2} \frac{1}{\gamma} \tan^{-1} \left(\frac{\epsilon}{\gamma} \right) \Big|_{-\epsilon_0}^{+\epsilon_0} \end{aligned} \quad (\text{V.20})$$

If ϵ_0 is large enough, \tan^{-1} becomes $\pi/2$ for ϵ_0 , and $-\pi/2$ for $-\epsilon_0$.

The response now becomes:

$$\overline{y^2} = \frac{\pi f_n}{4k^2 \gamma} W_F \quad (\text{V.21})$$

Remark:

When the power density of the excitation is expressed in $W(\omega)$ instead of $W(f)$, there follows from $\int_0^\infty W(\omega) d\omega = \int_0^\infty W(f) df$, that $W(\omega) = \frac{1}{2\pi} W(f)$.

V. 5 Response parameters

The response $\overline{y^2}$ can then be expressed as $\overline{y^2} = \frac{\pi \omega_n}{4k^2 \gamma} W(\omega_n)$, which leads to a similar expression as (V.21).

The limit of $\tan^{-1}(\frac{\epsilon}{\gamma})$ for "large" ϵ values was $\pi/2$, but it turns out that 80% of $\pi/2$ is reached when $\epsilon_0 = 3.1 \gamma$; so the total band width $\Delta f = 2 * (3.1 \gamma f_n)$. In this case, the standard deviation of y has 10% inaccuracy. Appreciation of the limited band width of real influence on the response is of importance when filter techniques are applied to the signal. It also enables one to judge whether peaks in the power density spectrum can still be treated with the theory of white noise excitation.

Another quantity which can be derived from (V.20) is the band width within which excitation can still be considered as periodic. If ϵ/γ is small, $\tan^{-1}(\frac{\epsilon}{\gamma}) \approx \frac{\epsilon}{\gamma}$. So, if the band width of excitation is small, equation (V.20) becomes:

$$\overline{y^2} = \frac{2 W_F \epsilon_0 f_n}{4k^2 \gamma^2} \quad (V.22)$$

The value $\epsilon = 1 - f/f_n$ varies from $-\epsilon_0$ to $+\epsilon_0$, so that the band width of excitation is $\Delta f = 2 \epsilon_0 f_n$ and

$$\overline{y^2} = W_F \Delta f / 4k^2 \gamma^2 \quad (V.23)$$

But as long as the excitation can be considered as purely periodic, there follows that $F = F \sin 2 \pi f_n t$. Consequently, the value $W_F \Delta f = \frac{1}{2} F_0^2$ and the response $Y_0 \sin(2\pi f_n t + \phi)$ give:

$$\overline{y^2} = \frac{1}{2} Y_0^2 = \frac{1}{2} F_0^2 / 4k^2 \gamma^2 \quad (V.24)$$

(V.24) is exactly the same as could have been found from (V.17) with periodic excitation at a frequency $f = f_n$.

The limit within which $\tan^{-1} \epsilon/\gamma \approx \epsilon/\gamma$ with an inaccuracy of 10% is $\epsilon/\gamma = 0.5$, which means that the total band width within which the signal may be considered as purely periodic is:

$$\Delta f = 2 * 0.5 \gamma f_n = \gamma f_n$$

5. PARAMETERS WHICH DETERMINE THE RESPONSE OF AN OSCILLATOR IN FLUID FLOW

The behaviour of a single oscillator in fluid flow is now considered, assuming that the excitation is random and conforms to the equations (V.8) to (V.11) of Paragraph 3, while the response is characterized by the equations (V.17 and 21) of Paragraph 4. The behaviour of the oscillator

Chapter V. Response to turbulence excitation

is described in terms of *internal force*, i.e. ky , whereas the hydrodynamic force will be called the *external force*.

Static force

If $f = 0$, the influence of the terms $m\ddot{y}$ and $c\dot{y}$ in equation (V.15) disappear, and ky becomes equal to the static load, expressed by equation (V.8). The static force becomes:

$$F_s = ky = F = c_F \times \frac{1}{2}\rho V^2 L^2$$

wherein $c_F = f(\text{geometry of flow})$ so that:

$$F_s / \frac{1}{2}\rho V^2 L^2 = c_F = f(\text{geometry of flow}) \quad (\text{V. 25})$$

Quasi-static force

It can be seen from equation (V.17) that even for $\gamma = 0$ the deflection is nearly a static one when $f/f_n < 0.32$ (at this value the deviation of the amplitude is 10%). If the first resonance frequency of a gate is sufficiently high relative to the dominant Strouhal number (one of the criteria of good design; see Chapter I), a large part of the excitation takes place in the low-frequency range. From vibration recordings, vibrations of resonance frequency can be eliminated with a band pass filter, and the internal quasi-static force is then representative of the external force of equation (V.9), except for frequencies higher than $0.32 f_n$.

$$F_{qs} = k\sqrt{y^2} \approx \sqrt{F'^2} = c_F' \times \frac{1}{2}\rho V^2 L^2$$

$$F_{qs} / \frac{1}{2}\rho V^2 L^2 = c_F' = f(\text{geometry of flow}) \quad (\text{V.26})$$

In the case of a submerged valve, the flow velocity can vary without changing the flow geometry. Tests with low water velocities form the most direct approach to obtain the power density spectrum of the force, because the dominant Strouhal number results in a low dominant frequency, compared with the resonance frequency of the structure. However, the accuracy of measurements decreases at low water velocities, because the force amplitude decreases proportionally to V^2 .

The shape of the power density spectrum in the low frequency range is of no importance for the strength of the structure, because tensions and displacements are determined only by c_F' (V.26), but information on the spectrum can give information on how the structure will react at

V. 5 Response parameters

higher velocities.

Dynamic force

The dynamic force is defined as the internal force in the resonance frequency range. The excitation is defined by equation (V.9) and (V.10). The power density spectrum $W(f)$ follows from (V.11):

$$W_F(f) = c_F'^2 (\frac{1}{2}\rho V^2 L^2)^2 LV^{-1} \phi_F$$

The response of the oscillator (supposing that damping is low) depends on the function W_F at the natural frequency f_n . Here is introduced the *reduced natural frequency*:

$$S_n = f_n L/V \tag{V.27}$$

giving:

$$W_F(f_n) = c_F'^2 (\frac{1}{2}\rho V^2 L^2)^2 LV^{-1} \phi_F(S_n) \tag{V.28}$$

The response of the structure follows from (V.21) and (V.28):

$$\overline{y^2} = \frac{\pi f_n}{4k^2 \gamma} W_F = \frac{\pi}{4k^2 \gamma} S_n c_F'^2 (\frac{1}{2}\rho V^2 L^2)^2 \phi_F(S_n) \tag{V.29}$$

The internal dynamic force F_d becomes:

$$F_d = \frac{1}{2} c_F' (\frac{1}{2}\rho V^2 L^2) \sqrt{\frac{\pi}{\gamma} S_n \phi_F(S_n)} \tag{V.30}$$

Because (V.10) states that $\phi_F(S) = f(\text{geometry of flow})$:

$$\frac{F_d \sqrt{\gamma}}{\frac{1}{2}\rho V^2 L^2} = c_F' \sqrt{\frac{\pi}{4} S_n \phi_F(S_n)} = f(S_n, \text{geometry of flow}) \tag{V.31}$$

The validity of this presentation has been checked experimentally (see Appendix B, fig. 9, wherein S_n is presented as $N_r D/V$).

DETERMINATION OF THE POWER DENSITY SPECTRUM FROM VIBRATION MEASUREMENTS:

If the damping of a structure is known for different water velocities (and consequently different S_n values), the power density spectrum of the excitation can be derived from the measurements of the internal force with the aid of equation (V. 21) and knowing $F_d = ky$:

$$W_F(f_n) = \frac{4F_d^2 \gamma}{\pi f_n^2} \tag{V.32}$$

Equation (V.32) can give the relation between measurements at low and high water velocities (supposing that the flow geometry remains constant).

Chapter V. Response to turbulence excitation

At low velocities, S_n lies far above the dominant S value of the excitation and the spectrum of the external force follows directly from the measured internal force, because the response is quasi-static. At high velocities, the dynamic response will dominate; at each velocity, one point of the power density spectrum can be determined from this response (if the flow geometry remains constant). When the low and high velocities measurements disagree, this can lead to conclusions regarding feedback phenomena between vibration and flow excitation.

CONSIDERATIONS ON THE CONDITION OF A "SINGLE DETERMINED FLOW CONDITION"

In a submerged culvert valve without aeration, it can be expected

- 1) that the flow geometry is determined by the position of the gate,
- 2) that the head difference is determined by the velocity and
- 3) that the absolute pressure has no influence on the forces acting on valves. So, at each valve position, there is a "single determined flow condition". However, for culvert valves the "single determined flow condition" is only true

- a) if there are no waves and/or resonance in the shafts,
- b) if the valve is fully submerged, also in open position, and
- c) if the valve is not aerated.

Attention must be paid to phenomena occurring in plug valves: if the leakage gap is small, a pistoning effect can occur (see Chapter II, par. 5), which causes a great change of the hydrodynamic mass during the valve raise. This mass variation must be considered in the analysis.

For an underflow gate controlling free-surface flow, different types of cross-section can be considered (fig. V.1).

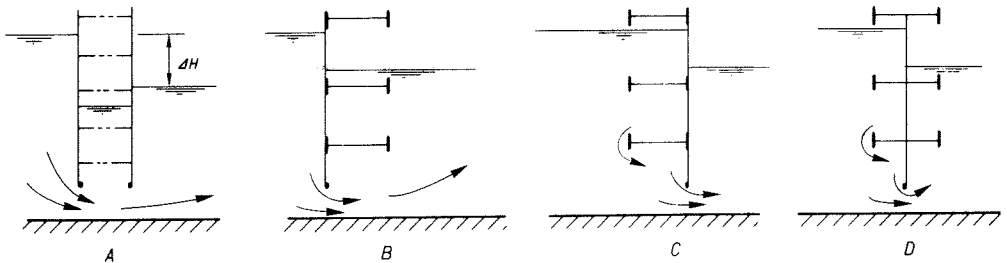


FIG. V.1

For gate types A and B, the upper water has no turbulence caused by the

V. 6 Measurement results

gate itself, and the turbulence which causes excitation is underneath and downstream of the gate. This means that the *geometry of flow* is determined only by the position of the gate and the downstream waterlevel, and that the velocity can be characterized by $\sqrt{2g \Delta H}$. When, however, the head is high and downstream water shallow, a hydraulic jump can occur, or even complete discharge, so that the downstream waterlevel has no longer any effect on the flow pattern. In this case, the flow pattern is determined by the gate elevation and the upper waterlevel. For gate type C, the turbulence caused by the girders is at the upstream side and the turbulence related to the deceleration of the flow under the gate is at the downstream side. The latter will give no excitation in the vertical sense, because pressures acting on the flat retaining plate only cause horizontal forces. So, for vertical forces and vibration, the flow geometry is determined by the gate elevation and the upper waterlevel; but for horizontal forces and vibrations, the flow geometry is determined by gate elevation and both upper and downstream waterlevel. For gate type D and for gates with overflow, the flow geometry is determined by both upper and downstream waterlevel.

In the analysis of vibration measurements, it must be borne in mind that the excitation is determined by the flow velocity and flow geometry only, but that the response is also determined by the added water mass and hydrodynamic damping. For gates of type A and B, this signifies a certain extra influence of the upper waterlevel, especially on horizontal vibration.

6. MEASUREMENT RESULTS IN GATE MODELS OF THE SINGLE OSCILLATOR TYPE

In the preceding paragraph, the force coefficients c_F and c_F' and the normalized power density spectrum were introduced as a function of the flow geometry, assuming that no feedback exists between vibration and excitation by flow.

This case is demonstrated in Appendix B, dealing with the investigation of a model of a reversed Taintor valve. As was expected, the valve showed no feedback phenomena and the analysis was roughly confirmed on the following points:

- c_F was constant.
- c_F' was still somewhat variable with velocity V (fig. 8, Appendix B), the possible causes of which are discussed in the appendix.

Chapter V. Response to turbulence excitation

- A dominant Strouhall number could roughly be determined.
- For the dynamic force it was found that, in agreement with (V.31), $F_d \sqrt{\gamma / \frac{1}{2} \rho V^2 L^2}$ is a single function of S_n (fig. 9, Appendix B); this was extensively checked with varying V and varying mass, rigidity and damping of the valve. The power density spectrum at low velocities could not be measured accurately enough to compare it with the dynamic response at high velocities.

Measurements in a model of gate type B (fig. V.1), with variation of head, spring rigidity and mechanical damping, have been carried out for a section of the weir gate at Hagestein (fig. IV.2) and were published [46]. For the low-frequency range, a nearly constant c_F' value could be found; also that the power density spectrum as derived from the dynamic response was in a reasonable way a function of the S_n value like in (V. 10); and in accordance with the response function for random excitation of equation (V.21), the amplitudes in the resonance frequencies turned out to be proportional to $\gamma^{-\frac{1}{2}}$.

Remark:

In paper [46] of the author and in the D.H.L. report M 561 [19], the non-dimensional values c_F' and Φ are not presented directly. For the *low-frequency force* (quasi-static force), (V.26) is presented as follows:

$$c_F' = F_{qs} / \frac{1}{2} \rho V^2 L^2 = k Y_{qs} / \frac{1}{2} \rho V^2 L^2$$

wherein $k = m \omega_n^2$ (ω_n is the natural frequency), or $k = 4\pi^2 f_n^2 m$.

Furthermore, the reference velocity V is $\sqrt{2g \Delta H}$ and c_F' becomes:

$$c_F' = 4\pi^2 f_n^2 m / \rho g \Delta H L^2$$

In the paper the constant factors ρ , g and L^2 are left out.

For the *dynamic force*, Φ_F is derived from (V.28) stating that:

$$\Phi_F (S_n) = W_F (f_n) \approx V L^{-1} / c_F'^2 (\frac{1}{2} \rho V^2 L^2)^2$$

and (V.32) stating that with $F_d = k Y_d$:

$$W_F (f) = \frac{4F_d^2 \gamma}{\pi f_n} = \frac{4Y_d^2 k^2 \gamma}{\pi f_n}$$

Combining these two equations and introducing $k = 4\pi^2 f_n^2 m$ and $V^2 = 2g\Delta H$

V. 7 Continuously elastic gates

results in the following expression for Φ_F :

$$\Phi_F (S_n) = \frac{64 \pi^3 \sqrt{2}}{c_F^2} * \frac{m^2 f_n^3 \gamma Y_d^2}{L^5 \rho^2 g^{3/2} \Delta H^{3/2}}$$

wherein $S_n = f_n L \sqrt{2 g \Delta H}$

In the paper and in the D.H.L. report, this was presented with other symbols as:

$$32 \pi^2 m^2 f_n^3 \gamma Y_d^2 \Delta H^{-3/2} = f \{f_n (2 g \Delta H)^{-1/2}\}$$

7. DISCUSSION ON THE BEHAVIOUR OF CONTINUOUSLY ELASTIC GATES

If a continuously elastic body is schematized by a number of masses (each concentrated in a single point) which are interconnected by springs, the natural modes and the natural frequencies can be found by solving the eigen-value problem. This results in a series of natural frequencies, each with a specific mode of vibration (a single relation between all the local amplitudes, whatever their direction) and with a specific eigen-load distribution, i.e. the load distribution which statically causes deflection equal to the one belonging to the vibration mode. Each arbitrary load distribution can be developed into eigen-load components, each component transferring energy only into the vibration of its proper mode. In this way, the response of one vibration mode, due to its proper eigen-load (being a function of time), becomes identical with the response of a single oscillator excited by a dynamic force.

The concept is also valid when mechanical damping is introduced, assuming that dampers are connected to each of the springs and that the combination has a constant damping/rigidity ratio.

When the construction is submerged, this concept is not changed, not even by coupling forces related to the added mass of water. The computation methods of coupled systems are described in von Karman and Biot's "Mathematical Methods in Engineering" [4].

When a valve is *fully submerged*, the added water mass is nearly independent of the reduced natural frequency S_n , and so its modes of vibration, its resonance frequencies and its eigen-load distributions will vary only slightly with the water velocity. Because the distribution of the hydrodynamic load is independent of the water velocity V , the development into eigen-load components remains unchanged and the amplitude of

Chapter V. Response to turbulence excitation

each of the eigen-loads will vary proportionally to V^2 .

This eigen-load concept leads to the conclusion that, for each mode of vibration, all concepts found for the single oscillator remain valid. The internal force has to be replaced by a representative amplitude or tension, which is then representative of the eigen-load amplitude.

Static force:

$$Y :: \frac{1}{2}\rho V^2 L^2 * f(\text{geometry of flow})$$

Quasi-static force:

$$Y :: \frac{1}{2}\rho V^2 L^2 * f(\text{geometry of flow})$$

Dynamic force:

$$Y\sqrt{\gamma} :: \frac{1}{2}\rho V^2 L^2 * f(S_n, \text{geometry of flow})$$

For gates in free-surface flow, the considerations given for vibrations with only one degree of freedom are not valid, because the velocities are related to the head across the structure; consequently, a change of the waterlevels will modify the vibration mode and the eigen-load distribution. This, in its turn, will modify the resolution of the hydrodynamic load into eigen-load components.

8. THE RELATION BETWEEN STRUCTURE RESPONSE AND FATIGUE OF MATERIALS

The foregoing analysis is related to hydrodynamic excitation and mechanical response. In the end, however, there must be found a relation with material fatigue and the life expectancy of a structure.

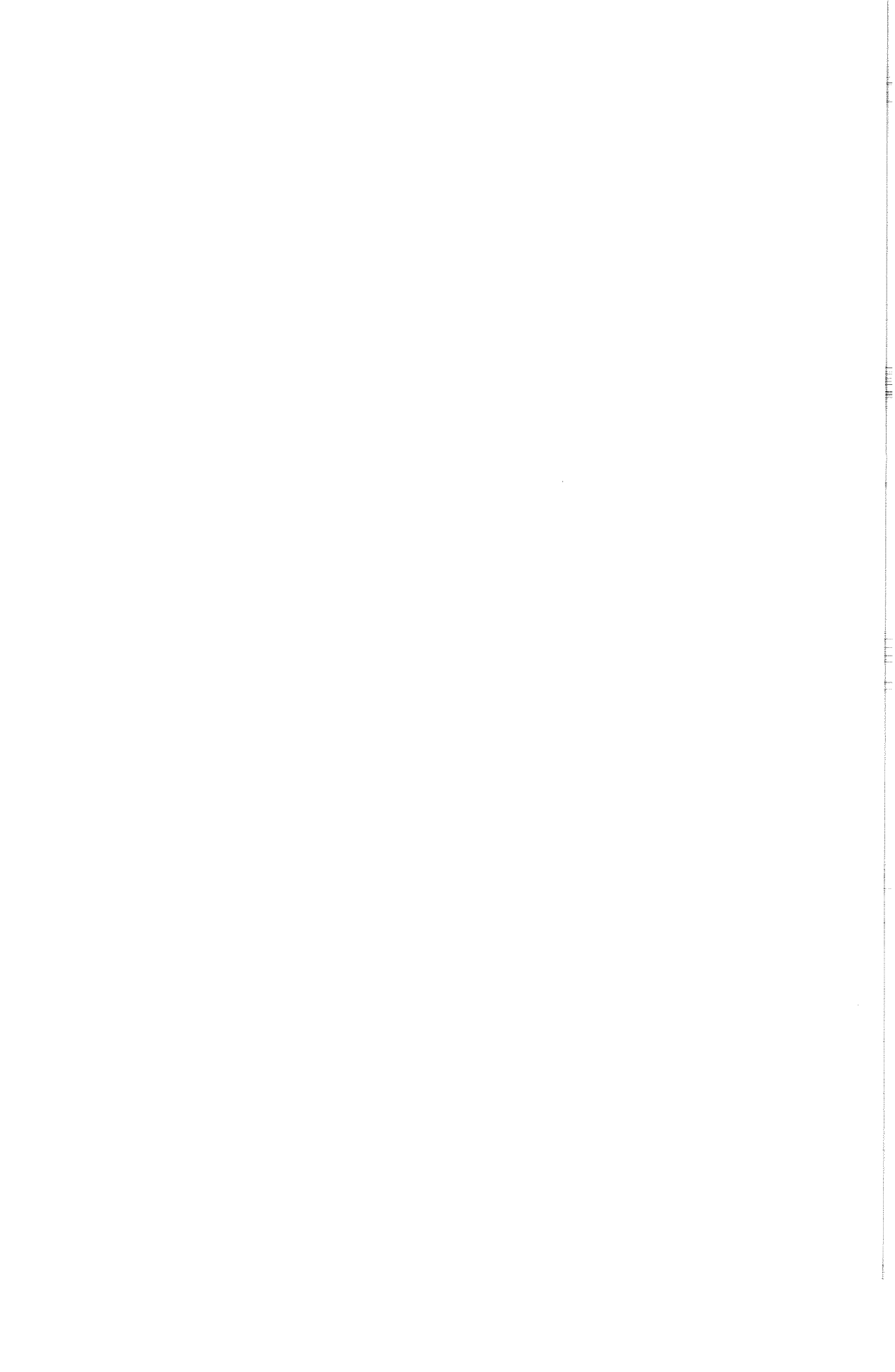
When in the preceding paragraphs the dynamic response of a structure was introduced, this was done in terms of internal force caused by the hydrodynamic load. Static, quasi-static and dynamic force components have been introduced, of which the quasi-static force can be presented in terms of a spectrum ($W(f)$).

The resistance of materials is, however, related to the sum of static and dynamic loads. Moreover, recent studies by Strating [95] on the fatigue of steel under stochastic load show that the shape of the spectrum W is hardly of importance, but that the statistical distribution of amplitudes is a dominant parameter, especially because peak values of tension have a relatively great influence on fatigue. Design criteria based on Wöhler diagrams (established with sinusoidal loads) are too

V. 8 Fatigue of materials

optimistic when applied to structures subjected to random loads having a comparable number of zero crossings and comparable root-mean-square amplitudes ($\sim 0.7A_{\max}$ for sinusoidal loads). In the case of random loads having a Gaussian amplitude distribution, admissible material strain as a function of the number of zero crossings is substantially lower. Increase of the duration of load condition always leads to a decrease of the acceptable load amplitude (in contrast to the Wöhler tests, wherein 2×10^6 periods stand for an infinite number), because longer duration increases the chance that still higher peaks might occur.

Further studies on the amplitude distribution function of hydraulic structures under hydrodynamic load will be of interest. The large structures for low-head conditions, which have till now been those most extensively investigated in our laboratory, did not lead to such studies, because, when certainty was obtained about the absence of self-exciting vibrations, the level of turbulence-excitation was too low to play an important role in the total load.



Chapter VI

The use of physical models in vibration research

This chapter is based on the article "Models with Elastic Similarity for the Investigation of Hydraulic Structures", which is reproduced as Appendix C.

1. SUMMARY

A survey is given of the potentials of hydraulic models for the investigation and improvement of gate and valve design as to hydrodynamic load and flow-induced vibration.

The different types of models discussed are:

- rigid models,
- single, free, oscillator models,
- activated oscillator models,
- models with continuous elasticity.

Scaling rules, presented in Appendix C, are discussed in relation to parameters which can disturb the reliability of models.

2. INTRODUCTION

The applicability of models with a reduced length scale is based on the fact that, when a number of modelling conditions are fulfilled, a valid reproduction of flow phenomena can be obtained. Because flow strength and pattern, together with fluid properties, fully determine the pressure differences and hence the forces, the latter are uniquely related to those in the prototype.

To reproduce the flow, the conditions at the boundaries must be correct and a number of non-dimensional parameters have to be simultaneously reproduced. This often leads to contradictory reproduction demands, and consequently only the dominant parameter is reproduced.

The influence of those parameters that are different in the model has to be judged from experience gained from other investigations wherein these parameters were systematically varied over a wide range. The magni-

Chapter VI. Physical models

tude of these parameters is a measure of their relative influence, and the limiting design conditions of a model consist in keeping these parameters out of their critical range.

The application of physical models is complementary to theoretical approach. Theory generally deals with solutions of equations based on a schematization of the real behaviour of fluid and structure in order to avoid a complicated integration procedure of micro behaviour.

Models give an integrated solution, but under conditions which are different from the ones in the prototype, due to, for instance, model fluid properties, simplified reproduction of flow boundaries and, in the case of gates, model elasticity.

The scaling rules for hydroelastic models are presented in Appendix C, which is a translation from "De Ingenieur", Jan. 27, 1967 section W9. A few additional remarks are made below on the possibility of reproducing phenomena which have not been treated therein. The parameters involved are, if not correctly reproduced, sources of possible scale effects in models, and as such some of them will be discussed in par. 4.

- Dynamic phenomena related to *the compressibility of air* (C_{air}) can occur if air is entrapped by the flow near a gate. The parameter to be modelled follows from the condition that the pressure, due to geometrically scaled compression, has the correct relation to the dynamic pressure head ρV^2 . The parameter to be reproduced, then becomes $C_{air}/\rho_{water} * V^2$ (the compressibility of a gas is related to its pressure; so a reduced V in the model requires a reduced ambient air pressure). This parameter is also of importance when, in a valve aeration system, the pressure variation of the air is not negligible compared with the atmospheric pressure.
- *Cavitation* can be an important cause of dynamic load. For gate design it is a primary requirement to be cavitation free, or to have only temporarily a low degree of cavitation. Theoretically, model research must be done in such a way that in model and prototype vapour pressure is reached at equivalent locations. The pressure at any other location in the flow is, in reference to the pressure in the critical location, related to ρV^2 . So the criterium is that in an arbitrary location $(p - p_{vapour})/\rho V^2$ (Thoma number) is correctly reproduced. If the zone where incipient cavitation is expected is large in vertical direction, hydrostatic pressure differences are important and the Froude number V^2/gL (Appendix C, p.204 subd) has to be reproduced also.

VI. 3 Types of models

Cavitation research, including scale effects in models, is a separate field of research and is not further treated in this report.

- *The density of the air* can play a role when air is not completely entrapped by the flow; shock pressures of water in a cavity are greatly influenced by the pressure needed for the escape of air. Because flow velocities of air and water are of equal scale, the related pressures are correct if the $\rho_{\text{water}}/\rho_{\text{air}}$ relation is re-produced in the model. This point has been discussed [15], for shock phenomena at the re-entry of space vehicles and missiles, but it can also be of importance for phenomena like wave attack, or when a hydraulic jump touches a gate. Also, when vibration of a thin water curtain is induced by boundary layer turbulence of the air [14] the correct reproduction of $\rho_{\text{air}}/\rho_{\text{water}}$ is of primary importance.

Aims of model investigation of a gate or valve follow from the design criteria mentioned in Chapter I:

- to check whether the gate is in all circumstances free of self-exciting vibrations;
- to check whether the lowest resonance frequencies are high enough relative to the dominant turbulence frequencies;
- to check whether the resulting force of proper weight minus static and dynamic uplift forces is in one definite direction;
- to check whether entrapped air or cavitation can cause an unstable water surface;
- to determine the total maximum load for the gate and the hoist system.

3. TYPES OF PHYSICAL MODELS FOR VIBRATION RESEARCH

There are different kinds of models used in gate research:

- rigid models,
- single oscillator models (free vibration models, with one vibration mode)
- activated oscillator models (with a forced frequency, amplitude and vibration direction)
- models with continuous elasticity (free vibration models)

An indication for the selection of the best one of these models can be found from Table VI.1. Which type of model is actually used depends on the type of measurement the laboratory is experienced in, the time in which the model can be made available, how easily the model can be modified, etc.

Chapter VI. Physical models

For the different types of dynamic models, it is often necessary to compromise in details because of the primary demand to suspend the gate in such a way that it is free of mechanical friction.

With regard to the geometry, an accurate reproduction of seals, slots, leakage gaps etc. is important because these elements sometimes are dominant factors in the generation of self-excited vibrations. Compromises have to be found if rubber seals in prototype are partly compressed and partly released, which alters their shape. An extra problem arises for culvert valves, when the whole culvert length can not be reproduced. The computation results of equation (II. 13) can lead to a correction factor for the results obtained in such models. In free oscillator type models, proper reproduction of weight can be a problem. However, if a variable spring rigidity is used, those measurements that belong to the correct resonance frequencies (in submerged condition) give the correct internal force in the low-frequency range and will give the correct final amplitudes when self-excited vibrations occur.

It can be said that each type of model has its own possibilities but still more its limitations, and often different types of models are employed for one gate investigation. The easiest studies are those where in reality only one degree of freedom is expected, like the reversed taintor valve described in Appendix B.

When the type of vibrations is not predictable, elastic models offer the greatest possibilities, but their disadvantage is that the prototype design must be roughly available to be able to reproduce its mechanical properties. Also the scale reduction (which is related to the materials available for models) has its limitations and, moreover, the compromise in material thickness endangers the geometry of flow. To overcome these disadvantages, sometimes a single oscillator model is built to develop the optimal shaping of the design, the elastic model is then used as a final check.

When shapes are involved, which are likely to be sensitive to a Reynolds number that is too small in the model (cylindrical shapes, rounded edges, etc.), a rigid model with dynamic pressure cells can give additional information. In a closed water or air tunnel, velocities can be chosen adapted to the Reynolds number of the prototype. The free-surface conditions can not be fulfilled at the same time, so the

VI. 4 Air models

boundary of the tunnel must follow the stream lines, which are determined theoretically or in other models. In this case, different models are built, none of which gives complete information. The designer must judge the results and then optimize the design.

4. AIR MODELS FOR GATE RESEARCH

One reason for the use of air models can be the availability of equipment. Additional advantages are that instruments, like pressure cells and strain gauges, do not need to be watertight and that the suspension of oscillator models, when placed in air, gives only little added fluid mass and damping. Hot wire instruments can be applied for three-dimensional, stationary and non-stationary flow velocity measurements. Pressure cells can be placed away from the surface on which the pressure measurements are done; the connection tube gives, due to the small air mass, hardly any deformation of the response, and the resonance frequency of the cell itself does not change. This permits the use of one probe for successive measurements at different spots by means of a selective air-tube switch.

Rigid gate models in air tunnels give the same information as can be obtained from rigid models placed in a water tunnel. The effect of a free surface can not be reproduced in air. The transsonic wind tunnel available in the Netherlands (at the National Aerospace Laboratory) enables research at very high Reynolds numbers; the dynamic viscosity can be lowered by using an air pressure of 4 atmospheres. Maximum air velocities in such research are limited, because the compressibility of air can not be allowed to interfere when non-compressible water conditions are to be reproduced.

Activated-oscillation models in air tunnels enable measurement of forces in phase with the vibrational displacement and with the vibrational velocity. These values are representative of forces in water. The forces in phase with the displacement however, are difficult to measure accurately, because the air forces are small compared with the inertia forces of the structure itself.

Free-vibration models in air are not applicable in the research of self-exciting vibrations, unless the type of vibration is sufficiently known to permit transformation of the measured forces into the real forces at the gate. The main problem is that the added air mass

Chapter VI. Physical models

is too small in relation to the gate mass, and this relation also interferes with the self-excitation mechanism. For instance, in equation (II. 13), the c_m value is not reproduced correctly.

5. THE RELIABILITY OF MODELS

It has been discussed in Appendix C that different, non-dimensional, parameters have to be reproduced in a model, which leads to contradictory requirements. For instance, the Reynolds number VL/ν , the Froude number V^2/gL and the Weber number $\rho LV^2/\sigma$ appear simultaneously. But, incidentally, the Thoma number $(p-p_{\text{vapour}})/\rho V^2$ related to cavitation phenomena, the Cauchy number related to air compressibility ($\equiv P_{\text{air}}/1/2\rho V^2$), in long pipes the relation of water compressibility C_{water} to dynamic pressure head $(C/\rho V^2)$, and sometimes the relation $\rho_{\text{air}}/\rho_{\text{water}}$ (when shock pressures occur or when in an aeration system suction pressures are so low that ρ_{air} varies) have to be considered.

The question of the reliability of models can, in fact, only be answered when theoretical or experimental studies have shown in which range of magnitude each parameter still has effect. Data of sufficient consistence are, however, not yet available. A few parameters will be discussed, taking into account that dynamic models of gates can for practical reasons not be too small, because of the demand that geometrical reproduction of seal shape etc. must be accurate.

Reynolds number. When flow separation is unstable, for instance at rounded edges, a comparison can be made with the experience gained with cylinders. Tests with cylinders having a diameter D have shown that between $Re (\equiv VD/\nu) 10^3$ and 5×10^5 the effect of the VD/ν relation is small on drag, dynamic lift and dominant Strouhall number; but roughly at $Re = 5 \times 10^5$ a transition occurs in the character of flow excitation. It is not yet clear whether above 10^6 a new stable region begins [17] [40] and [104]. When flow separation is stable, no indication exists that the Reynolds number influences drag and the magnitude of turbulence. An indication is found in Appendix B that even damping measurements under still water conditions show hardly any influence of the vibration velocity (\dot{y}) on the drag coefficient.

Experience has demonstrated [25] that self-exciting vibration can even occur in models where small Reynolds numbers are involved. The model of the gate of the Volkerak barrage showed heavy regular vibrations when the gap width was 1-2 mm and the level difference 0.3 m. No conclusion can, however, be drawn whether reproduction of this phenomenon is fully correct on this scale.

VI. 5 Reliability of models

Froude number. For gate research, the reproduction of the free water levels is necessary: the Froude number has to be reproduced. For valves, free surface influence interferes only when the water level in the gate shaft is low or when the valve is fully aerated at its downstream side. Under all other conditions, the Froude number has no influence on the behaviour of valves.

Weber number. This number only has effect when wave radiation is of importance. The curvature of the surface causes additional pressures, resulting in a quasi-increase of gravity. The number $4\pi^2\sigma/\lambda^2\rho g$ (λ = wave length) has to be much smaller than unity. For a sinusoidal wave, this number expresses the relation between the pressure due to surface tension (related to the curvature of the surface) and the pressure due to gravity. Indirectly, surface tension has an effect on the onset of cavitation (influence on the pressure inside of a small vapour bubble), on the velocity of rising air bubbles and on the suction of air by flowing water. In general, it is assumed that air suction is somewhat suppressed in a model, because of too high velocities of the rising air bubbles.

Thoma number. When cavitation is involved, the Thoma number has to be correctly reproduced (by testing the model under reduced pressure). Systematic tests have demonstrated [100] that the critical Thoma number (incipient cavitation number) becomes smaller when the size of the structure is reduced. This is probably due to the effect of surface tension on the pressure inside the small vapour bubbles and will disappear at fully developed cavitation.

Cauchy number related to air compressibility. In Appendix A it is discussed that for an air volume enclosed behind an overflow nappe, a model may be unsafe to predict vibrations. In other cases where air compressibility is involved (shock pressures when the water is mixed with air, etc.), no definite conclusions can be drawn about the interpretation of model results.

The importance of the different parameters has not yet been investigated in a systematic way, and generally it is very laborious and difficult to obtain information on the dynamic behaviour of prototype gates and valves to check the predictions obtained from models. For this reason, it was an unique opportunity, given by Rijkswaterstaat (Netherlands Public Works Department), to execute an extensive test

Chapter VI. Physical models

programme on the gates of the Hagestein barrage and to repeat model investigations (on a model with continuous elasticity) under exactly the same conditions as had been encountered during the prototype measurements.

These comparative studies have been published [32], [33] and [47] and are shortly summarized in Appendix C. The results justify confidence in vibration models in general and particularly in models with continuous elasticity. They also demonstrate the limitations residing in the fact that the local bending rigidity of plates and solid beams is exaggerated in such models; high-frequency vibrations in such members are obliterated thereby.

The model gate, with a height of 0.4 m and exposed to level differences of 0.15 m and less, was used with a range of Reynolds numbers normal for model investigations, and it could be concluded that the small Reynolds numbers in such a model do not limit its applicability. However, this conclusion is probably not true when vibrations arise from unstable flow separation at a convex surface, as it has been shown for cylinders that the dynamic excitation alters its character at a critical Reynolds number which lies above the value reached in models ($Re_{crit} = VD/\nu \approx 5 \cdot 10^5$). No phenomena related to cavitation or air suction occurred, and nearly no wave radiation was observed. So this study was mainly conclusive for the small influence of the Reynolds number and for the correct elastic reproduction of the prototype.

Table VI. 1	Type of measurement	Detection of self-excited vibrations	Detection of external (hydrodynamic) load	Detection of load on members	Detection of water mass and damping	Detection of local tensions	General applications	Application on gates and valves	Limitations	References
Rigid (gate) models	a. pressures. b. total external forces.	Indirect, by detection of the instability parameter.	Yes	Generally not possible	No	No	Turbulence and wake research. Forces on cylinders and similar cross-sections [30], [102].	Detection of dominant excitation frequency. Mostly used in preliminary study.	a. elaborate b. force meters + weight of model limit the frequency range of measurement.	[1] [3] [26] [42] [69]
Single, free, oscillator models	Internal force.	In one direction of vibration.	In the low frequency range or indirectly from dynamic force.	No	In one direction by means of damped free oscillation.	No	Research on self-excitation. Technique most extensively used for gates and valves.	When hoist system is weakest point. Check of predicted vibrations. Preliminary study.	One degree of freedom.	[19] [21] [23] [24] [59] [61] [62] [63] [80]
Activated oscillator models	Internal force during periodic oscillation.	In one direction of vibration. Detailed information (frequency and amplitude easily variable).	Yes	No	Yes	No	Fundamental research [98]	Fundamental research. Summation of energy transfer can predict total behaviour if vibration is nearly 2 dimensional.	Data elaborately obtained by subtraction of total force and inertia force of model.	[35] [70]
Models with continuous elasticity	a. displacement b. acceleration c. strain	Complete reproduction, as far as geometry and rigidity of members are sufficiently correct.	No	No; a rough indication can be obtained by strain measurements	Roughly by change in ω_n and mode of vibration.	Yes	Flutter research on wings (velocity scale $n_v = 1$).	Overall, 3 dimensional check of the final design. When used with free surface flow $n_v^2 = n \frac{n_1}{g L}$.	Final design must be available. Schematized: shape, rigidity and mass distribution.	[20] [26] [25] [37]

Appendix A

Instability of a vertical water-curtain closing an air-chamber*

SUMMARY

A study is presented on the water-curtain/air-chamber system. The aim of the study was to get an insight into the feedback mechanism, and to detect whether factors are involved on which scale effects in physical models have to be expected. The theoretical part of the study consists of the behaviour of the curtain when a periodic air pressure variation is assumed, and conditions are derived for the cushion rigidity and damping of the air-chamber for which the feedback mechanism can occur. Experiments in a small model show results which can be partly explained by the theory, but questions on the air compressibility still remain. Tests with an elastic membrane in the wall indicate that a physical model on which the air compressibility is too high gives results on the unsafe side for the prediction of instabilities.

INTRODUCTION

Interest in the problem of instabilities in a water curtain has tended to be limited because early studies showed that splitting the water curtain is a simple remedy to stop the vibrations and to ensure a safe design of the overflow type of gate. But in some cases the splitting of the curtain is not technically attractive (ice problems etc.) and aeration tubes are considered, the capacity of which is determined by model studies. The more recent interest (Schwarz [92,93] and Partensky [76,77]) has been more directed towards the fundamentals of the feedback

* This paper has been published in the IUTAM-IAHR symposium on Flow-Induced Structural Vibrations, Karlsruhe 1972, ref. [68].

Appendix A

mechanism which can be of importance for other vibration problems also. The work of Schwarz showed that an analytical approach is in principle possible and leads to good results in the determination of critical frequencies. Recently, Partensky [77] has shown also how the elasticity of the gate can be introduced. However, still missing at this moment is the explanation of the overall mechanism of the instability and the explanation why this instability of only the water curtain (rigid gate) can occur even when the air rigidity in test-installations is higher than acceptable in the computations [92]. As the compressibility of air is incorrect in small-scale models it is important to get information about this discrepancy.

To start with a disillusion: our recent work has not produced a complete solution either. Its interest is mainly connected with the fact that the theoretical and experimental set-ups are relatively simple to overlook because there is only a vertical water sheet enclosing a rectangular air-cushion (fig. 1).

THEORETICAL STUDY

When it is assumed that outside of the chamber (fig. 1) the pressure is constant (P_0) and inside it is varying ($P_0 + p$), then the horizontal acceleration of the falling water particle depends on the mass ($\rho\delta$) and the pressure variation (p). The inside pressure is supposed to be equal over the height of the curtain. Because the effect of p on the fall velocity has been neglected, the system is linear.

When the water curtain and the air-cushion form a feedback vibration, the air pressure will have the characteristic $p = \hat{p} * e^{zt}$, in which z is complex. When the real part of z is positive, the amplitude increases and the system is unstable and when negative, the system is damped. With this approach, however, the equations became too complicated to find the sign of the real part of z .

Thus, the following method was used. When a stationary vibration is assumed, the air pressure variation $\hat{p} \cos \omega t$ determines the behaviour of the curtain. (eq (4a) and fig. 3), and the variation of the volume ΔV can be computed. The volume variation can be written as $[\Delta V = A(\hat{p}, \omega\tau_H, v/g\tau_H) * \sin \omega t - B(\hat{p}, \omega\tau_H, v/g\tau_H) \cos \omega t]$ (eq. (6)), (Appendix I). Then a formulation is possible of the condition to be fulfilled for ΔV causing $\hat{p} \cos \omega t$ (Appendix II).

Appendix A

This leads to a "necessary rigidity" and a "necessary damping" which can be either positive or negative. When the "necessary damping" is positive for the stationary vibration ($A/B < 0$), and the real damping of the air is smaller, the real system will have a surplus of energy and will amplify.

The computations were made for variations of the height (H) and frequency (ω), and it appears (Appendix I and II) that the spring rigidity of the air, expressed in L with the assumption of $pV = \text{constant}$ (isotherm), can be found from:

$$\Psi = P_o V_o^2 / L g^2 \rho_w \delta_o = \Psi(\omega \tau_H, V/g\tau_H),$$

in which τ_H is the time of fall ($H = V_o \tau_H + \frac{1}{2} g \tau_H^2$). The value of Ψ is to be found in fig. 2.

When a real situation is given, Ψ and $V/g\tau_H$ are known, and a number of values will be found for $\omega \tau_H$, of which some have a positive "necessary damping" (fig. 2). At these values of $\omega \tau_H$ vibrations can occur.

Theoretically the amplitude in the case of instability of a linear system grows indefinitely. Only the speed of increase is coupled to the "necessary damping" (log. incr. = $-\pi A/B$, eq.(11)). The limit of the amplitude is only due to non-linear effects.

The use of this linear theory is limited to infinitely small amplitudes, which is to be seen from an energy balance. The incoming water has a certain energy (kinetic + potential). The energy of the curtain increases due to the horizontal (vibration) velocities and also, for negative A/B values, energy is "pumped" into the air. This means that the fall energy has to decrease to obtain a correct energy balance.

EXPERIMENTAL STUDY

With a small model it was checked how far the computations are valuable. The total height over which the curtain could fall (H) was up to 0.5 m, the width 0.23 m, and the length L was variable up to 0.3 m (Fig. 4) H could be varied by regulation of the downstream water-level.

On the back wall, a rubber membrane was braced weakly and could be taken out of work by a valve inside of the air-chamber. The membrane rigidity was not calibrated, but the relations between the amplitudes of pressures and of the membrane movement during vibration indicated that 1 mm of water column gave 40 to 60 cm^3 volume variation.

Appendix A

This means roughly that the weakest air cushion during the test ($H = 0.5\text{ m}$, $L = 0.3\text{ m}$) became ten times weaker with the membrane.

The fall velocity V_o was determined accurately by photographing oil drops, injected intermittently at the same frequency as the frequency of a stroboscope lamp.

The test results are presented in fig. 5; the measured frequencies differ by a maximum of 5% from the average lines which are presented in fig. 5b.

The main conclusions which are drawn from a comparison between the measured and calculated values are:

1. *Frequencies.* The frequencies of vibration as presented in fig. 5b are, for the first harmonic, reasonably described by $\omega\tau_H \sim 8.2$; for the values of H , where vibrations could only occur with help of the membrane, this goes down to 6.8. For the second harmonic $\omega\tau_H$ is about 14.5 without and down to 12.5 with membrane. The measurement of the third harmonic was only incidentally obtained, with a value of $\omega\tau_H = 22.3$. In the region where vibration could occur without membrane, practically no influence was seen when the membrane was used.

The $\omega\tau_H$ values do not really correspond with the maxima of the $(-A/B)$ values as was expected from the computations (fig. 2), nor do the Ψ values of fig. 2 agree with the Ψ values of the model (mentioned in fig. 5a). The $\omega\tau_H$ values correspond better with the frequencies where the pressure variation $\hat{p} \cos \omega\tau$ has a maximum energy transfer from the curtain into the air; this is when $(-A)$ reaches the maximum value.

To demonstrate this, the A curves are also plotted in fig. 2. The $\omega\tau_H$ values correspond with the $2\pi(n + \frac{1}{4})$ criterium of Schwarz: this would result in $\omega\tau_H = 7.9, 14,$ and 20.4 for the first three harmonics.

The measurement of the third harmonic with $\omega\tau_H = 22.3$ comes just where A becomes positive. As this value was only taken at one measurement, no premature conclusions should be drawn.

2. *The Membrane.* As is seen in fig. 5, vibrations occurred at much greater ranges of H with the use of the membrane. Also, the vibration started much easier. *This indicates that a model on a reduced scale is on the unsafe side for the study of vibrations,* because then the air rigidity is relatively too high. In some cases, the membrane had

Appendix A

to be used to stimulate the vibrations; then, the vibrations remained also without it. In fig. 2, those cases are presented as vibrations without membrane.

3. *The Rigidity of the Air Cushion.* The results, as discussed under Point 1, are not at all related to the theoretical Ψ value of fig. 2. The rigidity of the aircushion in the model was much too large compared with the theoretical value, and discrepancies are more than 100-fold. Different possibilities, apart from the curtain itself, can be considered:

- (a) The downstream water-level under the airchamber is another elastic element. With the static deflection due to a pressure variation, the total rigidity can come in the right order of magnitude. However, wave studies indicate that this only occurs at very low frequencies. When they are high, the water acts as mass or as spring, depending on the frequency. Moreover, the quasi-rigidity of the water becomes much higher at the frequencies being dealt with here. Tests were carried out with the downstream water-level replaced by a sloping bottom. As the vibrations remained, it is concluded that the water cushion is definitely not the determining parameter for the rigidity of the system.
- (b) The downstream water-level is supposed to be a damper, being in series with the air "spring". This is analyzed in Appendix II; The resulting rigidity can be $(A^2/B^2 + 1)$ higher than the Ψ on fig. 2, where the damper was supposed to be in series with the spring. This results from eq.(10). For the range of measurements, the maximum of A/B is 1.2, so the theoretical Ψ value becomes 1 to 2.5 times the Ψ value of fig. 2.

4. *Pressure Variations in the Air Chamber.* Simultaneous pressure measurements were made on one side wall. Depending on L and H , the pick-ups could be placed on 2-12 locations. All pressure variations had the same amplitude without phase shift. Only at the corner where the curtain falls into the water, p was a little greater. *This shows that for this model the concept of a simple air cushion was correct.* When the dimensions of the air cushion are greater, resonance in the air can play a role; in this case, a small-scale model will also have scale effects.

Appendix A

5. *Magnitudes of Pressures.* Pressures have only been measured for the steady-state vibration. Roughly it can be said that for tests I and III \hat{p} is proportional to H^{-1} , and for the first harmonic the average value for $H = 0.5$ m varies from 0.65 mm of water column to 0.8 mm for test I and from 1.0 to 1.4 mm for test III (so roughly increasing proportional to δ_0). Lowest amplitudes are found for small L , the greatest for $L = 0.3$ m and with membrane. The second harmonic gives 1.3 to 1.6 times greater \hat{p} values. At smaller H values, near where the vibration ends, \hat{p} decreases to zero.

Test II has low \hat{p} values compared with test III (same δ_0 value but lower V_0), and decreases rapidly from 0.8 mm for $H = 0.5$ m w.c. to 0.2 mm for $H = 0.43$ m. For tests I and III computations show that 2 to 4% of the (kinetic + potential) energy of the curtain is transferred to the air. For test II, this is 0.3 to 1%.

6. *Shape of the Slit.* Shapes with round and sharp corners (stable and unstable separation) have been tested, without producing any effect.

7. *Aeration of the Air Chamber.* When the curtain is split or not attached to the side walls, there is no vibration. For thin curtains ($\delta = 0.6$ to 1.2 mm), aeration through holes in the side wall was possible up to 10% of the wall area. Without membrane this was somewhat less. For test III only 2% was acceptable, for test II nothing could be opened.

8. *Test with an L of 1.5 m but the Back Wall Removed.* Vibrations appeared to occur after some initial excitation; no further measurements were made. Theoretically, this means that Ψ can be negative.

9. *Influence of the Ψ Values of the Physical Model.* As is seen from fig. 5a, there is a tendency that a decrease of air rigidity (by greater L or membrane) gives rise to lower harmonics. This agrees with theory (fig. 2). On the other hand, test II with a low Ψ value only vibrated at the second harmonic. As it is concluded that the Ψ is not the relevant parameter, the effect of V_0 and δ_0 is discussed separately.

Appendix A

10. *Influence of the Initial Velocity V_0 .* Greater V_0 eases the vibration; this agrees with fig. 2 because A (or $-A/B$) increases at higher $V/g\tau_H$ values.
11. *Influence of δ_0 .* No vibrations were obtained for δ_0 greater than 2.5 to 3 mm. The limit of vibration depends on L and the membrane.
12. The elimination of the interference of the downstream water-level and the apparent *discrepancy in the Ψ value* indicates that the linear theory is too rough an approximation. Another indication for the importance of non-linear effects is the initial stimulation which is sometimes necessary to obtain the steady-state vibration. Non-linear effects, of which the most important are related to the influence of p on the fall velocity, can affect, for instance, the apparent Ψ value. But the magnitude of this influence will then be related to the amplitude of vibration. This makes it more understandable that, for instance, different \hat{p} values have been measured after the cushion rigidity has been varied. As the amplitude of the vibration is related to \hat{p}/δ_0 the remark under point 5 that \hat{p} is proportional to δ_0 also indicates that the influence of p on the fall velocity is the determining parameter.

CONCLUSION

The linear approach for the calculation of the water curtain is valid to predict the correct possible frequencies of vibrations, that is, those frequencies where maximum energy transfer from the curtain into the air occurs. Discrepancy between theory and experiment is found on the point of the air rigidity, but qualitative agreement is found on the fact that greater rigidity gives rise to higher harmonics and that higher initial velocity eases the vibration. No information is found for conditions where lower harmonics transform into higher, or where vibration stops. Indications are given that probable non-linear effects by periodic changes in the fall velocity have to be taken into account.

Experiments with a membrane in the wall show that a model with a too stiff air-cushion is on the unsafe side for the prediction of vibrations.

Appendix A

ACKNOWLEDGEMENT

The author is very grateful to W.C. Bisschoff van Heemskerck, Professor at the Delft Technical University, and to N. Schoenmakers. The former stimulated the set-up of this study and allowed Mr. Schoenmakers to do the experiments and a part of the elaborate computations for his engineering-degree work.

APPENDIX I (belongs to Appendix A: Instability of a water curtain)

CALCULATION OF THE MOMENTARY CURTAIN SHAPE DUE TO A HARMONIC PRESSURE VARIATION

The particle which is at time t on place Y left the top at time $t - \tau_Y$ (with $Y = v_0 \tau_Y + \frac{1}{2} g \tau_Y^2$). While $v = v_0 + g\tau$, the thickness of the curtain during falling, becomes:

$$\delta = \frac{\delta_0 v_0}{v_0 + g\tau} \quad (1)$$

(The notations are followed according to fig. 1).

Horizontal acceleration due to pressure difference $p = \hat{p} \cos \omega t$:

$$\frac{d^2 x}{d\tau^2} = \frac{p}{\rho_w \delta} = \frac{(v+g\tau)}{\rho_w v_0 \delta_0} * \hat{p} \cos \omega(t - \tau_Y + \tau) \quad (2)$$

The horizontal velocity at the moment τ after leaving the top:

$$\frac{dx}{d\tau} = \int_0^{\tau} \frac{d^2 x}{d\tau^2} d\tau \quad (3)$$

The horizontal displacement X of the particle being at y at the moment t (being τ_Y after leaving the top):

$$X(y) = \int_0^{\tau_Y} \frac{dx}{d\tau} d\tau \quad (4)$$

In complete form, eq. (4) becomes:

Appendix A

$$\begin{aligned}
 X(y) = X(\tau_y) = & \frac{\hat{p}}{\rho_w \delta_o \omega^2} \left[(\omega \tau_y \sin \omega \tau_y + \cos \omega \tau_y - 1) \cos \omega t + \right. \\
 & \left. + (\sin \omega \tau_y - \omega \tau_y \cos \omega \tau_y) \sin \omega t \right] + \\
 & + \frac{\hat{p}g}{v_o \rho_w \delta_o \omega^3} \left[(2 \sin \omega \tau_y - \omega \tau_y \cos \omega \tau_y - \omega \tau_y) \cos \omega t + \right. \\
 & \left. + (2 - \omega \tau_y \sin \omega \tau_y - 2 \cos \omega \tau_y) \sin \omega t \right] \tag{4a}
 \end{aligned}$$

One example is represented in fig. 3.

The variation of volume per unit of width becomes:

$$\Delta V = \int_0^H X dy = \int_0^{\tau_H} X(v + g\tau_y) d\tau_y \tag{5}$$

or:

$$\begin{aligned}
 \Delta V = & \frac{\hat{p}g^2}{\delta_o \rho_w v_o \omega^5} \left[\left\{ \omega^2 \tau_H^2 + 4 + (\omega^2 \tau_H^2 - 4) \cos \omega \tau_H - 4 \omega \tau_H \sin \omega \tau_H \right\} \sin \omega t - \right. \\
 & \left. - \left\{ \frac{1}{3} \omega^3 \tau_H^3 + 4 \omega \tau_H \cos \omega \tau_H + (\omega^2 \tau_H^2 - 4) \sin \omega \tau_H \right\} \cos \omega t \right] + \\
 & + \frac{\hat{p}v_o (v_o + g\tau_H)}{\delta_o \rho_w v_o \omega^3} \left[\left\{ 2 - 2 \cos \omega \tau_H - \omega \tau_H \sin \omega \tau_H \right\} \sin \omega t - \right. \\
 & \left. - \left\{ \omega \tau_H + \omega \tau_H \cos \omega \tau_H - 2 \sin \omega \tau_H \right\} \cos \omega t \right] = A \sin \omega t - B \cos \omega t \tag{6}
 \end{aligned}$$

In the evaluation $\alpha = \frac{v_o}{g\tau_H}$ is used, and

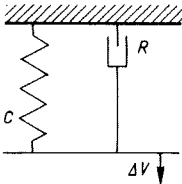
$$\frac{\hat{p}g^2}{\delta_o \rho_w v_o \omega^5} * (\alpha^2 + \alpha) (\omega \tau_H)^2 \text{ instead of } \frac{\hat{p}v_o (v_o + g\tau_H)}{\delta_o \rho_w v_o \omega^3}$$

APPENDIX II (belongs to Appendix A:
Instability of a water curtain)

CUSHION RIGIDITY AND DAMPING, RELATED TO HARMONIC OSCILLATION

It is supposed that the oscillation is steady, and that this is reached by the property of the air-cushion.

The air-cushion is compressed by a volume reduction ($-\Delta V$) and this causes an extra pressure of



$$\Delta p = c(-\Delta V) + R d(-\Delta V)/dt \quad (7)$$

It is assumed that the damping is in the air, so rigidity c and damping R work parallel. In reality, c and R will be positive; in the following computation these can be either positive or negative.

When Δp equals the value necessary to produce the volume variation ΔV (Appendix I), equilibrium is reached and steady oscillation is obtained. Eq. (6) of Appendix I is used.

$$\Delta p = \hat{p} \cos \omega t \text{ produces } \Delta V = A \sin \omega t - B \cos \omega t \quad (8)$$

Equation (7) results in:

$$\Delta p = \hat{p} \cos \omega t = -cA \sin \omega t + cB \cos \omega t - R\omega A \cos \omega t - R\omega B \sin \omega t \quad (9)$$

This results in:

$$c = \frac{\hat{p}B}{A^2 + B^2} \text{ and} \quad (10)$$

$$\frac{\omega R}{c} = -\frac{A}{B} \quad (11)$$

For comparison: with a free-damped motion of a mechanical oscillator ($m\ddot{y} + R\dot{y} + cy = 0$) the logarithmic decrement equals $\pi\omega R/c = -\pi A/B$.

For the water-curtain/air-cushion the value $\pi\omega R/c = -\pi A/B$ will,

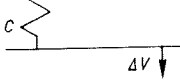
Appendix A

when the cushion is undamped, represent the logarithmic increment of the self-excited oscillation. The damping R can also be in series with the rigidity c (when the damping is in the downstream water, or when the air-cushion has a leakage with a linear resistance).



$$\Delta p = R \frac{d(-\Delta V_o)}{dt} \quad (12)$$

and



$$\Delta p = c(-\Delta V + \Delta V_o) \quad (13)$$

Integration of (12) and application of (8) results in:

$$V_o = \frac{-\hat{p}}{R} \sin \omega t \quad (14)$$

Equations (13) and (14) finally result in:

$$c = \frac{\hat{p}}{B} = \frac{\hat{p}B}{A^2 + B^2} \left(\frac{A^2}{B^2} + 1 \right) \quad (15)$$

$$\frac{\omega R}{c} = -\frac{B}{A} \quad (16)$$

With the A/B values of fig. 2, it is seen that for the region where $A/B < 0$, the $\frac{A^2}{B^2}$ becomes maximum $(1.2)^2$; this means the cushion rigidity can at a maximum be 2.5 times greater than the one found with fig. 2.

The value of the logarithmic increment remains $-\pi A/B$.

EXPLANATION OF FIG. 2

Calculations are made with the assumption of a damped air-cushion (rigidity c parallel to damping R). Equation (11) is represented in the lower graph of fig. 2. When $A/B < 0$ the system will be unstable and self-excitation can occur. The upper graph of fig. 2 has been determined for two conditions:

(A) Condition of isothermal compression of the air-cushion. Pressure * volume = constant (Volume per unit width), so $dP * Vol + dV * P_o = 0$.

$$c_I = \frac{-dP}{dV} = \frac{P_o}{Vol} = \frac{P_o}{LH} = \frac{P_o}{L(v_o \tau_H + \frac{1}{2} g \tau_H^2)} = \frac{P_o}{Lg \tau_H^2 (\alpha + \frac{1}{2})} \quad (17)$$

Appendix A

(B) Equation (10) is $c_2 = \hat{p}B/(A^2 + B^2)$

From eq. (6), Appendix I, it follows:

$$A = \frac{\hat{p}g^2}{\delta_o \rho_w v_o \omega^5} * f_A(\omega\tau_H, \alpha) \text{ and } B = \frac{\hat{p}g^2}{\delta_o \rho_w v_o \omega^5} * f_B(\omega\tau_H, \alpha).$$

$$c_2 \text{ can be written as } c_2 = \frac{\delta_o \rho_w v_o \omega^5}{g^2} f_{(AB)}(\omega\tau_H, \alpha).$$

The condition for a steady oscillation will arise when $c_1 = c_2$.

$$c_1 = c_2 = \frac{P_o}{Lg\tau_H^2 (\alpha + \frac{1}{2})} = \frac{\delta_o \rho_w v_o \omega^5}{g^2} f_{AB}(\omega\tau_H, \alpha), \text{ and it follows:}$$

$$\frac{P_o g}{L\tau_H^2 \delta_o \rho_w v_o \omega^5} \equiv \frac{P_o v_o^2}{L\delta_o \rho_w g^2} * \frac{1}{\alpha^3 (\omega\tau_H)^5} = (\alpha + \frac{1}{2}) f_{ab}(\omega\tau_H, \alpha),$$

and consequently:

$$\frac{P_o v_o^2}{L\delta_o \rho_w g^2} = \Psi(\omega\tau_H, \alpha). \tag{18}$$

Ψ is presented in fig. 2.

Appendix A

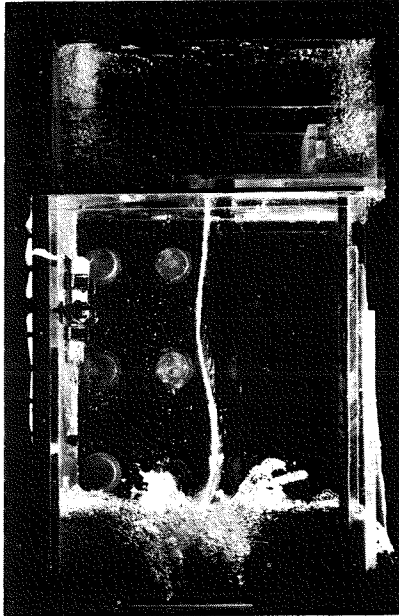
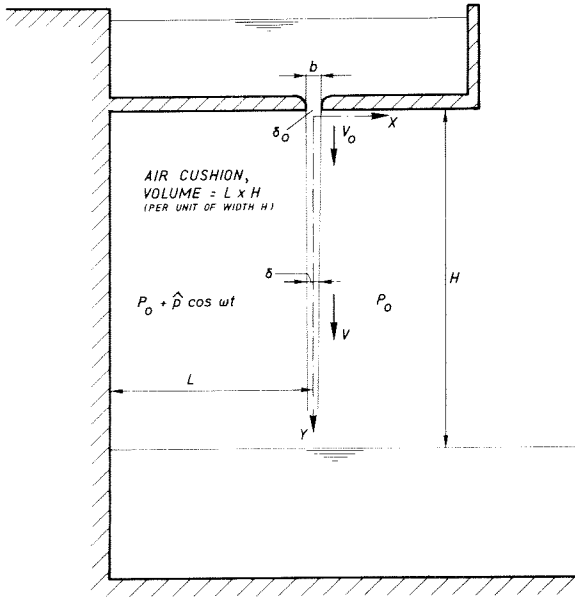


Fig. 1 Symbols

Appendix A

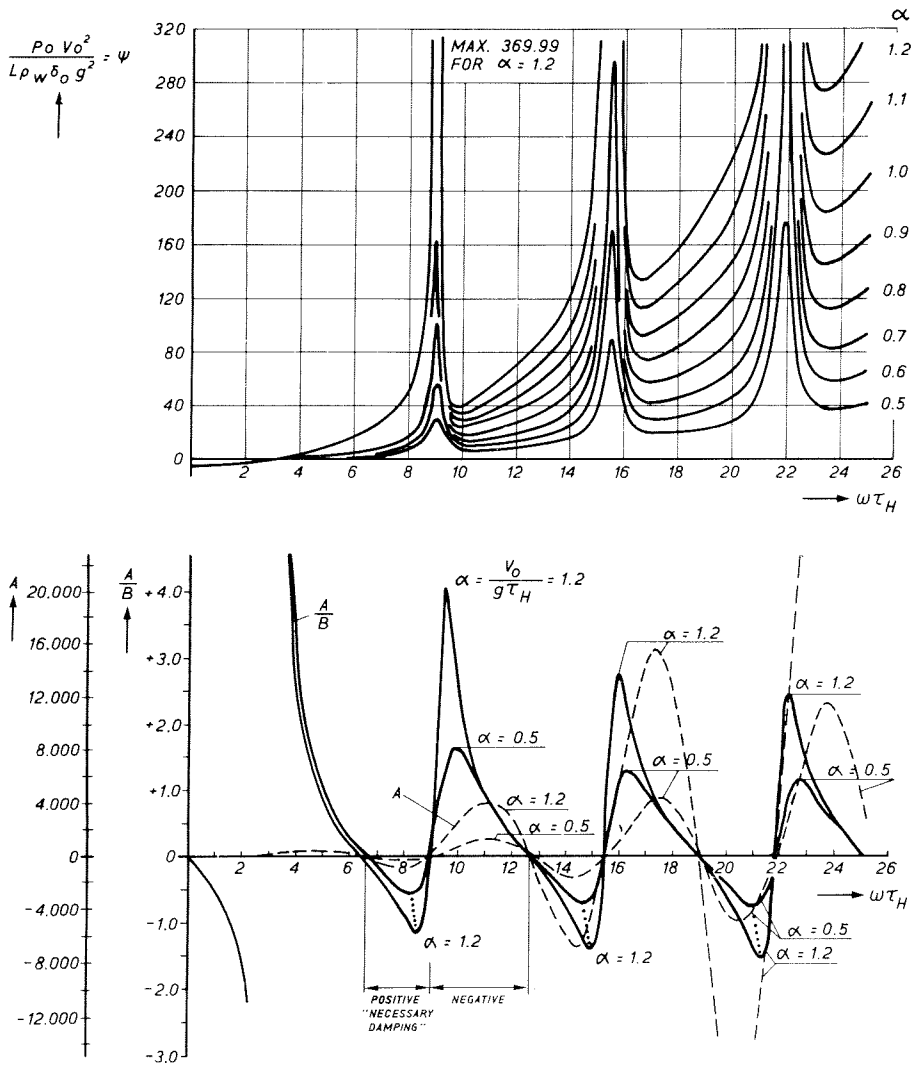


Fig. 2 Theoretical relation of Ψ and A/B with $\omega\tau_H$
(from Appendix I and II)

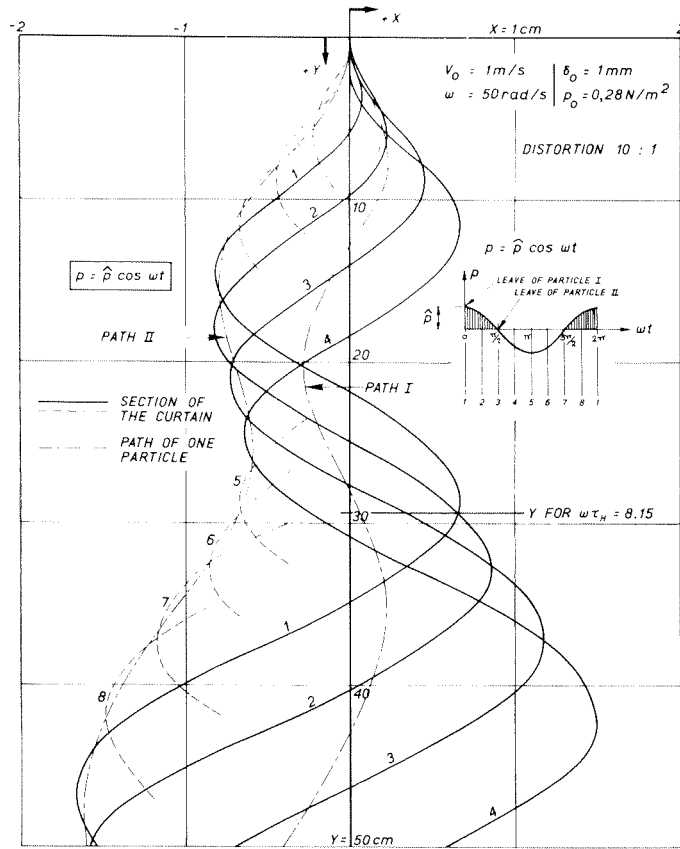


Fig. 3 Vibration of the curtain (eq.(4a), Appendix I)

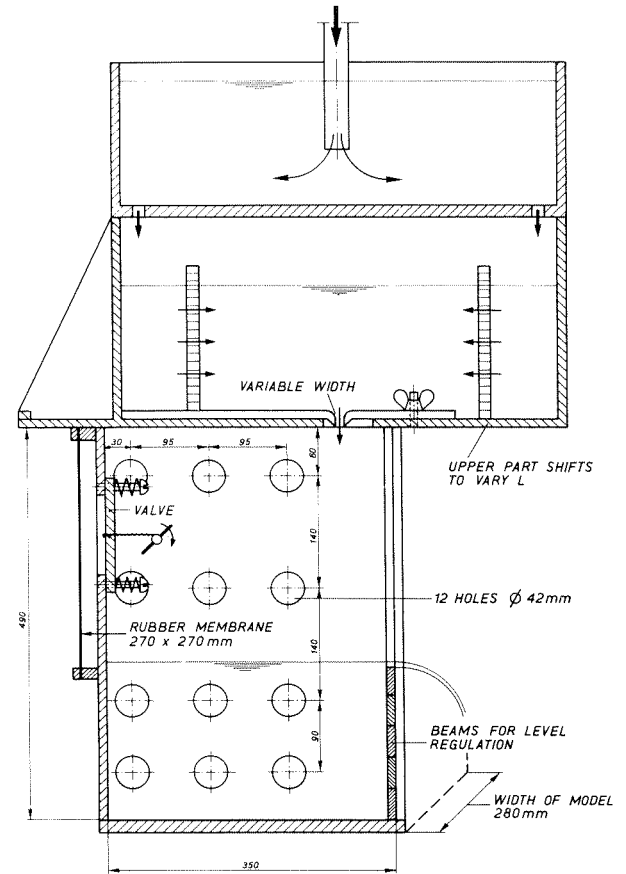


Fig. 4 Section of the model (sizes in mm)

Appendix A

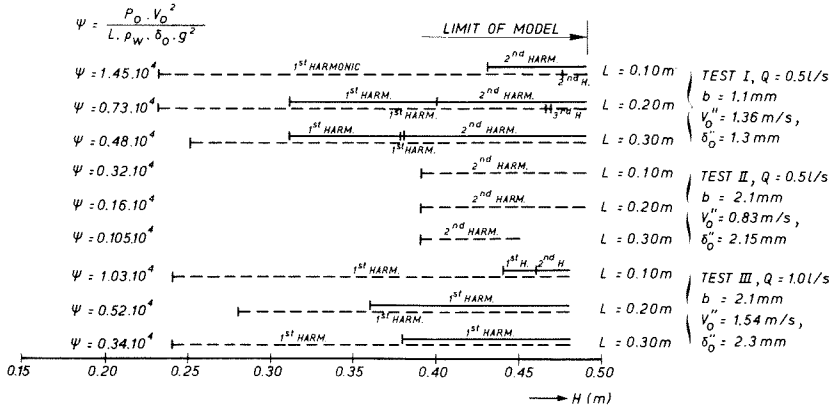


Fig. 5a Ranges of H where vibrations occur

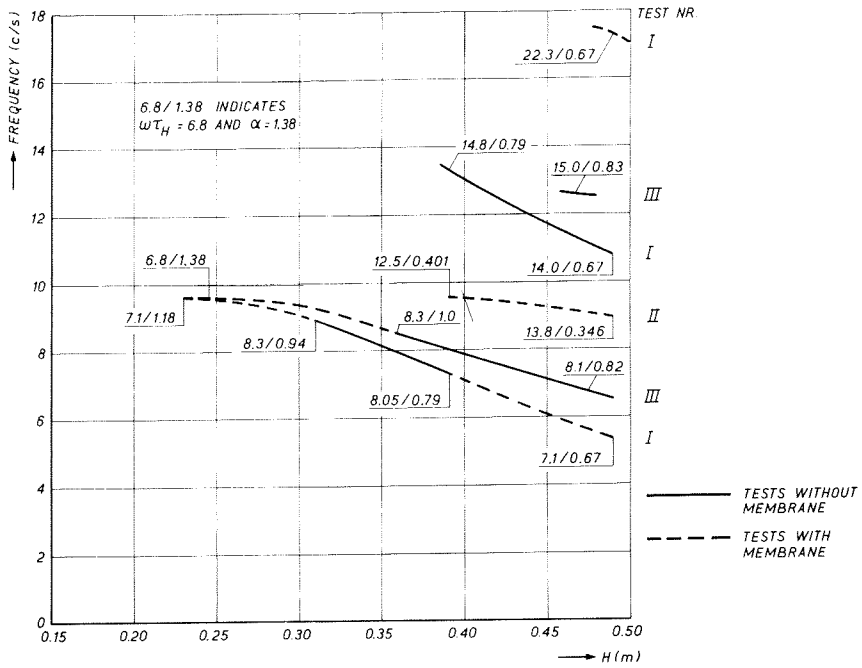


Fig. 5b Measured frequencies

Appendix B

Analysis of vibration and damping measurements on a reversed Tainter valve*

SUMMARY

An outline is given of a research program on hydro-elastic vibrations, in progress in the Delft Hydraulics Laboratory. In a culvert a reversed tainter valve has been suspended by a spring. Because only rotation on the pivot is possible, the valve-spring acts as a single oscillator. The shape of the valve is such that self-excited vibrations are not likely to occur. Vibration measurements are made with a range of water velocities and with varying gate position, valve mass, suspension rigidity and mechanical damping. The water damping is determined separately. The research program is:

- a. to study the determining factors for vibration: excitation by flow and turbulence, water inertia and water damping;
- b. to develop analysis techniques for vibration measurements;
- c. to compile systematically the dynamic behaviour of the valve.

The measurements, show that for this valve the water excitation, water mass and water damping can be treated separately.

INTRODUCTION

On different types of gates and culvert valves, force and vibration measurements have been made on small scale models taking into account the mass and rigidity of the valve and the hoist system. Solutions are found

* Presented at the IAHR symposium on Hydraulic Machinery, Stockholm 1970.

Appendix B

for the shape of seals etc. to prevent regular self-excited vibrations with large amplitudes.

It is important however to get more general information about the forces and dynamic behaviour of valves in such a way that this is applicable in a variety of conditions. Since for each application the strength and weight of the valve will always be adapted to the forces, a variation of water velocities (discharges), valve mass, hoist and other rigidities and mechanical damping has to be considered.

For the research program has been chosen a reversed tainter valve placed in a culvert, which is already applied in relatively high head navigation locks. The design was copied from lit. [62] A confirmation of the good qualities of this valve has been found in the Delft Hydraulics Laboratory by comparing different tainter valves. The qualities of the valve are mainly due to the sharp under edge which assures stable flow separation, and the vertical girder support of the skin plate which reduces resistance against tangential flow and consequently vertical forces. Moreover the great radial rigidity prevents vibration in flow direction and the pre-stressed rubber side seals, sliding against stainless steel strips, prevent transverse vibration. From model tests it is known that an upper seal as shown in fig. 2 is effective in reducing vertical vibrations at small openings.

For this type of valve the only degree of freedom of interest for a vibration study, is the vertical vibration; this simplification has been an added reason for choosing this valve type for research purposes.

As was stated by Mr. Murphy in [62] one of the interests of a study is to check that for all valve positions the submerged weight of the valve exceeds the static and dynamic uplift force due to flow, preventing play in pivoting joints causing extra vibrations.

The aims of the research program can be summarised as follows:

- a. to study the determining factors for vibration excitation by flow and turbulence, water inertia and water damping;
- b. to develop analysis techniques for vibration measurements;
- c. to compile systematically the dynamic behaviour of the valve.

Appendix B

CHOICE OF DIMENSIONLESS PARAMETERS

The investigation of forces and vibrations of the valve has been restricted to vertical forces (hoist load); the valve-hoist system is considered to be a single mass-spring system. For the sake of simplicity the polar moments of mass, spring, and damping of the valve and the water during the rotation of the valve have been recalculated in this paper to equivalent values for vertical movement. So the mass, the spring, the damping and the excitation are supposed to act on a horizontal distance of 37.6 cm of the pivot, on the skin plate (fig. 2).

In a closed conduit the geometry of flow is independent of the water velocity, and all pressures are proportional to ρV^2 . The excitation on geometric similar models will be proportional to ρDWV^2 (preference is given to separate height and width dimensions because the flow is more or less two dimensional), and the frequencies of turbulence are proportional to V/D . The response of a single mass spring system (i.e. the internal forces in the spring) depends on the ratio of turbulence to resonance frequencies and on the damping (expressed in the amplification factor $(2\gamma)^{-1}$ at periodic excitation in the resonance frequency). But the response of the structure, $y(t)$, can also affect the turbulence and the excitation. So in general the excitation can be described as:

$$F = f(D, d, W, \Sigma L, \rho, V, \nu, y, t) \quad (1)$$

in which F = external force, D = culvert height, d = valve raise, W = culvert width, ΣL = all the sizes determining the shape of the gate and the culvert, ρ = density of water, V = average water velocity in the culvert, ν = kinematic viscosity, y = movement of valve, t = time. The response of the valve is:

$$y = f(D, W, d, \Sigma L, \rho, V, \nu, m, c, R, t) \quad (2)$$

in which m , c and R are the mass, the spring and the damping which determine the equation for the mass-spring system:

$$m \frac{d^2 y}{dt^2} + R \frac{dy}{dt} + cy = F$$

When only the main hydraulic parameters V , D and ρ are considered, the following dimensionless parameters will be found:

$$\frac{y}{D} = f\left(\frac{W}{D}, \frac{d}{D}, \frac{\Sigma L}{D}, \frac{VD}{\nu}, \frac{c}{\rho V^2 D}, \frac{m}{\rho D^3}, \frac{R}{\rho V D^2}, \frac{Vt}{D}\right) \quad (3)$$

In this way relevant scale factors of a model are obtained.

Appendix B

To choose optimum dimensionless parameters from eq. (2), for analysis purpose it has been judged useful to follow the response equation of the mass-spring system:

$$\frac{F_{\text{intern}}}{F_{\text{extern}}} = f\left(\frac{N_{\text{res}}}{N_{\text{exc}}}, \gamma\right), \text{ and therefore the following parameters}$$

have been chosen:

$$\frac{cy}{\frac{1}{2}\rho V^2 WD} = f\left(\frac{d}{D}, \frac{W}{D}, \frac{\Sigma L}{D}, \frac{VD}{v}, \frac{N_r D}{V}, \gamma, \frac{y}{D}, \frac{Vt}{D}\right) \quad (4)$$

(a) (b) (c) (d) (e) (f) (g)(h)(i)

(a) gives the relation between internal force in the spring and the external force; (b), (c) and (d) are geometrical factors. W/D indicates that not only the vertical cross section is of interest to the excitation, mass and damping effect of the water; (d/D) is the relative valve opening; $\frac{\Sigma L}{D}$ represents mainly the vertical cross section of the culvert, the shaft and the valve. (e) is the Reynolds number. (f) is an important number indicating the relation between resonance and turbulence frequencies. N_r is the resonance frequency in water; for its computation the equivalent mass of the water m_w has to be known:

$$N_r = \frac{1}{2\pi} \sqrt{\frac{c}{m+m_w}} \quad (5)$$

$m_w/\rho D^2 W$ is generally considered independent of V , v , N_r , y and t , so the mass number can be introduced:

$$\frac{m_w}{\rho D^2 W} = f\left(\frac{d}{D}, \frac{W}{D}, \frac{\Sigma L}{D}\right) \quad (6)$$

(g) is the ratio damping/critical damping:

$$\gamma = \frac{R + R_w}{2(m+m_w)\omega_r} = \pi N_r \frac{R + R_w}{c} \quad (7)$$

(h) indicates the feed back of the vibration on the turbulent excitation. This parameter is also significant when non linear parameters interfere (springs, mechanical- and waterdamping can be non linear, joints with play can interfere).

(i) indicates that y is a function of time. This parameter can be suppressed when $y(t)$ can be described in a representative way by an equivalent amplitude, see next paragraph.

Appendix B

REPRESENTATIVE AMPLITUDES

The response of an oscillator is such that static load and low frequency excitation ($N_{\text{turb}} \ll N_r$) gives no or little amplification. Periodic excitation in resonance frequency gives an amplification of $(2\gamma)^{-1}$, while white-noise excitation gives an amplification proportional to $\gamma^{-1/2}$. High frequency excitation ($N_{\text{turb}} \gg N_r$) will give no response. For this reason the internal force (cy) has been divided in:

- static force F_s , of which only the force caused by the flow will be considered.

- Quasi-static force F_{qs} , which is the low frequency force.

- Dynamic force F_d , which is the resonance response.

The separation in F_{qs} and F_d is useful only if a clear frequency separation can be made between the two vibrations. The force F_{qs} and F_d will vary with the separation frequency N_s . It can be expected that:

$$F_s / \frac{1}{2} \rho V^2 W D = f_1 \left(\frac{d}{D}, \frac{W}{D}, \frac{\Sigma L}{D}, \frac{VD}{v} \right) \quad (8)$$

$$F_{qs} / \frac{1}{2} \rho V^2 W D = f_2 \left(\frac{d}{D}, \frac{W}{D}, \frac{\Sigma L}{D}, \frac{VD}{v}, \frac{N_s D}{V} \right) \quad (9)$$

$$F_d / \frac{1}{2} \rho V^2 W D = f_3 \left(\frac{d}{D}, \frac{W}{D}, \frac{\Sigma L}{D}, \frac{VD}{v}, \frac{N_r D}{V}, \frac{N_s D}{V}, \gamma, \frac{y}{D} \right) \quad (10)$$

In the research program these relations are investigated.

For F_{qs} and F_d the standard deviations are taken as representative amplitudes. This value has been obtained by filtering the signal in the frequency N_s , and by averaging the square value of the signal; the root equals the standard deviation. Approximately the same results have been obtained by taking of the filtered signal some arbitrary levels and by determining the percentage of time the level is exceeded. Plotting the points on "gaussian" paper enables finding the standard deviation.

The standard deviation of the total dynamic force can be calculated by $F_t = (F_{qs}^2 + F_d^2)^{1/2}$ which value corresponds with the standard deviation of the unfiltered signal. It has been checked that vibrations have approximately a normal distribution. For practical application a crash factor 3 to 5 has to be applied to the standard deviation.

ANALYSIS OF THE WATERDAMPING

From lit. [45] it is seen that waterdamping consists partly of a drag force $f = \frac{1}{2} \rho V_t^2 A C_D$, and partly of viscosity effects. Combination

Appendix B

of flow and vibration gives for the former:

$$f = \frac{1}{2} \rho (V_t - \frac{dy}{dt}) |V_t - \frac{dy}{dt}| AC_D \quad (11)$$

A = valve area \perp vibration direction

V_t = tangential or vertical velocity component

C_D = drag coefficient.

The force f gives per period of a stationary vibration ($y = Y_o \sin \omega t$) an energy dissipation which has to be compared with the energy dissipation due to the damping term $R dy/dt$ of the mass-spring equation (being $\pi R Y_o^2 \omega$).

When $V_t = 0$, $f = \frac{1}{2} \rho (\frac{dy}{dt}) |\frac{dy}{dt}| AC_D$ and the energy dissipation per period is $\frac{4}{3} \rho AC_D Y_o^3 \omega^2$, so the damping term R can be calculated:

$$R = \frac{4}{3\pi} \rho AC_D \omega Y_o \quad (12)$$

When $|V_t| > |\frac{dy}{dt}|$ eq. (11) becomes $f = \frac{1}{2} (V_t - \frac{dy}{dt})^2 AC_D$, of which only the double product contributes to the damping. The double product is equal to the term $R \frac{dy}{dt}$ in the mass-spring equation, so:

$$R = \rho V_t AC_D \quad (13)$$

For all values of V_t , it is found:

$$\frac{R}{\rho AC_D V_t} = f\left(\frac{\omega Y_o}{V_t}\right) \quad (14)$$

In this function eq. (12) gives the asymptote (for $\omega Y_o / V_t \rightarrow \infty$) being $R / \rho AC_D V_t = 4 \omega Y_o / 3\pi V_t$, and eq. (13) gives for $\omega Y_o / V_t < 1$ that $R / \rho V_t AC_D = 1$.

Because measurements with $V = V_t = 0$ have shown $C_D = f(Y_o/D)$, without an influence of viscosity, eq. (14) becomes:

$$\frac{R}{\rho W D V} = \frac{V_t}{V} * \frac{A}{W D} * C_D \left(\frac{Y_o}{D}\right) * f\left(\frac{\omega Y_o}{V_t}\right) \quad (14')$$

$$\text{which means } \frac{R}{\rho W D V} = f'\left(\frac{\omega Y_o}{V_t}, \frac{Y_o}{D}\right) \quad (14'')$$

With the same variable parameters this can be presented as:

$$\frac{R}{\rho W D V} = f''\left(\frac{N D}{V}, \frac{Y_o}{D}\right) \quad (14''')$$

This presentation has been used for analysis, as the terms are in accor-

Appendix B

dance with eq.(4). When viscosity is not negligible eq.(14''') becomes:

$$\frac{R}{\rho W D V} = f'''\left(\frac{N D}{V}, \frac{Y_0}{D}, \frac{V D}{\nu}\right) \quad (15)$$

The damping measurements have been done by recording the free damped vibration after a short blow. The envelope curve of the vibration has been drawn, the tangent on the amplitude Y on the moment t goes through the zero line a time $\tau = (2\pi N_r \gamma)^{-1}$ later. With eq (7) the $R + R_w$ can be calculated, while R was measured from tests under dry conditions.

THE MODEL

Fig. 1 shows the test installation, with diffuser and stilling chamber to suppress turbulence. The culvert $D = W = 0.25$ m, has an up-stream length from the valve of 2 m, and a downstream length of 3 m. The discharge and the pressure (the water-level in the shaft) can be regulated by a valve upstream and by bulkheads downstream of the culvert.

The valve hangs on a steel wire attached to a pair of leaf springs on top of the shaft. Between the leaf springs additional mass can be attached which makes the same movements as the valve, so that it is possible to vary the valve mass without affecting the geometry in water.

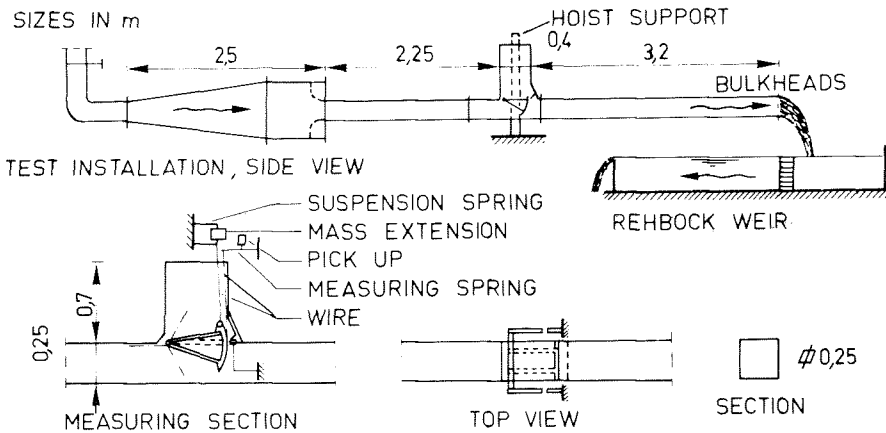


Fig. 1 Tests installation

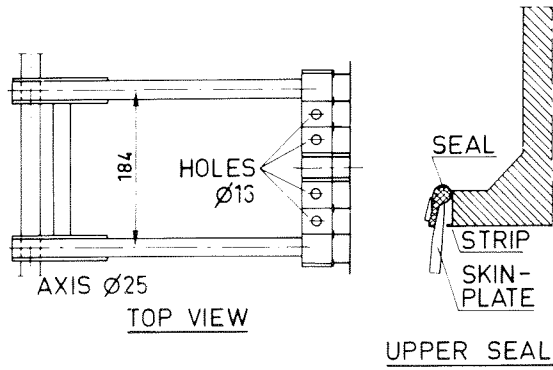
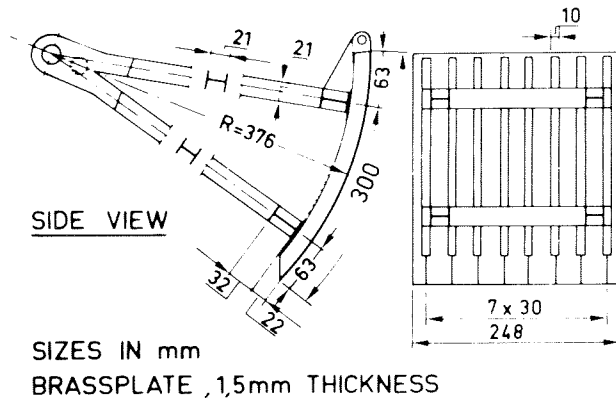


Fig. 2 Valve, shape and sizes

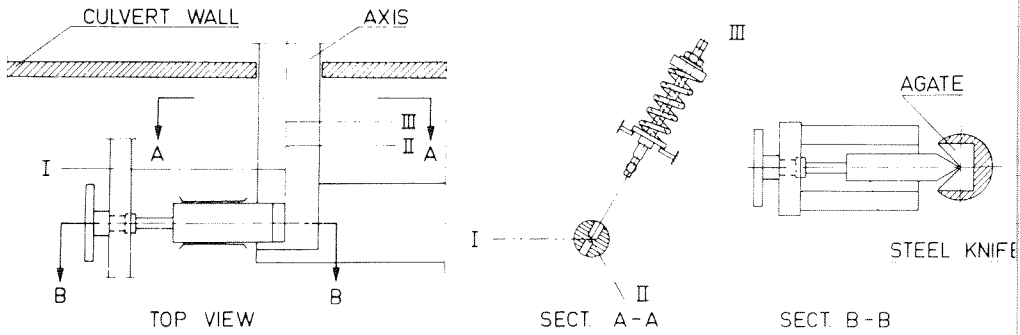


Fig. 3 Knife bearing for low friction pivoting

Appendix B

The length of the leaf spring is variable to vary the rigidity. A second steel wire has been attached to the downstream side of the skin-plate to measure vibrations at all valve positions at a constant distance from the axis. On top of the shaft this wire is suspended to a relatively weak leaf spring, the deflection of which is measured with an inductive displacement meter. For calibration purposes a micrometer is used.

The valve rotates on special pivots, which are placed beside the culvert. The axis penetrates the side walls with a leakage of 1 mm around. The pivots are shown in fig. 3. The damping had to be as low as possible and had to be fully constant and independent of the water load. Therefore two knife edge supports with three springs are applied. Initially at each water velocity the test had to start with unscrewing the knives, and by centering the axis with the springs; then the knives were placed in touch with the axis and the back springs were given a constant extra force. Since practice shows that the knife supports are not sensitive to the spring loads, and so not sensitive to water load, constant spring tensions are used. To prevent additional damping the valve has no side seals.

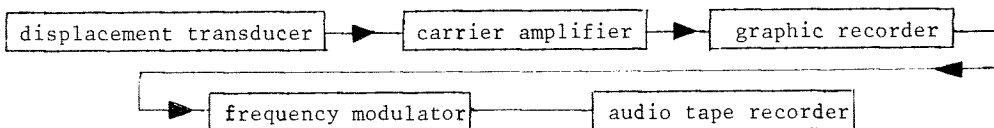
Outside the culvert two horizontal arms are attached to the axis, which are pulled down by extra springs. These serve for stretching the steel wires, to obtain maximum rigidity.

The position of the axis cannot be changed. To adjust the valve opening the valve is clamped on the axis.

The signal of the displacement meter is recorded on paper and on magnetic tape. The latter signal is used for spectrum analysis, and for the determination of the standard deviation. To separate the low frequency and the resonance vibration an electronic filter is used.

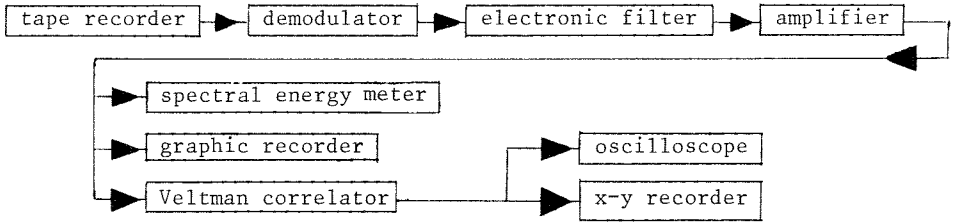
EQUIPMENT

Recording:



Appendix B

Analysis:



REMARKS:

The electronic filter is a band pass filter with variable frequencies. It can also be used as low pass filter which enables static calibration.

The Veltman correlator is an on-line computer for correlation functions and Fourier transforms, developed by the Technical University of Delft. The principle of the apparatus is described in [105].

RESULTS OF MEASUREMENTS WITH A VALVE OPENING $d/D = 0.3$

Valve loss coefficient

The valve loss coefficient is defined as $\xi_v = \Delta p / \frac{1}{2} \rho V^2$, where Δp is the difference in pressure measured in the culvert just upstream of the shaft and on about $10D (= 2.5 \text{ m})$ distance downstream of the valve.

$$\xi_v = 19.2$$

result I

An estimate can be made of the force in the pivot. This is in first order $\xi_v W D \frac{1}{2} \rho V^2$, but due to valve shape and valve position, and local effects at the top seal of the culvert the pivot force will be 10-15% higher (for $d/D = 0.3$).

Equivalent mass of water

The equivalent mass of water has been calculated with eq. (5) by comparing the frequencies recorded after a short blow, in dry and in submerged conditions:

$$c = 4\pi^2 m (N_{r_{\text{dry}}})^2 = 4\pi^2 (m + m_w) (N_{r_{\text{subm}}})^2 \quad (16)$$

The experiments have shown:

$$m_{\text{water}} / \rho D^2 W = 0.04$$

result II

This is independent of the resonance frequency (5-15 c/s) and the water velocity. The scatter in the results was rather great due to the fact

Appendix B

that m/m_w was about 10, so N_r varied only 5% by the water. But this also means that errors in m_w have no great effect on the vibration analysis.

Damping of the water

When $V = 0$, eq. (12) should be valid when viscosity has no effect.

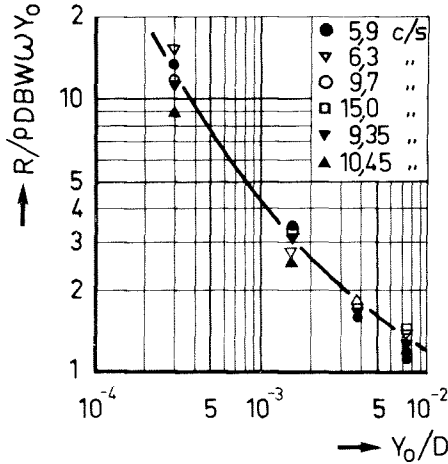


Fig. 4 Water damping with stagnant water

In fig. 4 is shown $R_w/\rho DW \omega Y_0$. This equals $4C_D A/3\pi DW$, and one would expect this value to be constant. From fig. 4 it is seen however that C_D depends on the vibration amplitude, but not on the vibration velocity ωY_0 . This means that the length of the vortex street induced by the vibration is the determining parameter, and also that the Reynolds number $\omega Y_0 D/\nu$ is of no importance. Similar results are known for the drag coefficient of strips and cylinders in sea waves or during oscillatory movements. Because with water velocity $V = 0$ viscosity can be neglected, its influence is still less probable at increasing water velocities. Even the possibility that viscosity has an effect on the excitation can now be considered small.

When $V > 0$, eq. (15) has been used for the presentation in fig. 5.

As was expected it has been found that for small amplitudes or for great water velocities the damping tends to be constant:

$$R_w/\rho VDW = 0.35$$

result III

For practical use this relation only is important, because vibration amplitudes due to flow are small. It is clearly shown that determination

Appendix B

of damping has to be done with the correct water velocity and with vibration amplitudes as small as possible.

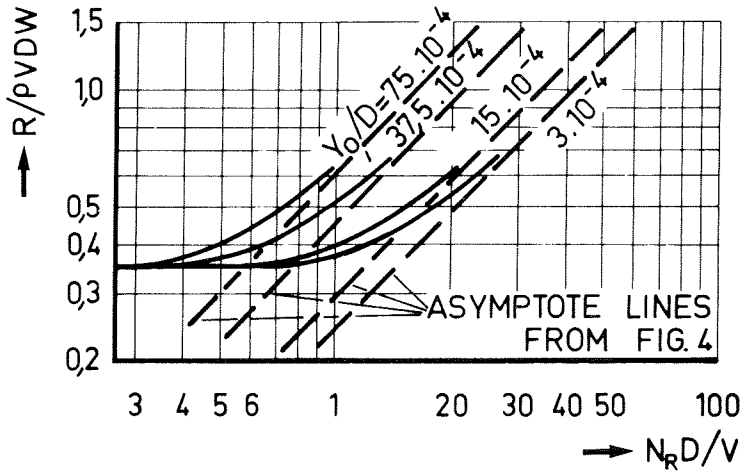


Fig. 5 Water damping with varied water velocities

Static force F_s

The downpull force due to the flow of the water only, is:

$$F_s / \rho V^2 W D = 0.315 \quad \text{result IV}$$

This value is independent of V , so the Reynolds number has no considerable effect.

Quasi static force F_{qs}

Some recordings have been analysed with the spectrum analyser, The duration of the recordings was 5-10 min.

The first impression of the recordings (fig. 6) was, that only two peaks are of importance, one being representative for the low frequency force and the other for the force in the resonance frequency; the separation frequency N_s has remained constant.

As the frequency of turbulence varies with V/D it was expected that $N_L D/V$ was constant, in which N_L is the main frequency of the quasi static force. It appeared however, that with V varying from 0.17 to 0.75 m/s a dominant frequency occurred of about 1 c/s. The probable explanation is that the free surface in the shaft together with the culvert and the downstream atmospheric pressure constituted a system of communicating vessels

Appendix B

with a dominant resonance frequency, which is excited by the flow turbulence.

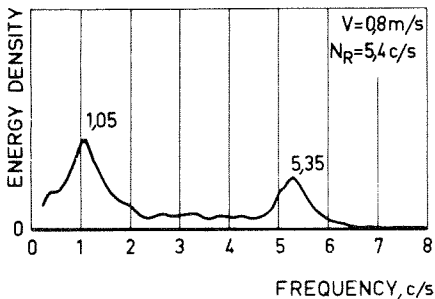


Fig. 6 Example of vibration spectrum

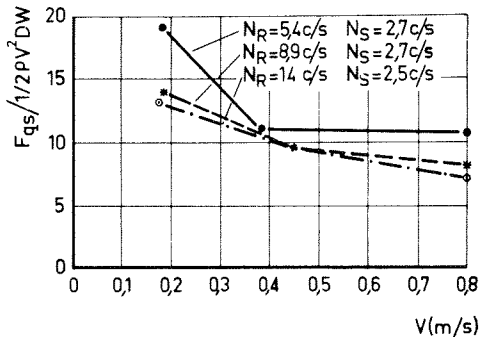


Fig. 7 Low frequency force, measured with constant separation frequency

By covering the shaft, a little under the free water level, with only a little leakage for passing the wires of the hoist and measuring system, the low frequency N_L varied as expected with the water velocity:

$$\frac{N_L D}{V} \sim 0.35 \text{ (scattering from 0.3 to 0.45)} \quad \boxed{\text{result V}}$$

For low water velocity N_L has been measured somewhat too high because the under limit of the spectrum analyser is 0.1 c/s. while with $V = 0.2$ m/s $N_L \sim 0.25$ c/s. A cut-off of lower frequencies gives a too high reading for N .

The amplitude of the quasi static force is represented in fig. 7. result VI

As is seen $F_{qs} / \frac{1}{2} \rho D W V^2$ varies with the water velocity. This can have two reasons: a. The turbulence of the upstream valve is relatively higher at low velocity since pressure upstream of this valve was constant for all discharges.

b. The separation frequency N_s had been kept constant, instead of $N_s D/V$.

To check b. the value of N_s has been varied for one test. The results are shown in fig. 8. Also the results of fig. 7 are plotted against $N_s D/V$ in this graph.

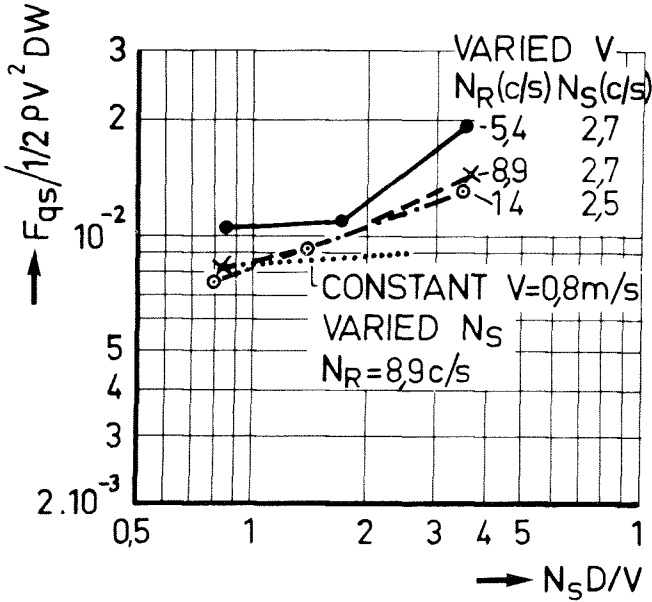


Fig. 8 Results of fig. 7 compared with tests with varied separation frequency

It appears that $F_{qs} / \frac{1}{2} \rho D W V^2$ is not uniquely dependent on $N_s D / V$ since especially the measurements with $V = 0.18$ m/s give high amplitudes. The explanation of this will be studied further; with vibrations of such small amplitudes (for $V = 0.18$ m/s Y_L is between 0.5 and 2 μ m) the background noise and the excitation caused by the leaking water at the pivot can be relatively important.

The quasi static force is nearly independent of the resonance frequency and independent of the mechanical damping as was expected from eq.(9).

Dynamic force F_d

Tests have been done with three resonance frequencies, and varied dampers.

N_r	$m + m_w$	c	γ	
			($V \sim 0.2$ m/s)	($V \sim 0.8$ m/s)
5.38 c/s	10.7 kg	12200 Nm^{-1}	0.01 -0.045	0.029-0.051
8.9 c/s	4.15 kg	13000 Nm^{-1}	0.017-0.041	0.045-0.069
14 c/s	4.15 kg	32100 Nm^{-1}	0.012-0.027	0.028-0.048

The damping has been varied by fixing disks to the hoist spring, which

Appendix B

are damped in an oil bath. It appeared that F_d varies with $\gamma^{-\frac{1}{2}}$, a relation which is connected to random, non periodic, excitation. This means also that the vibration does not effect the turbulence, because then a periodicity would have been introduced. So the factor Y/D in eq. (7) has no effect.

The amplitude of the dynamic force, with constant N_s of 2.7 c/s is presented in fig. 9. result VII

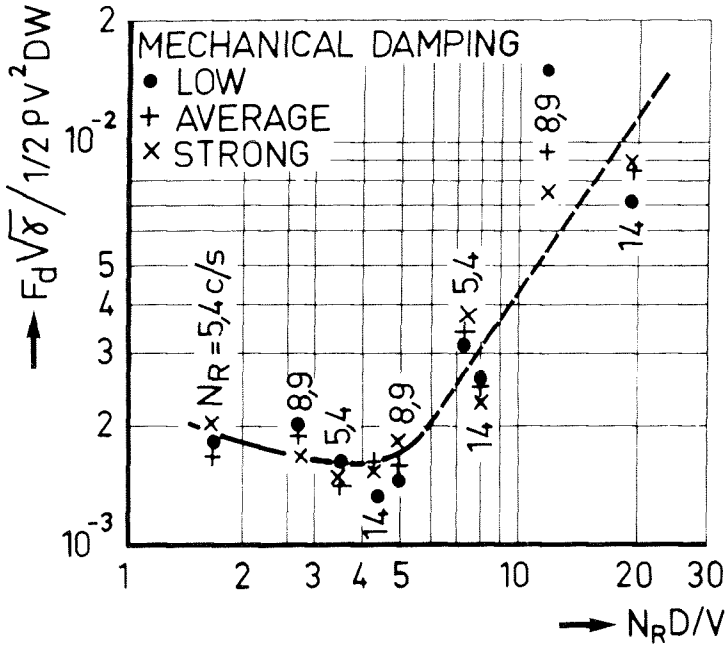


Fig. 9 Dynamic force; varied water velocities, mechanical dampings and resonance frequencies.

It is seen that, except for low discharge, a simple relation exists between $F_d \sqrt{\gamma} / 1/2 \rho V^2 D W$ and $N_r D / V$. Only a small influence of the separation frequency N_s has been found, but for future measurements it has been decided to take for the F_{dyn} the separation frequency $N_s = \frac{1}{2} N_r$. The quasi static force will then be determined with as well $N_s = \frac{1}{2} N_r$ as with $N_s D / V$ being about 2 times $N_r D / V$. The fact that N_s has been kept constant should theoretically give a too low amplitude for tests with low resonance frequencies; some tests indicated that a variation of 20% can be expected when N_r varies between 5 and 15 c/s.

Again there has been found a relative increase in amplitude for high

Appendix B

values of $N_r D/V$, being the measurements with low water velocities. As is stated previously measurements with low discharges can easily be disturbed; this will be studied further.

CONCLUSIONS

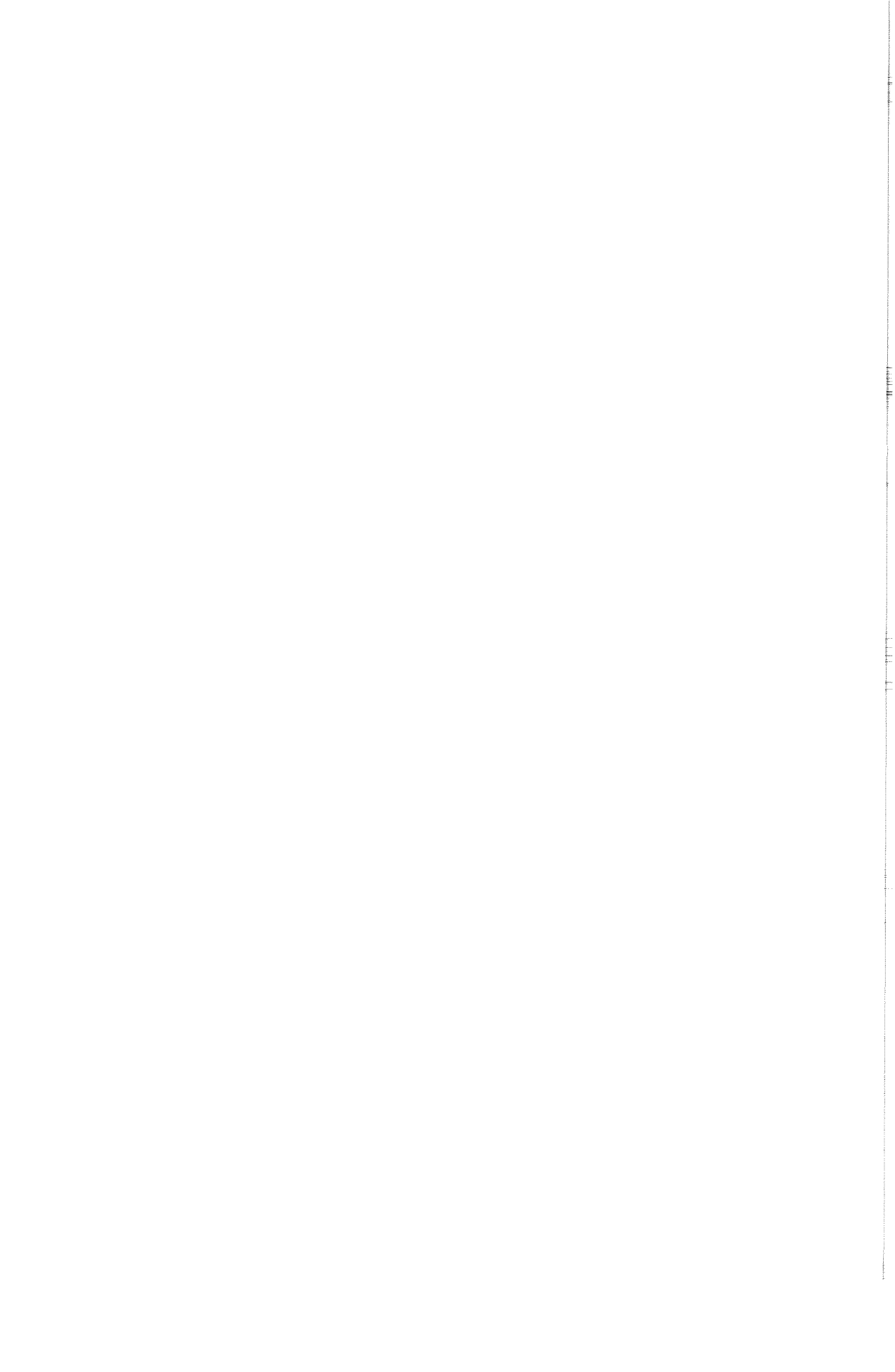
In this stage where the research program is still in progress some conclusions can already be drawn:

- a. For a valve with girders with well defined stream separations (sharp edges) the influence of water viscosity on damping and most probably on excitation by the flow is of no importance.
- b. The parameter $N_r D/V$ is a dominant factor for the vibration amplitude.
- c. The static and low frequency force is independent of the resonance frequency and the mechanical damping. $F_{qs} / \frac{1}{2} \rho V^2 WD$ was expected to be a constant, but with low discharge and a low resonance frequency this term tends to increase. It has to be studied if low discharge measurements have been disturbed by imperfections of the test installation.
- d. The water damping, as far as it is important for the vibration, is proportional to the water velocity. When measured at higher amplitudes a greater damping value, with non linear character, will be found.
- e. Separation of low frequency and resonance vibration is useful, because the effect of mechanical damping can be studied more easily, and in the design its effect can be taken into account. But the separation frequency has always some influence on the results.
- f. For the dynamic force it has been found that $F_d :: \gamma^{-\frac{1}{2}}$, which means that resonance vibration occurs only due to random excitation and there is no feed back of vibration on turbulence. The term $F_d \sqrt{\gamma} / \frac{1}{2} \rho V^2 WD$ can be expressed as a function of $N_r D/V$.
- g. When no feed back exists between vibration and flow excitation, measurements of forces combined with a spectrum analysis should be sufficient to predict the vibration amplitudes.

Appendix B

NOTATION

A	= Area of valve perpendicular to direction of vibration (m^2)	V_t	= Water velocity in tangent direction (ms^{-1})
C_D	= Drag coefficient	W	= Culvert width (m)
D	= Culvert height (m)	Y_o	= Single amplitude of vibration (m)
F	= External force (Newton = N)	c	= Spring rigidity (Nm^{-1})
F_d	= Internal dynamic force in resonance frequency (N)	d	= Raise of the valve (m)
F_{qs}	= Internal low frequency force (N)	f	= Resistance force due to flow (N)
F_s	= Internal permanent force due to the flow (N)	m	= Mass of valve (kg)
F_T	= Total dynamic force (N)	m_w	= Equivalent mass of water (kg)
N_L	= Frequency of low frequency excitation (cs^{-1})	t	= Time (s)
N_r	= Resonance frequency (cs^{-1})	y	= Displacement, static and dynamic
N_s	= Separation frequency (cs^{-1})	γ	= Ratio damping/critical damping
R	= Damping factor for mechanical damping (Nsm^{-1})	ν	= Kinematic viscosity of water ($m^2 s^{-1}$)
R_w	= Damping factor for water damping (Nsm^{-1})	ω	= Angular frequency of vibration ($rad s^{-1}$)
V	= Average water velocity in culvert (ms^{-1})	ρ	= Density of the water ($kg m^{-3}$)
		ξ_v	= Valve loss coefficient



Appendix C

Models with elastic similarity for the investigation of hydraulic structures*

The development of elastic similarity models for hydraulic structures was greatly stimulated by the Delta Works and the Rhine canalization, projects which required large control gates that would occasionally be subject to extreme dynamic loads resulting from wave attack and sustained turbulence. Economic considerations demanded design along new principles. The Delft Hydraulics Laboratory was entrusted with the study of the problems of safety of the new type of constructions, particularly the vibration caused by long-lasting flow and the resistance against the impact of waves.

The application of elastic similarity models is not a new one, as even before 1940 the resonance frequency determination on plastic models of machine parts was known. As the ratios of specific weight and modulus of the elasticity of steel and plastic are known, it was possible to calculate the conversion scale for frequencies. Models are also being used for flutter investigation in wind tunnels, but in these cases the same materials are used as for the prototype. A good reproduction of static and dynamic behaviour is obtained if the wind velocities are the same as in the prototype. This subject will be dealt with later in this article.

* Lecture held for a Symposium on Models and Reproduction Laws, organized by the Section of Mechanical Engineering and Naval Architecture of the Royal Institute of Engineers, January 18 and 19, 1966, in Eindhoven, Holland. Published in De Ingenieur, January 27, 1967, Section W 9.

Appendix C

In hydraulic models with a free water surface, the length scale determines the velocity scale. The flow velocities in the model are lower because the water level variations, and therefore the pressure variations, are smaller. From this there arises the necessity of selecting different model materials in elastic models.

The model technique set forth here was developed in co-operation with Ir. F.K. Ligtenberg, now Director of the TNO Institute for Building Materials and Constructions.

The applicability of this technique can best be demonstrated by an enumeration of the problems that will arise before a numerical approach can be tried: In the calculation of the response of a construction on an external dynamic load, not only must its elasticity and mass be taken into account, but also the additional mass effect of the water. The magnitude and distribution of the apparent mass increase is dependent on the vibration frequency, amplitude, etc. Also the damping effect of the structure and the energy absorption by the water must be known. In the case of vibrations connected with the instability of the flow pattern, movements of the structure may influence the load thereon so that there exists an interaction between load and movement.

All these factors mean that many data must be known: the mechanical properties of the structure; the load as a function of its point of attack and time and the degree of its interaction with movements of the structure; and the vibrating water mass and the damping effect of the water. Simple vibration calculations of complex structures being already laborious, a complete solution without the use of an elastic model is quite impossible.

For the sake of a systematic approach, the hydraulic reproduction laws and the reproduction laws for elastic models are separately deduced, and afterwards combined.

HYDRAULIC REPRODUCTION LAWS

For complete reproduction in a model of the flow pattern in the prototype, it is necessary that in a similar situation the internal and external forces that act on an elementary water particle keep operating in the same proportion.

In the equation of the dynamic equilibrium of an elementary water particle, the following terms occur:

Appendix C

I. Acceleration

$$\rho \frac{\partial v_x}{\partial t} + \rho \left(v_x \frac{\partial v_x}{\partial x} + v_y \frac{\partial v_x}{\partial y} + v_z \frac{\partial v_x}{\partial z} \right), \text{ etc.}$$

ρ = liquid density

v = velocity component

x, y and z = co-ordinates

t = time

II. Pressure

$$\frac{\partial P}{\partial x} \text{ etc., wherein } P = p + \rho gh$$

p = local pressure

g = gravity

h = height with respect to a reference level

III. Viscous shear-stress

$$k_x = \frac{\partial \tau_x}{\partial y} + \frac{\partial \tau_x}{\partial z}, \text{ etc.}$$

which corresponds with:

$$\rho \nu \left(\frac{\partial^2 v_x}{\partial x^2} + \frac{\partial^2 v_x}{\partial y^2} + \frac{\partial^2 v_x}{\partial z^2} \right), \text{ etc.}$$

τ_x = shear tension in x direction, etc.

ν = kinematic viscosity of liquid.

IV. Free liquid surface

At the surface is $p = p_{\text{atm.}}$ (= constant)

$$\frac{\partial P}{\partial x} = \rho g \frac{\partial h}{\partial x}$$

V. Surface tension

$$(p_{\text{gas}} - p_{\text{liq}}) = \pm \sigma \left(\frac{1}{R_1} + \frac{1}{R_2} \right)$$

σ = surface tension

R_1 and R_2 = radius of curvature of the surface in two directions.

Appendix C

If all the length dimensions are reduced by a factor n_L , it is possible to deduce the reproduction factors by the introduction of invariance in the relation of terms enumerated above.

- a. From I follows: $n_t = n_L/n_v$
b. From II/I follows: $n_p = n_\rho n_v^2$
c. From III/I follows: $n_v n_L/n_v = 1$

The Reynolds number ($Re = v L/\nu$) is invariant.

- d. From IV/I follows: $n_v^2/n_g n_L = 1$

The Froude number ($Fr = v^2/gL$) is invariant.

- e. From V follows: $n_p = n_\sigma/n_L$
and from V/b: $n_\rho n_L n_v^2/n_\sigma = 1$

The Weber number ($We = \frac{\rho L v^2}{\sigma}$) is invariant.

The variance of the Reynolds, Froude and Weber numbers provides the conditions for the velocity scale, from which the pressure and time scales can be deduced by means of the relations a. and b. If the gas or liquid used in the model is the same as in the prototype, the conditions for the velocity scale are always contradictory, because in such a case there would be the relation: $n_\rho = n_v = n_\sigma = n_g = 1$. This would mean that in a 1:20 model the flow velocity according to Reynolds must be 20 times faster than in the prototype, according to Froude $\sqrt{20}$ times slower, and according to Weber $\sqrt{20}$ times faster. The choice will depend on the purpose of the investigation.

Because of the wave action and the turbulence of the sea and rivers and because hydraulic structures are seldom perfectly streamlined, the water particles are always in strongly accelerated or decelerated motion. It turns out that viscosity and surface tension play a minor role compared to the forces of acceleration and gravity (i.e., Re and We are very great). Even during constant flow in wide pipes or in concrete irrigation ditches, the turbulence caused by surface roughness turns out to be so great that the influence of viscosity is comparatively small.

These considerations lead to a certain liberty to depart from the correct magnitude of Re in the model, provided this magnitude is still sufficiently great. Literature provides adequate information on this subject.

Appendix C

In the laboratory, of course, certain inaccuracies in models are accepted for practical reasons.

From the foregoing it follows that in a model without free liquid surface the velocity scale may be freely chosen, if only Re does not drop below a critical minimum. If there is free liquid surface, the invariance of Fr will determine the velocity scale.

We and Re magnitudes that are too small may be corrected in a free surface model by increasing the vertical scale, and by the use of a wire to promote boundary layer turbulence. It will be clear, however, that both methods endanger the conformity of the flow pattern.

ELASTIC PROPERTIES OF MODELS

For a simple mass-spring system the ultimate vibration amplitude resulting from periodic excitation is depicted in the graph of fig. 1, the shape of which is dependent only on the damping effect.

- c = elasticity of the spring K = force
- m = mass ω = angular frequency of excitation
- A = amplitude ω_r = resonance frequency

For reproduction in a hydraulic model, it is necessary that n_A = n_L, from which follows:

$$n_c n_L / n_K = 1 \tag{1}$$

Also, the scale of ω_r must be equal to the scale of the excitation frequency (for example, the wave or turbulence frequency), i.e.:

$$n_\omega / n_{\omega_r} = 1 \tag{2}$$

The relative damping effect γ (= damping effect/critical damping effect) must be the same in the prototype and in the model:

$$n_\gamma = 1 \tag{3}$$

The conditions (1) and (2) determine the mass scale:

$$n_m = n_c / n_{\omega_r}^2 = n_K / n_L n_{\omega_r}^2 \tag{4}$$

Because of the apparent mass increase of a structure vibrating in liquid, this condition must be satisfied by the scale of the model mass together with the additional water mass.

For elastical models of composite structures the condition (1) can be replaced by:

Appendix C

$$n_\epsilon = n_\sigma / n_E = n_K / n_L^2 n_E = 1 \quad (5)$$

ϵ = relative deformation

E = elasticity modulus

σ = material stress

For shear stress there is obtained the analogous formula:

$$n_K / n_L^2 n_G = 1 \quad (5a)$$

From the combination of (5) and (5a) there follows: $n_G = n_E$. This condition is mostly automatically fulfilled.

COMBINATION FOR FLOW WITHOUT FREE LIQUID SURFACE

For the flow conditions it is found that $n_p = n_\rho n_v^2$, because any force can be expressed as a pressure multiplied by an area:

$$n_K = n_p n_L^2 = n_\rho n_L^2 n_v^2 \quad (6)$$

The elasticity of an elastic model follows from (1):

$$n_c n_L / n_K = n_c n_L / n_\rho n_L^2 n_v^2 = n_c / n_\rho n_L n_v^2 = 1 \quad (7)$$

which means that the Cauchy number ($Ca = \frac{c}{\rho L v^2}$) is invariant.

For the frequency of excitation by flow or waves it has been found that $n_t = n_L / n_v$, or expressed otherwise $n_\omega = n_v / n_L$.

Combining this with (2), the resonance frequency of the model is obtained:

$$n_L n_\omega / n_v = 1 \quad (8)$$

which means that the reduced natural frequency ($\frac{\omega_r L}{v}$) is invariant.

For the mass scale it is found from (4), (6) and (8) that

$$n_m / n_\rho n_L^3 = 1 \quad (9)$$

It could, therefore, be said that the "mass number" ($\frac{m}{\rho L^3}$) is invariant.

According to (9) the total mass, i.e., $m_{\text{struct.}} + m_{\text{water}}$, must be, so to say, geometrically reduced while preserving the same density in relation to the surrounding liquid. This condition is already satisfied by the vibrating water mass, so that it is only necessary to take care that $m_{\text{struct.}}$ complies with it.

A correct reproduction of vibration phenomena in mass-spring systems can thus be obtained in a model, for any velocity, by adaptation of the

Appendix C

elasticity; the model mass being independent of velocity.

For complex structures and the use of the same liquid, the model is preferably made of the same materials as the prototype, in which case it has the correct mass for all vibration phenomena. If $n_E = n_\rho = 1$, it follows now from (5) and (6) that

$$n_\epsilon = n_K/n_L^2 n_E = n_\rho n_L^2 n_V^2/n_L^2 n_E = n_V^2 = 1 \quad (10)$$

This means that the flow velocity in the model must be the same as in the prototype. As already mentioned, this is done in wind tunnel investigation of flutter of aircraft wings, whereby also the correct Mach number is achieved. This results from the fact that materials and air keep the same deformability, which leads to the same reproduction laws.

COMBINATION FOR FLOW WITH FREE LIQUID SURFACE

The invariance of the Froude number is now introduced as an additional condition, which results in:

$$n_V = (n_g n_L)^{\frac{1}{2}} \quad (11)$$

The elasticity of a model of a mass-spring system follows from the invariance of the Cauchy number.

For composite structures there can be deduced from (5) and (6) that

$$n_\epsilon = n_K/n_L^2 n_E = n_\rho n_L^2 n_V^2/n_L^2 n_E = 1, \text{ resulting in:} \\ n_L/n_E = 1 \quad (12)$$

The condition $n_{\rho;\text{struct.}} = n_\rho = 1$ must also be satisfied. For acceptable model scales no material exists that satisfies these conditions. But as the elasticity of composite structures is directly proportional to plate thickness (except for the local bending resistance of plates and solid beams), the rigidity of the model can be adjusted at the cost of some sacrifice of geometry.

For practical reasons it is preferred to use a model material whose E is too low, in order to be able to increase the plate thickness. Thus far, plastic models have been used with a value of $n_E \approx 60$ in relation to the steel prototype. According to (11) this would require a value of $n_L = 60$, but such a value would mean that the models became too small with regard to the permissible value of the Reynolds number. For the model of the Hagestein visor gates (in the Netherlands) a value of

Appendix C

$n_L = 20$ was used, so that E was a factor 3 too low. This was compensated by increasing the plate thickness by factor 3. As the plastic material used (Trovidur) is $5\frac{1}{2}$ times lighter than steel, the model mass was still too low, and so small lead ballast weights were used to compensate the lack of mass without affecting the rigidity. Their distribution was approximately proportional to the local mass deficiency.

The damping condition $n_\gamma = 1$ (3) remains valid, of course, under all circumstances. It is possible in a geometric model made of the same materials as the prototype that γ has the same value, as γ is to a high degree a material constant. For sliding members, hinges, rubber seals, etc. the damping effect is not automatically reproduced on the right scale. In the case of damping by liquid, scale effects are also to be expected. Damping by drag forces on beams, etc. in turbulent flow, however, will be to scale, but not if viscosity is the dominant factor as, for example, in the case of a plate which vibrates in its own plane. Often it is necessary to consider separately the damping effect of hinges, etc. and also to investigate whether or not the liquid damping is to scale.

In the case of resonance, the equilibrium amplitude is determined by the degree of damping. In general, however, the occurrence of resonance will necessitate a change of design to suppress it. If the degree of damping in a model is low enough, preferably lower than in the prototype, model tests will give a useful indication of the possible occurrence of resonance.

If there is no resonance, damping is still a matter of consequence, as the response to a periodic excitation by a turbulent flow pattern can include components of resonance frequency (see fig. 10). Their influence will, however, be smaller than that of resonance frequency vibrations.

Damping is of minor importance for the response to impact, as the maximum amplitude will occur shortly after the impact, before a substantial dissipation of energy can take place.

In plastic models the degree of damping is too great. On the other hand, verification measurements on the Hagestein visor gates showed that friction effects dominated damping effects to such an extent that the model as a whole often had less damping than the prototype.

Deformation in elastic similarity models can be directly measured by means of strain gauges. As $n_\epsilon = 1$, the right prototype strain value is

Appendix C

immediately obtained therefrom. If the material is relatively thin, glue and seals will influence the elasticity to such a degree that strain gauges can be employed only to a limited extent.

MODEL RESEARCH AND VERIFICATION MEASUREMENT ON THE HAGESTEIN VISOR GATES

The gates serve to regulate the level and flow rate in the lower Rhine. As they must be capable of operating for months on end in their regulating positions, it is a prime requirement that no resonance vibration will occur. The gate design was of a new type, characterized by a light, non-rigid, semi-circular construction (see figs. 2 and 3).

Briefly, the model research included the following phases:

- a. Determination of vibration patterns and resonance frequencies (fig. 4) by means of an elastic similarity model. Because of the non-rigidity of the construction in horizontal directions, the lowest resonance frequency was very low: in dry condition 1.3 c/sec and submerged 0.6 c/sec.
- b. Measurement of the pressure fluctuations in a rigid model of a section of the gate. All the pressure fluctuations had frequencies between 0 and 10 Herz, so that some vibration has always to be expected. Variations in the shape of the lower edge of the model had little influence.
- c. Testing of the lower edge. A spring-suspended model (scale 1:6) of a gate section was examined for the occurrence of resonance vibrations during horizontal and vertical motion and at several resonance frequencies. Resonance vibrations did not occur at the chosen profile of the edge.
- d. Measurements on the elastic similarity model. Perforation of the base reinforcement rib gave an appreciable reduction of vertical vibrations. Systematic measurements at different vertical positions of the gate and at different water levels showed no important vibration amplitudes; the amplitude in horizontal direction was 7 mm, and in vertical direction 1.7 mm.
- e. Comparison of the flow-induced vibrations in the model of c. and in a similar 1:20 model thereof. The water-damping in these models was also compared.

As the results of d. showed a wide safety margin and the tests of e. did not give rise to the expectation of important scale effects, the

Appendix C

construction was considered to be sufficiently safe. In practice it turned out that under special conditions some resonance occurred in certain parts of the plating, but this could be redressed by a slight change in the position of the gate. This resonance in the plating did not become obvious in the model because of its greater plate thickness and the resulting too great rigidity.

Verification measurements:

To test the model technique, measurements were executed on the prototype by the TNO Institute for Mechanical Constructions, while the gate model was mounted once more so as to be able to reproduce those measurements under all conditions. The elasticity of the rubber side seal was separately tested under dynamic load. This elasticity was reproduced in the model.

As the cables were not yet mounted during the dry excitation tests, the gate was temporarily suspended by means of strips (see fig. 5). For verification purposes this was useful, as the elasticity of the cables would have so dominated all measurements that no reliable comparison could be made of the gate elasticity in prototype and model.

The graphs of figs. 7 and 8 show a comparison of the responses of prototype and model to periodic excitation in tangential and radial horizontal directions. The similarity of resonance frequencies in dry and in submerged condition is satisfactory. The amplification of amplitude at resonance frequencies in the model was mostly greater than in the prototype. The influence of water on the resonance frequencies was also satisfactorily reproduced.

Fig. 9 shows similar results for vertical excitation. Too great rigidity of the model, a result of its highly schematized construction, resulted in a shift of the resonance to a higher frequency. This shift was reasonably predictable. Remarkable was the great water-damping in the prototype; during the prototype measurements a high-frequency vibration was observed in the plating, and this vibration probably absorbed much energy.

In fig. 10 vibration recordings are shown of prototype and model, both cable-suspended, during (simulated) operation conditions. The similarity was again satisfactory.

The tests have demonstrated that the model technique is a reliable tool if the difficulties of too great material damping are taken into

Appendix C

account from the beginning, and if much attention is given to such details as the elasticity of and damping in rubber seals, friction and damping in hinges, elasticity of cables, etc.

FURTHER APPLICATION OF ELASTIC SIMILARITY MODELS

After the research on the Hagestein gates, elastic similarity model investigation was applied to several other gates and valves. Often a highly simplified model could be used, when hoist elasticity was a dominant factor. The model was then designed as a simple mass-spring system as, for instance, in the case of the culvert valve for the great lock at Terneuzen (fig. 11).

Fig. 12 shows successive stages of the lowering of tubular steel stop logs to be used as emergency bulkhead in a lock. Their dancing and vigorously vibrating movement was predicted by an elastic similarity model, so that a better solution could be found.

Also for an investigation of the response to wave impact of the Haringvliet tainter gates an elastic similarity model was used. Apart from some models that were executed as simple mass-spring systems for measurement of the forces required to raise the gates in current and waves, an elastic similarity model of one entire span with its two tainter gates was constructed (fig. 13). The elastic properties of the concrete bridge, as well as those of the steel gates, were reproduced in the plastic model. Care was taken that the rigidity of the plating was also correctly reproduced, so that it was possible to determine exactly how the structure would respond to wave impact. The thickness of the material was sufficient to permit the use of strain gauges. With the aid of wind-generated waves in the model, the statistical distribution of stress could be correlated to the statistical distribution of wave heights.

The results of the model tests could be verified in certain aspects by measurements made in an electrical analogon model.

Appendix C

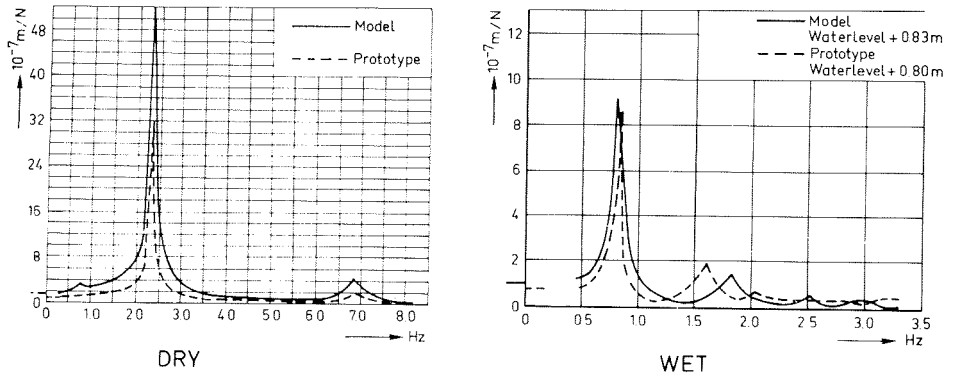


Fig. 8 Response characteristics of prototype and model subjected to horizontal radial excitation.

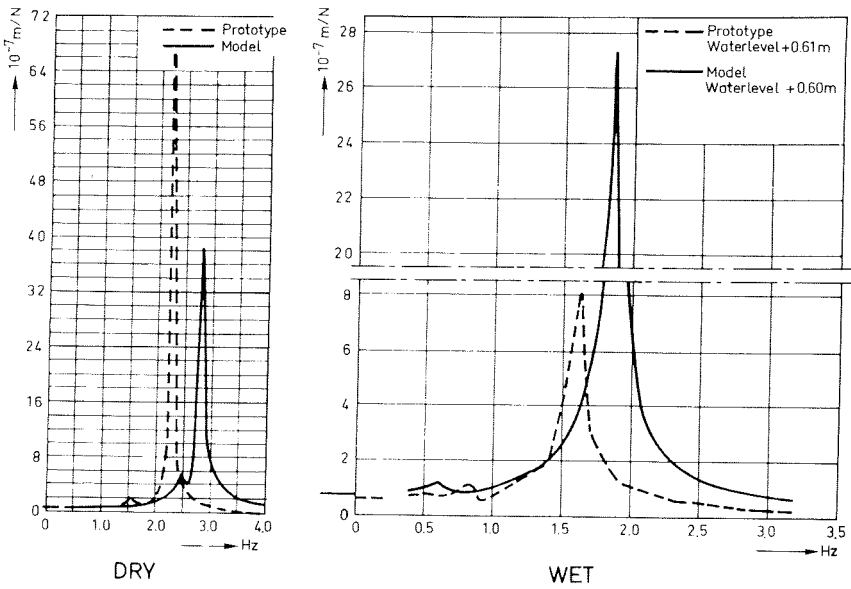


Fig. 9 Response characteristics of prototype and model subjected to vertical excitation.

Appendix C

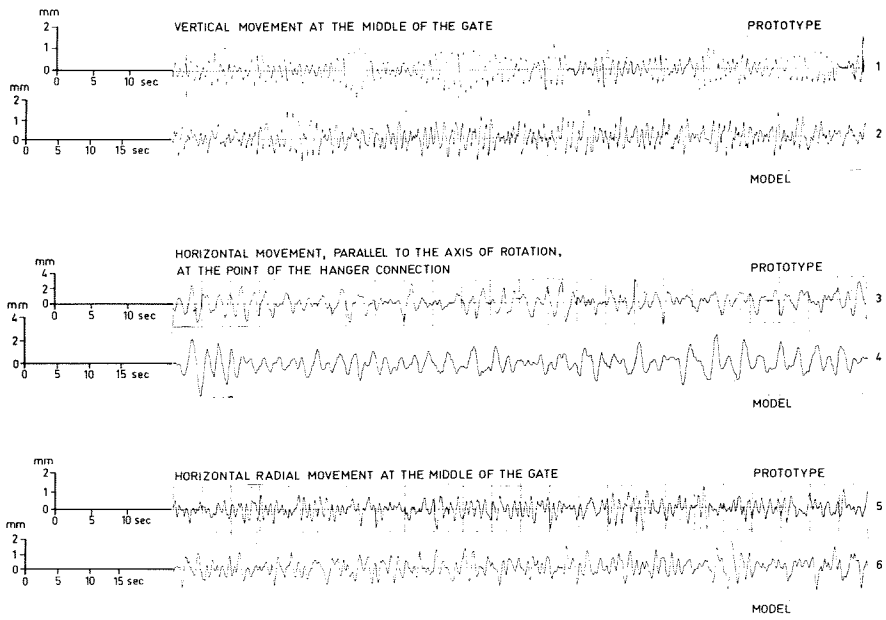


Fig. 10 Recorded vibration in prototype and model under flow conditions.

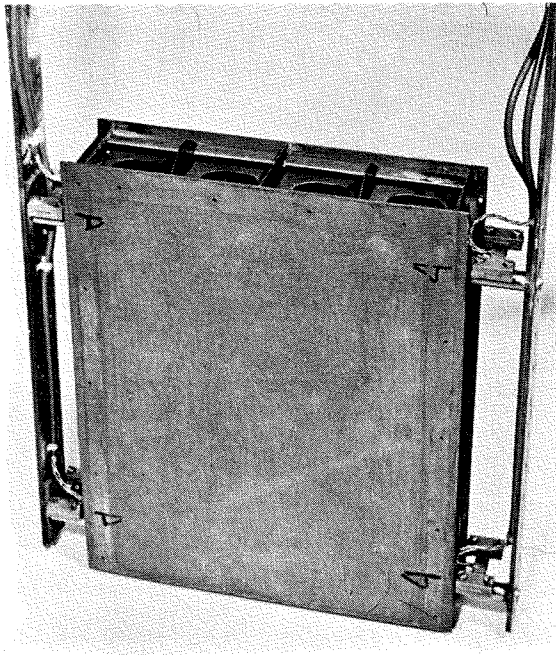
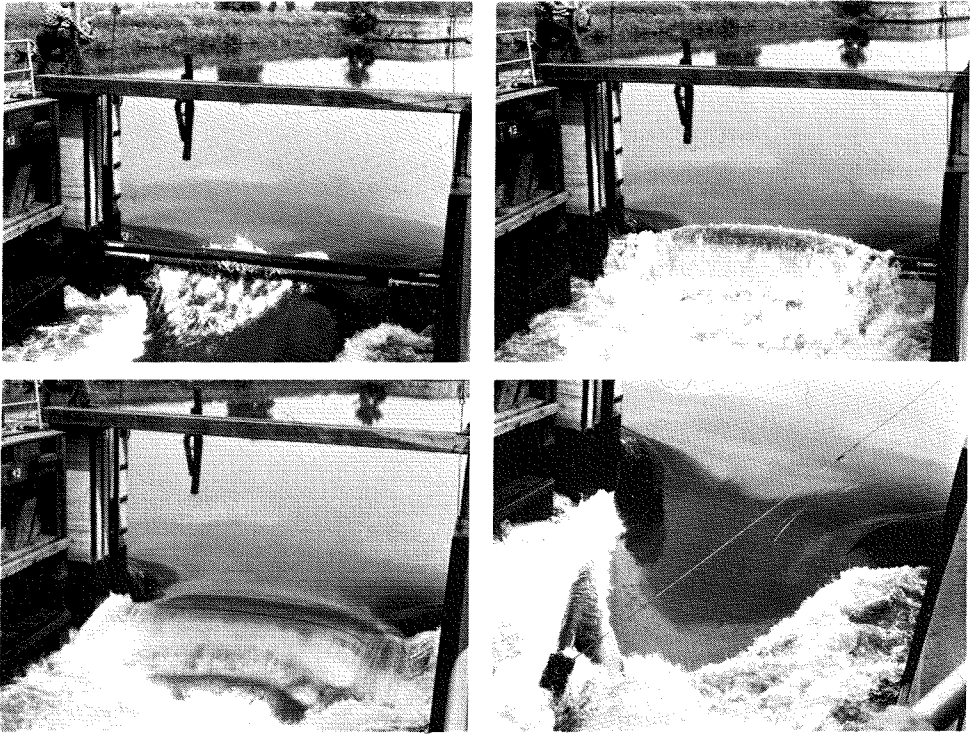


Fig. 11. Model of a culvert valve for the great lock at Terneuzen, executed as a simple mass-spring system.



Figs. 12 a-d Lowering of tubular stop logs in stream entering a lock-chamber



Fig. 13 Elastic similarity model of box girder and one of the tainter gates of the Haringvliet sluices.

References

- 1 ABELEV, A.S., "Investigations of the Total Pulsating Hydrodynamic Load acting on Bottom Outlet Sliding Gates and its Scale Modelling", 8th congress of the Int. Ass. of Hydraulic Research, Montreal 1959, paper A.10.
- 2 ABELEV, A.S., "Etude de la pulsation des charges hydrodynamiques globales s'exerçant sur des vannes d'étranglement", Traduction 1152 Centre de Recherches et d'Essais de Chatou, E.D.F.; orig: Izvestia Guidrotekniki, Vol. 69, 1962, pp. 21 - 24.
- 3 ABELEV, A.S., "Pulsations of Hydrodynamic Loads acting on Bottom Gates of Hydraulic Structures and their Calculation Methods", 10th congress of the Int. Ass. of Hydraulic Research, London 1963, paper 3.21.
- 4 ABELEV, A.S., DOLNIKOV, L.L., "Experimental Investigations of Self-Excited Vibrations of Submerged Vertical-Lift Hydraulic Gates", I.U.T.A.M./I.A.H.R. Symp. on Flow-Induced Vibrations, Karlsruhe 1972, see [68] pp. 265 - 277.
- 5 ABLES, J.H., MURPHY, T.E., "Culvert Taintor Valves, New Lock no. 19, Mississippi River", Techn. Rep. 2-537, June 1961 U.S. Army Eng. Waterways Exp. Stat., Corps of Engineers.
- 6 ABRAMSON, H.N., "Hydrofoil flutter: some recent developments", I.U.T.A.M./I.A.H.R. Symp. on Flow-Induced Vibrations, Karlsruhe 1972, see [68] pp. 640 - 649.
- 7 ALLERSMA, E., "The Virtual Mass of a Submerged Sluice Gate", 8th congress of the Int. Ass. of Hydraulic Research, Montreal 1959, paper A.23, also published as Delft Hydraulics Laboratory publ. no. 18.
- 8 ASHLEY, H., "Aeroelasticity", Appl. Mech. Review, 1970 no. 2, Febr. pp. 119 - 129.
- 9 BAVINK, H., GRASMAN, J., "Relaxatietrillingen", publ. Mathematisch Centrum, Amsterdam 1969.
- 10 BECKER, E., "Das Wellenbild einer unter der Oberfläche eines Stromes schwerer Flüssigkeit pulsierenden Quelle", Zeitschr. für Angew. Math. u. Mech. 38, 1958 Heft 9/10 pp. 391 - 399.
- 11 BERGH, H., "Het meten van luchtkrachten op trillende vleugels", De Ingenieur, 7 juni 1957, no. 23, L7.

References

- 12 BERKHOFF, J., "Trilling van Sluisdeuren", internal Delft Hydr. Lab. report which will appear later in the series W 254.
- 13 BIESEL, F., SUQUET, F., "Les appareils générateurs de houle en laboratoire", Ed. La Houille Blanche, Grenoble.
- 14 BINNIE, A.M., "The Stability of a Falling Sheet of Water", Proc. Royal Soc. of London, Series A, 326, Jan. 1972.
- 15 BIRKHOFF, G., "Hydrodynamics, a study in Logic, Fact and Similitude", Princeton Univ. Press, 1960.
- 16 CREMER, L., ISING, H., "Selbsterregte Schwingungen von Überfallstrahlen", Acoustica, no. 2, pp. 94 - 107.
- 17 DELANY, N.K., SORENSEN, N., "Low Speed Drag of Cylinders of various Shapes", Naca techn. note 3038.
- 18 Delft Hydraulics Laboratory report M 561^A, "Trillingsonderzoek vizerschuiven Stuw Hagestein; schaalproeven".
- 19 Delft Hydraulics Laboratory report M 561^B, "Trillingsonderzoek vizerschuiven Stuw Hagestein; onderrandproeven".
- 20 Delft Hydraulics Laboratory report M 561^C, "Vizerschuiven Stuw Hagestein", ontwerp elastisch gelijkvormig model".
- 21 Delft Hydraulics Laboratory report M 620 I and II, "Trillen Stuw Haringvliet".
- 22 Delft Hydraulics Laboratory report M 667^{II}, an investigation on the culvert valves of the sea-vessel navigation lock at Terneuzen.
- 23 Delft Hydraulics Laboratory report M 780^{II}, "Shipping Locks Kainji Dam, Reversed Taintor Valves".
- 24 Delft Hydraulics Laboratory report M 865^{VI}, "Zoutbestrijding Kreekraksluizen, onderzoek rioolschuiven en woelbak".
- 25 Delft Hydraulics Laboratory report M 1129, "Inlaatsluis Volkerak, modelonderzoek elastisch gelijkvormig model".
- 26 Delft Hydraulics Laboratory report S 50/M 583, "Nota, onderzoek aan ronde schotbalken".
- 27 DEN HARTOG, J.P., "Mechanical Vibrations". McGraw Hill Book Co 1956.
- 28 DOUMA, J.H., "Field Experiments with Hydraulic Structures, I.U.T.A.M./I.A.H.R. Symp. on Flow-Induced Vibrations, Karlsruhe 1972, see [68] pp. 223 - 249.
- 29 FISCHER, H., "Die Beseitigung von Schwingungen an über- und unterströmten Wehren". Mitteilungen aus der Forschungsanstalten v. Gutehoffnungshütte Konzern, no. 5, 1937, p. 75.

References

- 30 FUNG, Y.C., "Fluctuating Lift and Drag on a Cylinder in a Flow at supercritical Reynolds Numbers", Inst. of Aerospace Sciences, Paper 60-6, presented as IAS 28th annual meeting, N.Y. Jan. 1960.
- 31 GAL, A., "Bestimmung der mitschwingenden Wassermassa bei überströmten Fischbauchklappen mit kreiszylindrischem Staubleck", Thesis of Univ. of Stuttgart, 1970.
- 32 GELEEDST, M., KOLKMAN, P.A., "Elastic Similarity of Models of Structures; Comparison of Measurements on the Prototype and the Elastically Similar Model of the Hagestein Weir", 10th congress of the Int. Ass. of Hydraulic Research, London 1963, paper 3.21.
- 33 GELEEDST, M., KOLKMAN, P.A., "Comparative Vibration Measurements on the Prototype and the Elastically Similar Model of the Hagestein Weir under Flow Conditions", 11th congress of the Int. Ass. of Hydraulic Research, Leningrad 1965, paper 4.7.
- 34 HARDING, D.A., "The Stability of a Relief Valve connected to a Long Pipe", 10th congress of the Int. Ass. of Hydraulic Research, London 1963, paper 3.18.
- 35 HARDWICK, J.D., "Flow-Induced Vibration of Vertical Lift Gate", Proc. of Am. Soc. of Civil Eng. Journ. of Hydr. Div., May 1974, HY 5, paper 10546.
- 36 HARRIS, C.M., CREDE, C.E. (editors), "Shock and Vibration Handbook", McGraw Hill Book Cy 1961.
- 37 HASZPRA, O., "Hydroelastic Experiments on a Stop-Log Model of a River Barrage", Symposium of the Int. Ass. of Hydraulic Research, Stockholm 1971, part 1, paper 15.
- 38 HASZPRA, O., Contribution to the discussion in section C of the I.U.T.A.M./I.A.H.R. Symposium on Flow-Induced Structural Vibrations, Karlsruhe 1972, publ. by Univ. of Karlsruhe, Inst. of Hydrodynamics.
- 39 HUNT, J.C., Contribution to the discussions of the I.U.T.A.M./I.A.H.R. Symposium on Flow-Induced Vibrations, Karlsruhe 1972, publ. by Univ. of Karlsruhe, Inst. of Hydrodynamics.
- 40 JONES, G.W., CINCOTTA, J.J., WALKER, R.W., "Aerodynamic Forces on Stationary and Oscillating Circular Cylinders at High Reynolds Numbers", NASA, TR-300, 1969.
- 41 VON KÁRMÁN, T., BIOT, M.A., "Mathematical Methods in Engineering", McGraw Hill Book Cy 1940.
- 42 KEIR, G., UNNY, T.E., HILL, H.M., "Pressure Fluctuations on Submerged Sluice Gate", Proc. of Am. Soc. of Civil Eng. Journ. of Hydr. Div., Nov. 1969, HY 6, paper 6875.
- 43 KING, R., PROSSER, M.J., "Criteria for Flow-Induced Oscillations of a Cantilevered Cylinder in Water", I.U.T.A.M./I.A.H.R. Symposium on Flow-Induced Structural Vibrations, Karlsruhe 1972, see [68] pp. 488 - 503.

References

- 44 KNAPP, R.T., DAILY, J.W., HAMMITT, F.G., "Cavitation", McGraw Hill Book Co 1970, Engng. Sc. Monographs, 578.
- 45 KOLKMAN, P.A., "Vibration Tests in a Model of a Weir with Elastic Similarity on Froude Scale", 8th congress of the Int. Ass. of Hydraulic Research, Montreal 1959, paper A.29.
- 46 KOLKMAN, P.A., "Analysis of Vibration Measurements on an Underflow Type of Gate", 10th congress of the Int. Ass. of Hydraulic Research, London 1963, paper 3.23, (Appendix B to this report).
- 47 KOLKMAN, P.A., "Vibrations des vannes en position partiellement montées du barrage de Hagestein", Soc. Hydrotechnique de France, VIII ieme Journées de l'Hydraulique, Lille 1964, Question III, rapport 9.
- 48 KOLKMAN, P.A., "Analysis of Vibration and Damping Measurements on a Reversed Taintor Valve", Symposium of the Int. Ass. of Hydraulic Research, Stockholm 1970, paper G.2.
- 49 KOLKMAN, P.A., Discussion on paper F.1, p. 149 of the Symposium of the Int. Ass. of Hydraulic Research, Stockholm 1970, in reaction on an intervention of Prof. E. Naudascher.
- 50 KOLKMAN, P.A., "Resonantiertellingen bij schuiven", Notitie "Hydraulica bij schutsluizen" no. 8, Jan. 1972 (Delft Techn. Univ., vakgroep Constructieve Waterbouwkunde), also: "Informatieblad" Delft Hydr. Lab.
- 51 KOLKMAN, P.A., "Methoden ter bepaling van de toegevoegde massa bij oscillerende beweging van voorwerpen in een vloeistof", Notitie "Hydraulica, Algemeen" no. 2, April 1971 (Delft Techn. Univ., vakgroep Constructieve Waterbouwkunde), also: "Informatieblad" Delft Hydr. Lab.
- 52 KORNECKI, A., "On the Character of Instability of certain Aeroelastic Systems", Transact. Am. Soc. of Mechanical Eng., June 1973, pp. 616/617.
- 53 KRUMMET, R., "Schwingungsverhalten von Verschlussorganen im Stahlwasserbau bei grossen Druckhöhen, insbesondere von Tiefschützen", Forsch. Ing.-Wes. 31 (1965) pp. 133 - 141.
- 54 LAMB, SIR HORACE, "Hydrodynamics", 6th ed. Cambridge Univ. Press, 1932.
- 55 LANGE, F., "On the Problem of Apparent Mass", Symposium of the Int. Ass. of Hydraulic Research, Stockholm 1970, paper E.3.
- 56 LIEBL, A., "High Pressure Sluice Gates", 11th Congrès des Grands Barrages, Madrid 1973, paper Q.41/R.42.
- 57 LYSENKO, P.E., CHEPAJKIN, G.A., "On Self-Excited Oscillations of Gate Seals", I.U.T.A.M./I.A.H.R. Symposium on Flow-Induced Structural Vibrations, Karlsruhe 1972, see [68] pp. 278 - 296.

References

- 58 MARTIN, W., NAUDASCHER, E., PADMANABHAN, M., "Fluid Dynamic Excitation involving Flow Instability", Proc. of Am. Soc. of Civil Eng. Journ. of Hydr. Div., HY 6, June 1975, paper 11361.
- 59 MINOR, H.E., "Beitrag zur Bestimmung der Schwingungsanfunktionsfunktion überströmter Stauklappen", Thesis Univ. of Stuttgart, 1972. Mitt. Inst. f. Wasserbau no. 24.
- 60 MÜLLER, O., "Schwingungsuntersuchungen an unterströmten Wehren", Mitt. Preuss. Versuchs Anst. f. Wasserb. u. Schiffbau, Heft 13, Berlin, 1933.
- 61 MÜLLER, O., "Schwingungsuntersuchungen an einem unterströmten Wehrmodell", Mitt. Preuss. Vers. Anst. f. Wasserbau, no. 31, Berlin, 1937.
- 62 MURPHY, T.E., "Model and Prototype Observations of Gate Oscillations", 10th congress of the Int. Ass. of Hydraulic Research, London 1963, paper 3.1.
- 63 NAUDASCHER, E., "Beitrag zur Untersuchung der schwingungserregenden Kräfte an gleichzeitig über- und unterströmten Wehrverschlüssen", Tech - Mitt. Krupp no. 17, 1959 no. 5, pp. 230 - 275; abstract from thesis, also published in Proc. of Am. Soc. of Civil Eng. 87, HY 5, paper 2927 pp. 63 - 86.
- 64 NAUDASCHER, E., "On the Role of Eddies in Flow-Induced Vibrations", 10th congress of the Int. Ass. of Hydraulic Research, London 1963, paper 3.9.
- 65 NAUDASCHER, E., "Hydrodynamische und hydroelastische Beanspruchung von Tiefschützen", Der Stahlbau 1964 no. 7, pp. 199 - 208 and no. 9, pp. 277 - 286. Also ed. in Proc. of Am. Soc. of Civil Eng. 90, 1964, HY 3 (part 1).
- 66 NAUDASCHER, E., "From Flow Instability to Flow-Induced Excitation", Proc. of Am. Soc. of Civil Eng. Journ. of Hydr. Div., July 1967, HY 4, paper 5336.
- 67 NAUDASCHER, E., Discussion on paper F.1 (Problems with recent High-Head Gate Installations by B.T.A. Sagar and J.P. Tullis) of the Symposium of the Int. Ass. of Hydraulic Research, Stockholm 1970.
- 68 NAUDASCHER, E. (editor), "Flow-Induced Structural Vibrations", Symposium of the Int. Union of Theor. and Appl. Mechanics (I.U.T.A.M.) and the Int. Ass. of Hydraulic Research (I.A.H.R.). Karlsruhe 1972, Springer Verlag, 1974.
- 69 NAUDASCHER, E., KOBUS, H.E., RAO, R.R.R., "Hydrodynamic Analysis for High-Head Leaf Gates", Proc. of Am. Soc. of Civil Eng. Journ. of Hydr. Div., 1964, HY 3, paper 3904.
- 70 NAUDASCHER, E., LOCHER, A., "Flow-Induced Forces on Protruding Walls", Proc. of Am. Soc. of Civil Eng. Journ. of Hydr. Div., Febr. 1974, HY 2, paper 10347.

References

- 71 ODEN, J.T. et al. (editors), "Finite Element Methods in Flow Problems", Int. Symp. 1974, Swansea, Publ. U.A.H. Press 1974, Univ. of Alabama.
- 72 PARISET, E., "Study on Vibration of Weir Nappes", 6th congress of the Int. Ass. of Hydraulic Research, The Hague, 1955, paper C.21.
- 73 PARKINSON, G.V., "Mathematical Models of Flow-Induced Vibrations of Bluff Bodies", see [68] pp. 81 - 127.
- 74 PARTENSKY, H.W., "Phénomènes d'oscillation observés aux vantaux ouverts d'une porte busquée", 10th congress of the Int. Ass. of Hydraulic Research, London 1963, paper 3.13.
- 75 PARTENSKY, H.W., "Forces dynamiques agissant sur les portes des écluses lors de la dérivation partielle des crues", Thesis of University of Toulouse, 1964.
- 76 PARTENSKY, H.W., SAR KHLOEUNG, I., "Oscillations de lames déversantes non aérées", Seminar S 6, 12th congress of the Int. Ass. of Hydraulic Research, Ft. Collins, 1967.
- 77 PARTENSKY, H.W., SWAIN, A., "Theoretical Study of Flap-Gate Oscillation", 14th congress of the Int. Ass. of Hydraulic Research, Paris, 1971, paper B.26.
- 78 PETRIKAT, K., "Die schwingungsanfachende Kräfte im Wehrbau", MAN Forschungsheft 69 - 100 (1953).
- 79 PETRIKAT, K., "Schwingungsuntersuchungen an Stahlwasserbauten", Der Stahlbau 1955 pp. 198 - 202 and pp. 272 - 289. Also edited in Water Power 1958 no. 2, 3, 4 and 5.
- 80 PETRIKAT, K., "Vibration Tests on Weirs and Bottom Gates", Water Power, 1958 nr. 2, 3, 4 and 5.
- 81 PETRIKAT, K., "Bestimmung der schwingungserregenden Vertikalkräfte an Sohldichtungen von Hubschützen und Segmentwehrverschlüssen", Mitt. Inst. f. Wasserbau, Univ. Stuttgart, no. 21, 1972, pp. 95 - 114.
- 82 PETRIKAT, K., MINOR, H.E., Contribution to the discussion in section C of the I.U.T.A.M./I.A.H.R. Symposium on Flow-Induced Vibrations, Karlsruhe 1972, publ. by Univ. of Karlsruhe, Inst. of Hydrodynamics.
- 83 PETRIKAT, K., RUEFF, H., Contribution to the discussion in section C of the I.U.T.A.M./I.A.H.R. Symposium on Flow-Induced Vibrations, Karlsruhe 1972, publ. by Univ. of Karlsruhe, Inst. of Hydrodynamics.
- 84 PICKETT, E.B., "Hydraulic Prototype Tests of Taintor Valve McNary Lock, Columbia river, Washington, Techn. Report no. 2-552, U.S. Army Eng. Waterw. Exp. Stat., Corps of Engineers.
- 85 RANDSFORD, G., "La théorie du premier ordre des lames vibrantes", Proc. 3th Canad. Congr. of Appl. Mech. C.A.N.C.A.M., Univ. of Calgary, May 1971.

References

- 86 RENAUD, H., "Le Béliier Hydraulique", Ed. Dunod, Paris 1950.
- 87 ROSEMEIER, G., "Zur aerodynamischen Stabilität von H-Querschnitten", Der Bauingenieur, 1973, no. 11, Nov. 1973, pp. 401-409.
- 88 ROSHKO, A., "On the Drag and Shedding Frequency of two dimensional Bluff Bodies", Naca TN 3169, July 1964, Washington.
- 89 SCHMIDGALL, T., "Spillway Vibrations on Arkansas River Dams", Proc. of Am. Soc. of Civil Eng. Journ. of Hydr. Div., Jan. 1972, HY 1, paper 8676.
- 90 SCHOEMAKER, H.J., "Virtuele massa bij golfklappen en daarop volgende trillingen in een constructie", Delft Hydraulics Laboratory publication G 6, "Manuscripten van H.J. Schoemaker in de periode 1946 - 1971".
- 91 SCHOEMAKER, H.J., "Belasting van stuwdammen bij aardbevingen", Autograph annex to lectures on irrigation, Delft Technical University.
- 92 SCHWARZ, H.I., "Nappe oscillation", Proc. of Am. Soc. of Civil Eng. Journ. of Hydr. Div., Nov. 1964, HY 6, paper 4138.
- 93 SCHWARZ, H.I., "Edgetones and Nappe Oscillation", Journ. of Acoust. Soc. of Amer., 1966/3.
- 94 SHERMAN, S., DI PAOLA, J., FRISSEL, H.F., "The simplification of flutter calculations by use of an extended form of the Routh-Hurwitz Discriminant", Journ. of Aer. Sc. Oct. 1945.
- 95 STRATING, J., "Fatigue and Stochastic Loadings", Thesis 1974 of Delft Univ. of Technology, publication Stevin Laboratory, Dept. of Civ. Eng.
- 96 THEODORSEN, Th., "General Theory of Aerodynamical Instability and the Mechanism of Flutter" Naca Report 496 (1935).
- 97 THOMSON, W.T., BARTON, M.V., "The Response of Mechanical Systems to Random Excitation", Journ. of Appl. Mechanics Vol. 24 no. 2 pp. 248 - 251.
- 98 TOEBES, G.H., RAMAMURTHY, A.S., "Fluidelastic Forces on Circular Cylinders", Proc. of Am. Soc. of Civil Eng. Journ. of Hydr. Div., Dec. 1967, no. E.M. 6, paper 5627.
- 99 TREIBER, B., "Theoretical Study of Nappe Oscillation", I.U.T.A.M./I.A.H.R. Symp. on Flow-Induced Vibrations, Karlsruhe 1972, see [68] pp. 34 - 46.
- 100 TULLIS, P., HOGAN, R.A., WHITTINGTON, N.C., "Predicting Cavitation in Valves", Symposium of the Int. Ass. of Hydraulic Research, Stockholm 1970, paper G.5.
- 101 Univ. of Washington Engng. Exp. Stat. "Aerodynamic Stability of Suspension Bridges with special reference to the Tacoma narrows Bridge", Bull. 116, Part I - IV.

References

- 102 Univ. of Washington Engng. Exp. Stat. "The Role of Vortex in the Aerodynamic Excitation of Suspension Bridges", Bull. 116, part III, Appendix III, 1952.
- 103 URATA, E., "Stability Problem of the Mass, Spring and Fluid System", Bull. Japanese Soc. Mech. Eng., 1972, no. 83, pp. 575 - 584.
- 104 VAN NUNEN, J.W.G., "Pressures and Forces on a Circular Cylinder in a Cross Flow at High Reynolds Numbers", I.U.T.A.M./I.A.H.R. Symposium on Flow-Induced Structural Vibrations, Karlsruhe 1972, see [68] pp. 748 - 754.
- 105 VELTMAN, B.P.Th., VAN DEN BOS, A., "On the Applicability of the Relay and Polaritycoincidence Correlator in Automatic Control", Proc. IFAC congress 1963, Basel.
- 106 WENDEL, K., "Hydrodynamische Massen und hydrodynamische Massenträgheitsmomente", Jahrbuch der Schiffbautechnischen Gesellschaft, Vol. 44, 1950.
- 107 WESTERGAART, H.M., "Water Pressures on Dams During Earthquakes", Trans. Am. Soc. of Civil Eng. 1933, paper 1835.
- 108 WICKERT, G., SCHMAUSZER, G., "Stahlwasserbau", Publ. by Springer, Berlin, Heidelberg, New York, 1971. Vibrations are treated on pp. 433 - 445.
- 109 ZIENKIEWICZ, O.C., NATH, B., "Analogue Procedure for Determination of Virtual Mass", Proc. of Am. Soc. of Civil Eng. Journ. of Hydr. Div., Sept. 1964, HY 5, pp. 69 - 81.

Summary

The objective of this study is to develop design criteria for the dynamic behaviour of gates and valves. To this end, a résumé of existing theories is given as well as an extended analysis of the added water mass, hydrodynamic rigidity and damping (also negative damping or self-excitation) and excitation by turbulent flow.

New computation methods are presented for self-exciting vibrations: The ensuing introduction of an instability indicator permits the prediction of such vibrations in the design phase.

Methods are described to calculate the added water mass and water damping in flowing water.

Also treated are the instability of overflowing and falling water nappes, the response of a mass-spring system to noise excitation by turbulence, and the technique of hydroelastic models. Prior publications by the author on these subjects are to be found in the Appendices.

SAMENVATTING

De doelstelling is ontwerpcriteria te ontwikkelen ten aanzien van het dynamisch gedrag van schuiven en afsluiters. Hiertoe wordt een overzicht van bestaande theorieën en een voortgezette analyse gegeven betreffende de toegevoegde watermassa, de hydrodynamische stijfheid en demping (ook negatieve demping of zelf-excitatie) en de excitatie door turbulente stroming.

Nieuwe berekeningsmethoden worden gepresenteerd voor zelf-exciterende trillingen. De introductie van een instabiliteitsindicator maakt het mogelijk dit type trillingen in het ontwerpstadium reeds te onderkennen.

Voorts worden rekenmethoden ten aanzien van de toegevoegde watermassa en de waterdemping bij stromend water gegeven.

Verder worden nog behandeld het instabiele gedrag van een vallend of overstortend watergordijn, de responsie van een massa-veersysteem op ruis-excitatie door turbulentie, en de techniek van elastisch-hydraulische modellen. Over deze onderwerpen zijn enkele vroegere publicaties van de auteur als bijlage toegevoegd.